Nitric oxide-mediated cGMP signal transduction in the central nervous system

Katalin Bartus

Thesis submitted in fulfilment of the degree of Doctor of Philosophy, University College London (Wolfson Institute for Biomedical Research).

I, Katalin Bartus, confirm that the work presented in this thesis is my own. Where information has been derived from other sources, I confirm that this has been indicated in the thesis.

Data presented in figures 3.2, 3.3, and 3.4 have been published in Garthwaite *et al.* (2006).

13th September 2009

Abstract

Nitric oxide (NO) functions as a signalling molecule throughout the brain where, via the intracellular generation of cGMP, it participates in many functions, such as in synaptic plasticity. The initial experiments were based on the finding that, in optic nerve, NO released from blood vessels tonically depolarises axons. The aim was to test the hypothesis that the tonic NO production is maintained by phosphorylation of endothelial NO synthase (eNOS). The results from extracellular recordings of changes in the axonal membrane potential suggested that PI3 kinase-mediated eNOS phosphorylation is partially responsible. The subsequent aim was to determine if blood vessel-neuron communication may be more widespread, by investigating if this mechanism accounts for basal NO production in the developing rat hippocampus. For this purpose, measurements of cGMP were chosen as a sensitive index of the local NO concentration. Contrary to expectations, no clear evidence for a dominant role of either eNOS or the neuronal NO synthase emerged, although the data suggested that NO formation was calcium-dependent. The next step was to characterise the target cells of endogenous and exogenous NO in the hippocampus, particularly in the light of findings that, with a better tool for inhibiting the dominant phosphodiesterase activity (phosphodiesterase-2), much higher cGMP levels could be evoked than previously. Accordingly, instead of a predominant location in astrocytes, cGMP immunocytochemistry showed widespread staining of neuronal elements (somata, dendrites, neuropil) throughout the tissue. The final objective was to begin to analyse NO transduction in cells in real-time, using a newly developed fluorescent cGMP sensor. Cell lines expressing various levels of guanylyl cyclase and phosphodiesterase were selected for study. Cellular responsiveness to extremely low NO concentrations (down to 3 pM) could be detected. Moreover, the findings illustrated how the interplay between guanylyl cyclase and phosphodiesterase activities serves to generate distinct cellular cGMP profiles.

Acknowledgements

I would like to express my gratitude to my supervisor John Garthwaite for his guidance, critique and support throughout the course of my research. Special thanks go to Giti Garthwaite for unrelenting encouragement and support, and her expertise in immunohistochemistry. I thank you both for giving me the chance to start fulfilling my ambitions. Your enthusiasm and guidance have been invaluable, I have learnt a lot from you.

Jeff Vernon deserves thanks not only for introducing me to tissue culture and Western blotting with a lot of patience along the way, but also for numerous insightful and motivating conversations, and new recipe ideas. Many thanks go to Barrie Lancaster for his advice whenever the grease-gap wasn't behaving, for preventing me from causing a global shortage in silver wire, and for his friendship. A big thanks goes to Andrew Batchelor for his outstanding expertise in imaging and all his help. Importantly, the camaraderie of past and present members of the Garthwaite lab has been invaluable. I thank you for your support and good laughs along the way.

I was given the great opportunity to visit the Dostmann lab in the University of Vermont to get introduced to the world of FlincG. I would like to express my appreciation to Wolfgang and Evelyn Dostmann, Kara and Matt Held, and Brent and Carmel Osborne for making me feel so welcome and for making my time in Vermont an unforgettable one.

My deepest thanks goes to my friends who have played a big part in keeping me reasonably sane. Thank you for your friendship, all the great chinwags and fun times, and – not to forget – for all the great sessions at the MA and Coffee Republic-get-togethers. I want to especially thank Elaine Irvine, Tanya Small, Jan Hendrich, Kieran Boyle, Curtis Asante, Rugina Ali and Rosie Milton for helping me rid myself of negative thoughts and emotions by inducing cell death to the responsible neurons.

Tremendous thanks goes to my mother for always supporting me to do what I wanted and for believing in me. En tudom hogy szerencses vagyok hogy nekem ilyen anyukam van. I want to thank you and Karli for your support and all the long phone conversations.

My heartfelt thanks go to Maurizio. You were always there when I was ready to give up, if only for those moments. I personally would award you the Nobel Prize in patience, unrelenting emotional support and constant encouragement.

I thank the generous financial support of the MRC and the Wellcome Trust.

Table of Contents

List of Figures

List of Tables

Abbreviations

ACh	acetylcholine
aCSF	artificial cerebrospinal fluid
Akt (PKB)	protein kinase B
AMPA	alpha-amino-3-hydroxyl-5-methyl-4-isoxazole-propionate
AMPK	5’ adenosine monophosphate-activated kinase
ATP	adenosine 5’-triphosphate
BH_4	tetrahydrobiopterin
BK	bradykinin
cAK (PKA)	cAMP-dependent protein kinase
cAMP	adenosine 3’-5’-cyclic monophosphate
Ca^{2+}	calcium
CaM	calmodulin
CaMKII	Ca^{2+}/CaM-dependent protein kinase
cGK (PKG)	cGMP-dependent protein kinase
cGMP	guanosine 3’-5’-cyclic monophosphate
cGMP-IR	cGMP immunoreactivity
CNBD	cyclic nucleotide binding domain
CNG	cyclic nucleotide gated
CNPase	2’,3’-cyclic nucleotide 3’-phosphodiesterase
CNS	central nervous system
CPTIO	2-(4-Carboxyphenyl)-4,4,5,5-tetramethylimidazoline-1-oxyl-3-oxide
Cys	cysteine
DAPI	4’,6’-diamidino-2-phenylindole
DEA/NO	2-(N,N-diethylamino)-diazenolate-2-oxide
DMSO	dimethyl sulphoxide
EDRF	endothelium-derived relaxing factor
eNOS	endothelial nitric oxide synthase
FAD	flavin adenine dinucleotide

FlincG	fluorescent indicator for cGMP
FMN	flavin mononucleotide
$GC\beta_1$	guanylyl cyclase beta-1 subunit
GFAP	glial fibrillary acidic protein
GTP	guanosine 5'-triphosphate
HCN	hyperpolarisation-activated cyclic nucleotide-modulated
HEK	human embryonic kidney
His	histidine
Hsp90	heat shock protein 90
IBMX	3-isobutyl-1-methylxanthine
iNOS	inducible nitric oxide synthase
L-MeArg	N^G-monomethyl-L-arginine acetate
L-NNA	N^G-nitro-L-arginine
LTP	long-term potentiation
NADPH	nicotinamide adenine dinucleotide phosphate
NeuN	neuronal nuclei
NF200	neurofilament 200
NMDA	N-methyl-d-aspartate
nNOS	neuronal nitric oxide synthase
NO_3^-	nitrate
NO_2^-	nitrite
NOS	nitric oxide synthase
NO	nitric oxide
NOC-12	1-hydroxy-2-oxo-3-(N-ethyl-2-aminoethyl)-3-ethyl-1-triazene
$NO_{GC}R$	guanylyl cyclase-coupled nitric oxide receptor (formerly sGC)
ODQ	1-*H*-[1,2,4]oxadiazolo[4,3-a]quinoxalin-1-one
$ONNO^-$	peroxynitrite
$O_2^{\cdot -}$	superoxide
PAPA/NO	(Z)-1-[N-(3-ammoniopropyl)-N-(n-propyl)-amino]/NO
PDE	cyclic 3'-5' monophosphate phosphodiesterase
PFA	paraformaldehyde
PI3 kinase	phosphatidylinositol-3-kinase

PP1	protein phosphatase 1
PP2A	protein phosphatase 2A
PSD-95	post-synaptic density-95
RIA	radioimmunoassay
Ser	serine
sGC	souble guanylyl cyclase (= $NO_{GC}R$)
SOD	superoxide dismutase
Thr	threonine
Val	valine

CHAPTER 1

General introduction

1.1 NITRIC OXIDE EMERGING AS A BIOLOGICALLY SIGNIFICANT MOLECULE

Nitric oxide (NO) was first discovered by Joseph Priestley in 1772, describing it as a colourless, toxic gas, with a lifetime of only a few seconds. Indeed, NO first came to medical prominence as a poison when Sir Humphrey Davy spoke of a terrible burning in his tongue, throat and chest upon inhaling NO during his investigations into nitrous oxide and other gases as anaesthetic agents (Sprigge, 2002). The rediscovery of NO as a poison owed to the tragedy reported in 1967 wherein a contaminated stock of nitrous oxide killed one patient and gravely injured a second (Clutton-Brock, 1967). Nonetheless, although being a noxious constituent of car fumes and cigarette smoke, and having long been regarded as a harmful pollutant, a string of seminal experiments which will be outlined below provided the stepping stone for NO to rise to biological fame. Having been proclaimed as the molecule of the year by the journal *Science* in 1992, the importance of the discovery of NO was further recognised by awarding the 1998-Nobel Prize in Physiology and Medicine to the late Robert Francis Furchgott, Louis Ignarro, and Ferid Murad. By the end of the 20th century the plethora of NO's implications was spanning almost every area of biomedicine, including cardiovascular function, neurotransmission and neuropathology, pain, diabetes, wound healing and tissue repair, skin, cancer, immune function, infection, respiratory function, eye physiology and pathology, and many others. It continues to be one of the most researched molecules.

Prior to the groundbreaking work in the 1980s, the first implications of NO in biology date back as far as the late 1860s when Alfred Nobel discovered nitroglycerin to have an anti-anginal effect. He utilised nitroglycerin in his factories to synthesise dynamite, in the course of which he observed that some of his workers complained of recurrent headaches, which would disappear over the weekends, while those suffering from angina pectoris often reported relief from chest pains during the working week. Although initially attributed to the vasodilatory action of nitroglycerin, about a century later the underlying mechanism was elucidated to involve metabolic

conversion of nitroglycerin to NO (Arnold *et al.*, 1977; Ignarro *et al.*, 1981). The potential of NO as a vasodilator was further confirmed by experiments conducted by Gruetter and colleagues, demonstrating relaxation of the vascular smooth muscle in experiments in which a gaseous mixture of NO in nitrogen or argon was delivered into an organ bath containing isolated pre-contracted strips of bovine coronary artery (Gruetter *et al.*, 1979).

In 1980, Furchgott and Zawadzki initiated the avalanche of NO research. Initially interested in studying the difference between *in vivo* and *in vitro* responses of blood vessels to acetylcholine, *in vitro* preparations generally contracting in response to stimulation by acetylcholine, experiments usually utilised only "pure" smooth muscle preparations where isolated arteries had been cleared of both the adventitia and the endothelium. On one occasion, Furchgott's technician, John Zawadzki, forgot to remove the endothelium in their rabbit aorta preparation and, to their surprise, acetylcholine caused a potent relaxation (Furchgott, 1999). This culminated in the first serendipitous discovery in the NO story in which Furchgott demonstrated that endothelial cells produce a relaxing factor in response to acetylcholine in vessels with intact endothelium, which was termed endothelium-derived relaxing factor or "EDRF" (Furchgott & Zawadzki, 1980). In this study, Furchgott established that arterial relaxation in response to acetylcholine strictly required the presence of the endothelium, and found relaxation to be prevented by atropine, implying that acetylcholine was acting on muscarinic receptors to initiate the production of a diffusible substance, which could ultimately reach the smooth muscle to evoke relaxation. At that time, the vasorelaxant effect of nitrovasodilators such as nitroglycerin and sodium nitroprusside had already been linked to stimulation of the enzyme guanylyl cyclase and resultant rise in cGMP, and also NO, which was known to be spontaneously liberated from sodium nitroprusside, was shown to increase cGMP (Arnold *et al.*, 1977; Gruetter *et al.*, 1981; Feelisch & Noack, 1987). Moreover, the endothelium-dependent relaxation was thought to be mediated by cGMP and cGMP-dependent phosphorylation (Rapoport & Murad 1983; Rapoport *et al.*, 1983). Nevertheless, a direct connection between NO and Furchgott's discovery was not made until nearly a decade later. Following numerous studies indicating striking similarities between the properties of NO and EDRF, it was only in 1987 that

two separate laboratories published direct evidence that NO and EDRF were in fact one and the same molecule (Palmer *et al.*, 1987; Ignarro *et al.*, 1987a; Ignarro *et al.*, 1987b). The group of Ignarro showed that EDRF derived from the pulmonary artery and vein with intact endothelium had identical vasorelaxant properties to NO applied to endothelium-denuded tissue preparations. They also provided chemical evidence that EDRF released from both artery and vein is NO, demonstrating that EDRF also reacts with haemoglobin and causes an identical shift in the absorbance spectrum as authentic NO. More-or-less at the same time, Palmer and colleagues found that cultured endothelial cells release an unstable vasodilating agent upon exposure to bradykinin with identical biological activity to NO. Moreover, using a chemiluminesence technique, Palmer et al. provided direct evidence that the vaso-active molecule produced in their experiments was NO.

Only about one year after the identification of EDRF as NO, it was discovered that NO is also produced in the brain following activation of the N-methyl-D-aspartate (NMDA) class of glutamate receptors in neurons, proposing that it may relay signals to neighboring cells (Garthwaite *et al.*, 1988). The potential of NO to diffuse between its sources and targets was particularly evident as NMDA elicited relaxation of rat aorta only in the presence of cerebellar cells (Garthwaite *et al.*, 1988). This groundbreaking discovery was preceded by a string of evidence indicating the presence of a transmitter which evokes accumulation of cGMP upon NMDA receptor stimulation. Already in the mid-1970s, Ferrendelli and colleagues speculated that there could be an intermediate transmitter between glutamate-evoked Ca^{2+} influx and resultant cGMP elevation, observing a rise in cGMP in mouse cerebellar slices upon exposure to glutamate, which was found to be dependent on the presence of Ca^{2+} (Ferrendelli *et al.*, 1974; Ferrendelli *et al.*, 1976). About a year later, Arnold et al. reported an increase in the activity of the guanylyl cyclase in brain homogenates upon exposure to pure NO gas (Arnold *et al.*, 1977), which was later found to closely resemble the increase in enzyme activity induced by L-arginine (Deguchi & Yoshioka, 1982). In 1985, the glutamate-evoked rise in cGMP was finally linked to NMDA receptor activation by pharmacological means (Garthwaite, 1985). Eventually, the experimental evidence indicating NO to be the connective element

between NMDA receptor activation and cGMP accumulation (Garthwaite *et al.*, 1988) potentially explained the earlier finding in the cerebellum of cGMP accumulation not predominantly occurring in the same cells stimulated by NMDA, suggesting an intercellular messenger (Garthwaite & Garthwaite 1987). More evidence that it was indeed NO that was the missing transmitter followed rapidly when it was demonstrated that NMDA receptor activation failed to evoke cGMP accumulation when the enzyme synthesising NO was inhibited, while this remained intact and was augmented in the presence of L-arginine (Garthwaite *et al.*, 1989). NO as a neurophysiological messenger was discovered, initiating the extensive research into NO signalling in the central nervous system.

Around the same time of NO being discovered to be a transmitter in the brain, parallel unrelated investigations identified the potential of NO to also serve in the immune system. Previously, it had been shown that urinary levels of nitrate (NO_3^-) exceeded dietary intake, indicative of a synthetic pathway (Green *et al.*, 1981). Following an inflammatory stimulus, the synthesis of NO_3^- was increased (Wagner *et al.*, 1983), which echoed findings of increased urinary nitrate excretion in patients suffering from diarrhoea and fever (Hegesh & Shiloah, 1982). This was later attributed to activated macrophages (Stuehr & Marletta, 1985). The dependence of the cytotoxic action of activated macrophages on L-arginine (Hibbs *et al.*, 1987) led to the confirmation of NO being part of the repertoire of defenses against foreign organisms (Hibbs *et al.*, 1988), exerting its cytotoxicity via mechanisms such as metabolic inhibition of DNA synthesis and mitochondrial respiration, which eventually culminates in the induction of apoptosis (MacMicking *et al.*, 1997).

These three diverse functions – smooth muscle relaxation, neural communication, and immune defense – remain at the core of NO biology and are mediated largely by the processes outlined in the following sections.

*

1.1 FORMATION OF NO

1.2.1 Nitric oxide synthases

The identification of EDRF as NO was rapidly followed by the discovery of the synthetic machinery for NO. The group of enzymes responsible for NO production was first described in 1989 to be the Ca^{2+}/calmodulin (CaM)-dependent NO synthases (NOS), and was subsequently characterised throughout the 1990's. The isolation and cloning of NOS from rat cerebellum (Bredt & Snyder, 1990; Bredt *et al.*, 1991a) was rapidly conjoined with immunohistochemical evidence demonstrating NOS not only to be localised in endothelial cells but also to be highly expressed in the brain (Bredt *et al.*, 1990; Vincent & Kimura, 1992), being discretely localised in neuronal populations (Bredt *et al.*, 1991b; Vincent & Kimura, 1992).

Currently there are three acknowledged isoforms of NOS responsible for NO production throughout the mammalian system, each of which catalyses the conversion of the amino acid L-arginine and molecular oxygen to L-citrulline and NO. There are three distinct genes in the mammalian genome encoding, respectively, the neuronal (n)NOS in neurons, endothelial (e)NOS in endothelial cells of the vasculature, and inducible (i)NOS. Inducible NOS is not found in any healthy cell but is instead, as the name implies, induced in various cell types, including macrophages and microglia, generally occurring in response to products of infection, such as bacterial endotoxin, or to inflammatory mediators, including cytokines, interleukin-1 and tumour necrosis factor, resulting in long-term NO production to cytotoxic levels.

Splice variants of some of the NOS isoforms have also been reported. Identified variants of nNOS include nNOSα, nNOSβ and nNOSγ. A fourth variant termed nNOS-2 has been reported in the mouse brain, but only at its mRNA level (Ogura *et al.*, 1993). The most relevant nNOS variant is the α-variant as it is the only one known to physically associate with NMDA receptors in synapses (Brenman *et al.*, 1996 and see later) and appears to be the most abundant nNOS subtype, accounting for approximately 95% of all enzyme activity in the brain (Huang *et al.*, 1993). In

contrast, both the β- and γ-variants appear to lack capacity to associate with NMDA receptors, the former being up-regulated in some brain regions (including striatum, hippocampus, brain stem and cortex) at its protein level in mice devoid of the nNOSα and suggested to be the only functional alternative to nNOSα, since the γ-variant appears to have little or no enzymatic activity (Brenman *et al.*, 1996; Eliasson *et al.*, 1997; Langnaese *et al.*, 2007). No splice variants of eNOS have so far been reported, while relatively little information exists on iNOS variants. Alternatively spliced mRNA transcripts of iNOS have been detected in human epithelial and alveolar macrophages (Eissa *et al.*, 1996). Due to its principal importance in host defence mechanisms as well as pathology, being largely irrelevant to the work presented in this thesis, iNOS will not be considered in much further detail.

1.2.2 NOS structure and reaction mechanism

NOS proteins are dimers, each monomer comprising a N-terminal oxygenase domain and a C-terminal reductase domain, these two domains being linked by a CaM-recognition site *(Fig. 1.1)*. The oxygenase domain possesses binding motifs for haem, the cofactor tetrahydrobiopterin (BH_4), and the substrate L-arginine, BH_4 thought to be predominantly promoting and stabilising the active dimeric form of all NOS isoforms. The reductase domain is equipped with the binding sites for NADPH, FAD and FMN.

The synthesis of NO by NOS involves electron flow through the enzyme, which is facilitated by Ca^{2+}-CaM binding to the CaM-recognition site, and a two-step oxidation of L-arginine to L-citrulline with the concomitant generation of NO. Functionally, electrons are donated by NADPH to the reductase domain and are transported through the reductase domain by the FAD and FMN redox carriers, eventually reaching the oxygenase domain of the opposite monomer. Upon arrival of the electrons at the oxygenase domain, the haem iron is initially reduced from Fe^{3+} to Fe^{2+}, allowing it to bind molecular oxygen, the cleavage of which in turn leads to the oxidation of L-arginine at the catalytic site, the end-products being L-citrulline and NO (Alderton *et al.*, 2001).

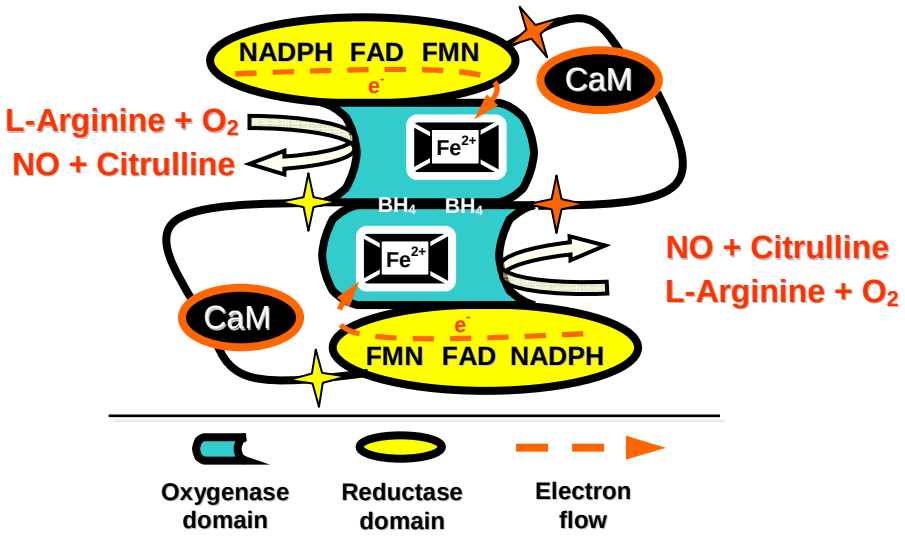

Fig. 1.1 Synthesis of NO by NOS: structure and catalytic function. Proposed arrangements of monomers; activity requires the dimeric interaction between two oxygenase domains and CaM binding between the reductase and oxygenase domains, which triggers electron transfer. The reductase reduces NADPH to NADP+, yielding electrons, which are then carried onto the haem moiety in the oxygenase domain of the other monomer via the bound flavins FMN and FAD. Subsequently, two cycles of L-arginine oxygenation occur. The first cycle yields the intermediate product N-hydroxyl-L-arginine (NHA) via oxygenation of the guanidine group of L-arginine to a N-hydroxyl group, a reaction that requires BH_4 as a cofactor. In the second cycle, NHA is converted to L-citrulline and NO by oxidative cleavage. *Adapted from Alderton et al., 2001*

1.2.3 Catalytic modulation

CaM and Ca^{2+}

The binding of Ca^{2+}-CaM is a pivotal requisite for NOS activity (Bredt & Snyder, 1990), functioning as a sensor of intracellular Ca^{2+} concentrations, where the binding of Ca^{2+} to CaM promotes CaM interaction with NOS. A conformational change in the NOS dimer upon CaM binding supports the flow of electrons within the reductase domain as well as the interdomain electron transfer (Panda *et al.*, 2001). The Ca^{2+}-dependence varies among NOS isoforms in that both eNOS and nNOS require higher concentrations than iNOS. The iNOS is held in an activated state even at low Ca^{2+} levels as it binds CaM very tightly, rendering it largely Ca^{2+}-independent. The varying

Ca^{2+}-sensitivity of the different NOS isoforms is determined by the presence of an auto-inhibitory loop insert of 40-50 amino acids in the FMN-binding subdomain. While absent in iNOS (Salerno *et al.*, 1997), this insert acts to destabilise CaM binding to eNOS and nNOS at low Ca^{2+} concentrations, thereby preventing the flow of electrons to the haem moiety. Upon CaM binding, this insert polypeptide is displaced, initiating the ability of CaM to gate electron flow through NOS (Salerno *et al.*, 1997).

Phosphorylation

nNOS:

Although having long been regarded to be predominantly Ca^{2+}-dependent, it is now clear that enzyme activity of both eNOS and nNOS may also be influenced via protein phosphorylation on several putative sites. The first indication that NOS can be regulated by many different factors came from cloning studies, revealing recognition sites not only for NADPH, CaM, and flavins, but also phosphorylation sites (Bredt *et al.*, 1991a).

Phosphorylation of nNOS on Ser-847 by CaM-dependent protein kinases has been demonstrated to reduce nNOS activity. Initial studies on purified nNOS from rat brain found Ser-847 to be phosphorylated by several CaM-dependent kinases, which was confirmed by the lack of phosphorylation observed upon mutation of this site (Hayashi *et al.*, 1999). Phosphorylation of Ser-847 was found to result in an overall 50-60% reduction in enzyme activity, attributed partially to suppressed CaM binding. Later studies in cultured hippocampal neurons confirmed this finding, demonstrating NMDA receptor-dependent phosphorylation of nNOS-Ser-847 by Ca^{2+}-CaM protein kinase II (CaMKII) in dendritic spines, which was slow in onset (Rameau *et al.*, 2004). An interesting observation made by Rameau and colleagues was that of a bidirectional regulation of this phosphorylation process depending on the concentration of glutamate applied to the neurons. While low micromolar concentrations of glutamate elicited enhanced nNOS phosphorylation, concentrations

in the several hundred-micromolar ranges were associated with reduced phosphorylation of the enzyme, indicating that the alleviation of this negative feedback control on nNOS activity may be a potential mechanism contributing to excessive NO output under conditions of excitotoxicity. Sustained CaMKII-mediated phosphorylation of nNOS-Ser-847, evoked by low glutamate concentrations, was also detected in cultured cortical neurons (Rameau *et al.*, 2007).

Other sites on nNOS the phosphorylation of which have been suggested to cause a reduction in nNOS activity are Ser-741 by CaMKI (Song *et al.*, 2004), and Thr-1296 (Song *et al.*, 2005), where the latter study employed phosphatase inhibitors and mutations mimicking Thr-phosphorylation to come to their conclusion. However, both studies based their conclusions on observations made either in HEK cells or in a neuroblastoma cell line transfected with nNOS (and CaMKI in the case of Song *et al.*, 2004).

Phosphorylation of Ser-1412 on nNOS, mediated by the Ser/Thr protein kinase Akt in a NMDA receptor-dependent manner, has also been proposed based on studies in cultured cortical neurons (Rameau *et al.*, 2007). In contrast to Ser-847 phosphorylation, however, this was found to occur more rapidly in response to low glutamate concentrations and to lead to rapid enhancement in nNOS activity.

eNOS:

While a fairly new concept in the field of nNOS research, protein phosphorylation on a number of putative sites by various types of protein kinases is a well-established feature of eNOS activity regulation. In fact, phosphorylation is now considered to be one of the most important mechanisms by which eNOS activity is controlled.

The two most extensively studied phosphorylation sites on eNOS have been Ser-1179, which is located in the reductase domain close to the C-terminus of eNOS, and Thr-497, which is located in the CaM-binding site. Phosphorylation of Ser-1179 enhances eNOS activity by reducing the enzyme's Ca^{2+}-dependence (Chen *et al.*, 1999) with an increase in the rate of NO production (Dimmeler *et al.*, 1999; Fulton *et al.*, 1999), while phosphorylation of Thr-497 reduces enzyme activity by increasing the

Ca^{2+}/CaM dependence of eNOS (Chen *et al.*, 1999; Fleming *et al.*, 2001). Physiologically, phosphorylation and dephosphorylation of these sites are regulated in a highly balanced manner. For instance, selective stimulation of eNOS by means of exposure of endothelial cells to bradykinin results in a transient dephosphorylation of the inhibitory site Thr-497 in conjunction with Ser-1179 phosphorylation (Fleming *et al.*, 2001; Harris *et al.*, 2001). Under unstimulated conditions Thr-497 appears to be strongly phosphorylated, with weak phosphorylation of Ser-1179 (Fleming *et al.*, 2001). Phosphorylation of eNOS is thought to be able to regulate eNOS activity in a Ca^{2+}-independent fashion (Corson *et al.*, 1996; Fleming *et al.*, 1998), the physiologically most important pathway for eNOS activation being fluid sheer stress. The activation of eNOS by fluid sheer stress is unique in that it can be maintained over hours and occurs in the absence of extracellular Ca^{2+} (Kuchan & Frangos, 1994; Ayajiki *et al.*, 1996). Moreover, mimicking Ser-1179 phosphorylation enhances eNOS activity, even in the absence of Ca^{2+} (Dimmeler *et al.*, 1999).

While being the target of multiple protein kinases, various studies have implicated a key signal transduction pathway in which activation of phosphatidylinositol-3-kinase (PI3 kinase) and the Ser/Thr protein kinase Akt results in eNOS phosphorylation on the Ser-1179 site. Initial studies demonstrated that treatment of endothelial cells with vascular endothelial growth factor (VEGF) or insulin stimulates NO synthesis in a PI3 kinase-dependent manner, PI3 kinase inhibition partially preventing NO release (Zeng & Quon, 1996; Papapetropoulos *et al.*, 1997). Subsequently, the kinase Akt, a downstream effector of PI3 kinase, was found to activate eNOS in endothelial cells exposed to shear stress, leading to enhanced NO production via Ser-1179 phosphorylation and cGMP accumulation, where inhibition of PI3 kinase or mutation of Ser-1179 attenuated phosphorylation and prevented eNOS activation and cGMP formation (Dimmeler *et al.*, 1999). This was joined by the finding that Akt phosphorylates eNOS-Ser-1179 directly, thereby activating basal NO output from eNOS in endothelial cells, which is diminished upon mutation of the Ser-1179 site (Fulton *et al.*, 1999). The detection of Akt in immunoprecipitates of eNOS from bovine aortic endothelial cells suggests that Akt and eNOS associate *in vivo* (Michell *et al.*, 1999). Apart from fluid shear stress, a number of eNOS agonists, including

VEGF, insulin, and bradykinin, can also increase eNOS activity through the PI3 kinase-Akt-Ser-1179 phosphorylation pathway (Dudzinski *et al.*, 2006).

The phosphorylation of eNOS is preventable by PI3 kinase inhibition, the two main inhibitors of PI3 kinase in use being wortmannin and LY 294002. Wortmannin is a fungal metabolite, isolated from *Penicillium wortmannii*, and inhibits PI3 kinase at a low nanomolar IC_{50}. The synthetic compound LY 294002 has a reported IC_{50} value for PI3 kinase inhibition in the low micromolar range (Walker *et al.*, 2000; Djordjevic & Driscoll, 2002). Both of these compounds are competitive inhibitors of ATP binding. X-ray crystallography revealed that both wortmannin and LY 294002 bind in the ATP binding site of the PI3 kinase that is located in a cleft between the N- and C-terminal lobes of the catalytic domain. However, while the interaction of LY 294002 with PI3 kinase is reversible, wortmannin causes irreversible inhibition of the kinase by forming a covalent complex with a lysine residue in the catalytic site, which leads to a large conformational rearrangement (Walker *et al.*, 2000). Both compounds were shown to be selective towards PI3 kinase at the concentrations used in the present work (Davies *et al.*, 2000).

Other eNOS phosphorylation sites include Ser-635, the phosphorylation of which is also stimulatory, and Ser-617 and Ser-116. The impact of the latter two on eNOS activity remains controversial, based on mixed findings from different laboratories observing either no change in enzyme activity, or enhanced or reduced activity, depending on the stimulating factor used (Mount *et al.*, 2007).

Protein-protein interactions

nNOS:

A number of proteins have been identified that may bind and regulate nNOS. These include the termed protein inhibitor of NOS (PIN), the C-terminal PDZ ligand of NOS (CAPON), heat shock protein 90 (hsp90), and NOS interacting protein (NOSIP). Overall, however, their functions remain poorly understood.

PIN, identified as a dynein light chain, may contribute to axonal transport of nNOS as indicated by the finding of it binding to nNOS, while having no direct influence on enzyme activity (Rodriguez-Crespo *et al.*, 1998). CAPON may aid membrane association of nNOS via synapsins at synaptic sites. The synapsin family of proteins have been identified as binding partners of CAPON, CAPON suggested to serve as an intermediate linking nNOS and synapsin. Comparing different subcellular fractions of forebrain obtained from mice lacking synapsin I and II revealed changes in the subcellular localisation of nNOS and CAPON in that both were increased in the soluble fractions (Jaffrey *et al.*, 2002). NOSIP interaction with nNOS may act to indirectly reduce nNOS activity by relocating the enzyme away from its site of action at the cell membrane as it has been demonstrated to modulate both the localisation and activity of nNOS. This hypothesis arose from a number of observations made by Dreyer and colleagues (Dreyer *et al.*, 2004). These included co-immunoprecipitation of nNOS and NOSIP from brain lysates, co-localisation of NOSIP and nNOS in neuronal synapses in various rat brain regions (including hippocampus), reduced enzyme activity upon stimulation with a Ca^{2+} ionophore in a cell line stably expressing nNOS and transiently transfected with NOSIP, and neuronal activity-dependent shuttling of NOSIP between synaptic, cytosolic and nuclear subcellular location in cultured hippocampal neurons. Silencing of neuronal activity favoured nuclear localisation of NOSIP, while non-nuclear localisation predominated under conditions of basal activity or NMDA receptor-evoked neuronal activity. Finally, hsp90 inhibition has been reported to reduce nNOS activity in insect cells by approximately 75%, suggested to be due to impaired haem insertion (Billecke *et al.*, 2002). Additionally, studies on purified nNOS have shown hsp90 to enhance enzyme activity directly and to increase CaM affinity for nNOS with resultant elevated catalytic activity (Song *et al.*, 2001).

eNOS:

Just as with phosphorylation, the significance of eNOS interacting with other proteins is better established than in the case of nNOS. The most extensively studied proteins

that can interact with eNOS, and regulate enzyme activity negatively or positively, include caveolin-1, NOSIP, and hsp90.

Caveolin-1 is an integral membrane protein abundant in endothelial cells, and serves as a structural scaffold within caveolae, which are enriched with cholesterol and sphingolipids, which minimise the fluidity of these discrete membrane regions. The limited fluidity in caveolae, which eNOS is localised to, draws together proteins, supporting protein-protein interactions. Studies on endothelial cell lysates demonstrated eNOS co-immunoprecipitation with caveolin-1 (Feron *et al.*, 1996; Garcia-Cardena *et al.*, 1996). Subsequently, *in vitro* studies and experiments with eNOS and caveolin-1 expressed in cells revealed that both the N- and C-terminal domains of caveolin-1 interact directly with the oxygenase domain of eNOS and thereby inhibits enzyme activity (Garcia-Cardena *et al.*, 1997; Ju *et al.*, 1997; Michel *et al.*, 1997). Moreover, *in vitro* manipulations further indicated that Ca^{2+}-CaM binding to eNOS disrupts the interaction between eNOS and caveolin-1, resulting in enhanced catalytic activity (Michel *et al.*, 1997). Later, experiments using particulate and soluble cellular fractions indicated that the association and dissociation of eNOS and caveolin-1 may be a cyclic event, in which dissociation leads to the mobilisation of eNOS from the particulate fraction upon agonist stimulation, followed by re-association of eNOS and caveolin-1 in the particulate fraction (Feron *et al.*, 1998). In intact blood vessels, the caveolin-1 was shown to potently inhibit eNOS *in vivo* (Bucci *et al.*, 2000). Bucci and colleagues used a membrane-permeable form of the caveolin-1 scaffolding domain (amino acids 82-101) and fused it to a cell-permeable leader sequence. Exposure of mouse aortas to the peptide resulted in uptake into the blood vessel, localising to endothelial cells, and prevention of ACh-mediated relaxation, with no effect on relaxation in response to exogenous NO. In aortas from mice lacking caveolin-1, on the other hand, the relaxant response to ACh is enhanced, attributable to increased basal NO production (Drab *et al.*, 2001).

NOSIP is another binding partner of eNOS that is proposed to have a negative regulatory impact on enzyme activity. Although the true function of NOSIP remains to be elucidated, the interaction between NOSIP and eNOS has been shown by co-immunoprecipitation studies in cells (Dedio *et al.*, 2001). Although NOSIP did not

affect eNOS activity when examined by *in vitro* assays, when co-expressed in cells, NO release was reduced, which was suggested, based on immunohistochemical data, to be caused by redistribution of eNOS from the plasma membrane caveolae to intracellular compartments (Dedio *et al.*, 2001).

In addition to CaM, another positive regulatory protein of eNOS is hsp90. First, hsp90 was shown to co-precipitate with eNOS, being associated with eNOS in resting endothelial cells (Garcia-Cardena *et al.*, 1998; Russell *et al.*, 2000). The treatment of cells with different stimuli including shear stress and VEGF enhanced hsp90-eNOS interaction. Mechanistically, it has been proposed that hsp90 may facilitate the ability of CaM to displace caveolin-1 from eNOS, the three constituents having been found to be present in the same complex in endothelial cells (Gratton *et al.*, 2000). Also, studies on purified enzyme have demonstrated hsp90 to enhance eNOS activity in the presence of CaM both at low and high Ca^{2+} concentrations, the EC_{50} values for both Ca^{2+} and CaM being reduced in the presence of hsp90 (Takahashi & Mendelsohn, 2003a). More direct evidence supporting the eNOS-hsp90 interaction emerged from experiments showing that hsp90 inhibition not only prevents VEGF-stimulated cGMP production in cultured endothelial cells, but also the ACh-evoked vasorelaxation of rat aortic rings (Garcia-Cardena *et al.*, 1998) as well as flow-induced dilation of rat middle cerebral artery to a similar extent as direct NOS inhibition with a non-selective NOS inhibitor (Viswanathan *et al.*, 1999).

Hsp90 may also affect eNOS activity indirectly by acting on the kinase Akt. Hsp90 has been shown to bind both the inactive or active Akt and is required for the interaction of Akt with eNOS (Garcia-Cardena *et al.*, 1998). Furthermore, it has been suggested that hsp90 stimulates eNOS by increasing the rate of Akt-dependent phosphorylation of eNOS, and that the kinase Akt and hsp90 synergistically activate eNOS at both physiological Ca^{2+} concentrations as well as independently of Ca^{2+}, indicating that hsp90-mediated Akt activation and the Akt-unrelated effects of hsp90 could be occurring simultaneously (Takahashi & Mendelsohn, 2003b). A summary of the proposed mechanism for eNOS activation via the PI3 kinase-Akt pathway is depicted in *Fig. 1.2*.

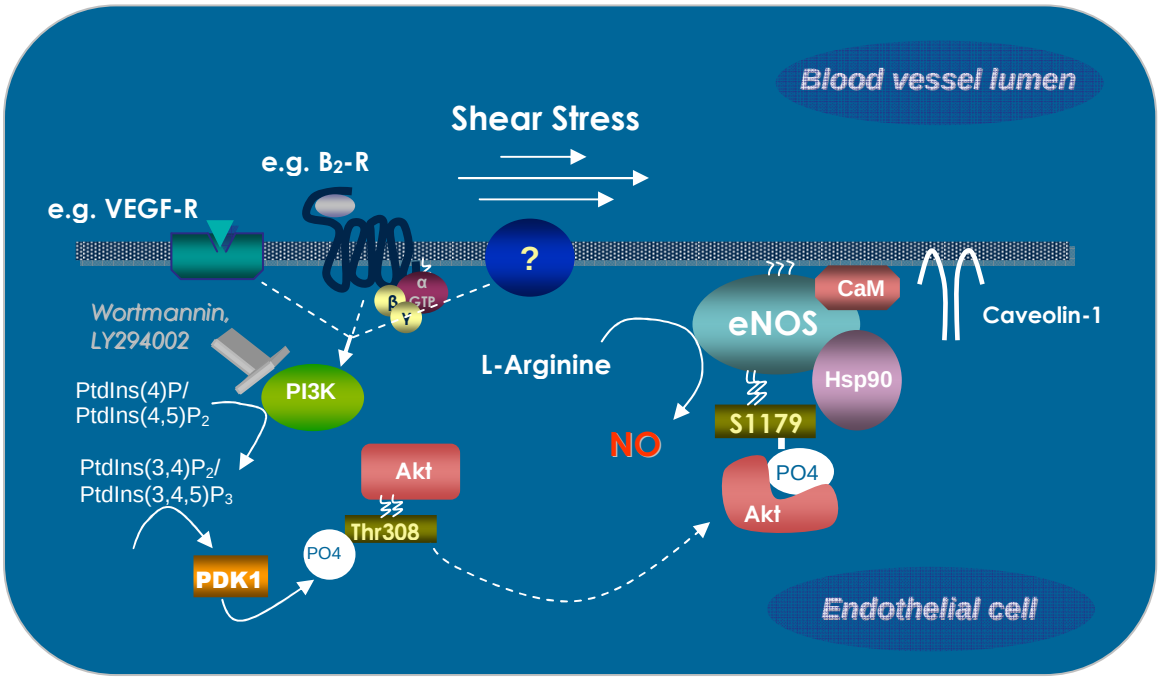

Fig. 1.2 Proposed scheme of PI3 kinase-Akt-mediated eNOS phosphorylation. Upon binding to their respective receptors, shear stress and various ligands can lead to activation of PI3 kinase. PI3 kinase then catalyses the formation of phosphatidylinositol bi- and triphosphates, which are required for the downstream activation of the phospholipid-dependent-kinase-1 (PDK-1). Upon activation, the PDK-1 then phosphorylates Akt, which initiates the translocation of Akt to the plasma membrane where Akt then phosphorylates eNOS on Ser-1179. Upon eNOS phosphorylation, caveolin-1, to which eNOS is bound in its inactive state, dissociates from the enzyme as it is displaced by calmodulin (CaM), initiating eNOS activation and NO formation from L-arginine. *Adapted from Sessa, 2004*

1.2.4 Pharmacological intervention for NOS inhibition

Inhibitors of NOS have become invaluable tools for investigating the biological roles of endogenous NO. The first series of inhibitors developed were derivatives of the NOS substrate L-arginine, which have a substituent on the guanidine nitrogen normally used for NO synthesis. The most commonly used of these inhibitors include N^G-nitro-L-arginine (L-NNA), N-methyl-L-arginine (L-NMMA), and N^G-nitro-L-arginine methyl ester (L-NAME), the latter being the prodrug of L-NNA. These compounds exert their inhibitory action non-selectively by competing with L-arginine

for its binding site. All of these broad-spectrum NOS inhibitors have reasonable potencies with K_i values in the low micromolar range (Alderton *et al.*, 2001). Among the first evidence for the inhibitory action of L-NNA and L-NMMA at the tissue level were results from rabbit aorta, in which both compounds were demonstrated to evoke concentration-dependent contractions and to prevent ACh-induced relaxation while leaving relaxation in response to exogenous NO intact (Moore *et al.*, 1990).

Considerable effort has also been dedicated towards the development of isoform-selective inhibitors. Compounds showing good selectivity for nNOS over eNOS and iNOS include N-propyl-L-arginine (NPA; Zhang *et al.*, 1997; Cooper *et al.*, 2000) and N^5-(1-Imino-3-butenyl)-L-ornithine (L-VNIO; Babu & Griffith, 1998). To date, L-VNIO is the most potent nNOS-selective inhibitor, with a Ki value in the low nanomolar range, being 120-fold and 600-fold higher for eNOS and iNOS respectively (Babu & Griffith, 1998). A compound showing good selectivity for iNOS over the other two NOS isoforms is [N-(3-aminoethylyl)benzyl]-acetamidine (1400W; Garvey *et al.*, 1997; Boer *et al.*, 2000). This inhibitor was found to be approximately 5000-fold or 200-fold more selective for iNOS over eNOS or nNOS respectively (Garvey *et al.*, 1997). All of these isoform-preferring inhibitors act by targeting the L-arginine binding site on NOS, competing with L-arginine for binding. No selective eNOS inhibitors are known to date.

1.2.5 nNOS and eNOS in the brain

nNOS

In neurons the predominant isoform of NOS is nNOS, which is widely distributed throughout the brain and spinal cord, albeit at varying amounts among different regions. For example, the highest activity and expression of nNOS is found in the cerebellum (Bredt *et al.*, 1990; Bredt *et al.*, 1991b), with nNOS localising to virtually all neuronal cells. On the other hand, in other areas such as the cerebral cortex and striatum, nNOS appears in a subpopulation of interneurons. Nevertheless, dense nNOS-containing networks of fibres can be seen throughout the neuropil, including areas with relatively sparse numbers of nNOS-bearing neurons, indicating that the

majority of neurons receive NO signals (Vincent & Kimura, 1992; Rodrigo *et al.*, 1994). Potential sites of NO synthesis have largely been identified in the past by means of immunohistochemistry (Bredt et al., 1990; Rodrigo et al., 1994; de Vente et al., 1998; Burette *et al.*, 2002), *in situ* hybridisation (Keilhoff *et al.*, 1996), and the NADPH-diaphorase staining methodology (Vincent & Kimura, 1992; Southam & Garthwaite, 1993; Keilhoff *et al.*, 1996), the latter exploiting NOS activity to reduce tetrazolium salts to visible formazans in an NADPH-dependent manner, thereby allowing the histochemical visualisation of sites of NOS activity.

In the hippocampus there have been mixed reports concerning nNOS expression. Initially, intense immunoreactivity was described in the dentate gyrus (Bredt *et al.*, 1990), and also some scattered immunoreactive neurons in the CA1 subfield were reported (Bredt *et al.*, 1991b). In both cases, however, pyramidal neurons appeared to be devoid of nNOS staining. Subsequent immunohistochemical studies suggested nNOS to be largely confined to interneurons in the CA1 and CA3 subregions of the hippocampus (Valtschanoff *et al.*, 1993; Lumme *et al.*, 2000), which was at odds with some of the immunohistochemical evidence finding immunoreactivity in CA1-CA3 and subicular pyramidal neurons (Rodrigo *et al.*, 1994), and NADPH-diaphorase results finding strong pyramidal cell staining in the subiculum (Vincent & Kimura, 1992) and CA1 region (Southam & Garthwaite, 1993). Eventually, the use of weaker fixation protocols and electron microscopy in conjunction with light microscopy clearly revealed the presence of nNOS in a number of pyramidal neurons (Endoh *et al.*, 1994; Wendland *et al.*, 1994; Blackshaw *et al.*, 2003) and in dendritic spines (Burette *et al.*, 2002). Strongly labelled cells were demonstrated to express nNOS staining diffusely in the cytosol, while weakly stained cells, or those appearing unlabelled at the light microscopic level, were revealed to express nNOS localised to membranes when examined by means of electron microscopy (Burette *et al.*, 2002). It transpired from these studies that not only the method of fixation but also antibody incubation times were crucial factors in determining the visibility of nNOS. In order to achieve optimal staining in interneurons, the reaction must be terminated before any nNOS could be revealed in pyramidal neurons.

The membrane localisation of nNOS visualised by Burette et al. (2002) is consistent with the known interaction of nNOS with NMDA receptors at synaptic membranes, thereby coupling NO formation to NMDA receptor activity, the entry of Ca^{2+} in the vicinity of the receptor resulting in NOS activation. The association between nNOS and the NMDA receptor is provided by the post-synaptic density-95 (PSD-95), which acts as the intermediate interaction partner. PSD-95 protein contains several PDZ domains, which are protein-protein interaction motifs. nNOS also contains a PDZ domain in its N-terminal region, which interacts with the second PDZ-domain of PSD-95 (Brenman *et al.*, 1996). The ternary complex is achieved by the second PDZ domain of PSD-95 also interacting with a C-terminal Ser/Thr-X-Val motif of the NMDA receptor (Kornau *et al.*, 1995; Christopherson *et al.*, 1999). Disruption of the interaction between nNOS and PSD-95 by deletion of the N-terminus of nNOS has been demonstrated to prevent membrane association without affecting the catalytic activity of the enzyme. Membrane association of nNOS with NMDA receptors, however, is functionally significant in terms of NMDA receptor-dependent synaptic activation of NO synthesis. Suppression of PSD-95 in cultured cortical neurons by means of anti-sense oligonucleotide techniques was found to attenuate cGMP production by more than 60% in response to NMDA receptor-mediated Ca^{2+} influx but not that in response to Ca^{2+} channel activation (Sattler *et al.*, 1999). As mentioned earlier, the splice variants nNOSβ and nNOSγ identified in nNOS mutant mice fail to associate with NMDA receptors at synaptic membranes via PSD-95 as they lack the PDZ motif, rendering these nNOS isoforms cytosolic (Brenman *et al.*, 1996; Eliasson *et al.*, 1997). While nNOSγ has been shown to be catalytically inactive, nNOSβ has been found to retain catalytic activity when purified (Brenman *et al.*, 1996). Moreover, *in vivo* examination of nNOS activity by visualising citrulline-immunoreactivity in brain sections obtained from mice with disrupted nNOSα revealed the presence of active nNOS, although the type of the splice variant responsible (nNOSβ or γ) was not identified (Eliasson *et al.*, 1997). Overall, this indicates that cytosolic nNOS may be activated by Ca^{2+} coming from entry sources other than NMDA receptors.

eNOS

In contrast to nNOS, eNOS expression is restricted to the vascular endothelium. Although initially reported to localise in hippocampal pyramidal neurons (Dinerman *et al.*, 1994), the same group could not confirm their finding, detecting eNOS mRNA exclusively in brain blood vessels (Demas *et al.*, 1999), and attributing their earlier observations to poor antibody specificity arising from possible cross-reactivity of the antibody with other forms of NOS. The exclusive presence of eNOS in endothelial cells lining the brain vasculature, but lacking in neurons or glia, was confirmed by other independent *in situ* hybridisation studies in both mouse and rat brain (Seidel *et al.*, 1997; Blackshaw *et al.*, 2003), immunocytochemical studies at the light- and electronmicroscopic level (Stanarius *et al.*, 1997; Topel *et al.*, 1998), and single-cell PCR investigations of eNOS mRNA in single hippocampal neurons (Chiang *et al.*, 1994). The cell-specific expression of eNOS was later suggested to be down to DNA methylation, finding cell-specific methylation patterns *in vivo* in endothelial cells and vascular smooth muscle cells of mouse aorta, and robust expression of eNOS mRNA in non-endothelial cell types upon inhibition of DNA methyltransferase activity (Chan *et al.*, 2004).

At the subcellular level, eNOS is localised to the cell membrane. The N-terminal region of eNOS contains consensus sequences for irreversible myristoylation and reversible palmitoylation (Shaul, 2002). These modifications associate eNOS with caveolae in plasma membranes, localising the enzyme to sites of Ca^{2+} entry. While both myristoylation and palmitoylation firmly anchor eNOS to the caveolar lipid bilayer, reversible palmitoylation is thought to be involved in dynamic regulation of eNOS activity. Prolonged stimulation of eNOS has been shown to induce depalmitoylation with resultant translocation of eNOS to the cytosol, a process suggested to serve as an additional mechanism for modulating eNOS activity (Michel *et al.*, 1997).

Physiologically, NO produced from endothelial cells, contributes to the maintenance of cerebral blood flow via the regulation of small artery and arteriolar tone (Umans & Levi, 1995). The smallest vessels penetrating the brain are the capillaries, the

capillary endothelial cells releasing NO tonically (Mitchell & Tyml, 1996). While it has been a relatively old concept that neuronal-derived NO can influence the vasculature, emerging evidence suggests that NO from eNOS in blood vessels could also influence neurons directly. Previously, it has been found that application of NMDA to rabbit brain *in vivo* produces dilatation of the cerebral microcirculation and results in an increase in blood flow, which could be prevented by the Na^+ channel blocker tetrodotoxin (TTX), a NMDA receptor antagonist, and by nNOS-selective inhibition (Faraci & Breese, 1993; Faraci & Brian, 1995). This led to the implication that NO released from neurons can signal to the vasculature. On the other hand, at least *in vitro*, it appears now that NO derived from blood vessels may also influence neuronal function. Vascular-derived NO has been found to modify the membrane potential of rat optic nerve axons (Garthwaite *et al.*, 2006) and the capacity for synaptic plasticity in the hippocampus (Hopper & Garthwaite, 2006).

1.2.6 The NO signal

The physico-chemical properties of NO distinguish it markedly from conventional signalling molecules such as neurotransmitters. Being a small non-polar molecule, NO is highly diffusible in both lipid and aqueous environments. Therefore, it can readily cross cell membranes without the need of specialised release mechanisms, thereby accessing all cell compartments unhindered. An extra, unpaired electron confers radical status upon NO. Nonetheless, NO is relatively stable at physiological concentrations, which are thought to be in the low nanomolar-to-picomolar range (Garthwaite *et al.*, 2005; Hall & Garthwaite, 2009). One or several simultaneous source(s) of NO, such as for example from the microvasculature and a presynaptic terminal, can influence neighbouring cells within milliseconds of NO production (Garthwaite, 2008). The potential area for signalling will contain a variety of brain constituents, including neurons (dendrites, somata, and axons), glia, and the vasculature. While the vasculature may be providing a tonic NO source, repeated activity of groups of neurons may generate a ‘cloud’ of NO. On the other hand, limited neuronal activity may result in a much more localised NO signal (Garthwaite, 2008). Taking a 400-nm-diameter postsynaptic density as an example, containing

NMDA receptors associated with nNOS molecules, maximal nNOS activity would result in an estimated 2 nM NO at its site of synthesis, reducing to 1 nM NO just on the other side of the synaptic cleft, and 0.25 nM at the periphery of the nerve terminal where it still would evoke approximately 0.4 μM cGMP (Garthwaite, 2008), enough to trigger cGMP-dependent phosphorylation (Mo *et al.*, 2004). While the concentration profile of NO based purely on its diffusion away from its source implies a high degree of synapse specificity, neighbouring structures close-by would also be penetrated by low NO concentrations (Garthwaite, 2008). Considering a tonic NO source, such as blood vessels, any point in the brain is at most a typical cell diameter (25 μm) away from a capillary (Pawlik *et al.*, 1981), the endothelial cells of which release NO tonically (Mitchell & Tyml, 1996), with the three-dimensional arrangement of the capillary system being as well suited for delivering NO globally to the tissue as it is for delivering oxygen (Garthwaite, 2008).

Recently, it has been proposed that, in addition to the rate and pattern of NO synthesis, active NO inactivation may also be important in shaping the NO signal under conditions of multiple-source-NO synthesis (Hall & Garthwaite, 2006). Brain tissue actively consumes NO, limiting its half-life at physiological concentrations to an estimated 10-millisecond timescale (Hall & Garthwaite, 2006). A high rate of NO inactivation was also indicated by the pattern of cGMP immunostaining of sections from 400 μm brain slices exposed to different NO concentrations, finding a marked gradient. It was revealed that at intermediate bath concentrations of NO (around 100 nM) the edges of the slice appeared cGMP-positive, while the centre did not, indicating that NO failed to access this region in active concentrations. Mechanistically, NO consumption was found to be independent of other putative routes for NO inactivation, such as NO reacting with oxygen. A novel mechanism for shaping the NO signal when several sources are active has been uncovered and found to take place in brain slices, but the identity of this mechanism remains to be elucidated. Recent evidence points to a possible involvement of cytochrome P450 oxidoreductase (Hall *et al.*, 2009).

1.2 NO SIGNAL TRANSDUCTION

1.3.1 The NO_{GC} receptor

The key component for translating NO signals into biological messages is the soluble guanylyl cyclase (sGC), and to date it is the only well-established physiological signal transduction partner for NO. Subsequent to observations in the late 1960s of cGMP-forming activity being present in mammalian tissues, early work during the 1970s established sGC as the principal transducer of NO signals, preceding the identification of NO as a biologically important messenger molecule. Shortly after the purification of sGC from bovine lung, it was found that NO stimulates sGC activity and increases cGMP levels in slices from rat cerebral cortex and cerebellum (Kimura *et al.*, 1975). This line of enquiry was crucial for building the hypothesis that EDRF was NO, as the smooth muscle relaxation evoked by EDRF was observed to be associated with cGMP formation. The enzyme became initially known as sGC as it was detected in the soluble fraction of tissue homogenates. However, based on the present knowledge that sGC can also localise to membranes (see below), and it bearing attributes such as the presence of a ligand-binding site for NO and a transduction unit, it is preferable to refer to it as the guanylyl cyclase-coupled NO (NO_{GC}) receptor (Bellamy & Garthwaite, 2002). In a nutshell, activation of the NO_{GC} receptor by NO initiates a conformational change, which is translated into the fast conversion of GTP to cGMP. This event, as well as structural aspects of the NO_{GC} receptor, its pharmacology, and its prevalence in the brain will be outlined in more detail in the following section.

General Features

The NO_{GC} receptor has the capacity to capture and communicate very low-level NO signals, even when the latter are very transient. The known complement at present is two α subunits (α_1 and α_2) and two β subunits (β_1 and β_2). The active enzyme exists as a heterodimer of one α and one β subunit, the $\alpha_1\beta_1$ heterodimer being the one initially purified from bovine lung (Russwurm & Koesling, 2002). Currently, there are

two known isoforms of the NO_{GC} receptor, namely $\alpha_1\beta_1$ and $\alpha_2\beta_1$, both of which have been detected at the protein level with widespread tissue distribution, and shown to be enzymatically active in response to NO (Russwurm & Koesling, 2002). Both isoforms share similar kinetic properties with an estimated EC_{50} value of 10 nM for NO under steady-state conditions in cells (Garthwaite, 2005). Conflicting results exist concerning the functioning of heterodimers consisting of a β_2 subunit rather than the β_1 subunit. One study reported that $\alpha_1\beta_2$ dimers have a reduced (30%) activity relative to the $\alpha_1\beta_1$ form of the enzyme when expressed in cells (Gupta *et al.*, 1997). However, this observation could not be reproduced to date, and no line of enquiry has shown so far that the β_2-protein exists physiologically (Koesling, 1999; Russwurm & Koesling, 2002; Gibb *et al.*, 2003).

The primary structure of the NO_{GC} receptor consists of a C-terminal catalytic domain, a dimerisation domain, and a N-terminal regulatory haem-binding domain *(Fig. 1.3)*. Stimulation of the receptor by NO requires the presence of intact N-terminal regions from both subunits, as it is this part of the enzyme that is responsible for the incorporation of the ligand-binding site into the receptor (Wedel *et al.*, 1994; Foerster *et al.*, 1996). The β_2 subunit lacks the initial 63 amino acids of the N-terminal region relative to residues of the β_1 subunit (Koesling, 1999), and deletion of this string of amino acids from β_1 leads to the formation of an inactive $\alpha_1\beta_1$ heterodimer as a result of its inability to incorporate the haem moiety (Foerster *et al.*, 1996).

The ligand-binding site for NO is a specialised haem moiety (Bellamy & Garthwaite, 2002), which could potentially be targeted by other haemprotein ligands that are present in the environment the NO_{GC} receptors function in, such as oxygen and carbon monoxide. However, it has been established that the haem moiety of the NO_{GC} receptor selectively binds NO, rigorously excluding both oxygen and carbon monoxide (Martin *et al.*, 2006), allowing NO to associate and dissociate freely without oxidising the haem iron and forming nitrate as occurs in the course of the NO-oxyhaemoglobin interaction. Detailed structure-function studies are still being awaited in order to identify the determinants responsible for this high ligand-selectivity. Furthermore, among the different redox forms of NO ($NO^{\bullet}$, NO^{-}, and

NO^+), only the uncharged NO radical ($NO^\bullet$) has been shown to significantly activate the NO_{GC} receptor (Dierks & Burstyn, 1996). Moreover, NO can bind to other haem-containing proteins such as haemoglobin. The capacity of haemoglobin to bind and inactivate NO has been known for long, in fact before NO was recognised as a biological molecule, and has also been crucial in posing and testing the hypothesis of NO being a biological messenger. For instance, early studies demonstrated that the endothelium-dependent ACh-evoked relaxation of rabbit aortic rings and the associated rise in cGMP could be prevented by haemoglobin (Martin *et al.*, 1985a), which was subsequently demonstrated to also occur upon exposure to another ferrous haemprotein, namely myoglobin (Martin *et al.*, 1985b). However, the binding of NO to most haem groups is extremely tight, taking hours or even days for it to dissociate. This feature alone would immediately disqualify NO from being a viable dynamic signalling molecule. On the contrary, however, despite the NO_{GC} receptor having a high affinity for NO (K_D ~ 20 nM; Garthwaite, 2005), the binding of NO to the purified haem of its receptor is a readily reversible process, with the rate of dissociation being 0.04 s^{-1}. This allows the cyclase to switch off with a half-life of 2-5 sec under physiological conditions upon removal of NO (Kharitonov *et al.*, 1997). While this applies to NO interacting with its purified receptor, in cells the rate of deactivation is even faster, being on a 100-millisecond timescale. Albeit at the expense of lowered NO sensitivity, this important attribute of NO-receptor interaction allows the NO_{GC} receptor to respond to brief NO transients more faithfully, providing a system that detects NO with high sensitivity and allows efficient NO signal transduction (Garthwaite, 2005).

The prevailing model for NO_{GC} receptor activation and its structure are summarised in *Fig. 1.3*. As aforementioned, the NO_{GC} receptor exists as a heterodimer comprising α and β subunits, ultimately forming the transduction unit the haem moiety is attached to. Each heterodimer incorporates a single haem moiety, with the haem binding site located in the β_1 subunit, where a histidine residue (his-105) forms a covalent link to the Fe^{2+} centre of the haem group (Wedel *et al.*, 1994). A pivotal requisite for enzyme activity is the concurrence of both subunits and the haem group. Homodimers of the

receptor could be formed in transfected cells, but were inactive (Zabel *et al.*, 1998). Additionally demonstrating the requisite of both complementary subunits were results from experiments showing that transfection of different population of cells with α or β subunits individually did not generate enzyme activity (Harteneck *et al.*, 1990). Moreover, change of the his-105 residue to a phenyl in the β_1 subunit resulted in a receptor species insensitive to NO, which was found to be because of failure of the haem to attach to the enzyme (Wedel *et al.*, 1994).

There are three phases in the NO-receptor interaction *(Fig. 1.3)*, each involving the formation of a distinct haem species. This was studied by monitoring the characteristic absorbance spectra for each species, the absorbance maximum (known as the Soret band) shifting as the receptor moves through the binding and activation steps upon NO challenge (Zhao *et al.*, 1999; Friebe & Koesling, 2003). Activation of the NO_{GC} receptor commences with the binding of NO to the vacant co-ordination site on the haem moiety, which is an extremely rapid event that is nearly diffusion-limited (Zhao *et al.*, 1999). Additionally, the rate of association of NO with its receptor was reported to accelerate with increasing temperatures, while the time for NO to dissociate slows down (Zhao *et al.*, 1999). Upon binding of NO to the haem group, within a millisecond-timescale a 6-coordinate nitrosyl-haem complex is formed first as an intermediate, which is followed by snapping of the bond between the haem-Fe^{2+} and the his-105 residue, leading to the formation of a 5-coordinate species (Zhao *et al.*, 1999). This bond cleavage causes a conformational change, thought to be the rate-limiting step for activation, which propagates to the catalytic domain of the enzyme, accelerating the conversion of GTP to cGMP by up to 1000-fold probably by supporting access of GTP to the catalytic site (Garthwaite, 2005; Roy *et al.*, 2008). The conversion of GTP to cGMP in the cyclase domain of the receptor is a simple displacement reaction constituting no covalent intermediate but an inversion of the GTP configuration at the proximal phosphate of GTP, followed by direct displacement of pyrophosphate by a 3'-hydroxyl group leading to the formation of cGMP (Senter *et al.*, 1983).

Catalysis of GTP to cGMP also requires a number of substrate co-factors. The divalent cation Mg^{2+} is suggested to be a necessity to facilitate the binding of GTP, while binding of Ca^{2+} to two negative allosteric sites results in inhibition of the NO_{GC}

receptor (Kazerounian *et al.*, 2002). Although both subunits that are partnered to form the receptor contribute to the catalytic domain, there is only one single active site NO binds to (Bellamy *et al.*, 2002a; Roy & Garthwaite, 2006). A second 'pseudosymmetric' site may have a regulatory function. ATP is an allosteric inhibitor of the NO_{GC} receptor. This has been postulated to be via ATP competing with GTP for binding at a regulatory site preferring ATP to GTP (Ruiz-Stewart *et al.*, 2004), which may be the 'pseudosymmetric' site (Roy *et al.*, 2008). Another factor suggested to inhibit the NO_{GC} receptor involves the cGMP-dependent kinase (PKG), which is among the major downstream effectors for cGMP (see later). It has been demonstrated in smooth muscle cells that NO induces PKG-dependent phosphorylation of NO_{GC} receptors, inhibiting enzyme activity and cGMP formation (Murthy, 2004). In this way, cGMP appears to provide its own production with a negative feedback mechanism.

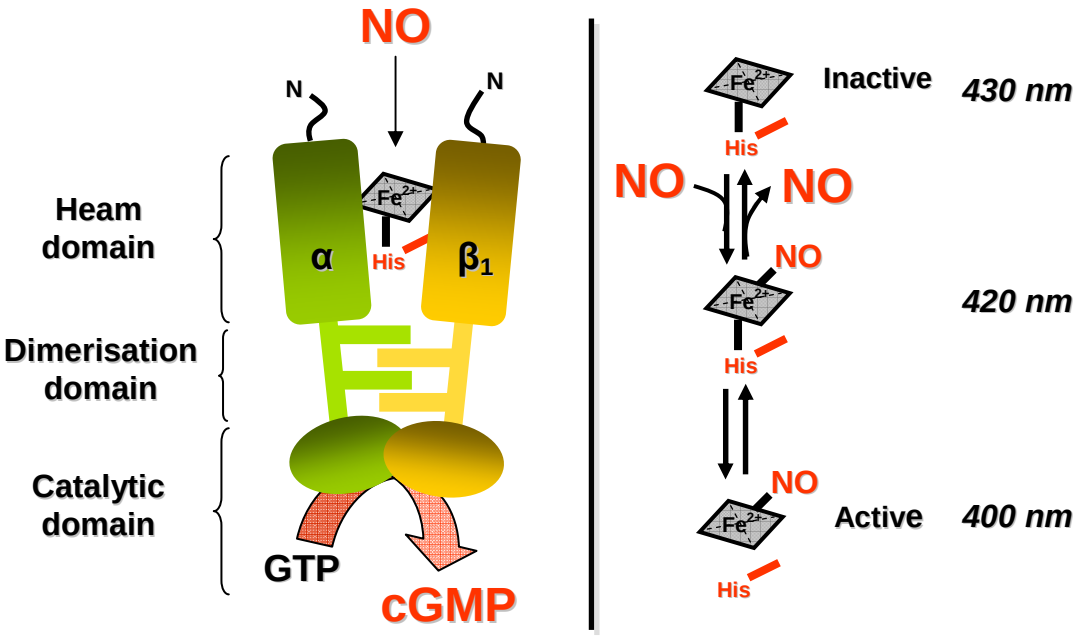

Fig. 1.3 Activation of the NO_{GC} receptor. The resting inactive state of the receptor exists with the Fe^{2+} centre of the haem moiety bound by his-105 of the β_1 subunit (absorption maximum ~ 430 nm). Upon binding of NO, a 6-coordinated haem is formed (absorption maximum ~ 420 nm), followed by cleavage of the proximal histidine bond leading to the formation of a 5-coordinate nitrosyl haem (absorption maximum ~ 400 nm), and a conformational change, which is propagated to the catalytic site. *Adapted from Bellamy & Garthwaite, 2002*

Pharmacology of the NO_{GC} receptor

Inhibition of the NO_{GC} receptor:

The most widely used inhibitor of the NO_{GC} receptor, and certainly the most selective one, is the compound ODQ. This compound has been well characterised in terms of its potency, selectivity, and mechanism of action, and is an invaluable tool in differentiating cGMP-mediated from cGMP-independent effects of NO. ODQ has been shown to inhibit cGMP formation in intact brain slices in response to NMDA receptor stimulation or exogenous NO with similar potency (IC_{50} ~ 20 nM), with no effect on NOS in the relevant concentration range for NO_{GC} receptor inhibition, and no effect on the other type of guanylyl cyclase, leaving atrial natriuretic peptide (ANP)-evoked cGMP accumulation in endothelial cells intact (Garthwaite *et al.*, 1995). Moreover, probing the inhibitory action of ODQ on purified enzyme revealed that inhibition occurred non-competitively with respect to the substrate GTP (Garthwaite *et al.*, 1995). ODQ has been shown to work at the haem moiety of the NO_{GC} receptor, incubation periods of several minutes (half-time ~ 3 min) leading to irreversible inhibition of purified enzyme as a result of oxidation of the ferric centre of the haem group from Fe^{2+} to Fe^{3+} as evaluated by spectroscopic measurements finding a characteristic Soret peak shift (Schrammel *et al.*, 1996). Non-specific effects of ODQ have been reported, finding inhibition of other haem-containing proteins, including NOS (Feelisch *et al.*, 1999). However, non-specificity of ODQ is observed only at much higher concentrations (> 30 μM) than those required for maximal inhibition of the NO_{GC} receptor. A benchmark concentration of 10 μM ODQ to be used to selectively inhibit NO-cGMP-mediated effects applies accordingly.

In the past other inhibitors had been presented as selective NO_{GC} receptor antagonists, which are spuriously still used sometimes nowadays. These include methylene blue and LY83583. They are very poorly selective compounds, both being known to compromise NOS activity (Mayer *et al.*, 1993; Luo *et al.*, 1995) and, in the case of methylene blue, to also generate superoxide anions which react rapidly with NO, thereby inactivating NO (Wolin *et al.*, 1990). Also to mention is that there have been

reports of LY83583 blocking neuronal cyclic nucleotide-gated ion channels in the same concentration range (1-10 µM) required for compromising 50% of NO_{GC} receptor activity *in vitro* (Leinders-Zufall & Zufall, 1995). These non-selective effects make data interpretation difficult, and these compounds should not be used to evaluate NO-cGMP-mediated effects.

NO donors:

A number of compounds can be used to stimulate NO_{GC} receptor activity independently of NOS-generated NO, evoking an increase in cGMP levels. Originally, these comprised the so-called nitrovasodilators, including nitroglycerin and sodium nitroprusside (SNP; Katsuki *et al.*, 1977). The essential trouble with these compounds, however, includes that they do not directly release authentic NO, often necessitating metabolism by cellular proteins, and often produce other NO-derivatives (Feelisch, 1993). For instance, SNP can generate NO^+ and NO^- additionally to $NO^\bullet$, as well as cyanide ions, and its decomposition depends on light and thiols. Equally troublesome compounds include SIN-1, SNAP, and GSNO. SIN-1 releases superoxide (O_2^-) alongside NO, thereby generating peroxynitrite ($ONOO^-$), the latter being a highly oxidising species that has a plethora of toxic effects on cells ranging from irreversible respiratory inhibition to DNA damage. SNAP and GSNO are S-nitrosothiols, also generating the other two redox forms of NO, and their decomposition also being light-sensitive and dependent on the presence of thiols and transition metals (Feelisch, 1998). The general consensus is that the interpretation of results achieved through the use of these NO-releasing compounds is complicated and they should not be used. Unfortunately, however, many of them are still used to the present day, often at very high concentrations.

The pharmacological solution to the problems associated with earlier compounds came with the development of the so-called NONOates (Morley & Keefer, 1993; Feelisch, 1998). These compounds are invaluable tools to study the actions of NO as they deliver authentic NO to tissues. These compounds are a series of nucleophile/NO adducts, which are synthesised by exposing a nucleophile in solution to NO gas, and

contain a characteristic [N(O)NO$^-$] functional group. The essential advantages offered by NONOates include stability when they are in solid form, and spontaneous decomposition in aqueous solution, releasing authentic NO with a stoichiometry of 1-2 mol NO per mol NONOate. Moreover, decomposition of these compounds is exclusively governed by temperature, pH, and the identity of the nucleophile precursor, so that addition of a NONOate compound to a solution at physiological temperature and pH will result in the release of authentic NO with predictable kinetics which will further only depend on the NO donor concentration and half-life.

A series of NONOates have been produced and are commercially available, with the half-life of degradation ranging from only a couple of seconds to 24 hours. Which NO donor with what half-life should be chosen, will depend on the nature of the experiment and the desired NO release profile. In parallel to this, once a compound has been chosen with a particular half-life, it is important to select the application time sensibly, especially when working with one that has a relatively short half-life. The meaning of this can be illustrated well with the following example extracted from findings by Bellamy *et al.* (2002b). Experiments on purified NO_{GC} receptors demonstrated that the concentration of NO produced by 0.3 μM of the NONOate DEA/NO ($t_{1/2}$ = 2.1 min under physiological conditions) peaks at 50 nM after 2 min and then falls below detection limit after 5-6 min. The rate at which cGMP was accumulating was found to occur maximally for 3-4 min after NO exposure, followed by the rate rapidly falling to zero after approximately 6 min when NO fell below 20 nM and eventually disappeared. These results exemplify that it is important to measure the response under investigation at the appropriate time points when NO is still present at active concentrations.

Allosteric enhancers of NO_{GC} receptors:

A number of compounds have been developed that act as allosteric enhancers, sensitising the NO_{GC} receptor towards NO. These pharmacological tools are particularly useful when measuring the cGMP output corresponding to very low (picomolar) NO concentrations.

The first compound earning recognition as an allosteric enhancer of NO_{GC} receptor activity was YC-1. This compound was initially found to cause platelet disaggregation independently of NO by activating NO_{GC} receptors with ensuing cGMP formation (Wu *et al.*, 1995). Later it was revealed that YC-1 inhibits thrombosis in mice *in vivo* (Teng *et al.*, 1997). The novelties of this compound emerged to be that it increased the catalytic efficiency of the NO_{GC} receptor alongside increasing the potency of NO for its receptor by interacting with an allosteric site to slow the rate at which NO dissociates from its binding site, thereby stabilising the NO_{GC} receptor in its active form (Friebe & Koesling, 1998; Mayer & Koesling, 2001). The finding that YC-1 did not cause the characteristic shift in the Soret absorption band indicated that this compound was acting not at the haem moiety like NO, but was binding to a distinct site (Friebe & Koesling, 1998). Consequently, YC-1 became known as an 'allosteric' activator of NO_{GC} receptors. The synergistic effect of YC-1 with NO made it unclear whether the previously observed NO-independent effects are real, or the result of YC-1 synergising with trace levels of environmental NO (Friebe *et al.*, 1996a), or, in the case of a tissue sample, basal NO levels. Also, stimulation of NO_{GC} receptors by YC-1 required the presence of the haem moiety (Friebe *et al.*, 1996b). Later down the line, complications started to transpire with YC-1 based on a number of non-selective effects. YC-1 has been shown to inhibit a range of phosphodiesterases (PDEs; see below), making the aspirations of unravelling the characteristics of the NO_{GC} receptor by means of this compound difficult (Friebe *et al.*, 1998). Additionally, the reported inhibitory effect of YC-1 on K^+ channels (at concentrations lower than required for NO_{GC} receptor stimulation; Wu *et al.*, 2000a), and Na^+ channels (Garthwaite *et al.*, 2002b) further complicates the use of YC-1 in intact tissues.

A different compound, also acting as an allosteric enhancer of NO_{GC} receptor activity, is available, namely BAY 41-2272. This compound has so far proven to be a 'cleaner' compound compared to its forerunner YC-1, and has been demonstrated to reduce blood pressure in hypertensive rats *in vivo* when administered orally, increasing the survival rate in a low-NO rat model of hypertension (Stasch *et al.*, 2001). Analogous to YC-1, BAY 41-2272 is proposed to stimulate enzyme activity independently of NO, but dependently on the presence of the haem moiety in the NO_{GC} receptor (Straub *et al.*, 2001; Stasch *et al.*, 2001). Moreover, like YC-1, the

binding of BAY 41-2272 fails to initiate a Soret band change, indicative of it binding to a site distinct from the NO binding site (Stasch *et al.*, 2001). Although reported to affect PDE activity like YC-1, BAY 41-2272 is approximately two orders of magnitude more potent than YC-1 (nanomolar *versus* micromolar respectively), with no inhibitory effect on PDE appearing at concentrations of up to 10 μM (Stasch *et al.*, 2001; Mullershausen *et al.*, 2004a). Photoaffinity labelling studies have proposed the binding site for BAY 41-2272 (and YC-1) to be in the N-terminal region of the α_1 subunit of the receptor, being in close proximity to two cysteine residues (Cys-238 and Cys-243; Stasch *et al.*, 2001; Becker *et al.*, 2001).

A recent study has provided more insights concerning the alleged NO-independent modulation of enzyme activity by allosteric NO_{GC} receptor enhancers (Roy *et al.*, 2008). As aforementioned, these compounds are thought to act in a NO-independent manner based on findings that they have residual activity even in the absence of added NO or in the presence of NO scavengers such as haemoglobin. New data now suggests that when BAY 41-2272 is applied at saturating concentrations, the potency of NO for its receptor becomes astonishingly high (EC_{50} ~ 4 pM) so that trace environmental NO levels would be enough to significantly enhance enzyme activity (Friebe *et al.*, 1996a; Roy *et al.*, 2008). Additionally, it was found that the allosteric site that binds BAY 41-2272 (or YC-1) may be the same site that binds ATP, the latter, as mentioned earlier, acting as an allosteric inhibitor of enzyme activity. This was derived from the observation that BAY 41-2272 prevents ATP-mediated inhibition of NO_{GC} receptors (Roy *et al.*, 2008).

Localisation of the NO_{GC} receptor in the brain

The NO_{GC} receptor has been visualised in the brain both at its mRNA and protein level, with both isoforms of the receptor being present, albeit with uneven distribution. Some areas show more abundant $\alpha_1\beta_1$, while others express $\alpha_2\beta_1$ more prominently. For instance, the α_2 and β_1 subunits were shown to be particularly notable in the cerebellum and the hippocampus, with comparably weaker levels appearing for the α_1 subunit, while other areas such as the caudate putamen and

nucleus accumbens appeared rich in α_1 and β_1 but relatively poor in α_2 (Gibb & Garthwaite, 2001). Overall, however, while the predominating isoform in other tissues is the $\alpha_1\beta_1$ heterodimer, the highest occurrence of the $\alpha_2\beta_1$ isoform is found in the brain, with levels comparable to those of $\alpha_1\beta_1$ as judged by the β_1 subunit being present at twice as much as the two α subunits (Mergia *et al.*, 2003). While the $\alpha_1\beta_1$ isoform is mostly cytosolic, a special attribute of the $\alpha_2\beta_1$ isoform is its ability to interact with the third PDZ domain of PSD-95 *in vivo* (Russwurm *et al.*, 2001), NO_{GC} receptors having indeed been found to associate with nNOS at subpopulations of dendritic spines in the hippocampus (Burette *et al.*, 2002). Also presynaptically in the hippocampus, some axon terminals appear to co-localise nNOS, NO_{GC} receptors, and the presynaptic protein synaptophysin (Burette *et al.*, 2002). Moreover, while overall there appear to be comparable levels of the two NO_{GC} receptor isoforms in the brain, the hippocampus (and also cerebellum) is an exception in that it displays much higher mRNA levels for α_2 than α_1 (Gibb & Garthwaite, 2001; Mergia *et al.*, 2003). While previously it had been shown that the receptor for NO also localises to pyramidal neurons, appearing as a 'ring-like' immunostaining in cell somata (Burette *et al.*, 2002), a recent study investigated the expression profile of the two different functional subunit compositions at high resolution, employing light- and electronmicroscopy, as well as mRNA analysis (Szabadits *et al.*, 2007). Szabadits and her colleagues demonstrated that, at least in the hippocampus, the α_1 subunit is restricted to a large number of GABAergic interneurons, being detectable in axon terminals that establish synaptic contacts on somata, dendrites, and axon initial segments. On the contrary, the α_2 subunit was detected only in pyramidal neurons, while the β_1 subunit was visualised both in interneurons and pyramidal neurons. The authors speculated that the absence of α_2 subunits in interneurons might ensure that these neurons do not target the NO_{GC} receptor to their afferent excitatory inputs.

The relationship between neuronal NO sources and targets:

Establishment of the relationship between endogenous NO synthesis and its sites of action allows insights into the functioning of NO and its effector cGMP as a signal

transduction pathway, and is also revealing concerning the status of NO as an intercellular signalling molecule. This is generally achieved by comparing the distribution of NOS with that of the NO_{GC} receptor. An atlas for the expression profile of NO_{GC} receptors in parallel to a map of NOS localisation has been provided by means of immunohistochemistry and NADPH diaphorase histochemistry respectively in rat brain obtained from animals that had been perfused with an NO donor (Southam & Garthwaite, 1993). A good match between the presence of NO_{GC} receptors and cGMP formation is apparent in various brain regions, and the general consensus is that both proteins, NOS and the NO_{GC} receptor, are functionally expressed in close proximity, with the localisation of NO_{GC} receptors appearing complementary to that of nNOS. Hence, the direction of signalling by NO in different neuronal circuits can be either retrograde or anterograde as it can be synthesised presynaptically in axon terminals or postsynaptically in dendrites, accessing its pre- or postsynaptic receptors. For instance, a comparatively small number of NOS-positive multipolar neurons radiate throughout neocortical layers 2-6, while NO-stimulated cGMP accumulation is seen in nearly all neurons in these layers (Southam & Garthwaite, 1993). In the cerebellum, prominent NOS staining is apparent throughout the neuropil of the molecular layer containing the granule cell axons, while the downstream Purkinje cells lack nNOS (Vincent & Kimura, 1992), but express NO_{GC} receptors (Ariano *et al.*, 1982). This juxtaposition of source and target has also been demonstrated at the synaptic level (Burette *et al.*, 2002; Szabadits *et al.*, 2007), finding a good match where the expression of nNOS and NO_{GC} receptors on the two sides of the synapse coincide (i.e. NOS-positive postsynaptic densities are usually apposed to NO_{GC} receptor-bearing presynaptic axon terminals). Additionally, as outlined above, the $\alpha_2\beta_1$ isoform of the NO_{GC} receptor is, via interaction with PSD-95, able to localise to postsynaptic membranes where nNOS is, and co-localisation of nNOS and the NO_{GC} receptor has also been observed presynaptically (Burette *et al.*, 2002). This expression profile would place the NO_{GC} receptor in a convenient position for the transduction of localised nNOS-derived NO signals. Another feature to mention is that a rich expression of nNOS, appearing as a mesh of fibres radiating throughout a particular brain region, may correspond to fibres forming synapses and releasing NO elsewhere. For instance, a lack of cGMP staining was found around the distinctly nNOS-positive

neurons in the pedunculopontine tegmental nucleus of the brainstem, while clear cGMP-staining was apparent in the thalamus whereto these nNOS-positive neurons project (Southam & Garthwaite, 1993). This notion is in line with all grey matter regions that accumulate cGMP also containing nNOS (Southam & Garthwaite, 1993).

Overall, the remarkable coincidence of NOS and the NO_{GC} receptors also emphasises very well the 'major target-status' of the NO_{GC} receptor for NO throughout the brain.

1.3.2 Other NO signal transduction routes

S-Nitrosation

One route for NO signal transduction, which is independent of NO_{GC} receptor activation, and has been perceived to be important, is the chemical modification of protein function by the transfer of the NO moiety to protein thiol (-SH) groups (Stamler *et al.*, 2001), a process now termed S-nitrosation (Koppenol, 2002). Within the brain, modification of NMDA receptors has been reported to occur via S-nitrosation of cysteine residues, resulting in down-regulation of NMDA receptors, NO being claimed to act in this way as a feedback regulator of NMDA function (Stamler *et al.*, 2001; Lipton *et al.*, 2002). Overall, however, a role for S-nitrosation in physiological NO signalling is highly controversial.

The chemical reactivity of NO is such that it is not able to simply associate with thiols directly in a reversible manner. Formation of a S-nitrosothiol first requires the formation of an oxidised species of NO such as NO^+ or N_2O_3 to proceed. A direct reaction of NO with thiols would produce a thiol disulphide (not a nitrosothiol), and NO from S-nitrosothiols is not released spontaneously. Additionally, the sulphur and the nitrogen in a S-nitrosothiol interact by forming a stable covalent link, which is not particularly susceptible to bond breakage, unless when exposed to strong irradiation (Hogg, 2002). Recently, it has been demonstrated that NMDA receptor inhibition via S-nitrosation is a consequence of concomitant exposure to UV light and high, non-physiological NO concentrations, indicative of artefactual generation of a nitrosating species such as NO^+ (Hopper *et al.*, 2004). While high NO concentrations or UV light

alone had no significant effect on NMDA receptor activity, pairing of the two factors resulted in irreversible depression of NMDA receptor-mediated fEPSPs in hippocampal slices, as well as depression of NMDA receptor-mediated currents in HEK cells expressing NMDA receptors. Based on the doubtful physiological relevance of NO-mediated S-nitrosation of proteins, this matter will not be further considered here.

Cytochrome c oxidase

Another potential physiological target for NO has previously been suggested to be the cytochrome c oxidase of mitochondria. Previously, it has been postulated that NO-mediated inhibition of cytochrome c oxidase is a physiologically relevant scenario in which NO presumably regulates cellular oxygen consumption by competing with oxygen for binding, thereby regulating the affinity of mitochondrial respiration for oxygen (Brown, 1995). However, following extensive revision, the physiological concentration of NO has been revealed to be in the low-nanomolar to picomolar range, most likely not exceeding 10 nM (Garthwaite, 2005; Hall & Garthwaite, 2009). Studies in cerebellar cells estimated an IC_{50} value for NO-mediated cytochrome c oxidase inhibition of approximately 120 nM at physiological (30 μM) oxygen and steady-state NO delivery (Bellamy *et al.*, 2002b). Additionally, it was found that, in order for NO (at concentrations that would maximally engage the NO_{GC} receptor) to cause 50% inhibition of cellular respiration, the oxygen concentration would have to fall to 5 μM, which is an oxygen level that would be pathological if it prevailed in the brain for more than a few seconds (Bellamy, *et al.*, 2002b). Moreover, very high concentrations of NO (~ 10 μM) had to be applied to organotypic hippocampal slices in order to kill them by respiratory inhibition (Keynes *et al.*, 2004). Also in the rat optic nerve preparation, only a relatively high NO concentration (approximately 100 nM) was found to kill axons, attributable to metabolic disruption with consequent ATP depletion and loss of ionic homeostasis (Garthwaite *et al.*, 2002a). Importantly, it has also been demonstrated that the NO_{GC} receptor is not saturated during maximal endogenous NO synthase activity, the endogenous NO concentration under maximal stimulating conditions rising to an apparent 4 nM in cerebellar brain slices (Bellamy

et al., 2002b), which is consistent with the *in vivo* situation in which cGMP rises to only a fraction of the maximally achievable levels even during abnormally elevated neuronal activity. Overall, since the interaction of NO with cytochrome c oxidase may only be relevant under pathological conditions, it will not be subjected to further consideration here.

1.3.3 The cGMP signal – desensitisation and PDEs

The major components regulating the cGMP profile known to date comprise a finely controlled balance between cGMP synthesis via NO_{GC} receptor activation and cGMP degradation combined with rapid NO_{GC} receptor desensitisation, the 'switch-on' and 'switch-off' of the receptor upon NO removal being a process occurring on a millisecond timescale. These features render NO_{GC} receptors highly effective in transducing NO signals into cGMP signals with good spatiotemporal fidelity, enabling diverse patterns of cGMP responses to NO to be generated by different cells in different subcellular domains. The receptor for NO can activate in response to very low NO concentrations (down to the low picomolar range), rapidly convert the NO signal into up to 1000-fold higher concentrations of cGMP within a second, and then cease activity within a second when NO production stops.

A crucial factor in shaping cGMP signals is the counterbalance to the rate of cGMP synthesis that is mainly provided by PDEs. These are enzymes termed phosphohydrolases which selectively catalyse the hydrolysis of cyclic nucleotides to the corresponding inactive non-cyclised monophosphate (i.e. 3',5'-cGMP to 5'-GMP) by degrading the 3' cyclic phosphate bond in the cyclic nucleotide molecule. There are currently 11 PDE families known in mammals, comprising 21 different gene products, with additional splice variants that may exhibit different tissue distributions and subcellular localisations contributing to further diversity. The isoenzymes operating in the CNS include PDE5 and 9, which are highly selective for cGMP, and subtypes 1, 2, 3, and 10, all of which hydrolyse both cGMP and cAMP (Bender & Beavo, 2006). Also PDE4 may be involved to some extent in cGMP degradation when cGMP levels rise to very high levels as has been demonstrated in cerebellar

astrocytes (Bellamy & Garthwaite, 2001b). The vast diversity of the types and properties of PDEs are in stark contrast to the relatively limited molecular heterogeneity of NOS and the NO_{GC} receptors. Judging from the level of diversity of PDEs, it is not surprising that these enzymes can provide the generation of many different cGMP signals which may differ in amplitude, duration, and localisation, where, depending on the 'pattern' of PDE expression in a given cell, differently featured cGMP signals may be at play in the same cell. The presence of two or more different PDEs in the same cell, albeit localising to different subcellular compartments, enable PDEs to generate and maintain cGMP-signalling compartments within the cell.

The dynamic nature of NO_{GC} receptors is highlighted by very fast activation (within 20 ms) and rapid deactivation (half-time of 200 ms) on addition and removal of NO respectively (Bellamy & Garthwaite, 2001a). This dynamic behaviour goes hand in hand with the NO_{GC} receptor also desensitising within seconds (or less) in intact cells upon NO exposure, as has been demonstrated in cerebellar astrocytes, human platelets, and striatal neurons, finding a marked decline in enzyme activity with time, recovering only slowly (half-time of 16 min) and being more pronounced at higher NO concentrations with an EC_{50} of 10-20 nM for NO to cause desensitisation (Bellamy *et al.*, 2000; Wykes *et al.*, 2002; Mo *et al.*, 2004; Halvey *et al.*, 2009). The molecular mechanism of NO_{GC} receptor desensitisation remains to be identified, although a number of observations have pointed to some unknown, possibly cGMP-regulated, cellular factor(s) being responsible rather than it being an intrinsic property of the NO_{GC} receptor (Bellamy et al., 2000; Wykes *et al.*, 2002). This latter notion was indicated by desensitisation of the N_{GC} receptor not taking place when in its purified form or when studied in lysed cells, which are conditions in which the factor would be absent or may be destroyed or diluted, rendering it inactive. An alternative explanation for the response decline involves PDE. It has been proposed that in platelets the 'sag' in the cGMP response with time upon NO exposures is associated with enhanced PDE5 activity due to PKG-mediated phosphorylation of the PDE, while the desensitisation observed in the presence of PDE inhibitors may be due to depletion of the substrate GTP (Mullershausen *et al.*, 2001; Mullershausen *et al.*,

2003). However, not consistent with these suggestions were the findings that desensitisation in cerebellar cells, which also express PDE5, is unaffected by large variations in GTP utilisation, and that the profile of cGMP accumulation remains unaltered upon inhibition of PKG or phosphatases (Bellamy *et al.*, 2000; Wykes *et al.*, 2002). Moreover, in rat platelets receptor desensitisation was found to occur over the entire range of PDE activities (i.e. PDE activity left intact down to up to 100-fold reduction in PDE activity), with 80% of the maximum activity of the NO_{GC} receptor being subject to desensitisation (Mo *et al.*, 2004). The general consensus at present is that there may be a number of different factors governing desensitisation, which may be different among different types of cells.

How the concerted working of PDEs and desensitisation could be instrumental to shaping the cGMP signal is well exemplified by the situation observed in cerebellar astrocytes and platelets. In cerebellar astrocytes, the combination of rapid desensitisation but very low PDE activity results in a large increase in cGMP accumulation and a long-lived plateau in response to NO (Bellamy *et al.*, 2000). On the contrary, rat platelets respond to NO with a very transient increase in cGMP (peaking within 2-5 sec) based in part on NO_{GC} receptor desensitisation and partially on PDE5 activation (Mo *et al.*, 2004; Halvey *et al.*, 2009). The desensitisation component has been found to predominate, with receptor desensitisation reverting very slowly with a half-time of 16 min, while PDE5 activity subsides much quicker upon NO removal with a half-time for recovery of 25 sec (Halvey *et al.*, 2009).

1.4 DOWNSTREAM EFFECTORS OF cGMP

1.4.1 cGMP-dependent kinase (PKG)

The cGMP-dependent protein kinase (cGK) or protein kinase G (PKG; as it will be referred to here) belongs to a family of Ser/Thr protein kinases, and is activated by submicromolar cGMP concentrations (Gamm *et al.*, 1995), converting cGMP elevations into changes of cellular function via phosphorylation of Ser- or Thr-

residues of a number of substrate proteins. In mammals there are two genes that encode PKG proteins, generating two isoforms, namely PKGII and PKGI, the latter comprising the two variants PKGIα and PKGIβ. The PKGI family are cytosolic proteins, while PKGII is anchored to the plasma membrane via myristoylation at its N-terminal glycine residue (Vaandrager *et al.*, 1996).

All PKG isoforms exist as homodimers, being composed of two identical monomers, each of which contains an N-terminal domain, a regulatory domain which contains two allosteric cGMP binding sites, and a C-terminal catalytic domain, the latter comprising binding sites for ATP and the target protein. The N-terminal region contains regulatory sites for dimerisation, auto-inhibition, auto-phosphorylation, and, in the case of PKGII, myristoylation (Lohmann *et al.*, 1997). Activation of PKG requires the occupation of both cGMP-binding sites to achieve full catalytic activity, where the binding of cGMP induces a conformational change, ultimately relieving the N-terminal auto-inhibition of the C-terminal catalytic centre (Gamm *et al.*, 1995; Wall *et al.*, 2003). Phosphorylation of the target protein involves the transfer of a phosphate group from ATP, which is bound in the C-terminal catalytic domain of PKG, to a Ser- or Thr-residue of the target protein. As already mentioned, the N-terminal region of PKG contains a number of regulatory sites, one of which is the auto-inhibitory site which is responsible for the inhibition of kinase activity in the absence of cGMP. Among the other N-terminal regulatory sites, one is important for the homodimerisation of the PKG subunits, while another allows auto-phosphorylation of this region, leading to more persistent kinase activity which can outlast the timeframe of the original stimulus (Lohmann *et al.*, 1997). For example, PKGIβ auto-phosphorylation causes a nearly 4-fold increase in basal kinase activity, and an approximately 2-fold decrease in the EC_{50} for cGMP-evoked phosphorylation of target proteins (Smith *et al.*, 1996). Although being very similar, the different PKG isoforms do differ in terms of substrate sensitivity, which is conferred by differences in their N-terminal domain. The PKGI isoforms are about 8-fold more sensitive to cGMP than PKGII, while the PKGIα isoform is approximately 10-fold more sensitive to cGMP activation than the PKGIβ isoform (Gamm *et al.*, 1995).

All PKG isoforms have been detected in the brain, with recent analysis of mRNA expression (Lein *et al.*, 2007) and immunohistochemical evaluation (El-Husseini *et al.*, 1999; Feil *et al.*, 2005) suggesting PKGI to be the predominant isoform. Regions in which the PKGI protein has been detected include cerebellar Purkinje cells, suprachiasmatic nucleus, hypothalamus, medulla, cerebral cortex, amygdala, olfactory bulb, the ganglion cell layer of the retina, and the hippocampus. Results from studies employing mRNA *in situ* hybridisation and immunoblotting with isoform-selective probes (Geiselhorniger *et al.*, 2004) or antibodies (Feil *et al.*, 2005) suggest that the PKGIα is the predominating isoform in the cerebellum and the medulla, while the PKGIβ isoform exists at high levels in the cortex, the olfactory bulb, the hypothalamus, and the hippocampus. Similar levels of the two PKGI variants appear to be present in the eye. The expression profile of PKGII has also been studied at the mRNA level, as well as protein level by means of immunohistochemistry and Western blot analysis. A line of such enquiries suggests that PKGII has a widespread distribution in the brain, with particular abundance in the cerebral cortex, the olfactory bulb, the thalamus, and the superior colliculi (El-Husseini *et al.*, 1999; de Vente *et al.*, 2001b).

The target proteins for the different PKG types as well as their discrete physiological involvement in PKG-mediated effects in the CNS remain largely unexplored. Among the proposed targets for PKGI is the protein phosphatase-1 inhibitor G-substrate, which has been shown by immunoprecipitation as well as mRNA- and peptide-mapping techniques to be concentrated in cerebellar Purkinje cells (Detre *et al.*, 1984; Endo *et al.*, 1999; Hall *et al.*, 1999), and is only detected at negligible levels in the cortex and hippocampus (Detre *et al.*, 1984). Another phosphatase inhibitor is DARPP-32, which shares homology with G-substrate, and has also been suggested to be a target for PKGI-mediated phosphorylation (Tsou *et al.*, 1993). Other proposed targets for PKGI-mediated phosphorylation include the PDE5 (see below), inositol 1,3,4-triphosphate (IP_3) receptors, which supports stimulation of Ca^{2+} release from IP_3-sensitive stores in the cerebellum and vascular smooth muscle (Haug *et al.*, 1999; Wagner *et al.*, 2003), the vasodilator-stimulated protein (VASP), which is implicated in vesicle trafficking and the regulation of the actin cytoskeleton (Butt *et al.*, 1994; Hauser *et al.*, 1999), and the small GTPase

RhoA, which is implicated in vesicle trafficking (Ellerbroek *et al.*, 2003). A target protein for PKGII has been suggested to be the GluRI subunit of AMPA receptors in the hippocampus (Serulle *et al.*, 2007; see later). Broadly, cGMP-PKG signalling has been implicated in a number of processes, including synaptic plasticity and learning, behaviour, development, and nociception (Schlossmann *et al.*, 2005).

1.4.2 cGMP-regulated PDEs

As mentioned earlier, some members of the vast PDE family degrade cGMP and thereby affect cellular responses by shaping cGMP signals derived from NO_{GC} receptor activity. However, the role of PDEs in cGMP signalling is more sophisticated than that as they also act as downstream effectors of cGMP. The activity of some PDE isoforms can be modulated negatively or positively by cGMP, either directly by cGMP binding to a regulatory domain of the PDE, or indirectly via cGMP mediating phosphorylation of the PDE. Additionally, cross-talk between cGMP and cAMP signalling cascades occurs by cGMP-dependent modulation of cAMP-preferring PDEs (and *vice versa*). Moreover, different outcomes of cGMP signals may prevail in different microdomains of a cell, which is achieved by PDEs being associated with different macromolecular complexes, which may comprise regulatory proteins, such as kinases, anchoring or scaffolding proteins, and other signalling proteins. This latter aspect is thought of as a key supporter of the specificity of cGMP effects in a particular tissue (Bender & Beavo, 2006). For ease, *Table 1.1* provides a summary of PDEs hydrolysing cGMP and/or being regulated by it, outlining the main features. The majority of PDEs exist as homodimers, being composed of a catalytic C-terminal domain and a regulatory N-terminal domain. The catalytic C-terminal domains are highly homologous among the different PDE families, whereas the N-terminal domain is the crucial feature that imparts unique functional fingerprints upon the different PDEs based on the incorporation of one or more regulatory segments (Bender & Beavo, 2006).

cGMP-specific PDEs

PDE5:

PDE5 is highly selective for cGMP *(Table 1.1)* and has the special feature of containing two so-called GAF domains (GAF-A and GAF-B) in the N-terminal region, additionally to the catalytic cGMP-binding domain. The name of this motif is based on the three classes of proteins in which it was identified, including c**G**MP-regulated PDEs, the cyanobacterial *Anabaena* **A**denylyl cyclase, and the *E. coli* transcription factor **F**h1A, hence '**GAF**'. In PDEs, these GAF domains are known to exclusively bind cGMP, and serve as non-catalytic allosteric sites (Martinez *et al.*, 2002). Apart from cGMP binding to the catalytic site of the enzyme, these small molecule-binding motifs also bind cGMP, usually one cGMP molecule per monomer. Binding of cGMP to the GAF-A motif in PDE5 (K_D ~ 40 nM), which is more than 100-fold more selective for cGMP than cAMP (Zoraghi *et al.*, 2005), activates the PDE and accelerates the rate of cGMP hydrolysis. This event of cGMP-GAF interaction also makes PDE5 a target for PKGI, where the PKG-mediated phosphorylation of PDE5-Ser-93 enhances the affinity of PDE5 for cGMP and the stimulatory effect of cGMP on the rate of hydrolysis further (Thomas *et al.*, 1990; Turko *et al.*, 1998; Mullershausen *et al.*, 2001; Rybalkin *et al.*, 2003; Mullershausen *et al.*, 2003; Shimizu-Albergine *et al.*, 2003; Mullershausen *et al.*, 2004b). In the brain, injection of cGMP analogues into mouse brain has been found to evoke PDE5 phosphorylation in cerebellar Purkinje neurons *in vivo*, which was observed to be missing in PKGI knockout animals (Shimizu-Albergine *et al.*, 2003). It has been suggested that phosphorylation of PDE5 induces a conformational change, which increases the affinity of the GAF-A domain for cGMP by approximately 10-fold, and consequently enhances the catalytic activity of PDE5 by nearly 2-fold (Corbin *et al.*, 2000; Francis *et al.*, 2002). Overall, this feature of PDE5 is thought to provide a negative regulatory mechanism whereby cGMP regulates its own accumulation negatively.

PDE 5 is characterised by being localised in the cytosol, and only one subform, the PDE5A, is known to exist to date, albeit with a number of possible variants. It became a famous PDE isoform upon being discovered to be a regulator of vascular smooth muscle contraction, and the target for the drug sildenafil (Viagra; Turko *et al.*, 1999; Bender & Beavo, 2006). As deduced from mRNA analysis and immunohistochemical results, PDE5 shows the most abundant expression in cerebellar Purkinje cells, but is also expressed in the spinal cord, and pyramidal cells of the hippocampus as well as granule cells of the dentate gyrus, while it shows only little or negligible expression levels in other brain areas (Kotera *et al.*, 1997; Kotera *et al.*, 2000; Giordano *et al.*, 2001; van Staveren *et al.*, 2003; Shimizu-Albergine *et al.*, 2003; Bender & Beavo 2004; van Staveren *et al.*, 2004; de Vente *et al.*, 2006).

PDE9:

The highest affinity to bind cGMP is imparted on PDE9, having by far the lowest K_m for cGMP, with its K_m for cAMP being more than 1000-fold greater, rendering this PDE isoform highly cGMP-selective *(Table 1.1)*. To date the only isoform recognised is PDE9A. However, as with PDE5A, also here a number of variants have been identified. Unlike PDE5, PDE9 does not contain GAF motifs. Overall, there is not much else known concerning the regulation of PDE9 (Bender & Beavo, 2006). The high affinity of PDE9 to bind cGMP would predict that cells expressing this PDE isoform maintain very low basal cGMP levels, implicating PDE9 to be an important constituent in cGMP signalling. In this respect it is interesting that the pattern of PDE9 mRNA expression in the brain appears to closely resemble that of NO_{GC} receptors, suggesting a potential functional association or coupling of these two constituents in regulating cGMP levels (Andreeva *et al.*, 2001). To tailgate this latter aspect, the distribution pattern of PDE9 in the brain appears to be widespread, having been detected in neurons of the dentate gyrus as well as pyramidal cells of the hippocampus, and various other regions of the brain including the cerebellum (in Purkinje cells), olfactory system, neocortex, thalamus, and basal ganglia, with the highest mRNA expression levels detected in the dentate gyrus, olfactory bulb, and Purkinje neurons (Andreeva *et al.*, 2001; van Staveren *et al.*, 2002; van Staveren *et*

al., 2003; van Staveren *et al.*, 2004). Overall, PDE9 is thought to be predominantly a neuronal PDE, but its presence has also been postulated in astrocytes (van Staveren *et al.*, 2002). PDE9 enzymes are localised in the cytosol, except the PDE9A1 variant, which has been observed to localise to the nucleus (Wang *et al.*, 2003). However, the nuclear expression has been observed in HEK cells selectively transfected with PDE9A1, and a possible physiological relevance of this observation remains to be determined. One special feature of PDE9 is its resistance to the broad-spectrum PDE inhibitor IBMX.

PDE6:

The PDE6 family is highly abundant in the retina and is ultimately best known for its role in phototransduction, existing as a membrane-bound enzyme in rod and cone photoreceptors, where it mediates cGMP breakdown that leads to the hyperpolarisation of photoreceptor cells. PDE6 comprises two catalytically active subunits (α and β in rods, and two α subunits in cones), which are associated with two identical inhibitory γ subunits and a regulatory δ subunit, the latter thought to modulate enzyme localisation (Bender & Beavo, 2006). There are three PDE6 isoforms known to date, termed PDE6A, PDE6B, and PDE6C, where the former two are found in rods and PDE6C is expressed in cones. In the dark, PDE6 is kept in an inactive state by the presence of the inhibitory γ subunits. In common with PDE5, PDE6 is not only highly selective for cGMP, but also contains two N-terminal GAF domains (GAF-A and GAF-B). It has been suggested that occupation of the GAF-A by cGMP enhances the affinity between the inhibitory γ subunits and the C-terminal catalytic subunits (Muradov *et al.*, 2004). Upon light stimulation, GTP-bound transducin-α displaces the inhibitory γ subunits from the catalytic core, thereby allowing activation of the PDE6. The result is very rapid cGMP degradation, supporting phototransduction by leading to the closure of cGMP-gated channels and the consequent hyperpolarisation of the photoreceptor cells. A special feature of the PDE6 family is that it has the highest catalytic efficiency compared to all other PDEs, with more than 3000 cGMP molecules being hydrolysed per molecule of PDE6 per

second (Gillespie & Beavo, 1988). The extreme efficiency of PDE6 supports very rapid adaptations occurring to changes in light intensity.

PDEs with dual substrate selectivity

PDE 1:

PDE1 can hydrolyse both cGMP and cAMP and thereby provides a mechanism of cross-talk between the two signalling molecules in that competitive inhibition of cGMP breakdown can be achieved by elevations in cAMP levels, and *vice versa*. A distinguishing characteristic of the PDE1 family is that its members lack the GAF domains, but are instead regulated by Ca^{2+}/CaM binding to two N-terminal CaM binding domains, which are structurally followed by the C-terminal catalytic domain. At present, there are three isoforms known of PDE1, namely PDE1A, PDE1B, and PDE1C, which differ in their substrate preferences *(Table 1.1)*, but are all cytosolic proteins (except for the ones expressed in sperm; Bender & Beavo, 2006). A number of possible variants have been identified, with the PDE1A having the largest number of variants.

The binding of Ca^{2+}/CaM to PDE1 has the effect of enhancing the rate of catalysis, without much impact upon the K_m (Kincaid *et al.*, 1985). The mechanism by which CaM binding activates PDE1 is not well understood, but previous biochemical studies have suggested that it involves relieve of an inhibition imposed upon enzyme activity, where the CaM binding domain spans an inhibitory sequence (Sonnenburg *et al.*, 1995). Additional scope for regulation of enzyme activity is suggested to be provided by phosphorylation mediated by cAMP-dependent protein kinase (PKA) or, in the case of PDE1B, by CaM kinase II, all of which cause a reduction in the affinity of the enzyme for CaM binding, thereby compromising enzyme activity (Sharma & Wang, 1985; Hashimoto *et al.*, 1989; Ang & Antoni, 2002). What makes the PDE1 family of particular interest in the NO-cGMP pathway is its activation by Ca^{2+}/CaM. As outlined earlier, NOS activation is also sensitive to Ca^{2+}. Therefore, the presence of two enzymes in the pathway that are sensitive to Ca^{2+} levels may have important implications in that an increase of Ca^{2+} would, on the one hand, stimulate NO-

mediated cGMP production and, on the other hand, dampen it as a result of activation of the cGMP-hydrolysing constituent. Such scenario has been revealed by a study by Mayer and colleagues (1992), in which both NOS and PDE1 were found in the cytosolic fraction of brain synaptosomes, the two enzymes sharing a common range for Ca^{2+} sensitivity (EC_{50} ~ 200-300 nM; Mayer *et al.*, 1992). The authors suggested that the failure of NO_{GC} receptor-, NOS-, and PDE1-bearing cells to accumulate cGMP upon Ca^{2+} influx may be explained by the suppression of the cGMP signal because of Ca^{2+}-dependent acceleration of cGMP degradation by PDE1. However, the EC_{50} for activation by Ca^{2+} has been found to vary among different PDE1 variants (e.g. 0.27 μM for PDE1A1 and 3.2 μM for PDE1C1; Bender & Beavo, 2006).

In the brain, all three isoforms of PDE1 are expressed in various brain regions, including the cortex, hippocampus, cerebellum, and striatum, albeit at differing degrees not only among different areas, but also within a neuronal population of the same region. For instance, PDE1A and PDE1B are expressed in neurons of the neocortex, striatal neurons, and hippocampal pyramidal neurons (Menniti *et al.*, 2006). The heterogeneity of a neuronal population in terms of PDE1 expression is exemplified by the situation in the cerebellum, where PDE1B appears at high levels in some Purkinje cells but not in others (Shimizu-Albergine *et al.*, 2003; Bender & Beavo, 2004). Functionally, it has been reported that mice lacking PDE1B (the only PDE1 knockouts available) suffer deficits in spatial learning in the Morris water maze and also exhibit increased locomotor activity (Reed *et al.*, 2002). Overall, there is still an urgent need for potent and selective PDE1 pharmacological tools, and the development of mice with disruption of other PDE1 genes would also be beneficial in further elucidating the functional roles of the PDE1 family.

PDE2:

Of this PDE family only one isoform is known so far, the PDE2A, of which there are three known variants, namely PDE2A1, PDE2A2 and PDE2A3. PDE2 is characterised by dual substrate selectivity, hydrolysing both cAMP and cGMP efficiently with high V_{max} and low K_m *(Table 1.1)*. In terms of the subcellular expression profile, PDE2A1 is cytosolic, and PDE2A2 and PDE2A3 are both

membrane-bound enzymes (Bender & Beavo, 2006). Similar to PDE5 and PDE6, PDE2 also contains regulatory GAF domains, but in this case cGMP binds to the GAF-B motif (Martins *et al.*, 1982; Martinez *et al.*, 2002; Bender & Beavo, 2006). Exclusive binding of cGMP to the GAF-B domain renders the affinity of PDE2 greater for cGMP, and results in positive cooperativity in that hydrolysis of both cGMP and cAMP is enhanced upon cGMP-GAF interaction. Based on the marked increases in the rate of hydrolysis of both cGMP and cAMP that are observed upon incubation of the enzyme with cGMP, PDE2 is sometimes referred to as 'cGMP-activated PDE' (Bender & Beavo, 2006). This modulatory effect of cGMP on its own breakdown as well as on cAMP levels highlights the potential cross-talk between these two signalling pathways, and offers a mechanism by which a NO stimulus can indirectly affect cAMP signals in cells.

In the brain, PDE2 is found in the cortex, the striatum, and the hippocampus (Wykes *et al.*, 2002; Suvarna & O'Donnell, 2002; van Staveren *et al.*, 2003; van Staveren *et al.*, 2004; Menniti *et al.*, 2006). The matter of PDE2 in the hippocampus will be a subject in Chapters 4 and 5. PDE2 has been proposed to regulate cGMP levels that arise in response to NMDA receptor activation in rat neurons from cortex and hippocampus (Suvarna & O'Donnell, 2002), and also NO-evoked cGMP accumulation in rat striatal neurons (Wykes *et al.*, 2002). Functionally, PDE2 has been implicated in synaptic plasticity, and learning and memory. Inhibition of PDE2 has been reported to enhance hippocampal long-term potentiation (LTP), and to improve memory in social and object recognition tasks (Boess *et al.*, 2004; Rutten *et al.*, 2007).

PDE3:

This dual-substrate PDE family is also regulated by cGMP like PDE2. However, in this case cGMP binding does not limit cyclic nucleotide accumulation by stimulating PDE activity, but instead inhibits PDE activity, therefore enhancing cAMP levels. This again exemplifies how a NO stimulus may influence the cellular level of cAMP, but this time in a positive way. Another difference here is that cGMP does not affect

PDE3 activity in an allosteric manner. The catalytic site of PDE3 degrades cAMP much more effectively than cGMP (V_{max} is ~ 10-fold higher for cAMP than cGMP) but yet has a high affinity for cGMP. This latter feature renders cGMP a competitive antagonist, where it competes with cAMP for binding to the catalytic site of PDE3 (Degerman *et al.*, 1997). Furthermore, the activity of PDE3 has been demonstrated to be enhanced by approximately 2-fold via PKA- or PI3 kinase-mediated phosphorylation (Manganiello & Degerman, 1999). Currently, there are two known isoforms of PDE3, namely PDE3A and PDE3B, where several variants of the former have been identified (Bender & Beavo, 2006). The different isofoms can be cytosolic or particulate, where residues in the N-terminal region have been suggested to regulate membrane association (Shakur *et al.*, 2000). Expression of this PDE family has been reported in neurons in the striatum and hippocampus, but discrete functional roles remain to be elucidated (Menniti *et al.*, 2006).

PDE10:

Also the PDE10 family has the capacity to hydrolyse both cGMP and cAMP, binding cAMP with greater affinity than cGMP but hydrolysing cGMP about 5-fold more effectively than cAMP (Soderling *et al.*, 1999). The PDE10 family is suggested to be a cAMP-inhibited enzyme (analogues to cGMP-inhibited PDE3). There is currently one isoform known, the PDE10A, of which there are two recognised variants (Bender & Beavo, 2006). Several studies have documented PDE10A to be limited to the testis and the brain (Fujishige *et al.*, 1999; Soderling *et al.*, 1999; Seeger *et al.*, 2003). Particularly high levels of mRNA transcript are found in striatal neurons, other areas including the cerebellum, the hippocampus, the thalamus, and spinal cord. However, no protein was detectable in the hippocampus as determined by Western blotting (Seeger *et al.*, 2003). A possible function of PDE10 in synaptic plasticity has been speculated based on the finding that mRNA levels for PDE10A variants are upregulated following LTP (O'Connor *et al.*, 2004).

1 General introduction

1 General introduction

Isoform	Substrate specificity	K_m – cGMP (µM)	K_m – cAMP (µM)	V_{max} – cGMP (µmol/min/mg)	V_{max} – cAMP (µmol/min/mg)	Comments
PDE1A	cAMP < cGMP	2.6 – 3.5	72.7 – 124	50 – 300	70 – 150	Ca^{2+}/CaM activated; cytosolic
PDE1B	cAMP < cGMP	1.2 – 5.9	10 – 24	30	10	Ca^{2+}/CaM activated; cytosolic
PDE1C	cAMP = cGMP	0.6 – 2.2	0.3 – 1.1	-	-	Ca^{2+}/CaM activated; cytosolic
PDE2A	cAMP = cGMP	10	30	123	120	cGMP-activated; membrane-bound (2A2 and 2A3) or cytosolic (2A1)
PDE3A	cAMP > cGMP	0.02 – 0.15	0.18	0.34	3 – 6	cGMP-inhibited; membrane-bound or cytosolic
PDE3B	cAMP > cGMP	0.28	0.38	2	8.5	cGMP-inhibited; membrane-bound
PDE5A	cAMP < cGMP	2.9 – 6.2	290	1.3	1	cGMP-binding, cGMP-specific; cytosolic
PDE6A/B	cAMP < cGMP	15	700	2300	~ 500	cGMP-binding, cGMP-specific; membrane-bound
PDE6C	cAMP < cGMP	17	610	1400	-	cGMP-binding, cGMP-specific; cytosolic
PDE9A	cAMP < cGMP	0.07 – 0.17	230	4.9	-	High affinity, cGMP-specific; cytosolic
PDE10A	cAMP < cGMP	13 – 14	0.22 – 1.1	3.5	0.74	cGMP-binding; membrane-bound (10A2) or cytosolic (10A1 and 10A3)

Tabel 1.1 Overview of cGMP-degrading PDEs

1 General introduction

1.4.3 Cyclic nucleotide-gated (CNG) channels

The ability of cGMP to activate these cation-selective channels was first documented in retinal rod photoreceptors (Fesenko *et al.*, 1985), followed by the cloning and sequencing of rod photoreceptor CNG channels (Kaupp *et al.*, 1989) and the discovery of CNG channels in retinal cone cells (Bonigk *et al.*, 1993) and olfactory receptor cells (Dhallan *et al.*, 1990), where they are involved in visual and olfactory signal transduction by converting sensory information into changes in membrane potential. CNG channels are now known to have a more widespread distribution, at least at the mRNA level, including the hippocampus (Kingston *et al.*, 1996) and the cerebellum (Kingston *et al.*, 1999; Strijbos *et al.*, 1999), and may therefore play a role in the communication between central neurons. Characteristic features of CNG channels include weak sensitivity to voltage, and opening upon direct binding of either cGMP or cAMP. In the absence of extracellular Ca^{2+}, these channels are permeable to Na^{+} and K^{+}. However, they have a higher affinity for Ca^{2+} so that, at physiological extracellular Ca^{2+} concentrations (1-2 mM), the pore of the channels is blocked by the divalent cation excluding Na^{+} and K^{+}, and, consequently, Ca^{2+} becomes the dominant ion permeating the active channels (Kaupp & Seifert, 2002). Based on these channels allowing Ca^{2+} influx when they open upon cyclic nucleotide binding, it becomes apparent that these channels could trigger Ca^{2+}-dependent processes within a cell.

CNG channels closely resemble voltage-gated K^{+} channels, and are therefore thought to have evolved from these channels. Functional CNG channels exist as a tetrameric assembly of α and β subunits arranged around a central pore. Based on hydropathy plotting, all subunits are predicted to share a common architecture, comprising a 6-transmembrane domain (S1-6), an ion conducting pore region which is located between S5 and S6 and carries the inward cationic currents, and an intracellular C-terminal cyclic nucleotide-binding domain (CNBD) which follows the S6 domain (Kaupp *et al.*, 1989; Matulef & Zagotta, 2003). The pore region, which is the determinant of ion permeation properties of the channel, is very similar to the one in K^{+} channels except for two residues that are absent in CNG channels but present in K^{+}

channels. Indeed, mutation of these residues has implied that no other regions in the channel are required to confer the profoundly different permeation qualities of the two channel types (Heginbotham *et al.*, 1992). The CNBD consists of three α-helices and an eight-stranded anti-parallel β-roll, and it is the binding of cGMP (or cAMP) to the CNBD that evokes the direct opening of the channel (Matulef & Zagotta, 2003).

Molecular cloning has identified two subfamilies of subunits in vertebrates, which are termed CNGα(1-4) and CNGβ(1,3), where there are two splice variants (β1a and β1b) known to exist for the CNGβ1. Heterologous expression of subunits has suggested subunits CNGα1-3 to be core subunits, which are able to form functional homomeric channels. On the contrary, CNGα4 and the β subunits lack this capability, and are instead regarded to have regulatory roles influencing channel properties such as ligand sensitivity and gating properties (Kaupp & Seifert, 2002; Craven & Zagotta, 2006).

The CNGα1 and CNGβ1a subunits are primarily found in rod photoreceptors, the rod CNG channels thought to be made of three CNGα1 subunits and one CNGβ1a subunit (Weitz *et al.*, 2002). Cone photoreceptors appear to express mainly CNGα3 and CNGβ3, where two CNGα3 subunits are thought to pair up with two CNGβ3 subunits to form the native channel (Peng *et al.*, 2004). The CNGα2, CNGα4, and CNGβ1b subunits are found in olfactory receptors, the native channel being thought to comprise a tetramer of two core CNGα2 subunits and two regulatory subunits – one CNGα4 and one CNGβ1b (Zheng & Zagotta, 2004). The rod and cone CNG channels prefer cGMP as their ligand, while the olfactory-type channels are relatively non-selective between cGMP and cAMP (Kaupp & Seifert, 2002).

Functionally, much remains to be learned about these channels and how they may be participating in the NO-cGMP signal transduction cascade, which has been made difficult by the lack of good pharmacological tools. Based on the features of these channels, it is plausible to suggest that membrane potential and Ca^{2+} influx may be modulated through NO-cGMP-mediated activation of CNG channels (Biel *et al.*, 1998). For instance, based on defined NADPH-diaphorase activity in amacrine cells

and NO-activated CNG channel currents in cultured retinal ganglion cells, which were occluded upon pre-exposure to cGMP, it has been suggested that NO from nearby amacrine cells could elevate cGMP levels in retinal ganglion cells, thereby enhancing CNG channel activity (Ahmad *et al.,* 1994). Another suggested role for the NO-cGMP-CNG channel pathway is the modulation of neurotransmitter release. In retinas isolated from lizards, it has been demonstrated that NO-cGMP-mediated CNG channel activation promotes neurotransmitter release from cone presynaptic terminals, which was sensitive to NO_{GC} receptor inhibition, culminating in enhanced neuronal firing of the postsynaptic horizontal cells (Savchenko *et al.,* 1997). In the hippocampus, *in situ* hybridisation studies and patch clamp-recordings from cultured neurons demonstrated the presence of both olfactory- and rod-type CNG channels in this brain region, being localised in neuronal somata and dendrites of pyramidal neurons, as well as in granule cells of the dentate gyrus (Leinders-Zufall *et al.,* 1995; Kingston *et al.,* 1996). Consistent with the expression profile of CNG channels in the hippocampus, it has been suggested that the olfactory-type CNG channels support LTP in the Schaffer collateral/CA1 synapse recorded from hippocampal slices, based on the finding that theta-burst-evoked LTP in mice lacking the α subunit of the channel was reduced (Parent *et al.,* 1998). Also NO_{GC} receptor-sensitive depolarisation of the membrane potential of rat hippocampal CA1 pyramidal neurons in slices has been reported, that was, however, insensitive to NOS inhibition and the ODQ concentration used was twice the 'bench-mark' concentration, therefore questioning the physiological relevance of this observation (Kuzmiski & MacVicar, 2001).

1.4.4 Hyperpolarisation-activated cyclic nucleotide-modulated (HCN) channels

General features

HCN channels have only relatively recently emerged as a potential player in transducing NO-cGMP signals. Similar to CNG channels, also HCN channels are

modulated by cyclic nucleotide binding. However, while CNG channels are virtually voltage-insensitive and open directly upon cyclic nucleotide binding, HCN channels are quite different in that their binding of cyclic nucleotides modulates their voltage dependence for activation. HCN channels have long puzzled scientists due to their 'unorthodox' behaviour compared to other voltage-gated channels in that they activate at more hyperpolarised membrane potentials negative to or close to the resting membrane potential. This unique characteristic has led to the nicknaming of their current as 'funny' (I_f) or 'queer' (I_q), alongside the more 'conservative' nomenclature of 'hyperpolarisation-activated' (I_h). While CNG channels carry an inward current dominated by Ca^{2+}, but also to a lesser extent by monovalent cations such as K^+, Na^+, Li^+, and Cs^+ (Kaupp & Seifert, 2002), the inward current conducted by HCN channels is a mixed cation current of both K^+ and Na^+ at an average permeability ratio of 4:1 (Robinson & Siegelbaum, 2003; Wahl-Schott & Biel, 2009). There is some evidence suggesting that HCN channels expressed in HEK293 cells also conduct Ca^{2+} ions to a small extent (Yu *et al.*, 2004), but the functional relevance of this remains to be elucidated, and, unlike CNG channels, HCN channels are not blocked by divalent cations (Kaupp & Seifert, 2002). The binding of cyclic nucleotides has the effect of causing a depolarising shift in the voltage dependence of HCN channel activation. HCN channels are found in a variety of excitable cells, including neurons, cardiac pacemaker cells, and photoreceptors (Pape, 1996; Wahl-Schott & Biel, 2009), their function being best established in the heart where I_h controls heart rate and rhythm by acting as a 'pacemaker current' in the sinoatrial (SA) node (Accili *et al.*, 2002; Barbuti & DiFrancesco, 2008).

HCN channels have a proposed structure *(Fig. 1.4)* as described for CNG channels. Four isoforms have been cloned in mammals, termed HCN 1-4, homomeric expression of the different subtypes revealing differences in terms of activation kinetics, gating properties, and cyclic nucleotide sensitivity (Accili *et al.*, 2002; Robinson & Siegelbaum, 2003; Wahl-Schott & Biel, 2009). These subunits combine to form tetrameric channels, arranged around a central pore, but the subunit stoichiometry of native channels remains largely unknown. The different subunits share an unifying structure, each comprising a cytosolic N-terminus, which is

important for subunit association (Proenza *et al.*, 2002), six transmembrane domains (S1-S6) of which the S4 is the positively charged voltage sensor that moves inwards on hyperpolarisation to produce channel opening, a pore-forming region between S5 and S6, which determines ion selectivity, and a cytosolic C-terminal CNBD, which is preceded by a C-linker region and to which cyclic nucleotides bind. The difference in activation polarity compared to other voltage-dependent channels is suggested to be determined by the downstream coupling mechanism between the voltage sensor and the gate (Rosenbaum & Gordon, 2004). Binding of cGMP or cAMP to the CNBD speeds up channel opening and causes a shift in activation to more depolarised potentials and an increase in current amplitude by initiating the removal of a tonic inhibition of the channel (Robinson & Siegelbaum, 2003; Wahl-Schott & Biel, 2009).

The determination of the crystal structure of part of the HCN2, beginning just after the end of S6 and extending through the C-linker and CNBD, has provided insights into cyclic nucleotide-dependent channel modulation (Zagotta *et al.*, 2003). The CNBD is made of an eight-stranded anti-parallel β-roll, which is connected to the pore by the C-linker region consisting of six α-helices. The construction of truncation mutants has shown that, during the inactivated state, the channel is inhibited by the CNBD at its core transmembrane domain region S1-S6 (Wainger *et al.*, 2001). The same study suggested that differences in the efficacy of CNBD, exerting different levels of tonic inhibition, are the cause of varying activation gating and cyclic nucleotide-dependent modulation, where cyclic nucleotide binding relieves this inhibition. Indeed, the deletion of the CNBD was found to mimic the effect of cAMP by moving the voltage dependence of channel gating to more depolarised potentials to a similar level as cAMP. Subsequently, chimeric subunit studies demonstrated that the difference in cAMP efficacy also depends on the interaction of the CNBD with the 80 amino acid C-linker, which itself has no intrinsic inhibitory influence, but accounts for the differences in basal gating and cAMP modulation by interacting with the CNBD (Wang *et al.*, 2001).

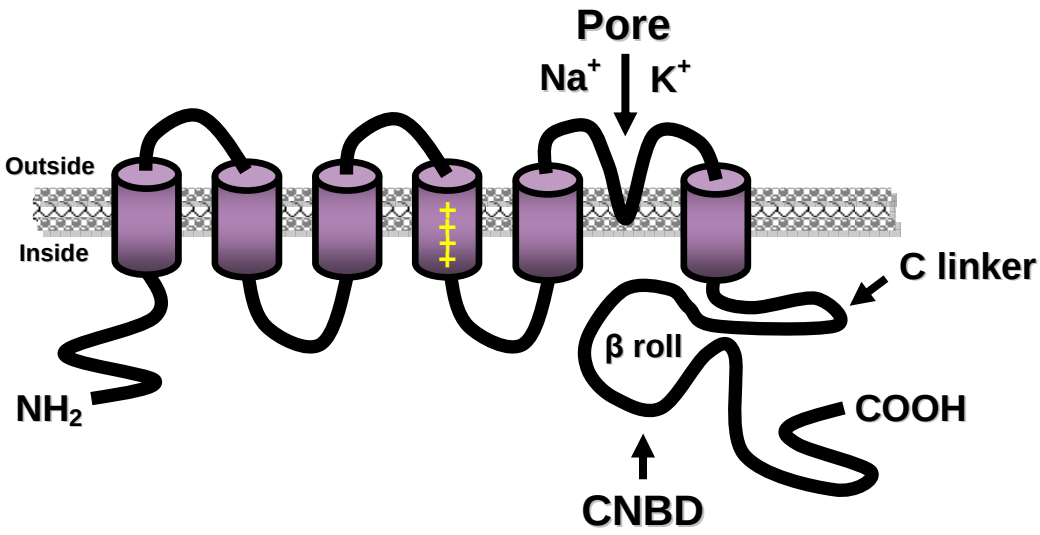

Fig. 1.4 The proposed topology and structure for HCN channel subunits. A single subunit comprises six α-helical membrane-spanning segments (S1-S6), a positively charged S4 domain, and cytoplasmic N- and C- termini. The putative pore region between S5 and S6 extends into the membrane, and the cyclic nucleotide binding domain (CNBD) is located in the C-terminal region. *Adapted from Robinson & Siegelbaum, 2003*

As aforementioned, the HCN subtypes exhibit marked differences in their biophysical properties, including voltage-dependence, activation kinetics, and cyclic nucleotide sensitivity. Homotetramers of HCN1 show the fastest activation kinetics, falling on a hundred-millisecond timescale, while HCN4 is the slowest channel, taking several seconds to activate at resting membrane potential but gradually becoming faster at more hyperpolarised potentials. HCN2 and HCN3 show activation kinetics intermediate to that of HCN1 and HCN4. Estimated values for the half-maximal voltages for activation are -70 mV for HCN1, -95 mV for HCN2, -85 mV for HCN3, and -100 mV for HCN4 (Wahl-Schott & Biel, 2009). In terms of cyclic nucleotide sensitivity, HCN1 and HCN3 homotetramers are the least sensitive, while HCN2 have greater sensitivity, followed by HCN4, which are strongly regulated by cyclic nucleotides. Although much remains to be learned about native channel compositions, HCN channels have been shown to co-assemble to form heteromers. A construct of HCN1 and HCN2 subunits has been found to exhibit modulation by cAMP and activation kinetics intermediate to those of HCN1 and HCN2 homomers (Ulens & Tytgat, 2001). Both native and heterologously expressed channels are activated by

cAMP and cGMP with similar efficacy, albeit with different sensitivity. Based on apparent dissociation constants, the channels appear to be about 30-fold less sensitive to cGMP as compared to cAMP, resulting in cAMP being often considered as the 'natural' ligand, showing approximately 10-fold greater potency to activate channels (DiFrancesco & Tortora, 1991; Ludwig *et al.*, 1998; Zagotta *et al.*, 2003). However, there have been instances where cAMP and cGMP were demonstrated to exhibit quite similar concentration-effect profiles (Ingram & Williams; 1996).

Initially, it had been proposed that I_h gating is directly regulated by cyclic nucleotide binding to the cytoplasmic CNBD, not involving other modulatory factors such as protein phosphorylation (Pape, 1996; Robinson & Siegelbaum, 2003). However, it has now emerged that also HCN channels may be modulated by other factors independently of cyclic nucleotides. The membrane lipid phosphatidylinositol-4,5-bisphosphate (PIP_2) apparently acts as an allosteric ligand, shifting the voltage-dependence of HCN channel activation to more depolarised values by about 20 mV (Zolles *et al.*, 2006; Pian *et al.*, 2006). A possible physiological significance for this has been proposed on the grounds of enzymatic degradation of phospholipids reducing channel activation and slowing neuronal firing frequency (Zolles *et al.*, 2006). How PIP_2 exerts this effect mechanistically is still unknown. Other proposed factors include the non-receptor tyrosine kinase c-Src and the Ser/Thr-kinase mitogen activated protein kinase p38-MAP, where c-Src has been found to enhance activation kinetics of the channels via C-linker domain phosphorylation, and p38-MAP is suggested to shift voltage-dependent activation to more positive potentials (Wahl-Schott & Biel, 2009). An involvement of PKA in channel modulation has so far only been reported in rat olfactory receptor neurons, where infusion of the PKA catalytic subunit was found to shift the activation voltage to more positive potentials (Vargas & Lucero, 2002). Furthermore, like with many other signalling components, it appears that there are 'context-dependent' mechanisms also at work in the case of HCN channels. A number of interacting proteins that may influence the coupling of HCN channels to signalling pathways and the trafficking of the channels to different cellular compartments have been identified, including the TPR-containing Rab8b-interacting protein (TRIP8b), which had no previously ascribed function, the mink-

related peptide 1 (MiRP1), and the cytoplasmic scaffold protein filamin A. Their functional implications in native tissue remain to be determined (Wahl-Schott & Biel, 2009).

Pharmacological manipulation of I_h

HCN channels can be blocked with Cs^+ and various organic compounds, including ZD 7288, zatebradine, and ivabradine. The two most commonly used inhibitors are caesium (Cs^+) and ZD 7288 (Harris & Constanti, 1995; Takigawa *et al.*, 1998; Ghamari-Langroudi & Bourque, 2001).

The compound ZD 7288 has been suggested to adapt properties of a lipophilic quaternary cation that can readily cross the cell membrane when applied externally, which is consistent with intracellular application of ZD 7288 also inhibiting I_h. Moreover, it has been proposed that ZD 7288 exerts its I_h-blocking effect in a non-use dependent manner, with an approximate half-maximal blocking concentration of 2 μM (Harris & Constanti, 1995). Inhibition of I_h by ZD 7288 occurs in a time- and concentration-dependent manner and is irreversible, its action being relatively slow (~ 10-15 min; Harris & Constanti, 1995; Takigawa *et al.*, 1998; Chevaleyre & Castillo, 2002). ZD 7288 has been reported to have also non-selective effects at high (> 30 μM) concentrations. At these higher concentrations, ZD 7288 has been observed to depress basal synaptic transmission, which did not occur upon Cs^+ application and was also not occluded by Cs^+ and therefore assumed to be I_h-independent (Chevaleyre & Castillo, 2002).

In contrast to ZD 7288, while also exerting its effect in a non-use dependent manner, Cs^+ induces block much more rapidly in a reversible manner, and has no effect on I_h when loaded into the cell interior, indicating that it acts on the extracellular site (Harris & Constanti, 1995). However, Cs^+ has the shortcoming of also blocking K^+ inward rectifier (I_{Kir}) channels (Pape, 1996; Ghamari-Langroudi & Bourque, 2001). Inhibition of I_{Kir} results in extracellular K^+ accumulation, leading to membrane depolarisation, which is indeed observed when using Cs^+ (Ghamari-Langroudi & Bourque, 2001). This may have great importance when using Cs^+ to block I_h, as the conductance of HCN channels is highly sensitive to external K^+ levels,

where a reduction below normal levels (2-4 mM) leads to a marked decrease in I_h magnitude and *vice versa* (Robinson & Siegelbaum, 2003).

Expression of HCN in the CNS and proposed functions

While in the heart HCN3 is absent (Shi *et al.*, 1999; Moosmang *et al.*, 2001), all four subtypes of HCN are found in the mammalian brain as determined by their expression pattern at protein and mRNA levels. HCN1 is found in the neocortex, hippocampus, brainstem, cerebellum, olfactory bulb, and spinal cord (Moosmang *et al.*, 1999; Santoro *et al.*, 2000; Notomi & Shigemoto, 2004; Milligan *et al.*, 2006). HCN2 has been reported to have widespread distribution, with highest expression levels detected in the thalamus, brainstem, hippocampus, and olfactory bulb (Moosmang *et al.*, 1999; Santoro *et al.*, 2000; Notomi & Shigemoto, 2004). In contrast, HCN3 is seen in the CNS at very low levels, appearing to be mainly restricted to the olfactory bulb and hypothalamus, whereas HCN4 is predominantly expressed in the thalamus and olfactory bulb (Moosmang *et al.*, 1999; Santoro *et al.*, 2000; Notomi & Shigemoto, 2004).

An emerging general consensus is that I_h plays an important role in influencing intrinsic neuronal excitability. Tonic activation of I_h sets the resting membrane potential at a depolarised level, and also reduces the input resistance so that the influence of any current on the membrane potential is reduced according to $V = I \times R$. These basic properties can lead to opposing effects of I_h on neuronal excitability, depending on the HCN isoform and the type of input reaching the cell. Dendritic I_h can reduce neuronal excitability on the basis of reducing membrane resistance, ultimately causing a decrease in dendritic summation in response to a dendritic depolarising input. In other words, I_h influences the cable properties of dendrites and in turn shapes the time course of the EPSP as it is propagated to the soma. On the other hand, by depolarising the resting membrane potential, I_h can enhance neuronal excitability by driving the neuron closer to firing threshold of action potentials. Based on these features, the physiological roles ascribed to HCN channels include control of oscillatory activity of neurons, maintenance of reliable conduction by counteracting

hyperpolarisation occurring during high-frequency activity, control of resting membrane potential, and modulation of membrane resistance and dendritic integration (Robinson & Siegelbaum, 2003; Wahl-Schott & Biel, 2009).

Evidence supporting the presence of a NO-cGMP-HCN pathway in the brain

It has been demonstrated *in vitro* that rhythmic oscillations of thalamic neurons are generated by the interplay between I_h and a low threshold Ca^{2+} current, termed 'I_T', that arises from T-type Ca^{2+} channels. It is proposed that I_h slowly depolarises the membrane, which in turn evokes a low-threshold Ca^{2+} spike via activation of I_T. These spikes are depolarising and last tens of milliseconds and therefore cause the generation of a series of Na^+ spikes. The prolonged depolarisation then leads up to the inactivation of T-type Ca^{2+} channels, terminating the low-threshold Ca^{2+} spike. During the spike, HCN channels are deactivated, therefore generating a hyperpolarising overshoot upon termination of the Ca^{2+} spike. This hyperpolarising overshoot removes the inactivation of the T-type Ca^{2+} channels and activates I_h again, initiating a new cycle. This 'burst mode' of thalamic neurons is characteristic for non-REM sleep and is thought to reduce sensory information transfer to the cortex during this sleep state (McCormick & Bal, 1997). One of the first reported observations suggesting NO as a potential regulator of I_h came from studies in guinea-pig and cat thalamocortical relay neurons maintained *in vitro* in slices (Pape & Mager, 1992). Using intracellular recordings it was found that both NO and a cGMP analogue depolarise the membrane potential of these neurons by 1-3 mV and reduce their membrane resistance. The target for the NO-cGMP pathway being I_h was deduced from the current-voltage relationship that suggested NO to have a greater effect at hyperpolarised potentials, the rate of rise and amplitude of I_h found to be enhanced by NO or cGMP. This work by Pape & Mager (1992) found NO to shift the voltage for half-maximal activation of the channels to a more depolarised value by approximately 5 mV. In this way, NO was demonstrated to potently and reversibly block the oscillatory activity in these spontaneously active neurons by causing a reduction in rebound depolarisation because of less de-inactivation of I_T, consequently reducing rebound action potentials (Pape & Mager, 1992).

During wakefulness and REM sleep, thalamocortical neurons are depolarised by afferent inputs and switch to a 'transmission' or 'single spike' mode, as opposed to the situation during non-REM sleep (McCormick & Bal, 1997). Fibres of the cholinergic tegmental neurons innervate the thalamus, and contain nNOS (Vincent & Kimura, 1992). These neurons are thought to increase their firing rate just before the transition from sleep to wakefulness (McCormick & Bal, 1997), which in turn would presumably facilitate the release of NO into the thalamus. Taken together, it appears that there is the possibility that NO regulates the switch between the two distinct firing modes of thalamic relay neurons, regulating the transition from the 'burst mode' associated with non-REM sleep to the 'transmission mode' prevailing during REM sleep and wakefulness, thereby supporting the increase in the transfer of sensory information to the cortex (Pape & Mager, 1992).

The above evidence suggesting the NO-cGMP pathway as a modulator of HCN channels was supported by a number of subsequent studies. Exogenously applied cGMP was demonstrated to enhance I_h in dissociated guinea-pig nodose and trigeminal neurons, finding the cGMP analogue to have a very similar concentration-effect profile to the related analogue for cAMP, where both analogues applied at 1 mM caused a shift in the half-maximal activation voltage of about 4 mV to more depolarised potentials (Ingram & Williams, 1996). This indicated that NO-cGMP signalling could play a role in nociceptive processing, which was further implied by a recent study by Kim and colleagues (2005), finding NO and exogenously applied cGMP to augment I_h in rat substantia gelatinosa neurons in spinal cord slices, the effect of the former being prevented by NO_{GC} receptor inhibition. Additionally, they reported NO to evoke depolarisation of the neurons by approximately 5 mV, which was sensitive to I_h block by Cs^+. Based on these findings a possible role of NO in central sensitisation was suggested (Kim *et al.*, 2005).

Exogenously applied cGMP or NO has also been demonstrated to increase I_h in guinea-pig trigeminal motor pool and rat mesencephalic neurons maintained *in vitro* in slices (Abudara *et al.*, 2002; Pose *et al.*, 2003). In these studies, NO (in an ODQ-sensitive manner) and exogenous cGMP reversibly depolarised the membrane potential by approximately 3-7 mV and reduced the threshold for firing so that the

enhanced I_h had an excitatory effect, suggested to have an importance in various jaw reflexes and movements. In both papers, these neurons were demonstrated, by immunohistochemical analysis, to be innervated by nNOS-bearing fibres, underscoring a possible physiological relevance of modulation of these neurons by NO.

Recently, it has been discovered that *in vitro* in the rat optic nerve, tonic eNOS-derived NO depolarises axons, this being transduced by cGMP engaging HCN channels. The prevailing tone of the NO-cGMP-HCN-maintained membrane potential was found to lie around the midpoint, indicating that the system is well balanced to respond to changes in eNOS activity (Garthwaite *et al.*, 2006).

1.5 OVERVIEW OF THE PHYSIOLOGICAL FUNCTIONS OF NO IN THE CNS

1.5.1 Development

There are three distinct steps NO has been suggested to play a role in during CNS development. These are inhibition of proliferation and promotion of cell differentiation, influence over the direction of neurite growth, and the refinement of topographical projections.

The indication of NO regulating neurogenesis in the developing embryo brain and in neurogenic areas in the adult brain came from studies demonstrating an inhibitory effect of NO on the rate of proliferation of undifferentiated neuronal precursors, and an accelerating effect on the neuronal differentiation process, NO thereby presumably acting as a switch between proliferation and differentiation. Inhibition of endogenous NO production by means of NOS inhibitors or application of haemoglobin to scavenge NO was found to increase the proliferation of cultured embryonic mouse brain neuronal progenitor cells or postnatal subventricular zone progenitors as

quantified by the expression of markers of proliferating cells such as nestin and bromodeoxyuridine (BrdU). Exogenous NO, on the other hand, was found to have the opposite effect (Cheng *et al.*, 2003; Matarredona *et al.*, 2004). Analogous results were obtained in studies investigating the role of NO in cell proliferation of neuronal progenitor cells in the adult mammalian brain (Park *et al.*, 2003; Packer *et al.*, 2003; Moreno-Lopez *et al.*, 2004).

Consistent with NO facilitating cell differentiation is the finding that the expression of neuronal phenotypic markers is delayed upon NOS inhibition or NO scavenging by haemoglobin, but increased upon NO application, which are the very same treatments that promote or suppress proliferation respectively (Cheng *et al.*, 2003; Moreno-Lopez *et al.*, 2004; Matarredona *et al.*, 2004). The spatiotemporal pattern of nNOS expression appears to correlate with NO acting as an anti-proliferative, pro-differentiation molecule. In the developing rodent CNS, transient increases in nNOS expression parallel cessation of proliferation and the beginning of differentiation, while in the adult brain NOS-bearing neurons are adjacent rather than within areas of adult neurogenesis (Moreno-Lopez *et al.*, 2000; Packer *et al.*, 2003; Moreno-Lopez *et al.*, 2004). Moreover, the growth factor brain-derived neurotrophic factor (BDNF) was shown to reduce cell proliferation and to augment nNOS levels in post-mitotic neurons nearby proliferating cells in the developing cortex, executing a stimulatory effect on neuronal differentiation that was sensitive to NOS inhibition or NO scavenging (Cheng *et al.*, 2003).

Additional evidence supporting the role of NO in these early developmental processes has been provided by studies using mice lacking nNOS, which were found to exhibit an increase in the number of proliferating cells, albeit to a lesser extent as compared to the effect observed upon non-selective NOS inhibition, indicating that NO sources other than the deleted NOS form may be involved in the regulation of proliferation and differentiation (Packer *et al.*, 2003). Overall, it appears that NO acts in a paracrine fashion during these early stages of neuronal development, being released from nearby differentiating neurons to stop neuronal precursors from further proliferation and to initiate differentiation into neuronal phenotypes. However, as the involvement of the NO_{GC} receptor and ensuing cGMP production has not been tested, the mechanism(s) through which NO exerts these actions remain elusive. The absence

of NO_{GC} receptors and cGMP in neurons prior to differentiation, as evaluated by means of immunohistochemistry, as well as the lack of effect of allosteric NO_{GC} enhancers on proliferation, have indicated that an alternative, as yet unidentified, signalling process may be at play (Arnhold *et al.*, 2002).

Several studies have proposed a role for NO in the control of neurite outgrowth. In the developing visual system of the ferret, based on a disruptive effect of NOS inhibition, NO has been suggested to be involved in directing retinal axons to the appropriate locations in the lateral geniculate nucleus of the thalamus (Cramer *et al.*, 1996). This finding parallels the proposed role of cyclic nucleotides in regulating neuronal growth cones, where it was observed that varying levels of cyclic nucleotides change the turning behaviour of isolated growth cones of *Xenopus* spinal neurons, NO-stimulation of cGMP formation or application of a cGMP analogue converting repulsion to attraction (Song *et al.*, 1998). There are a number of contradictory observations, however, showing either collapse and retraction of growth cones in response to NO (Ernst *et al.*, 2000; Gallo *et al.*, 2002; He *et al.*, 2002), or NO-cGMP-mediated attraction of growth cones and protection from collapse (Campbell *et al.*, 2001; Schmidt *et al.*, 2002; Xiang *et al.*, 2002; Steinbach *et al.*, 2002). Overall, the opposing observations appear to be related to the concentration of NO that is applied. Growth cone collapse occurs in studies applying NO donors at high micromolar to millimolar concentrations, while attraction and protection is observed in studies applying lower NO donor concentrations or cGMP analogues. Also, for instance, semaphorin-3A-mediated attraction of rat cortical pyramidal cell dendrites to the pial surface was demonstrated to depend on NO_{GC} receptors and PKG, localising NO_{GC} receptors to the region of the cells where apical dendrites are generated, and finding that inhibition of these two constituents disrupts oriented dendritic growth. However, pharmacological inhibition of these constituents did not cause the dendrites to be repelled by semaphorin-3A, implying that NO_{GC} receptor activity does not simply act as a polarity switch. Additionally, the repellent effect of semaphorin-3A on pyramidal cell axons was found to be independent of this pathway (Polleux *et al.*, 2000). Another study, although not identifying the site of action of cGMP (i.e. growth cones *vs.* their target cells), reported that reducing cGMP levels impairs synapse formation

between mossy fibres and CA3 pyramidal cell apical dendrites in the stratum lucidum, leading to random orientation of mossy fibres (Mizuhashi *et al.*, 2001). Evidence coming from studies documenting effects of exogenously applied NO or cGMP analogues therefore suggests a role for NO in regulating the direction of neurite outgrowth. The involvement of endogenous NO was first indicated in retinal axon path finding (Cramer *et al.*, 1996), and by a study on PC12h cells (Yamazaki *et al.*, 2001), showing prevention of nerve growth factor-mediated neurite outgrowth following NO_{GC} receptor inhibition or upon inhibition of endogenous NO production by means of broad-spectrum NOS inhibition or NO scavenging. Additionally, Yamazaki and colleagues found enhanced NADPH-diaphorase activity and nNOS protein in cells prior to neurite outgrowth. Recently, a study in organotypic hippocampal slice cultures from postnatal rats using electronmicroscopy demonstrated that the postsynaptic site promotes synapse formation with nearby axons via NO derived from the nNOS-PSD-95 interaction site (Nikonenko *et al.*, 2008). The key findings leading to this proposal included prevention of synapse formation upon deletion of the second PDZ domain of PSD-95, or through small interfering RNA-induced down-regulation of nNOS or pharmacological broad-spectrum inhibition of NOS. Interestingly, knockdown of nNOS had only a partial effect in this respect, while non-selective NOS inhibition caused complete inhibition of synapse formation. This could point towards another NO source (e.g. eNOS) contributing. Conversely, application of a cGMP analogue or slow-releasing NO donor enhanced synapse formation. Finally, the notion that NO is acting downstream of PSD-95 was indicated by the result that NO donor treatment also increased synapse formation in slices with deleted PDZ, which was prevented upon NO_{GC} receptor inhibition (Nikonenko *et al.*, 2008).

Overall, however, it appears difficult to propose a general model for NO-regulated neurite growth, as this may differ among species, and also may vary depending on the extracellular cue communicating with the NO-cGMP signalling cascade in a given brain region, as well as the cGMP effector engaged. For example, in postnatal dissociated dorsal root ganglion neurons, inhibition of endogenous NO synthesis by means of broad-spectrum NOS inhibition or a NO scavenger revealed a repulsive action of endogenous NO on axon guidance, the extracellular cue being the

neurotrophic factor neurotrophin-4. Additionally, NO scavenging or NO_{GC} receptor inhibition were both found to convert the neurotrophin-4-induced repulsion of the growth cones to attraction (Tojima *et al.*, 2009).

NO has also been implicated in mediating activity-dependent refinement of topographical projections after a coarse map has been laid down by guidance cues. However, this seems to be restricted to only a few specific areas. Inhibition of endogenous NO production has been demonstrated to cause disorganisation of refinement of ipsilateral retinotectal or retinocollicular projections in the chick and rat *in vivo* (Campello-Costa *et al.*, 2000; Wu *et al.*, 2001). In the rat, projections undergo topographical refinement within the first two postnatal weeks, and the role of NO in this process was compatible with the spatiotemporal expression profile of NOS in the tectum and colliculus during the period of refinement. Maximal NOS activity in tissue homogenates or NADPH-diaphorase levels were measured towards the end of the first postnatal week, followed by a slight decrease by the end of the third postnatal week, which is the time point marking the end of topographical fine-tuning, and an approximately two-third reduction in adulthood (Campello-Costa *et al.*, 2000). Overall, these findings are in line with double-knockout mice that lack eNOS and nNOS exhibiting delayed refinement with more diffuse ipsilateral retinocollicular projections that eventually become more refined with age presumably due to residual NOS activity in the knockouts (Wu *et al.*, 2000b). Additionally, the refinement process in normal mice or nNOS or eNOS knockouts is in progress before eye opening, but significantly delayed in double knockouts (Wu *et al.*, 2000c). Also, during visual system development, the terminals of retinal ganglion cell axons segregate first into eye-specific layers within the dorsal lateral geniculate nucleus (dLGN), which is followed by a process of sublamination during which the ON- and OFF-inputs from retinal ganglion cells are organised into sublayers. It has been demonstrated in ferret kittens that the period of retinogeniculate axon sublamination within the dLGN requires activity of the incoming fibres, NMDA receptor-mediated NO synthesis, and ensuing NO_{GC} receptor-dependent cGMP formation. This was accompanied by the finding that the period of connection refinement in the retinogeniculate pathway overlaps with transient upregulation of NO_{GC} receptor

activity in pre- and postsynaptic elements, as revealed by particularly strong cGMP staining during the second to third postnatal week (Leamey *et al.*, 2001). Also continuous infusion of ferrets with ODQ by means of osmotic mini-pumps led to impaired normal sublamination, indicating that the activity of the NO-cGMP pathway may be required for normal ON- OFF-sublamination *in vivo* (Leamey *et al.*, 2001).

The organisation of other sensory projections appears to be unrelated to the NO-cGMP transduction pathway. The lack of large scale neuroanatomical, neurochemical, or behavioural changes in adults following chronic neonatal NOS inhibition *in vivo* suggests that NO may not be a necessity in the formation and refinement of cortical neuronal maps during late development (Contestabile, 2000).

1.5.2 Acute effects on neuronal function

Neuronal function can be modulated by NO in an acute manner via influences upon neuronal excitability, firing rate, and neurotransmitter release. This section will outline the possibilities by a number of examples.

In a study in rat hypothalamic slices, NO was reported to reduce the firing rate of spinally projecting paraventricular nucleus (PVN) neurons by enhancing GABA release through a cGMP-PKG-dependent mechanism (Li *et al.*, 2002; Li *et al.*, 2004). In this case, L-arginine, a cGMP analogue or NO donor enhanced the frequency of GABAergic miniature IPSCs and reduced the discharge activity of PVN neurons, the NO-mediated effect being prevented by inhibiting $GABA_A$ receptors, scavenging NO, inhibiting NO_{GC} receptors or PKG, or selectively inhibiting nNOS. Furthermore, inhibition of NOS activity or scavenging of basal NO was found to have no effect, suggesting that the NO-mediated effect is stimulus-evoked rather than tonic. On the contrary, a subpopulation of PVN neurons in the hypothalamus that project to the rostral ventrolateral medulla have been found to increase their discharge rate in response to nNOS inhibition, demonstrating a tonic inhibitory function of NO, exogenous NO having the opposite effect (Stern *et al.*, 2003). Other proposed mechanisms via which the NO-cGMP signalling pathway could exert postsynaptic inhibitory effects on excitability include hyperpolarisation by activating various types

of K^+ channels as has been observed for delayed-rectifier K^+ channels in cultured mouse neocortical neurons (Han *et al.*, 2006), leak K^+ channels in basal forebrain neurons maintained *in vitro* in slices (Kang *et al.*, 2007), and ATP-sensitive K^+ channels in brainstem neurons maintained *in vitro* in slices (Mironov & Langohr, 2007). While the former two studies investigated this at the level of NO donors, cGMP analogues, and NO_{GC} receptor inhibition only, Mironov & Langohr (2007) also tested the effect of two different NO scavengers and a broad-spectrum NOS inhibitor. They found that exogenous NO suppressed spontaneous synaptic currents, activated K^+ channels, and inhibited L-type Ca^{2+} channels, inhibition of endogenous NO synthesis having the opposite effect. An *in vivo* example of NO acting in an inhibitory manner is derived from work in the cat visual cortex, where inhibition of endogenous NO levels caused an increase in the responses to visual stimuli in a small (5%) population of cells (Cudeiro *et al.*, 1997).

NO has also been shown to dis-inhibit by reducing GABAergic transmission, thereby acting in an excitatory manner indirectly. For example, in the cerebellum, endogenous NO appears to reduce GABA release from Golgi cells by tonically hyperpolarising them, possibly through mediating the opening of large conductance Ca^{2+}-activated K^+ channels (Wall, 2003). Also, $GABA_A$-mediated currents in cerebellar granule cells, which are innervated by GABAergic Golgi cells, appear to be tonically suppressed by NO through a PKG-dependent mechanism (Robello *et al.*, 1996). The overall result of this NO-mediated effect is dis-inhibition of granule cell activity due to the negative effect on GABAergic tone.

In the rat ventrobasal and lateral geniculate nucleus of the thalamus, exogenous NO or application of a cGMP analogue were found to depolarise neurons *in vitro*, and to enhance neuronal responses to whisker or light stimulation respectively, as well as to ionotropic glutamate receptor activation *in vivo*, indicating that NO enhances sensory transmission through the thalamus (Shaw *et al.*, 1999). An enhancing effect of NO has also been observed in the visual cortex, where inhibition of endogenous NO levels was found to lead to decreases in the responses to visual stimuli in a population (38%) of cells, while protocols enhancing NO levels endogenously or exogenously caused an

increase in the number of action potentials in response to visual stimuli (Cudeiro *et al.*, 1997; Kara & Friedlander, 1999). In rat medial vestibular nucleus neurons maintained *in vitro* in brain stem slices, the NO-cGMP pathway was shown to cause depolarisation and increase their spontaneous discharge rate via activation of CNG channels (Podda *et al.*, 2004; Podda *et al.*, 2008). Nitric oxide-cGMP-mediated depolarisation has also been observed *in vitro* in a number of different central neurons via HCN channel modulation (see above). Another possible route for NO to modulate excitation in a facilitating manner has been proposed to be via suppression of K^+ conductances. For instance, intracellular recordings from rat striatal neurons *in vivo* revealed NO, perhaps derived from local nNOS-bearing interneurons, to modulate the spontaneous up- and down-state membrane activity and synaptic responses (West & Grace, 2004). This study demonstrated that NO causes membrane depolarisation probably by cGMP-mediated suppression of K^+ currents, with the ultimate net effect of enhanced EPSPs. Pharmacological disruption of NO-NO_{GC} receptor signalling by means of infusion of a NO scavenger, nNOS inhibitor, or ODQ, on the other hand, was found to reduce neuronal responsiveness associated with membrane hyperpolarisation.

Direct excitatory effects of NO on synaptic transmission could also be based on NO-cGMP-PKG-dependent augmentation of glutamate release by potentiating Ca^{2+} entry through presynaptic N-type Ca^{2+} channels, as has been demonstrated in rostral ventrolateral medulla neurons in brainstem slices (Huang *et al.*, 2003). Another potential mechanism in NO-modulated transmitter release has been suggested to involve inhibition of presynaptic voltage-gated K^+ channels, including Kv1.1 and Kv1.2 subtypes, a mechanism reported to be involved in potentiating GABA release to PVN neurons (Yang *et al.*, 2007). Paradoxically, also NO-cGMP-mediated activation of K^+ channels has been found to facilitate neurotransmitter release. In peptidergic nerve terminals of the posterior pituitary, NO-cGMP-PKG-mediated enhancement of Ca^{2+}-activated K^+-channels activity at depolarised potentials has been found to facilitate transmitter release. This is suggested to be associated with increased action potential afterhyperpolarisation, which in turn facilitates the recovery of Na^+ channels from their inactivated state, ultimately reducing the rate of action

potential failure. This in turn would allow more Ca^{2+} influx and consequently increased neuropeptide release (Klyachko *et al.*, 2001).

1.5.3 Long-term modulation of neuronal function

The function of NO in the CNS that has been studied most extensively is its involvement in synaptic plasticity. This is an activity-dependent process in which neurons undergo long-term adjustments in the strength of their synaptic connections either in the 'upward' or 'downward' direction in response to brief periods of altered input. These processes are known as long-term potentiation (LTP) and long-term depression (LTD) respectively, and are commonly proposed to be a cellular correlate of learning and memory (Bliss & Collingridge, 1993; Neves *et al.*, 2008; Nader & Hardt, 2009). In LTP, the correlated firing of the pre- and postsynaptic neuron leads to an increase in the efficiency of synaptic transmission as such that subsequent presynaptic activity is able to exert a stronger influence on the firing of the postsynaptic neuron. Since the first observation of LTP at the perforant path/granule cell synapse in the rabbit hippocampus following brief high frequency stimulation (Bliss & Lomo, 1973), this structure in the medial temporal lobe became the dominant model of this process, with intense research aiming to elucidate the molecular mechanisms of synaptic plasticity. Nonetheless, LTP is not a phenomenon restricted to that brain region, but has – just as the reciprocal phenomenon to LTP, namely LTD, which has been most extensively described in the cerebellum – also been observed in other brain regions. The NO-cGMP pathway has been proposed to be involved in LTP in the hippocampus, cerebral cortex, cerebellum, amygdala, and the spinal cord, as well as in LTD in the cerebellum and the striatum. There has been much controversy in the vast research field of NO in synaptic plasticity, but one well-accepted hypothesis is that NO may act pre- and/or postsynaptically. This section will outline features of NO in LTP and LTD in the light of the hippocampus and the cerebellum respectively.

NO and LTP

The involvement of NO in LTP has been extensively studied at the Schaffer collateral/CA1 synapse in the hippocampus. Following the establishment that this involved postsynaptic NMDA receptors, in combination with NO's properties (i.e. association with NMDA receptor activation and diffusibility), NO became implicated in a scheme where NMDA receptor-mediated Ca^{2+} influx activates nNOS leading to postsynaptic NO formation, which then diffuses as a retrograde messenger across the synaptic cleft to activate its receptor in the presynaptic terminal, ultimately thought to converge on changes in neurotransmitter release (Garthwaite & Boulton, 1995).

Initial evidence showing that NO can augment neurotransmitter release came from experiments on cultured hippocampal neurons, finding that a low nanomolar concentration of exogenous NO increases the frequency of spontaneous miniature EPSPs, while bath application of the membrane-impermeable haemoglobin to scavenge NO, or postsynaptic injection of a NOS inhibitor, prevented LTP (O'Dell *et al.*, 1991). A number of subsequent studies have supported the proposition that presynaptic NO signalling involves NO_{GC} receptor activation, cGMP accumulation, and PKG activation. Evidence supporting a presynaptic localisation of the cGMP response came from studies on NMDA receptor-dependent LTP between pairs of cultured hippocampal pyramidal neurons, finding that injection of cGMP only into the presynaptic neuron is sufficient to facilitate activity-dependent LTP alongside an increase in miniature EPSPs, while inhibition of NO_{GC} receptors or PKG prevented the induction of LTP (Arancio *et al.*, 1995). This paralleled further experiments, using the same preparation, showing that tetanus-evoked LTP is prevented by injection of a NO scavenger into pre- or postsynaptic neurons, while under conditions of simultaneous NO application and tetanic stimulation the LTP was only prevented when the scavenger was injected into the presynaptic neuron. Additionally, tetanus-induced LTP was prevented upon injection of a NOS inhibitor into the postsynaptic neuron, but not the presynaptic neuron (Arancio *et al.*, 1996). A predominant involvement of PKG in presynaptic signalling was first proposed based on the detection of PKGI in presynaptic terminals, demonstrated to co-localise with the vesicle protein synaptophysin (Arancio *et al.*, 2001). Studying NMDA receptor-

dependent LTP between pairs of cultured hippocampal neurons, the same study reinforced the concept of presynaptic NO-cGMP signalling via PKG based on the observation that injection of purified PKGIα protein or a PKG inhibitor into the presynaptic neuron respectively facilitates or prevents LTP induced by a weak tetanus. At odds with these findings are results from studies in hippocampus-specific PKGI knockout mice, reporting not only normal LTP in juvenile animals (4-6 weeks) and reduced LTP in older animals (12 weeks), but also normal hippocampus-dependent learning of the older mice in contextual fear conditioning and spatial learning in a water maze (Kleppisch *et al.*, 2003).

There are a number of mechanisms suggested to underlie NO-mediated modulation of transmitter release, including changes in the mode of vesicle fusion, the number of vesicles released in response to afferent stimulation, and vesicle recycling. PKG targets suggested to link the cGMP signal to vesicle function include the Ca^{2+}/calmodulin-dependent protein kinase II (CaMKII) and the vasodilator-stimulated phosphoprotein (VASP). The possible presynaptic function of CaMKII in this scenario was provided by a study in cultured hippocampal neurons, demonstrating that presynaptic injection of a membrane-impermeable CaMKII inhibitor peptide prevented LTP in response to weak tetanic stimulation, glutamate, an NO donor, or PKG activator, while presynaptic injection of CaMKII itself paired with tetanic stimulation evoked LTP in the presence of a NOS or PKG inhibitor (Ninan & Arancio, 2004). However, this is at great odds with a study investigating hippocampal slices from mutant mice lacking the dominant CaMKII α isoform selectively in presynaptic CA3 neurons of the Schaffer collateral pathway, reporting an inhibitory rather than stimulatory function of CaMKII in activity-dependent transmitter release (Hinds *et al.*, 2003).

It is suggested that activity-dependent potentiation is accompanied by cytoskeletal changes at the presynaptic site, comprising a rapid increase in clusters of the vesicular proteins synaptophysin and synapsin I (Antonova *et al.*, 2001; Wang *et al.*, 2005). In these latter studies, at synapses between pairs of cultured hippocampal neurons, application of glutamate was shown to induce NO-dependent clustering of both pre- and postsynaptic proteins. A regulator of actin dynamics, namely VASP, has

been implicated as a downstream target of cGMP-PKG signalling, suggested to be a critical component in activity-dependent changes in transmitter release. It has been found in cultured hippocampal neurons that VASP appears to be an endogenous PKG-substrate and that PKG-dependent VASP-Ser-239 phosphorylation is important in the induction of LTP, all necessary components (i.e. NO_{GC} receptors, PKGI, and VASP) being expressed in presynaptic terminals (Arancio *et al.*, 2001; Wang *et al.*, 2005). Finally, a different set of work in cultured hippocampal neurons that monitored exo- and endocytosis in the neurons by means of fluorescence imaging suggested that NO promotes synaptic vesicle recycling in an activity-dependent manner, the NMDA receptor-dependent production of NO accelerating vesicle endocytosis in a cGMP-dependent manner (Micheva *et al.*, 2001; Micheva *et al.*, 2003).

There is also evidence suggesting routes for enhanced transmitter release independent of PKG. Experiments on cone/horizontal cell synapses in culture indicated that exocytosis can also be triggered by cGMP-evoked Ca^{2+} influx through CNG channels (Savchenko *et al.*, 1997). CNG channels are expressed in the hippocampus in cell bodies and processes of CA1 and CA3 neurons, and therefore they may serve as transducers that link activity-dependent generation of cGMP in the presynaptic terminal to increases in transmitter release (Kingston *et al.*, 1996; Bradley *et al.*, 1997). In support of this latter notion is the finding of reduced LTP in the Schaffer collateral pathway recorded in hippocampal slices from mice with disrupted CNG channels (Parent *et al.*, 1998).

In addition to its presynaptic action, NO may also act postsynaptically. While postsynaptic NMDA receptor activation requires glutamate release into the synaptic cleft and membrane depolarisation in order to be relieved of their Mg^{2+} block, fast excitatory transmission in the CNS is mediated by AMPA receptors. It has emerged that activity-regulated AMPA receptor trafficking represents an additional mechanism for the modification of synaptic strength. Initial evidence came from studies in cultured hippocampal neurons, reporting an increase in the amplitude of EPSPs in response to brief applications of glutamate, associated with an increase in the number of postsynaptic protein clusters containing the GluR1 subunit of AMPA receptors (Antonova *et al.*, 2001), which was later demonstrated to be replicable upon exposure

to a cGMP analogue and dependent on PKG (Wang *et al.*, 2005). A recent study in cultured hippocampal neurons and adult mouse hippocampal slices suggested that cGMP regulates AMPA receptor trafficking and subunit composition via PKGII (Serulle *et al.*, 2007). These authors reported PKGII and GluRI to co-localise and interact in a cGMP-dependent manner, resulting in the phosphorylation of the Ser-845 residue of the GluRI, ultimately leading to an increase of AMPA receptor surface expression at extrasynaptic sites. Impediment of phosphorylation by mutating the Ser-845 residue prevented the surface increase. Serulle and colleagues (2007) found the increase in AMPA receptors and the associated enhancement in synaptic strength to occur in response to exogenous NO as well as NMDA receptor activation in a NOS-, NO_{GC} receptor-, and PKG-dependent manner. Also, additionally to the data obtained in cultured neurons, the authors demonstrated a reduction in LTP in slices upon PKGII inhibition by a PKGII inhibitor peptide.

There is also evidence in terms of postsynaptic NO-cGMP actions regarding the regulation of gene expression. It has been reported that transcription via cAMP-response-element-binding protein (CREB) can be activated in a NO-cGMP-dependent manner in the hippocampus (Lu *et al.*, 1999; Lu & Hawkins, 2002; Chien *et al.*, 2003). These studies, employing protein analysis by means of Western blotting and immunofluorescence in slice preparations, showed that CREB in postsynaptic CA1 cell somata is phosphorylated via the NO-cGMP-PKG pathway. The complete signalling cascade for cGMP-mediated activation of CREB-regulated gene transcription remains to be clarified, but a mechanism involving Ca^{2+} release from ryanodine-sensitive stores has been proposed (Lu & Hawkins, 2002). Additionally, the possibility has been put forward that the cognitive decline in Alzheimer's disease might, at least partially, result from inhibition of hippocampal cGMP-CREB-interaction by amyloid-β peptide (Puzzo *et al.*, 2005). Puzzo and co-workers found in their experiments on hippocampal slices that application of low micromolar NO donor concentrations, a cGMP analogue, or an allosteric NO_{GC} receptor activator, protects against the impairment of LTP that is caused by exposure to amyloid-β in a PKG-dependent manner. Additionally, the authors demonstrated that amyloid-β prevents tetanus-induced phosphorylation of CREB in CA1 cell somata, which could be rescued by NO in a cGMP-dependent manner, as well as by PKG activation, the

amyloid-β possibly directly interfering with the NO-cGMP pathway as it prevented tetanus-evoked cGMP elevation.

Investigations using genetic approaches to study the importance of endogenous NO in LTP have yielded incoherent results. For example, mice lacking eNOS or nNOS were demonstrated to exhibit normal hippocampal LTP, while double knockouts lacking both NOS isoforms showed impaired LTP in the stratum radiatum containing CA1 pyramidal apical dendrite/CA3 axon synapses with no gross anatomical abnormalities and the reduction in LTP being quantitatively similar to that observed upon exposure to a broad-spectrum NOS inhibitor in wild-type mice (Son *et al.*, 1996). Others found impaired LTP in eNOS knockouts (Kantor *et al.*, 1996; Wilson *et al.*, 1999). An important role of eNOS was suggested as disrupting the localisation of eNOS to the cell membrane impaired LTP, which could be overcome by expressing a chimeric form of the eNOS constitutively targeted to the cell membrane (Kantor *et al.*, 1996). Complications may arise in nNOS knockouts due to the upregulation of active splice variants of the enzyme (Eliasson *et al.*, 1997; and see above). In eNOS knockout mice, disruptions in other second messenger pathways may make data interpretation difficult, as indicated by studies of the mossy fibre synapse in the dentate gyrus (Doreulee *et al.*, 2001). On the other hand, there is the implication that endogenous NO generated from both nNOS and eNOS play their part in LTP. NO appears to function not only as an acute signalling molecule that is evoked during the triggering of LTP, but also a tonic one (Bon & Garthwaite, 2003). Recently, it has been revealed that LTP induction at the Schaffer collateral/CA1 synapse requires both a tonic, low level eNOS-derived NO as well as activity-evoked phasic nNOS-generated NO (Hopper & Garthwaite, 2006). However, the precise roles of these two distinct NO signals remain to be uncovered.

Recent studies using genetic approaches have also explored the endogenous pathway at the level of NO_{GC} receptors. Mice lacking either the α_1 or α_2 subunit of the NO_{GC} receptor were shown to have reduced LTP in visual cortical slices, which could be restored in both strains by exposure to a cGMP analogue (Haghikia *et al.*, 2007). Also hippocampal LTP, recorded in slices from mice lacking either the α_1 or α_2 subunit of the NO_{GC} receptor, is abolished in both knockout strains (Taqatqeh *et*

al., 2009). Taqatqeh and colleagues (2009) also provided indication for a presynaptic role of the $\alpha_1\beta_1$ isoform of the NO_{GC} receptor in neurotransmitter release, observing increased paired-pulse ratios in mice lacking the α_1 subunit.

NO and LTD

LTD has been best characterised in the cerebellum, where the large dendritic tree of an individual Purkinje cell in the molecular layer of the cerebellar cortex receives excitatory inputs from a single climbing fibre and many parallel fibres originating from the granule cells in the granular layer. This form of plasticity is evoked when the parallel fibres are repeatedly activated simultaneously with the climbing fibre that converges onto the same Purkinje neuron, leading to postsynaptic Ca^{2+} rises, and is thought to underlie specific forms of motor learning such as adaptation of the vestibulo-ocular reflex, which keeps images stable on the retina during head movements (Ito, 2001).

A string of studies have implicated NO-cGMP signalling in this process. The prevention of LTD induction was demonstrated in cerebellar slices upon NOS or NO_{GC} receptor inhibition, substituting NO or applying cGMP analogues restoring it (Boxall & Garthwaite, 1996; Lev-Ram *et al.*, 1997). Here, NO is thought to act as an anterograde messenger that is produced upon repetitive activity-evoked NMDA receptor activation on presynaptic parallel fibres or liberated from interneurons (Casado *et al.*, 2002; Shin & Linden, 2005), and then evokes postsynaptic LTD via stimulating a cGMP-dependent signalling pathway in the postsynaptic cell (Boxall & Garthwaite, 1996; Ito, 2001). As mentioned earlier, Purkinje cells are rich in PKGIα, and it is this downstream effector of cGMP that is thought to play a key role in cerebellar LTD. Inhibition of PKG was shown to impair LTD in cerebellar slices (Hartell, 1994; Lev-Ram *et al.*, 1997), which was consistent with the later finding that mice with a Purkinje neuron-specific disruption of the PKGI gene exhibit abolished LTD recorded in acute slice preparations (Feil *et al.*, 2003). Additionally, these mutants were found to show marked deficits in their adaptation of the vestibulo-ocular reflex, while exhibiting normal general motor performance as assessed by foot print

patterns and the runway tests. The possibility of this specific phenotype arising due to structural or physiological abnormalities has been ruled out based on the demonstration that the Purkinje neurons in these mutants have normal climbing fibre innervations as revealed by normal dendritic Ca^{2+} signals in the Purkinje cells upon climbing fibre stimulation, without any notable morphological changes of the cerebellar cortex in general (Feil *et al.*, 2003).

Reciprocally to what has been suggested in LTP, in LTD the rapid internalisation of AMPA receptors has been proposed to contribute to the expression of cerebellar LTD (Wang & Linden, 2000). LTD induction is thought to comprise an increase in postsynaptic endocytosis of GluR2-containing AMPA receptors, a process that is proposed to involve phosphorylation of the Ser-880 residue of the GluR2 by protein kinase C (Wang & Linden, 2000; Chung *et al.*, 2003). A central role of the GluR2 subunit in this respect was highlighted by the finding that LTD is absent in cultured cerebellar Purkinje neurons from mice lacking this AMPA receptor subunit, which could, however, be rescued by transiently transfecting the cells with the wild-type GluR2 subunit (Chung *et al.*, 2003). An alternative mechanism suggested for enhanced AMPA receptor phosphorylation and consequent removal from the postsynaptic membrane is reduced phosphatase activity. Cerebellar Purkinje cells are rich in the PKG-target protein G-substrate, which is a phosphatase inhibitor (Detre *et al.*, 1984; Hall *et al.*, 1999; Endo *et al.*, 1999). Phosphorylation of G-substrate via the cGMP-PKGI cascade has been shown to suppress the activity of the protein phosphatases 1C and 2A (Hall *et al.*, 1999), inhibition of the latter having been found to lead to enhanced AMPA-GluR2 phosphorylation in cultured cerebellar neurons, in turn causing endocytosis of the receptors and reduced synaptic currents in a manner that occludes subsequent induction of LTD (Launey *et al.*, 2004).

*

1.6 GENERAL AIMS OF THIS WORK

Previous data obtained in the optic nerve pointed to a potential mechanism of vasculo-neuronal communication involving eNOS (Garthwaite *et al.*, 2006). The aim was to further test the involvement of eNOS and to investigate the underlying mechanism for the maintenance of tonic NO synthesis in the rat optic nerve, assessing the role of the PI3 kinase-Akt pathway, which is thought to be one of the key mechanisms for tonic eNOS stimulation. Previous work has indicated tonic eNOS-derived NO to be a requisite for LTP induction in the hippocampus (Hopper & Garthwaite, 2006). The subsequent aim was to determine if blood vessel-neuron communication may be more widespread, investigating further if a PI3 kinase-dependent mechanism also accounts for basal NO production in the rat hippocampus.

Taking advantage of the now available pharmacological tools, the following objective was to re-investigate the targets for NO in the hippocampus based on inconsistencies regarding NO_{GC} receptor expression *versus* cGMP accumulation and functional implications in this brain region.

The lack of information about endogenous NO and cGMP signals is a major deficit in the current understanding of this signalling pathway. A final objective of the present work was to begin to analyse NO transduction in cells in real-time combined with steady-state delivery of NO at physiological concentrations, using a newly developed fluorescent cGMP sensor (Nausch *et al.*, 2008) transfected into cell lines expressing various levels the NO_{GC} receptor and phosphodiesterase.

*

CHAPTER 2

General materials and methods

2.1 MATERIALS

2.1.1 Reagents

Pharmacological agents

Table 2.1: Overview of pharmacological compounds utilised

Compound	Abbreviation	Action	Solubility	Source
Acetylcholine chloride	ACh	Cholinergic agonist	10 mM Stock in dH_2O	Sigma
D-(-)-2-Amino-5-phosphonopentanoic acid	D-AP5	NMDA receptor antagonist	20 mM Stock in dH_2O	Tocris
(Z)-1-[N-(3-Ammoniopropyl)-N-(n-propyl)-amino]/NO	PAPA/NO	NO donor	10 mM Stock in 10 mM NaOH	Axxora
[R-(R*,S*)]-5-(6,8-Dihydro-8-oxofuro[3,4-e]-1,3-benzodioxol-6-yl)-5,6,7,8-tetrahydro-6,6-dimethyl-1,3-dioxolo[4,5-g]isoquinolinium chloride	Bicuculline	$GABA_A$ receptor antagonist	100 mM Stock in DMSO	Tocris
Bradykinin acetate	BK	Bradykinin receptor agonist	1 mM Stock in dH_2O	Sigma
Cadmium sulfate 8/3-hydrate	Cd^{2+}	Non-selective Ca^{2+} channel blocker	20 mM Stock in dH_2O	Sigma
2-(4-Carboxyphenyl)-4,4,5,5-tetramethylimidazoline-1-oxyl-3-oxide . potassium salt	CPTIO	NO scavenger	100 mM Stock in dH_2O	Axxora
(2S)-3-[[(1S)-1-(3,4-Dichlorophenyl)ethyl]amino-2-hydro xypropyl](phenylmethyl)phosphinic acid	CGP 55845	$GABA_B$ receptor antagonist	10 mM Stock in DMSO	Tocris
6-Cyano-7-nitroquinoxaline-2,3-dione	CNQX	AMPA/Kainate receptor antagonist	10 mM Stock in DMSO	Tocris
2-(N,N-Diethylamino)-diazenolate-2-oxide diethylammonium salt	DEA/NO	NO donor	10 mM Stock in 10 mM NaOH	Axxora

[2-(3,4-dimethoxybenzyl)-7-[(1R)-1-[(1R)-1-hydroxyethyl]-4-phenylbutyl]-5-methylimidazo[5,1-f][1,2,4]triazin-4(3H)-one	BAY 60-7550	PDE2 inhibitor	1 mM Stock in DMSO	Axxora
4-Ethylphenyl-amino-1,2-dimethyl-6-methylaminopyrimidinium chloride	ZD 7288	HCN channel blocker	10 mM Stock in dH_2O	Tocris
Forskolin	-	AC activator	10 mM Stock in DMSO	Tocris
Gadolinium(III) chloride hexahydrate	Gd^{3+}	TRP channel blocker	10 mM Stock in DMSO	Sigma
HOE-140	-	Bradykinin B_2 receptor antagonist	1 mM Stock in dH_2O	Sigma
1-Hydroxy-2-oxo-3-(N-ethyl-2-aminoethyl)-3-ethyl-1-triazene	NOC-12	NO donor	10 mM Stock in 10 mM NaOH	Axxora
3-Isobutyl-1-methylxanthine	IBMX	Non-selective PDE inhibitor (except PDE 9)	1 mM final concentration dissolved in aCSF	Sigma
Lanthanum(III) chloride heptahydrate	La^{3+}	TRP channel blocker	20 mM Stock in DMSO	Sigma
N-Methyl-D-aspartic acid	NMDA	NMDA receptor agonist	10 mM Stock in dH_2O	Tocris
N^G-Monomethyl-L-arginine acetate	L-MeArg	Non-selective NOS inhibitor	10 mM Stock in dH_2O	Tocris
2-(4-Morpholinyl)-8-phenyl-4H-1benzopyran-4-one hydrochloride	LY 294002	PI3K inhibitor	20 mM Stock in DMSO	Tocris
N^G-Nitro-L-arginine	L-NNA	Non-selective NOS inhibitor	10 mM Stock in 10 mM HCl	Tocris
1H-[1,2,4]Oxadiazolo[4,3-a]quinoxalin-1-one	ODQ	NO_{GC} receptor inhibitor	10 mM Stock in DMSO	Sigma
Phenylmethanesulphonylfluoride or phenylmethylsulphonyl fluoride	PMSF	Protease inhibitor	100x Stock made in DMSO	
N-Propyl-L-arginine	NPA	nNOS inhibitor	10 mM Stock in DMSO	Axoora
SKF 96365 hydrochloride	-	TRP channel blocker	10 mM Stock in dH_2O	Tocris
Superoxide dismutase (from bovine erythrocytes)	SOD	Catalyses the dismutation of	100K U/ml Stock in dH_2O	Sigma

		superoxide radicals to hydrogen peroxide and molecular oxygen		
Tetrodotoxin	TTX	Na^+ channel blocker	Soluble in acetic acid	Latoxan
Uric acid	-	Endogenous antioxidant; converts NO_2 into NO_2^-	30 mM Stock in 60 mM NaOH	Sigma
Vinyl-N-5-(1-imino-3-butenyl)-L-ornithine	L-VNIO	nNOS inhibitor	10 mM Stock in dH_2O	Axxora
Wortmannin	-	PI3K inhibitor	1 mM Stock in DMSO	Sigma

Other reagents

Table 2.2: Overview of other reagents used

Compound	Abbreviation	Source
Bicinchoninic acid Protein assay kit	BCA kit	Perbio
Bovine serum albumin (fraction V)	BSA	Sigma
Cyclic adenosine monophosphate (^3H) biotrak assay	^3H-cAMP kit	GEHealth-care
Chromium potassium sulfate	-	Sigma
3,3'-Diaminobenzadine tablets	DAB	Sigma
Dimethyldichlorosilane solution (for coating)	DMDS	Sigma
Dimethyl sulfoxide	DMSO	Sigma
Donkey serum	-	Chemicon
DPX mounting medium	-	VWR
Dulbecco's Modified Eagle Medium (1x), High Glucose	DMEM, high glucose	Invitrogen
Dulbecco's Phosphate Buffered Saline (1x)	D-PBS	Invitrogen
Ethylenediaminetetraacetic acid disodium	EDTA	Sigma
Ethylene glycol-bis(2-aminoethylether)-N,N,N',N'-tetra-acetic acid	EGTA	Sigma
Foetal Bovine Serum (Heat inactivated)	FBS	Invitrogen
Gelatine powder (for coating)	Gelatine	Sigma
Geneticin Selective Antibiotic (G-418 Sulfate)	G-418	Invitrogen
γ-Globulins bovine blood	γ-Glob	Sigma

Glycine	-	Sigma
Hygromycin B	-	Invitrogen
Hydrogen peroxide	H_2O_2	Sigma
Magermilchpulver (dried milk)	-	VWR
MEM Non Essential Amino Acids	MEM-NEAAs	Invitrogen
OCT embedding medium	OCT	Lamb
Paraformaldehyde	PFA	Sigma
Peroxidase suppressor	PS	Perbio
Poly-D-Lysine	PDL	Sigma
Sodium bisulfite	-	Sigma
Sodium dodecyl sulphate	SDS	VWR
Tris-hydrochloric acid	Tris-HCl	Calbio-chem
Tritiated cyclic guanosine monophosphate	^{3}H-cGMP	Amers-ham (GEHealthcare)
Trizma base	Tris base	Sigma
Triton X-100	Triton	Sigma
Trypsin, 0.05% with EDTA	Trypsin	Invitrogen
Tween 20	Tween	Sigma
Vectashield mounting medium with 4',6'-diamidino-2-phenylindole	DAPI	Vector
Vectastain Elite ABC complex	ABC reagent	Vector
Zeocin Selection Reagent	Zeocin	Invitrogen

Note: All standard reagents (including salts used for aCSF and other solutions) were obtained from BDH (VWR) unless otherwise stated.

Antibodies

Table 2.3: Overview of antibodies:

Primary Antibodies			
Antigen	**Host**	**Dilution**	**Source**
cGMP	Sheep	1 : 40 000	Gift from Dr. J. de Vente (Maastrich, Netherlands)
CNPase	Mouse	1 : 2000	Chemicon
eNOS	Mouse	1 : 200	Transduction

GCβ1	Rabbit	1 : 500	Cayman
GFAP	Rabbit	1 : 1000	Chemicon
NeuN	Mouse	1 : 1200	Chemicon
NF 200	Mouse	1 : 500	Chemicon
nNOS	Rabbit	1 : 500	Zymed
eNOS (for Western blot)	Rabbit	1 : 1000	BD Biosciences
Phospho-eNOS (Ser1179) (for Western blot)	Rabbit	1 : 2000	New England Biolabs

Secondary Antibodies

Antigen	Host	Tag	Dilution	Source
Mouse	Donkey	Alexa 594	1 : 600	Invitrogen
Rabbit	Donkey	Alexa 594	1 : 1500	Invitrogen
Rabbit	Donkey	Biotin	1 : 200	Chemicon
Sheep	Donkey	Alexa 488	1 : 1000	Invitrogen
Rabbit (for Western blot)	Goat	Horseradish peroxidase conjugated	1 : 25 000	Perbio

Suppliers key

Axxora	Axxora Ltd (Alexis Biochemicals), Nottingham, UK
Calbiochem	Calbiochem (Merck Chemicals Ltd), Nottingham, UK
Cayman	IDS Ltd (Cayman Chemical), Tyne & Wear, UK
Chemicon	Chemicon Europe Ltd, Hampshire, UK
GEHealthcare	GE Healthcare (Amersham Bioscience), Bucks, UK
Invitrogen	Invitrogen Ltd, Paisley, UK
Lamb	Raymond A Lamb Ltd, Eastbourne, UK
Latoxan	Latoxan Laboratories, Rosans, France
New England Biolabs	New England Biolabs (Cell signalling technology, Inc.) 3 Trask Lane, Danvers, MA 01923, USA
Perbio	Perbio Science UK Ltd, Northumberland, UK
Sigma	Sigma-Aldrich Company Ltd, Poole, Dorset, UK
Tocris	Tocris Cooksen Ltd, Avonmouth, Bristol, UK
Transduction	BD Transduction Laboratories (BD Biosciences), Oxford, UK

Vector	Vector Labs Ltd, Peterborough UK
VWR	VWR International, Dorset, UK
Zymed	Zymed Laboratories Inc, San Francisco, CA, USA

2.1.2 NO donors

Stock solutions at 10 mM were prepared freshly each day of experimentation in 10 mM NaOH, and kept on ice until use. The NO donors used are members of the 1-substituted diazen-1-ium-1,2-diolate (NONOate) class of compounds that generate authentic NO at predictable rates (Keefer *et al.*, 1996). These compounds have different half-lives and were chosen according to the timeframe requirements of the experiment.

Table 2.4: NO donor compounds

Donor	Structure	Half-life (pH 7.4; 37ºC)
PAPA/NONOate	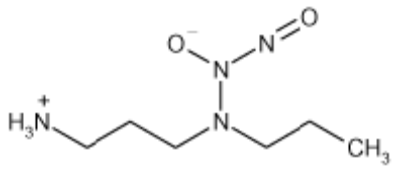	15 mins
DEA/NONOate	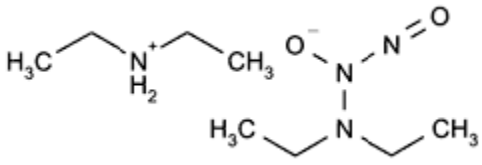	2 mins

NOC-12 100 mins

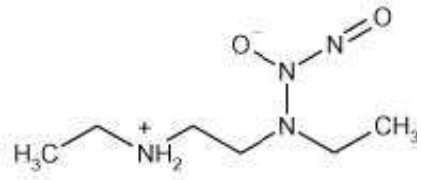

2.2 GENERAL SOLUTIONS

2.2.1 Artificial cerebral spinal fluid (aCSF)

Was composed of the following (in mM): NaCl (120), KCl (2.0), $MgSO_4$ $7H_2O$ (1.19), $NaHCO_3$ (26.0), KH_2PO_4 (1.18), $CaCl_2$ (2.0) and glucose (11.0); the aCSF was equilibrated with 95% O_2 / 5% CO_2; pH (37ºC) = 7.4.

2.2.2 Reagents used in cGMP radioimmunoassay

Inactivation buffer

Was composed of Tris-HCl (50 mM) and EDTA disodium salt (4 mM); pH was adjusted to 7.4 (solution kept at 4°C).

cGMP Standard stock solution (80 nM)

Stocks of 80 µM cGMP (sodium salt) were prepared in inactivation buffer (aliquots were kept at -20 ºC); for a working solution the 80 µM stock was diluted 1: 1000 in inactivation buffer to give a 80 nM cGMP solution (kept at 4ºC) which was used to prepare the standards (standards were diluted down from the 80 nM stock solution in inactivation buffer).

cGMP blank

Cyclic GMP at 10 µM was prepared in inactivation buffer (aliquots were kept at -20ºC and working stock was kept at 4ºC).

[^{3}H]-cGMP solution

Stock solutions, later diluted in inactivation buffer, were prepared by diluting the original [^{3}H]-cGMP supply 1: 1000 in 50% ethanol (aliquots were kept at -20ºC).

cGMP antibody (raised in rabbit; made by Giti Garthwaite)

Antibody (freeze-dried kept at -80ºC; reconstituted in dH_2O) was prepared in inactivation buffer containing γ-globulin (132 mg per 17.5 ml inactivation buffer; for precipitation purposes).

Ammonium sulphate solution ($[NH_4]_2SO_4$; saturated)

One litre of dH_2O to 390 g ammonium sulphate; stored at 4ºC.

2.2.3 Solutions used for immunohistochemistry

Phosphate buffer (PB)

Stock 'A' and stock 'B' solutions were prepared; 'A' contained 31.2 g NaH_2PO_4 . 2 H_2O dissolved in 1 L dH_2O; 'B' contained 35.6 g Na_2HPO_4 . 2 H_2O dissolved in 1 L dH_2O; a 0.2 M stock of PB solution was prepared adding 95 ml of 'A' to 405 ml of 'B'; pH was adjusted to 7.4; a 0.1 M stock of PB solution was prepared diluting the 0.2 M PB solution 1: 2 in dH_2O.

Tris-buffered saline (TBS)

5.85 g of Tris base (Trizma) was dissolved in 250 ml dH_2O; 3.4 ml HCl (37%) was added to 200 ml dH_2O; 250 ml Tris solution, 192 ml HCl solution and 8.77 g added NaCl were combined and topped up to a final volume of 1 L with dH_2O; pH was adjusted to 7.4.

Tris-buffered saline with Triton (TBST)

TBS with added Triton at 0.1%.

Paraformaldehyde (PFA) fixative (in 0.1 M PB)

To make 4% or 1% fixative, 4 g or 1 g PFA were added to 40 ml dH_2O; heated with stirrer to 65ºC; added 1-2 drops of 5 M NaOH to clear the solution (filtered if necessary); allowed to cool and made up to 50 ml with dH_2O; added 50 ml of 0.2 M PB solution to final volume of 100 ml; adjusted pH to 7.4 (stored at 4ºC; never kept for longer than a week).

Sucrose solutions

Prepared in 0.1 M PB.

Coating slides for immunohistochemistry

Dissolved 5 g of gelatine in 1 L of hot dH_2O; let cool while continuously stirring; added 0.5 g chromium potassium sulphate; dipped slides several times in the solution; drained and let dry in a dust free warm oven (37-40ºC).

2.2.4 Extracellular solutions used for the imaging experiments

Imaging buffer

Was composed of the following (in mM): NaCl (136), KCl (2.0), $MgSO_4$ (1.19), KH_2PO_4 (1.18), $CaCl_2$ (1.5) and glucose (5.5), HEPES (10); the pH was adjusted to 7.4 at 37ºC by adding 5 M NaOH solution (1-1.5 ml). The osmolality was adjusted to 285 mOsm (± 2).

Clamp buffer

To achieve a constant concentration of NO over a given period of time (Griffiths *et al.*, 2003), the following was added to the imaging buffer: CPTIO (100 µM), SOD (100 U/ml) and uric acid (300 µM). The broad-spectrum NOS inhibitor L-NNA (30 µM) was added to inhibit any endogenous NO production. To complete the attainment of a clamped NO profile, an NO donor with a long half-life was chosen (in this case NOC-12; see below).

2.2.5 Solutions used for Western blotting

SDS PAGE buffer ("Running buffer")

In a final volume of 1 L dissolved: 3 g Tris-base, 14 g glycine and 1 g SDS in dH_2O; stored at room temperature.

Transfer buffer ("Blotting buffer")

In a final volume of 2 L dissolved: 12 g Tris-base and 56 g glycine. Dissolved these in just under 2 L of dH_2O and add 50 ml methanol. Removed 500 ml to a fresh bottle for gel treatments and stored the remainder at 4ºC. Note: this buffer was used for soaking the polyvinylidene fluoride (PVDF) membrane, sponges, assembling cassettes.

Equilibration buffer

For each gel to be shaken, took 100 ml of transfer buffer and added 0.5 ml triton and 100 µl of antioxidant (see below).

1000x Antioxidant

Prepared a 10% solution of N'N'-dimethylformamide (DMF) in 5 ml dH_2O; dissolved 1 g of sodium bisulfite in this solution. Frozen in 1 ml aliquots and kept one working tube at 4ºC.

10x TBS (diluted to 1x TBS for use)

In a final volume of 1 L dissolved: 24 g Tris-base and 88 g NaCl in dH_2O. Added approximately 16.5 ml of concentrated HCl for pH 7.2-7.4 (adjusted if necessary).

TBS with detergents ("Washing buffer")

To 500 ml of 1x TBS added 1 ml of 10% Triton and 2.5 ml of 10% Tween. Note: This solution was used to wash the membranes in blotting experiments following antibody incubations and in some instances also to dilute antibodies.

Blocking and antibody dilution buffers

5% milk dissolved in 1x TBS were used to block the membranes to prevent non-specific background binding of the antibodies. The primary antibodies were diluted to their final concentration in 1x TBS containing 5% BSA and 0.075% Tween. The secondary antibody was diluted to its final concentration in 1x TBS containing 5% milk and 0.05% Tween.

2.3 METHODS

2.3.1 Protein measurement

Following homogenisation of the tissue by means of sonication, the protein concentrations of each sample were determined by comparison to bovine serum albumin (BSA) standards using the BCA Protein Assay Kit, which is based on the reduction of Cu^{2+} to Cu^{+} in the presence of protein under alkaline conditions. Briefly, 10 µl of sample or BSA standards (0-100 µg/ml made up from a 1 mg/ml BSA stock; all prepared in inactivation buffer) in triplicates was dispensed into a 96-well plate to which 200 µl of the BCA reagent was added. The plates were incubated for 30 min at 37°C, allowed to cool to room temperature followed by measuring the absorbance at 562 nm using a Spectra Max 250 spectrometer (Molecular devices, California, USA). The absorbance over the standard concentration range was linear, from which the unknown protein content of the samples was calculated. The remainder of the samples was centrifuged at 800 rpm for 10 min at 4°C to pellet the debris, the supernatant used for cGMP quantification by means of radioimmunoassay (see below). Samples not assayed immediately were kept at -20°C.

2.3.2 Quantitative evaluation of cGMP accumulation – radioimmunoassay (RIA)

The principle of RIA is based on competitive binding to an antibody raised specifically for cGMP. The test tube will contain a fixed quantity of tritium (^{3}H)-labelled cGMP, a fixed amount of antibody for cGMP and an aliquot of unlabelled cGMP (in this case the supernatant form the tissue suspension). The two cGMP 'species' will compete for the binding to the antibody and the more cGMP the tissue sample contains the less radioactively labelled cGMP will be bound to the antibody, which appears as a lower dpm count when reading the samples in the scintillation counter (and *vice versa*). The abbreviation 'dpm' stands for disintegrations per minute

and is the measure for the number of atoms in a quantity of radioactivity that decay per minute. Below is an overview of the RIA procedure.

RIA procedure in detail

Standard curve:

Standards were tested in duplicates (18 microfuge tubes required). To 6 ('A-F') tubes 250 µl inactivation buffer were added. To tube 'A' 250 µl of cGMP standard stock solution was added. From tube 'A' it was double diluted down to tube 'F' (i.e. 250 µl from 'A' to 'B' containing 250 µl inactivation buffer, 250 µl from tube 'B' to 'C' containing 250 µl inactivation buffer, etc). This series of dilutions gave the following amounts of cGMP (pmol/assay tube):

'A' = 4 pmol
'B'= 2 pmol
'C' = 1 pmol
'D' = 0.5 pmol
'E' = 0.25 pmol
'F' = 0.125 pmol

Tubes 1 + 2 contained inactivation buffer only, tubes 15 + 16 contained the 80 nM cGMP standard stock solution (giving 8 pmol cGMP/assay tube) and tubes 17 + 18 contained the cGMP blank. The tubes in between contained the standard dilutions in ascending order, producing a sigmoidal standard curve (see below).

The following quantities were added to the microfuge tubes:

Unknown Sample / Standard (µl)	[3H]-cGMP (µl)	Rabbit-anti-cGMP (µl)
100	50	50

Samples were incubated at 4ºC, placed on ice for a minimum of 2 hours or left under these conditions overnight.

Protocol following incubation period:

Ammonium sulphate solution (1 ml) was added to each tube to precipitate the antibody-bound complex and left for 5 min on ice, followed by centrifugation at 12500 rpm for 5 min at 4ºC to pellet the antibody-bound complex. The supernatant was removed by vacuum suction to separate the antibody-bound complex from the unbound cGMP and 1 ml of dH_2O was added to each tube to dissolve the pellet (left for 20-30 min or until dissolved). A volume of 0.95 ml was transferred to scintillation vials containing 5 ml scintillant. Vials were shaken vigorously to mix well and counted for 5 min per vial using a scintillation counter (LS6500 – ^{137}Cs; Beckman Coulter Ltd).

RIA analysis

The radioactivity in each sample is determined as disintegrations per minute (dpm). The dpm data was entered in and analysed with OriginPro 7.5 Client to obtain the amount of cGMP in a sample given as pmol cGMP per mg protein. First, the standard curve data was entered, plotting the dpm counts as a function of pmol cGMP per tube on a logarithmic scale. The data was fitted using the following logistic function:

$$y = \frac{A1 - A2}{1 + (\frac{x}{x_0})^p} + A2$$

Where y is dpm, A1 and A2 are the mean zero cGMP (i.e. top of the standard curve) and mean blank (i.e. bottom of the standard curve) respectively, p is the slope (that should approximate 1), x is pmol cGMP/assay tube and x_0 is the amount of cGMP at which half of the displacement has occurred. Below, in Fig. 2.1, an example of a typical calibration curve obtained in one of my experiments is shown.

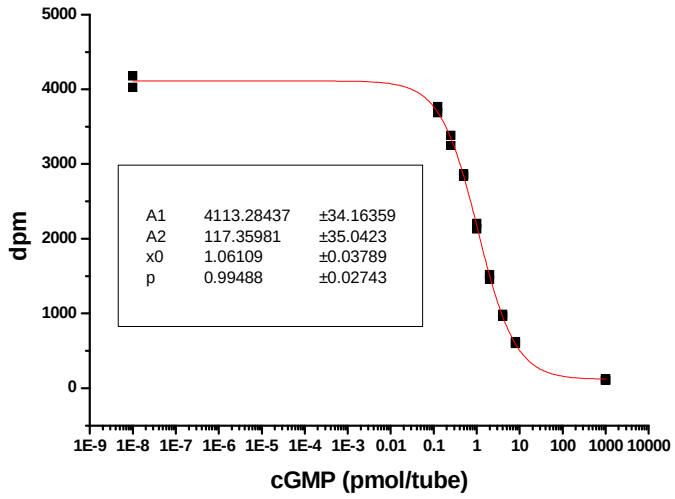

Fig. 2.1. Typical standard curve obtained for RIA

Having obtained the values for A1, A2 and x_0, it is possible to calculate the amount of cGMP in pmol normalised to 'per mg tissue protein', using OriginPro 8. This was achieved by the following series of steps:

- Spread sheet in Origin
- Enter dpm of unknown samples into column(A)
- Set column(B) equal to x
  i.e. $x = x_0 * (((A1 – A2) / (column(A) – A2))-1)$, where x = pmol cGMP per assay tube
- Set column(C) equal to 10 * column(B), giving the amount of cGMP in pmol per ml
- Set column(D) equal to the dilution factor for each sample (e.g. 2 for 1:2 dilution, 5 for 1:5 dilution etc)
- Set column(E) equal to column(C) * column(D), giving pmol cGMP per ml of the original sample
- Enter the concentration of protein (mg protein/ml) of the brain slice that where obtained by means of the protein assay for each sample into column(F)

- Set column(G) equal to column(E)/column(F), giving the amount of cGMP in pmol per mg of tissue protein

All data are presented as means ± SEM obtained from a minimum of three samples in duplicates derived from three different animals. Statistical evaluation of cGMP measurements was carried out in GraphPad InStat version 3 (GraphPad Software, Inc., San Diego, CA, USA) using ANOVA with Dunnett's test, statistical significance being accepted at $P < 0.05$.

*

CHAPTER 3

Mechanism of vasculo-neuronal communication through nitric oxide in optic nerve

3 Mechanism of vasculo-neuronal communication through nitric oxide in optic nerve

3.1 INTRODUCTION

The characteristics of NO set it apart from 'classical' neurotransmitters. Firstly, NO is not produced in advance or stored; additionally, it is freely diffusible and able to cross membranes rapidly. The unique nature of NO is highlighted by its ability to spread out in a three-dimensional fashion. Based on these properties, NO may act on different tissue elements within the brain, irrespective of anatomical connection (Garthwaite & Boulton, 1995; Garthwaite 2008).

Central axons have been proposed as a target for NO (de Vente *et al.*, 1998), but the functional changes it induces are largely unexplored. The optic nerve provides a good model to study white matter function as it consists solely of axons, blood vessels, and glial cells (Waxman *et al.*, 1991; Bolton & Butt, 2005). The NO-cGMP pathway has been shown to play an intriguing role in this tissue (Garthwaite *et al.*, 1999a; Garthwaite *et al.*, 1999b). Stimulation of optic nerves with NO has been demonstrated to induce the generation of cGMP in axons only (Garthwaite *et al.*, 1999b), followed by the finding that NO at high concentrations kills axons (Garthwaite *et al.*, 2002a). In association with the latter finding, it was shown that high concentrations of NO cause a biphasic depolarisation of optic nerve axons, the second large phase being associated with pathological actions of NO (Garthwaite *et al.*, 2002a). The second phase of the depolarisation was found to be blocked by the Na^+ channel blocker TTX, reflecting the Na^+-dependent toxicity under conditions of impaired cellular respiration and ATP loss. In contrast, the earlier small phase of the depolarising response persisted (Garthwaite *et al.*, 2002a). Based on these previous findings, initial work (Garthwaite *et al.*, 2006) was aimed at elucidating the cellular mechanism through which axons depolarise in response to a low concentration of NO. Garthwaite et al. (2006) discovered that the depolarising response induced by low concentrations of exogenous NO was cGMP-dependent, and that the underlying mechanism for this voltage response involved the direct modulation of HCN channels by cGMP, these channels being a potential downstream target for cGMP (see Chapter 1) and having been proposed to reside in the rat optic nerve previously (Eng *et al.*, 1990; Stys *et al.*, 1998). Yet, more strikingly, it emerged that there was a tonic source

of NO in the optic nerve that kept optic nerve axons in a depolarised state under basal conditions, the endogenous NO acting through the same mechanism as exogenous NO (Garthwaite *et al.*, 2006).

After setting out to identify the source of this continuous NO release, it was found that it was NO coming from the capillaries permeating the optic nerve that influences the membrane potential of optic nerve axons (Garthwaite *et al.*, 2006). While NO is usually considered a key player purely in terms of vascular function, communication between neurons and vascular elements is taking place during development, where it has been found that blood vessels send out signals via certain growth factors to aid axonal guidance (Carmeliet & Tessier-Lavigne, 2005). In terms of vascular function, NO is able to reach underlying smooth muscle cells to raise cGMP levels and, consequently, to induce vessel dilatation in large blood vessels over distances of several 100 µm (Martin *et al.*, 1985a; Gold *et al.*, 1990). In contrast, any point in the brain is at most a cell diameter (25 µm) away from a capillary (Pawlik *et al.*, 1981), the endothelial cells of which release NO tonically from the endothelial isoform of NOS (Mitchell & Tyml, 1996). The global levels of NO produced may depend on the geometrical arrangement of capillaries within the tissue (Tsoukias & Popel, 2003), and the three-dimensional arrangement of the capillary network around axons would be able to deliver NO just as well as it distributes O_2 (Garthwaite, 2008). Concerning the expression pattern of endothelial (e)NOS in the brain there have been disagreements in the past. Previous immunohistochemical studies claimed eNOS to be also expressed in some neurons (Dinerman *et al.*, 1994) or in astrocytes (Lin *et al.*, 2007). However, concerning the latter, the specificity and credibility of the staining has not yet been confirmed, and no astrocytic eNOS or neuronal (n)NOS was detected in the rat optic nerve (Garthwaite *et al.*, 2006). For instance in the work by Lin *et al.* (2007), only a very small number of structures appeared to be positive for both eNOS and the astrocytic marker GFAP, and, judging by the nature of the staining, the minor degree of co-localisation is likely to be arising from astrocytic endfeet contacting blood vessels. Additionally, the observations made in terms of eNOS residing in neurons has been disputed (Chiang *et al.*, 1994; Demas *et al.*, 1999) and based on more recent evidence the general notion is accepted of eNOS being primarily located

in endothelial cells (Seidel *et al.*, 1997; Stanarius *et al.*, 1997; Topel *et al.*, 1998; Demas *et al.*, 1999; Blackshaw *et al.*, 2003; Chan *et al.*, 2004). Taking these aspects and the unique characteristics of NO compared with other neurotransmitters into consideration, the possibility of components of the vascular system actively influencing neuronal function becomes readily conceivable.

3.2 AIM OVERVIEW

The overall evidence from preceding work led to the suggestion that the endothelial cells of the capillary network within the optic nerve persistently signal to axons, causing depolarisation by releasing NO from eNOS (Garthwaite *et al.*, 2006). Although direct communication between neurons and the vascular system has been implied, this has only been noted for 'neuron-to-blood vessel' rather than the opposite way around. Fergus & Lee (1997), for example, found that NMDA-evoked vasodilatation of microvessels monitored in a hippocampal slice preparation is diminished upon nNOS inhibition, implicating NO derived from local neurons in close apposition to blood vessels directly participating in the regulation of vascular tone. Foregoing work found expression of both nNOS and eNOS in rat optic nerves, but a lack of iNOS (Garthwaite *et al.*, 2006). However, nNOS was only detected in large blood vessels on the surface of the nerve, frequently co-localising with eNOS, as has been observed in pial blood vessels (Seidel *et al.*, 1997). This was in contrast to the restricted and rich expression pattern of eNOS throughout the microvascular network that runs within the optic nerve (Garthwaite *et al.*, 2006). A number of questions remained to be answered, which would help to further validate the hypothesis of blood vessels directly signalling to axons, and if it merited further examination. Additional experimental evidence was sought to further test the hypothesis that eNOS is indeed the chief endogenous source of NO in the optic nerve. Moreover, the electrophysiological technique used is not a direct readout of the actual changes in membrane potential. Hence, to further evaluate the significance of the findings, the aim was to carry out a calibration to estimate the actual change in

membrane potential, correlating to the DC potential detected by the extracellular recordings. Finally, it was of interest to elucidate the underlying cause of tonic NO release under basal conditions. Production of NO from endothelial cells is stimulated by a variety of factors, such as shear stress, which blood vessels are constantly exposed to, as well as a number of humoral factors, including acetylcholine, vascular endothelial growth factor (VEGF), bradykinin, and oestrogen (Dudzinski *et al.*, 2006). One of the key regulatory mechanisms of eNOS activity at basal level is thought to be the PI3 kinase-Akt phosphorylation pathway, which can mediate a 15- to 20-fold increase in eNOS activity, enabling the enzyme to function even at resting levels of cytosolic Ca^{2+} (Dimmeler *et al.*, 1999; Fulton *et al.*, 1999; Michell *et al.*, 1999; Dudzinski *et al.*, 2006). The present study aimed at investigating whether it is this mechanism prevailing in the rat optic nerve, thereby governing ongoing NO release. The rationale for testing this is not only to follow the mechanism upstream, but also to obtain more evidence that would test further the suggested involvement of eNOS in the proposed scenario. Some of the data that will be presented here have been published in conjunction with data that originated from preceding work (Garthwaite *et al.*, 2006).

3.3 METHODS

3.3.1 Optic nerve preparation and *in vitro* maintenance

Optic nerves *(Fig. 3.1)* from 10- to 11-day-old Sprague Dawley rats were used. All animals were purchased from Charles River UK Ltd. The animals were sacrificed by cervical dislocation followed by decapitation as approved by the UK Home Office Schedule 1 regulations. Following transection of the optic nerves immediately behind the eye, the cranium was cut along the hemisphere-midline and removed. The brain was then gently retracted, which has the effect of pulling the optic nerves through the optic canals, and placed into pre-oxygenated, ice-cold aCSF. Optic nerves were then excised as a pair by severing them from the optic chiasm, leaving a small piece of

chiasm attached, and were then separated by cutting along the midline of the chiasm. A piece of thread was tied to the retinal end, to allow the nerves to be physically manipulated into the chamber. Nerves were then transferred into a flask containing continuously oxygenated cold aCSF, and were left at room temperature to recover for at least 30-60 min before installing the tissue in the recording chamber.

Solutions for K^+ calibration experiments

Nerves were perfused and allowed to stabilise in aCSF composed of the following (in mM): NaCl (120), KCl (2.0), $MgSO_4$ $7H_2O$ (1.19), $NaHCO_3$ (26.0), KH_2PO_4 (1.18), $CaCl_2$ (2.0) and glucose (11.0); the aCSF was equilibrated with 95% O_2 / 5% CO_2; pH (37ºC) = 7.4. Taking into account that the aCSF contained 3.18 mM K^+, appropriate volumes of a 4 mM KCl stock solution were added to the aCSF (Na^+ replaced isotonically with K^+) to expose the nerve to 15, 40, and 130 mM K^+, the depolarising responses to which were recorded.

3.3.2 The grease-gap technique

Principle and method procedure

The isolated optic nerve was mounted in a three-compartment grease-gap recording chamber *(Fig. 3.1)*, similar to the one designed and described in detail by Garthwaite and Batchelor (1996). The principle of the grease-gap method is the imposition of an extracellular resistance formed by a greased barrier separating two chambers of a tissue bath. A voltage change in the middle chamber (where the main body of the nerve lies) leads to intra- and extracellular current flow. The extracellular component of the current generates a voltage between the two sides of the barrier as it flows across the resistance. This voltage change is monitored using Ag/AgCl electrodes. The observed voltage deflection corresponds to voltage changes in the population of axons that cross the barrier, where the amplitude will depend on the quality of the greased seal (i.e. the size of the extracellular resistance). Apart from its simplicity, the

grease-gap technique provides a number of advantages such as stable responses over long periods of time (usually several hours) and a low noise level with a good baseline stability, which allows small potential changes to be detected. In addition, it is a relatively non-invasive method, therefore avoiding tissue damage due to experimental procedure.

The central chamber (0.5 ml capacity) was connected to a pump, allowing continuous perfusion with aCSF with or without test compounds at a rate of 1.5-2 ml/min, and the perfusate was removed by a suction arm in the middle chamber. The recording bath was separated into a three-compartment unit by two pairs of Perspex slats that would be placed on top of each other. The Perspex slats that would be positioned on top of the nerve had a groove so that the nerve would not be crushed. The regions that come into contact with the sides of the recording bath, as well as the grooves of the partitions were greased with Dow Corning High-Vacuum Grease (Cole-Parmer Instrument Company Ltd, London, UK) in order to obtain a good seal that provided the resistance between the chambers. The main body of the nerve was contained in the middle compartment. Once the nerve was installed, the central compartment was immediately perfused with aCSF and the two side-chambers were filled with aCSF to a suitable level but were not perfused. Nerves were left for further recovery until a stable recording baseline was obtained (normally for approximately 1 hour). The whole chamber and the perfusates were kept at 37 ± 0.5°C throughout the experiments and all perfusates were continuously equilibrated with 95% O_2 / 5% CO_2. Experiments were started once a stable baseline had been obtained. Potential changes in response to pharmacological agents were recorded using Ag/AgCl electrodes embedded in agar (see below) and monitored on a personal computer using Clampex 8.0 (Molecular Devices, Palo Alto, CA) for data collection. To check the stability of the recordings and nerve viability, control responses to the NO donor PAPA/NO (1 µM) and/or K^+ (1-3 mM, added as KCl) were obtained before the start and after completion of each recording. Changes in DC potential provided the readout of changes in membrane potential.

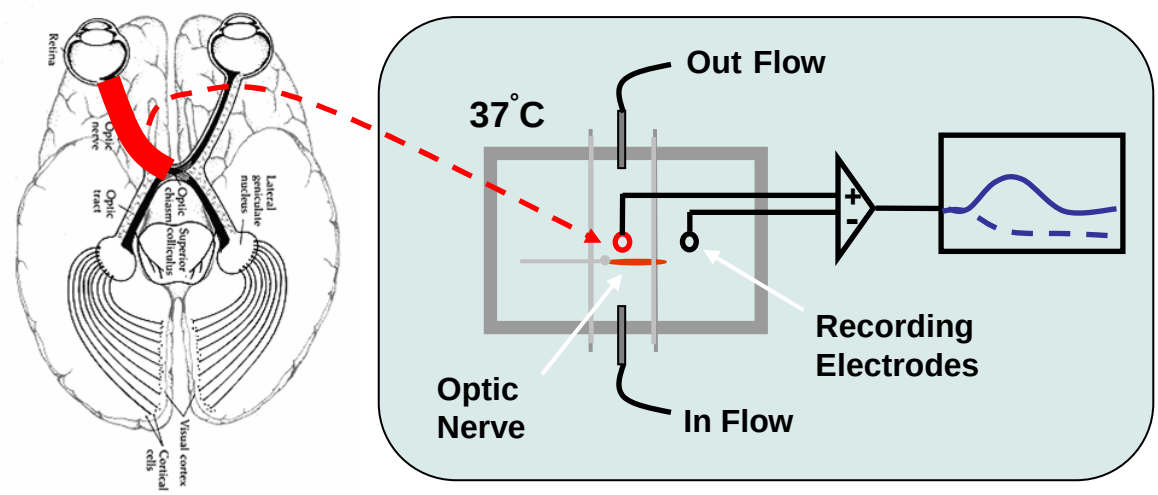

Fig. 3.1. Schematic showing the grease-gap set up

Ingredients and method for Ag/AgCl electrodes:

2 x 2 mm sockets

2 x 20 cm lengths of silver wire (AG10-W 2 m 0.25 mm dia.; Harvard apparatus Ltd)

Rapid Araldite

2 x pipette tips (size P20/P200)

2 x 1 ml syringes

Agar

NaCl solution 0.9%

Chloriding setup (battery and NaCl solution slightly acidified with HCl)

Storage vessels for electrodes

Shorting wire (5 cm wire with 2 mm plug either end)

The silver wire was soldered to the sockets. Two trimmed and bent tips were glued to the end of the syringes with Araldite and left to set. The silver wires were then cleaned with acetone and wound around a metal stick to give a spiral that would fit in the syringes. This was followed by careful cleaning to remove grease, and coating with chloride until the wires had turned black-red-coloured. Subsequently, 100 ml of 4% agar made up in 0.9% NaCl solution was heated in a Pyrex beaker. Once the agar

was dissolved, it was left for a few minutes until the solution was clear and free of air bubbles. The hot agar was sucked up into the syringes to a level that would cover the spiral portion of the wires. With finger over the syringe tip, the spiral was inserted and the socket pushed in firmly. When the agar had cooled enough to stop it from flowing back out, the syringes were returned to the beaker containing agar. This was then left at 4°C allowing it to set completely before removing the electrodes. The electrodes were stored in 0.9% NaCl solution at 4°C. Before starting an experiment the recording electrodes were allowed to equilibrate at room temperature and returned to 4°C after the experiment. A pair of electrodes was usually used for approximately 2-3 months, if their quality was very good. Running down of the quality of the electrodes was normally judged by drifts during the recordings and/or variable control responses in successive experiments.

3.3.3 Western blot

Following isolation (see above for details), optic nerves from 10- to 11- day old Sprague Dawley rat pups were kept in 50 ml Erlenmeyer flasks containing 20 ml pre-oxygenated, ice-cold aCSF. Flasks were transferred to a shaking water bath for a recovery period of 1-2 hours at 37°C with a constant stream of carbogen flowing through the inlet stopper, mimicking the recovery period optic nerves were normally given before commencing electrophysiological experiments. Subsequent to recovery, the PI3 kinase inhibitors LY 294002 and wortmannin were added to their respective flasks for an incubation period of 20 min. In the meantime, control nerves not receiving pharmacological treatment, were snap-frozen over dry ice / iso-pentane into an Eppendorf tube. The same was carried out for the other nerves that had been exposed to PI3 kinase inhibitors following the exposure period. For each condition, at least ten nerves were pooled into one Eppendorf tube in order to obtain plenty of protein for the Western blot. The frozen optic nerves were stored at -80ºC until Western blotting.

Sample preparation

Eppendorf tubes containing the frozen optic nerves were placed on ice and left to thaw (samples were kept cold at all times). Lysis buffer was then added at 100 µl to each tube, followed by addition of PMSF at 1% final concentration. Samples were sonicated, and 10% Triton at 1% final concentration was added to the protein suspension. Samples were spun for 5 min at 6000 rpm at 4ºC, the supernatant placed into a fresh Eppendorf tube (discarding the pellet), and protein contents determined using the BCA Protein Assay kit. 4x loading buffer was added to an appropriate amount of sample (e.g. 12 µl of 4x loading buffer to 36 µl protein sample) followed by loading the samples into the gel pockets (see below). The protein / loading buffer mix was not denatured by boiling at 95ºC before loading the sample onto the gel (when done so, no staining was obtained).

Western blotting

Proteins were separated by means of SDS-polyacrylamid gel electrophoresis loading crude protein homogenate (70 µg) plus loading buffer onto a 4-15% Tris-HCl ready gel (Bio-Rad), loading a total of 40 µl into each well. The gel was then left for 30 min gently shaking in equilibration buffer before proceeding to the protein transfer onto a PVDF membrane. Using electrophoresis, the protein bands were blotted onto a piece of PVDF membrane that had previously been hydrated by soaking it in methanol followed by dH_2O and then equilibration buffer. To achieve the protein transfer, the negative charge was on the side of the gel and the positive charge on the side of the PVDF membrane, so that the negatively charged proteins would be driven over onto the PVDF membrane. Following the blot, the side of the membrane that had been facing down on the gel was marked and the membrane dried at 37ºC. The membrane was stored at 4ºC until proceeding for staining the protein of interest.

Probing for phospho-eNOS (Ser1179) and total eNOS protein

Note: Where not specified, steps were carried out at room temperature.

The PVDF membrane was first re-hydrated by placing it in methanol (shaking) for a couple of minutes followed by a couple of rinses with dH_2O. The membrane was then placed into 1x TBS for 5 min (shaking). Non-specific background binding was blocked by immersing the membrane in 5% dried milk emulsion (made in 1x TBS) for 1-2 hours (shaking). Following blocking, the membrane was washed in 1x TBS (no detergents) for 5 min (shaking). Primary antibody was added made up to its final concentration in 1x TBS containing 5% BSA and 0.075% Tween and left incubating overnight at 4ºC (gently shaking). The final concentrations for the primary antibodies used were 1: 2000 and 1: 1000 for phospho-eNOS and eNOS protein respectively. To prevent protein degradation the preservative sodium azide was added to the antibody dilutions (50 µl of 10% sodium azide per 10 ml). Primary antibody incubation was followed by 3x 5 min washes with washing buffer. Secondary antibody (horseradish peroxidase anti-rabbit) was applied to the membrane at 1: 25 000 made in 1x TBS containing 5% dried milk and 0.05% Tween and left incubating at room temperature for approximately 2 hours (shaking), which was followed by 3x 5 min washes with washing buffer. The membrane was rinsed several times with dH_2O to get rid of any residual detergent contained in the washing buffer. Finally, the membrane was placed into developer solution (1: 1 ratio of SuperSignal West Pico Luminol/ Enhancer solution: SuperSignal West Pico Stable Peroxide solution; Thermo Scientific, Rockford, IL, USA) for 5 min (shaking) and put into the developer cassette. The stained protein blot was developed in the dark room by placing a piece of film into the cassette onto the membrane, which was then developed utilising the X-Ograph Compact X2 film processor (Xograph Imaging systems, Tetbury, Gloucestershire, UK). Following developing, the PVDF membrane was prepared for re-probing with a different primary antibody by leaving it in Restore Western Blot Stripping buffer (Thermo Scientific, Rockford, IL, USA) for 10-20 min at 37ºC, followed by a few rinses with dH_2O. The membrane was let to dry at room temperature on a piece of

filter paper and, if not immediately re-probed, stored at 4ºC. To re-probe the PVDF membrane with a different primary antibody, the above steps were repeated exclusive of the blocking procedure.

3.3.4 Analysis

Electrophysiology

Response amplitudes, when reversible, were measured relative to the interpolated baseline, obtained by fitting a linear regression to 5 min periods on either side. Otherwise, measurements were made relative to the mean voltage during a 5 min period of preceding baseline. The data were analysed using Clampfit 8.0 (Molecular Devices, Palo Alto, CA) and OriginPro 7.5 Client. All data are presented as means ± SEM of a minimum of three experiments obtained from three different animals. Statistical evaluation was carried out in OriginPro 7.5 using Student's *t*-test and statistical significance was accepted at $P < 0.05$.

Western blot

Time of antibody incubations (primary and secondary), washing intervals, and exposure time in developer solution were kept the same between the phospho-eNOS and total eNOS blots. Western blots were captured and then analysed by means of densitometry using the Gel Analysis Software GeneTools (Syngene, Cambridge, UK). This was performed for the bands stained for the phospho-eNOS and total eNOS, the latter serving as the reference which was used for correcting for uneven protein loading. The ratios of the densities of the bands corresponding to phospho-eNOS over the density of the respective bands corresponding to total eNOS protein were determined in arbitrary units and expressed as percentage of controls (i.e. protein from untreated optic nerves). For each condition tested, at least ten nerves were pooled into one Eppendorf tube in order to obtain plenty of protein for the Western blot, and each condition was tested in three independent experiments. The remaining analysis was

carried out in OriginPro 8. Statistical analysis was performed in GraphPad InStat version 3 (GraphPad Software, Inc., San Diego, CA, USA) using ANOVA with Dunnett's test, statistical significance being accepted at $P < 0.05$.

3.4 RESULTS

3.4.1 NOS isoforms responsible for tonic NO production in the optic nerve

Effect of bradykinin, an eNOS stimulator

To test further the hypothesis that eNOS is the endogenous source of NO in the optic nerve by which blood vessels signal to axons, experiments were conducted that investigated the action of bradykinin, a well established stimulator of eNOS in endothelial cells, where the receptors for this endogenous eNOS activator, the bradykinin B_2 receptors, exist in a complex with eNOS (Ju *et al.*, 1998; Marrero *et al.*, 1999; Prado *et al*., 2002).

Exposure of rat optic nerves to bradykinin (300 nM) evoked reproducible depolarisations *(Fig. 3.2a),* peaking after 2-3 min and reversing on washing out the agonist. Both the general NOS inhibitor L-NNA (100 µM) and the NO_{GC} receptor antagonist ODQ (10 µM) caused hyperpolarisations (-0.451 ± 0.074 mV, $n = 4$ for L-NNA; -0.233 ± 0.034 mV, $n = 4$ for ODQ) signifying the loss of basal, tonic NO, and inhibited the bradykinin-evoked depolarisation *(Fig. 3.2b,c,f).* The depolarisation in response to bradykinin was also significantly prevented in the presence of the bradykinin B_2 receptor antagonist HOE-140 (1 µM; *Fig. 3.2d,f*). However, the lack of an obvious hyperpolarising effect of HOE-140 on the basal membrane potential *(Fig. 3.2d)* indicates that endogenous bradykinin is unlikely to contribute to the tonic NO release in rat optic nerve measurably. Measurements were made on random stretches of baseline for the same duration (15-20 min) to account for possible drifts; positive

peaks averaged 0.045 ± 0.009 mV (*n* = 5) and negative peaks averaged -0.060 ± 0.006 mV (*n* = 7), with the average of both in the same records being 0.019 ± 0.002 mV (*n* = 8). The average effect of HOE-140 on the baseline (-0.067 ± 0.0028 mV; *n* = 3) was not significantly different from average fluctuations in the baseline.

To further test if bradykinin is acting through the cellular mechanism suggested for NO-induced depolarisation (Garthwaite *et al.*, 2006), the role of HCN channels was explored. Perfusion of the HCN channel inhibitor ZD 7288 (10 µM) elicited a marked hyperpolarisation (-1.6 ± 0.27 mV, *n* = 4) and prevented the response to bradykinin *(Fig. 3.2e,f)*, implying that HCN channels are mediating the bradykinin-induced depolarisation. Overall, if NO synthesised by eNOS in endothelial cells signals persistently to axons, as indicated by preceding data (Garthwaite *et al.*, 2006), it would be predicted that an agonist that selectively increases eNOS activity evokes a NO-dependent depolarisation through HCN channels that is associated with cGMP formation. The data presented here are consistent with these predictions.

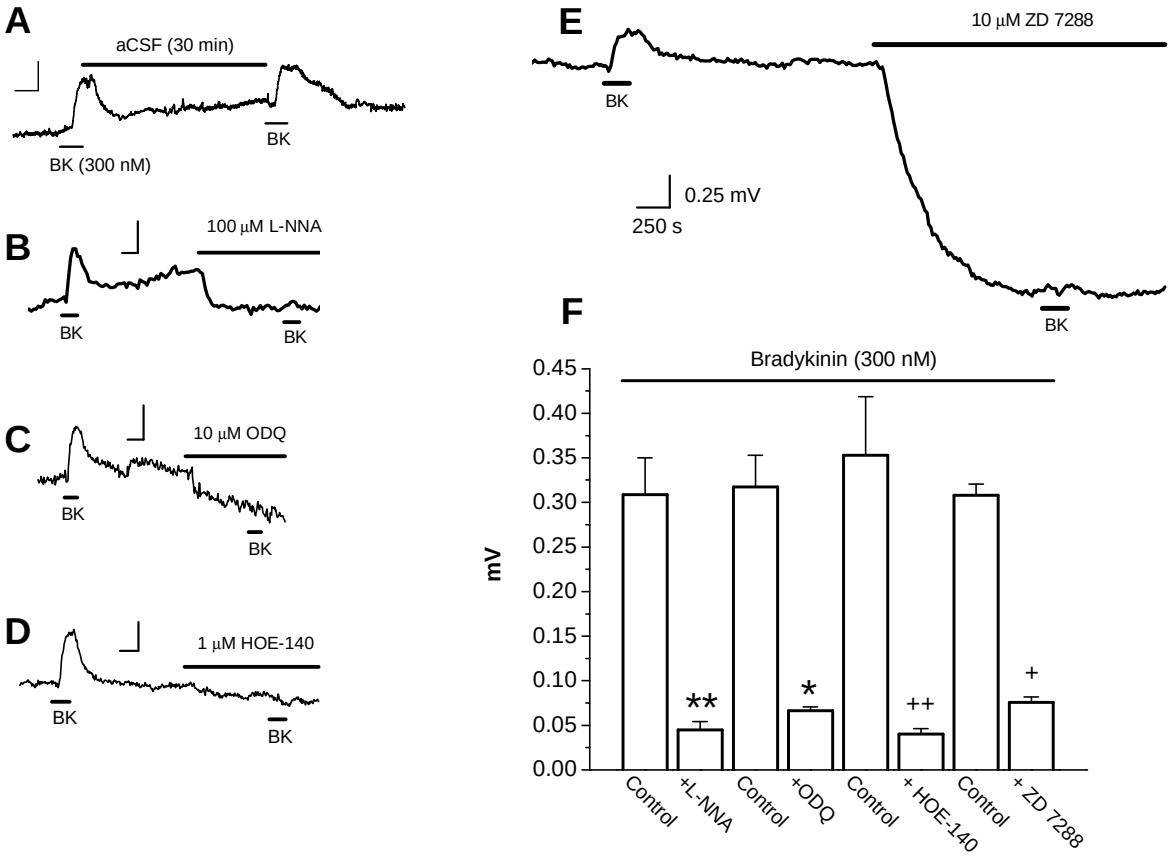

FIG. 3.2. Effect of the eNOS stimulator bradykinin (BK) on rat optic nerve. *A:* BK evokes reproducible depolarisation of optic nerves (n = 4). *B-E:* Inhibition of BK-induced depolarisation by L-NNA (*B*, n = 4), ODQ (*C*; n = 3), HOE-140 (*D*; n = 3) and ZD 7288 (*E*; n = 4). *F:* Summary data for experiments illustrated in *B-E* (n = 3-4; $^{**}p < 0.009$, $^{*}p < 0.002$, $^{++}p < 0.001$, $^{+}p < 0.00001$). *Note:* Applications of compounds in *A-E* were for the duration shown by the horizontal bars. The scaling in *E* applies to all scale bars.

Possible involvement of NOS isoforms other than eNOS

Although foregoing data (Garthwaite *et al.*, 2006) as well as data presented here strongly imply eNOS as the main source responsible for the ongoing NO synthesis in optic nerves, more evidence was sought to exclude the possible involvement of other NOS isoforms in the rat optic nerve. One way to test the involvement of nNOS more directly would be the use of mice lacking the gene for nNOS. However, such knock-out mice are problematic due to remaining

compensatory active splice variants (see Chapter 1). Therefore, instead, a pharmacological approach was adopted to investigate this issue, utilising three inhibitors (NPA, L-VNIO and 1400W) that have been shown to have good selectivity for nNOS over eNOS in enzymatic studies (Babu & Griffith, 1998; Bretscher *et al.*, 2003; Erdal *et al.*, 2005) and in whole tissue (Hopper & Garthwaite, 2006). This also provided a way of testing for the involvement of iNOS, as one of the compounds (1400W) also inhibits iNOS more potently than eNOS (and nNOS; Garvey *et al.*, 1997).

Perfusion of the nerves with the nNOS/iNOS inhibitor 1400W (1 µM), or the nNOS inhibitors L-VNIO (100 nM) or NPA (1 µM) had no significant antagonistic effect on the bradykinin-evoked depolarisation, the hyperpolarisation caused by L-NNA (100 µM) being retained *(Fig. 3.3a-d)*. Also, no significant effect was observed on the baseline under basal conditions during pre-incubation of these inhibitors (-0.056 ± 0.0043 mV, n = 5 for 1400W; -0.085 ± 0.0093 mV, n = 4 for L-VNIO; -0.062 ± 0.007 mV, n = 3 for NPA) as compared to fluctuations in the baseline (see above). These data suggest that there is no measurable contribution of the other NOS isoforms to the tonic level of NO in the optic nerve, or to the increase in NO in response to bradykinin. Taken together, these data further strengthen the implication that eNOS as is the principal endogenous NO source.

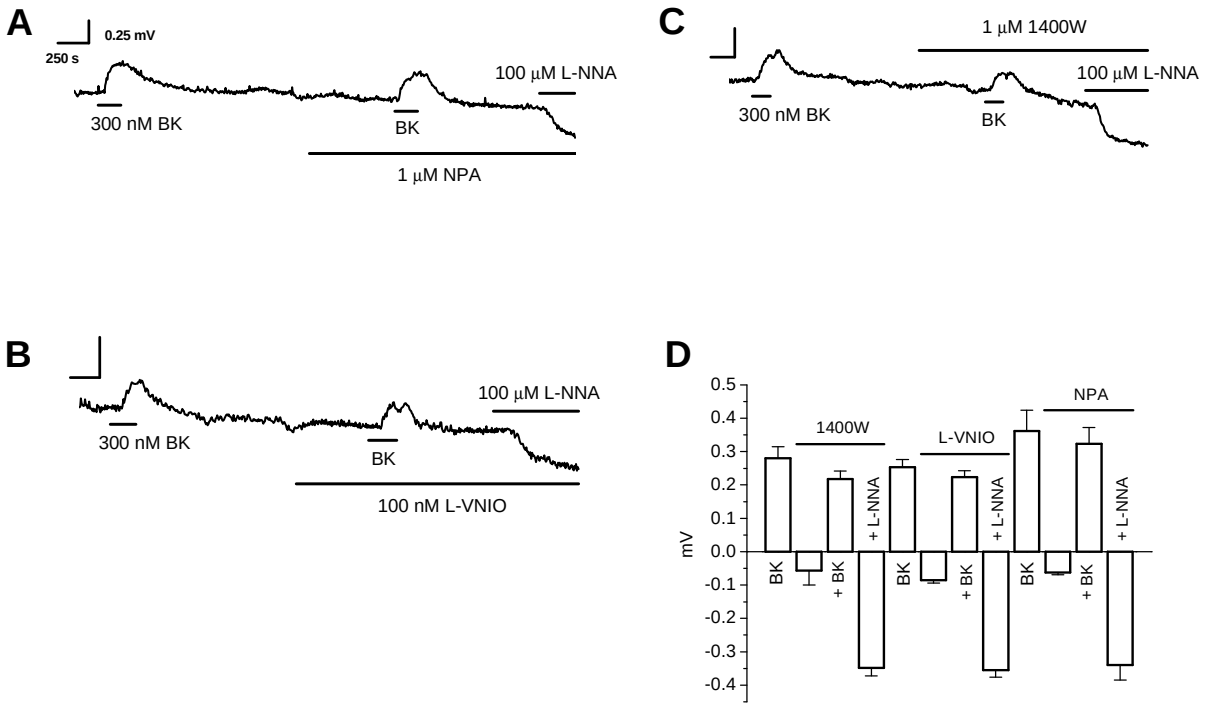

FIG. 3.3. Testing for the role of nNOS and iNOS in tonic NO production in the rat optic nerve. *A-C:* Compounds inhibiting nNOS (NPA, *A*; L-VNIO, *B*; 1400 W, *C*) and iNOS (1400W, *C*) had no significant antagonistic effect on the depolarisation elicited by bradykinin (BK) and, unlike L-NNA, did not cause a noticeable hyperpolarisation. In the presence of the nNOS/iNOS inhibitors, L-NNA retained its hyperpolarising action of the usual magnitude that was observed in experiments discussed and illustrated earlier. *D:* Summary data for experiments illustrated in *A-C* (n = 3-5). *Note:* Applications of compounds in *A-C* were for the duration shown by the horizontal bars. The scaling in *A* applies to all scale bars.

3.4.2 Estimation of the true magnitude of membrane potential changes that occur using the grease-gap technique

To estimate the true magnitude of the membrane potential changes obtained from recordings using the grease-gap method, calibration experiments were carried out that were based on a previously adopted approach (Stys *et al.*, 1993; Leppanen & Stys, 1997). Voltage responses to PAPA/NO (1 μM) were recorded at the beginning of each experiment (0.44 ± 0.13 mV; n = 4), serving as a control for nerve viability and recording stability. This was followed by perfusing the nerve with ascending

concentrations of K^+ (15 mM, 40 mM and 130 mM; added as KCl), correcting for junction potentials before each application and during the plateau phase of the depolarisation evoked by K^+. Sufficient wash-out time was allowed after each application until the response had returned to baseline. Presuming an intracellular K^+ concentration of 130 mM in the rat optic nerve (Stys *et al.*, 1993; Leppanen & Stys, 1997; Stys *et al.*, 1997), the application of 130 mM K^+ should drive the membrane potential to near zero. The mean recorded depolarisation under these conditions at steady state were 18.9 ± 2.4 mV (*n* = 4; *Fig. 3.4*). Mean depolarisation at steady-state in response to 15 and 40 mM K^+ solution were 4.4 ± 0.64 mV and 11.7 ± 1.9 mV, respectively (*n* = 4; *Fig. 3.4*). The ratios of the responses to isotonic (130 mM) K^+ solution and to PAPA/NO were very similar in the different nerves, ranging from 39 to 46 (mean: 43 ± 1.7, *n* = 4). The mean magnitude of depolarisation in response to each of the tested K^+ concentrations was obtained, and a value of -80 mV was assumed for the resting membrane potential of the optic nerve (Stys *et al.*, 1997). From these data it was possible to estimate (from the Goldman equation) the actual membrane potential at each of the respective K^+ concentrations *(Fig 3.4).* Having determined that a mean depolarisation of 18.9 mV in response to isotonic K^+ solution corresponds to a shift in membrane potential from -80 to 0 mV *(Fig. 3.4),* it is possible to estimate the true magnitude of membrane potential changes occurring in the experiments in response to pharmacological agents. The results obtained from these calibration experiments imply that the actual mean depolarisation produced by 1 µM PAPA/NO is approximately 2 mV, while the size of the ZD 7288-evoked hyperpolarisation corresponds to an actual change of about 6-8 mV (Garthwaite *et al.*, 2006). The overall scope of NO for altering the membrane potential in optic nerve axons is approximately 6 mV.

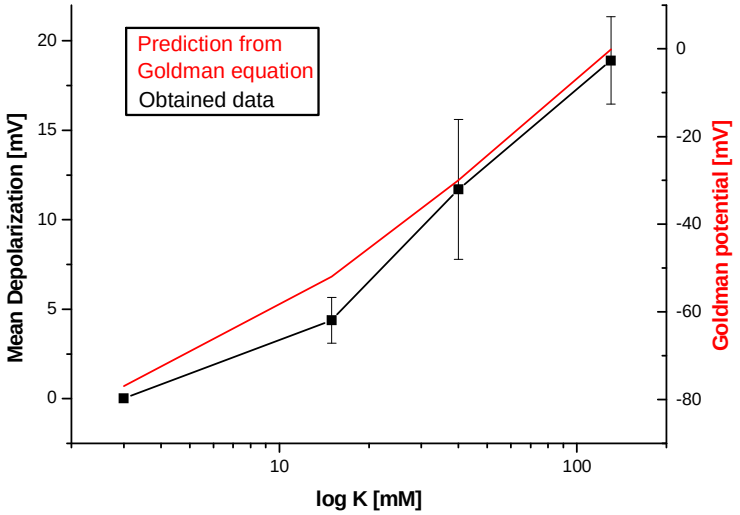

FIG. 3.4. Calibration experiments for estimation of the true value of membrane potential changes in rat optic nerve, recorded by means of the grease-gap recording method. The magnitude of the depolarisations in response to ascending K^+ concentrations were in close relation with the changes in membrane potential that would be predicted by the Goldman equation, assuming the same extracellular K^+ concentrations.

The above was determined from the Goldman equation as follows:

Goldman equation is given as

$$E = \frac{RT}{zF} \ln \frac{P_K[K^+]_o + P_{Na}[Na^+]_o + P_{Cl}[Cl^-]_i}{P_K[K^+]_i + P_{Na}[Na^+]_i + P_{Cl}[Cl^-]_o}$$

As estimated previously (Stys *et al.*, 1993; Leppanen & Stys, 1997; Stys *et al.*, 1997), in the rat optic nerve $[K^+]_i$ is 130 mM ($[K^+]_o$ = 3 mM), $[Na^+]_i$ is 25 mM ($[Na^+]_o$ = 146 mM), and $[Cl^-]_i$ is 55 mM ($[Cl^-]_o$ = 122 mM), the permeability ratios being 35:1:0.1 for P_K:P_{Na}:P_{Cl} (Stys *et al.*, 1993; Leppanen & Stys, 1997). Incorporating these ion concentrations that have been estimated to prevail in the rat optic nerve (Stys *et al.*, 1993; Leppanen & Stys, 1997; Stys *et al.*, 1997) into the Goldman equation predicts a resting potential of -77 mV, a value consistent with previous experimental determinations of the resting membrane potential (Stys *et al.*, 1997). The respective

concentrations of K^+ applied in the experiments (i.e. 15, 40 and 130 mM) were incorporated into the Goldman equation, giving a number of values for the resting membrane potential that would exist at these respective extracellular K^+ concentrations. This ultimately provided the calibration curve against which it would be possible to estimate the magnitude of change in the membrane potential *(Fig. 3.4)*.

3.4.3 Underlying cause of tonic NO synthesis – role of PI3 kinase

One of the key mechanisms for maintaining tonic eNOS activity in endothelial cells is phosphorylation of the enzyme, in part through the PI3 kinase-Akt pathway (Dimmeler *et al.*, 1999; Fulton *et al.*, 1999; Michell *et al.*, 1999; Dudzinski *et al.*, 2006). The following sets of experiments investigated whether this mechanism is also responsible for the continuous NO release from eNOS in optic nerves. If the endogenous NO level in rat optic nerves is sustained through this phosphorylation pathway, inhibition of the PI3 kinase should occlude the hyperpolarising response to a general NOS inhibitor, and *vice versa*. Inhibition of PI3 kinase would be expected to cause hyperpolarisation in itself, which should be prevented upon NO_{GC} receptor inhibition presuming that the NO is acting via its receptors and cGMP accumulation. To test these assumptions, the general NOS inhibitor L-MeArg (100 µM) was used. In contrast to the previously used inhibitor L-NNA, L-MeArg is reversible, which was a requisite in this set of experiments. It has been shown in earlier work that this reversible NOS inhibitor causes hyperpolarisation repeatedly, given that sufficient time is allowed for wash-out of the compound (Garthwaite *et al.*, 2006).

Two different PI3 kinase inhibitors, wortmannin (1 µM) and LY 294002 (30 µM), both induced comparable hyperpolarisations which were, however, of slightly smaller magnitude than that seen in response to the general NOS inhibitor (wortmannin *vs.* L-MeArg: 0.24 ± 0.03 *vs.* 0.37 ± 0.07 mV; LY 294002 *vs.* L-MeArg: 0.25 ± 0.01 *vs.* 0.34 ± 0.03 mV; n = 4-6; *Figs. 3.5c and 3.6c*). Both PI3 kinase inhibitors partly prevented the hyperpolarisation caused by L-MeArg *(Fig. 3.5a,b,c)*, whereas the hyperpolarisations evoked by the PI3 kinase inhibitors were occluded

when L-MeArg was added beforehand *(Fig. 3.6a,b,c)*. Upon inhibition of the NO_{GC} receptors by ODQ (10 µM) the hyperpolarisations to both wortmannin and LY 294002 were prevented *(Fig. 3.7a,b,c)*, confirming that the PI3 kinase inhibitors act through inhibition of NO which acts via its guanylyl cyclase-coupled receptors. In all experiments, control voltage responses to PAPA/NO (1 µM) were recorded which were of the usual magnitudes found in previous experiments (Garthwaite *et al.*, 2006), and were unaffected in the presence of PI3 kinase or general NOS inhibitors (0.34 ± 0.03 *vs.* 0.39 ± 0.04 mV in the presence of inhibitors). However, as would be expected, the response to PAPA/NO was prevented in the presence of ODQ *(Fig. 3.7a,b,c)*. In summary, these data suggest that the tonic NO release from eNOS in the rat optic nerves is, at least partly, maintained by PI3 kinase-mediated phosphorylation.

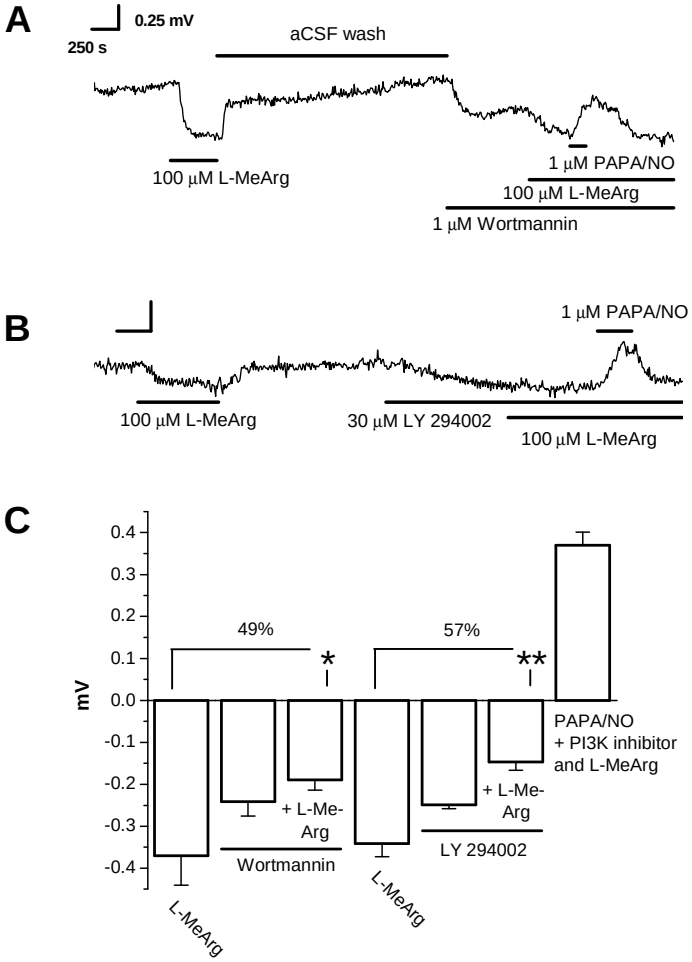

FIG. 3.5. Effect of PI3 kinase inhibition on the response to a general NOS inhibitor. *A-B:* The hyperpolarising action of L-MeArg was partially prevented by both PI3 kinase inhibitors, wortmannin (*A*; $n = 6$) and LY 294002 (*B*; $n = 4$), while the PI3 kinase inhibitors alone produced a hyperpolarising response. The PAPA/NO-evoked depolarisation was not different from what is usually observed under normal conditions. *C:* Summary data for experiments depicted in *A* and *B*. The mean hyperpolarising effect of L-MeArg was greater as compared to that in response to wortmannin or LY 294002, and was partially prevented by both PI3 kinase inhibitors ($n = 4$-6; $*p < 0.03$, $**p < 0.002$). *Note:* Applications of compounds in *A* and *B* were for the duration indicated by the horizontal bars. The scaling in *A* applies to all scale bars.

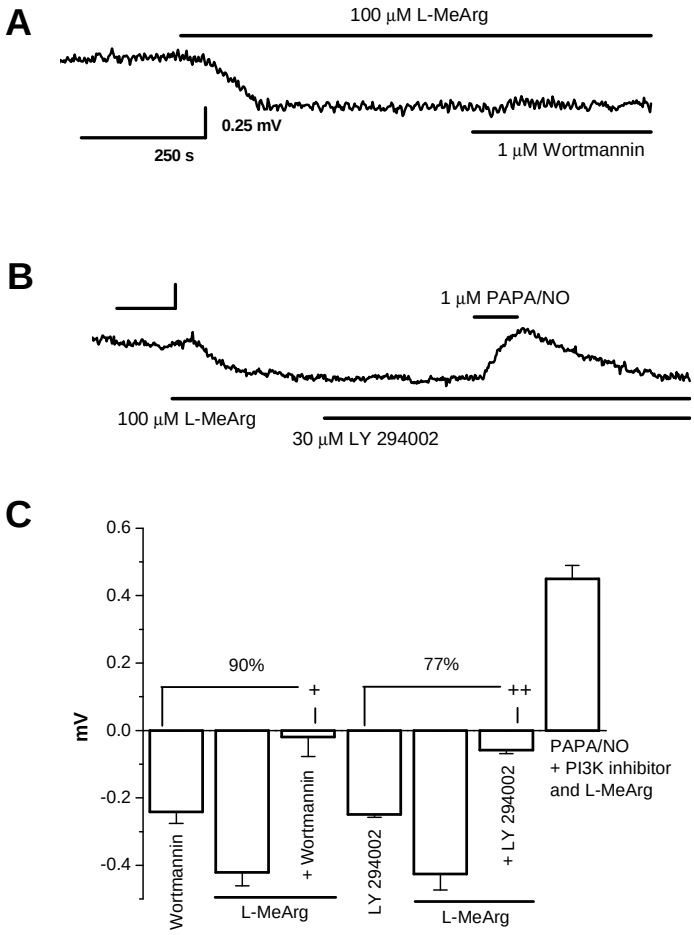

FIG. 3.6. Effect of NOS inhibition on the response to PI3 kinase inhibitors. *A-B:* The hyperpolarising effect of both, wortmannin (*C*; $n = 4$) and LY 294002 (*D*; $n = 4$), was near to completely occluded in the presence of L-MeArg, the latter having the usual hyperpolarising effect under control conditions. The voltage responses to PAPA/NO remained unaffected, as compared to what is usually observed under control conditions. *C:* Summary data for experiments shown in *A* and *B* ($n = 4$; $^{+}p < 0.008$, $^{++}p < 0.001$). *Note:* Applications of compounds in *A* and *B* were for the duration indicated by the horizontal bars. The scaling in *A* applies to all scale bars.

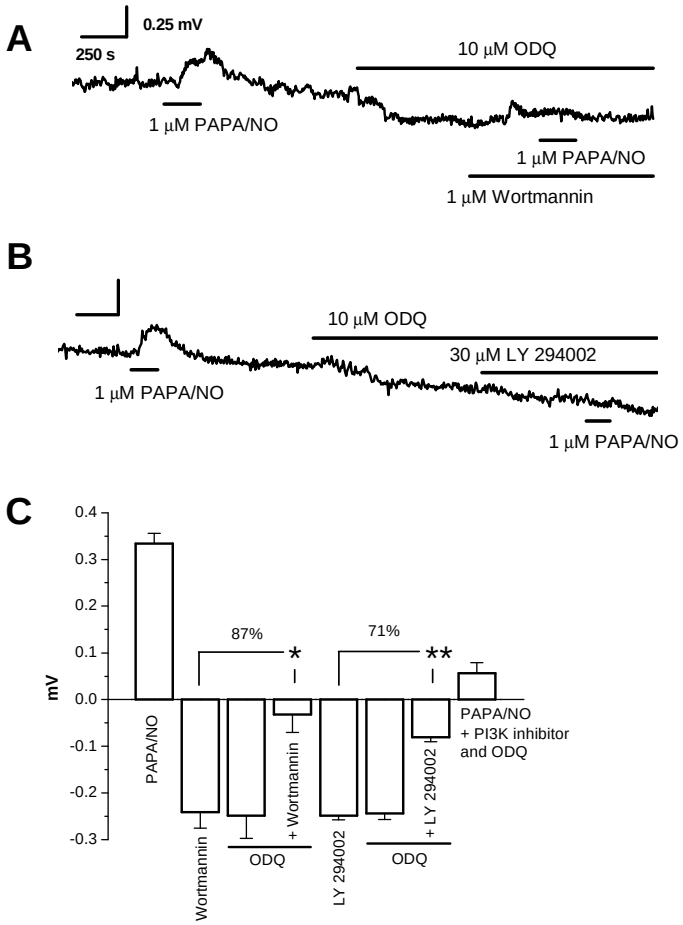

FIG. 3.7. Role of the PI3 kinase phosphorylation pathway in the maintenance of tonic NO release from eNOS in rat optic nerve – cGMP dependence. *A-B:* The hyperpolarisation induced by wortmannin (*E*; $n = 4$) or LY 294002 (*F*; $n = 4$) was prevented by ODQ, as was, expectedly, the PAPA/NO-evoked depolarisation. *C:* Summary data for experiments illustrated in *A* and *B* ($n = 4$; $*p < 0.004$, $**p < 0.001$). *Note:* Applications of compounds in *A* and *B* were for the duration indicated by the horizontal bars. The scaling in *A* applies to all scale bars.

Quantitative evaluation of eNOS phosphorylation by means of Western blotting

As the data derived from the electrophysiological experiments only provide circumstantial evidence with regard to the involvement of the PI3 kinase pathway in eNOS phosphorylation, Western blotting was employed in order to investigate this more directly. Optic nerves were exposed *in vitro* to either LY 294002 (30 μM) or

wortmannin (1 µM) and then snap frozen before proceeding to perform Western blotting. Control nerves were treated in the same way except for the exposure to PI3 kinase inhibitors. Antibodies directed against phosphorylated eNOS at the residue serine 1179 (S1179) or to total eNOS protein were used. This provided the possibility to try evaluating, first, the amount of phosphorylated eNOS protein relative to total eNOS protein, and, secondly, whether the amount of basal phosphorylated eNOS was reduced after optic nerves had been exposed to the PI3 kinase inhibitors LY 294002 or wortmannin. As determined by means of densitometry, and normalised to total eNOS protein to correct for uneven protein loading, neither of the PI3 kinase inhibitors led to a detectable decline in the degree of phosphorylation of native eNOS at S1179 *(Fig. 3.8)*.

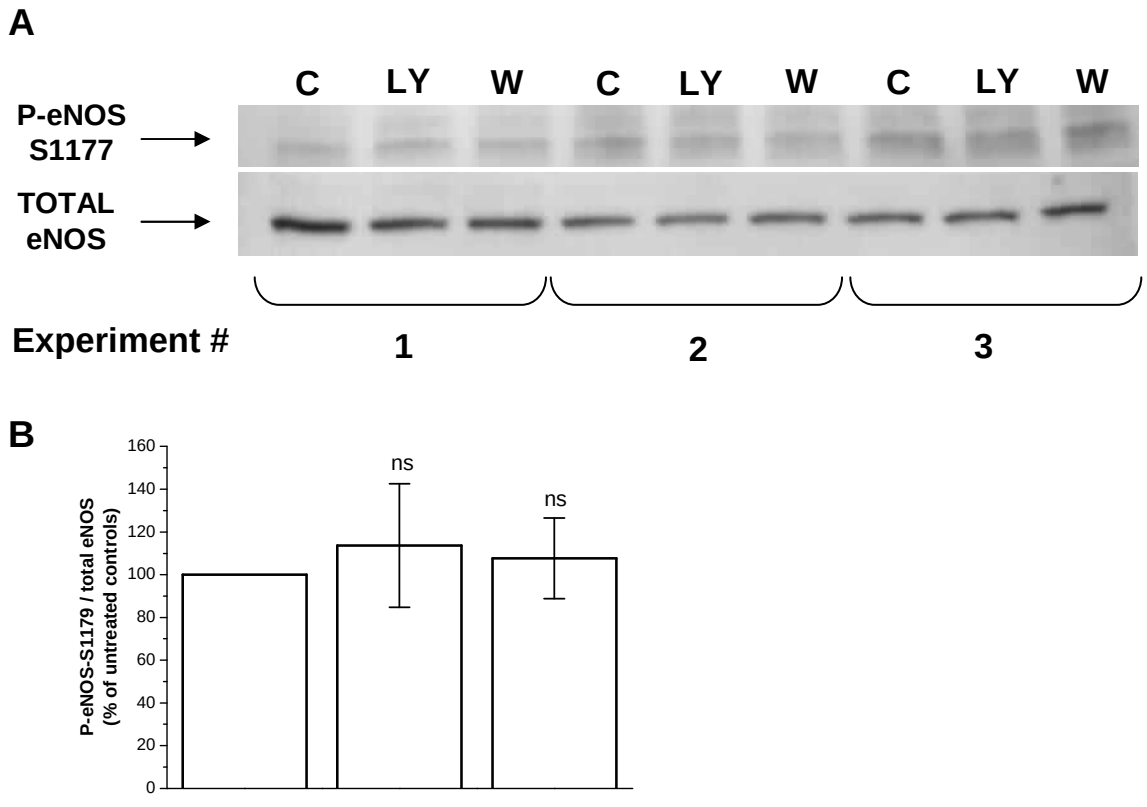

FIG. 3.8. Effect of PI3 kinase inhibition on eNOS phosphorylation as determined by means of Western blotting. *A:* Representative Western immunoblots of phospho-eNOS-S1179 (top row) and total eNOS (bottom row) in the absence or presence of LY 294002 (30 µM) or wortmannin (1 µM). *B:* Summary data for experiments illustrated in *A* (n = 3; $^{ns}p > 0.05$). The ratio of the densities of phophorylated-eNOS-S1177 bands to their respective total

eNOS bands was determined in arbitrary units. Each bar represents the mean ± SEM of phospho-eNOS / total eNOS expressed relative to the results obtained from untreated control optic nerves. C, control (i.e. untreated optic nerves); LY, LY 294002-treated nerves; W, wortmannin-treated nerves; P-eNOS S1179, phospho-eNOS-Ser-1179

3.5 DISCUSSION

Data from foregoing work (Garthwaite *et al.*, 2006) pointed to an intriguing concept, in which two distinct structures, namely blood vessels and axons, display an unexpected sequence of communication. These data suggested a scenario in which endothelial cells of the microvasculature permeating the optic nerve persistently signal to optic nerve axons by releasing NO derived from eNOS. The ultimate result of the NO signal was axonal depolarisation, the underlying transduction pathway engaging cGMP-mediated HCN channel modulation. The results presented here address several questions, which required answering to further confirm the proposed hypothesis of blood vessels actively influencing axonal function. The current work provides further evidence indicating that eNOS is the chief contributor to tonic NO synthesis in the rat optic nerve, and suggests that basal eNOS activity is partially maintained by a PI3 kinase-mediated mechanism.

Direct signalling from blood vessels to neurons is a relatively unusual concept, and further evidence was sought that would test whether eNOS is indeed the principal source of NO in the optic nerve that influences the axonal membrane potential (Garthwaite *et al.*, 2006). Display of the right characteristics upon eNOS stimulation with bradykinin provided further indication concerning eNOS being the tonic NO source, including bradykinin-evoked depolarisation that is prevented upon NOS and NO_{GC} receptor inhibition and mediated by HCN channels. Moreover, the lack of effect of pharmacological tools that exhibit selective inhibition of nNOS (and iNOS) over eNOS further argues against the participation of NOS isoforms other than eNOS in the proposed scenario, which is in support of foregoing findings (Garthwaite *et al.*, 2006). Also the observation of HCN channel inhibition evoking hyperpolarisation is

in line with previous work (Garthwaite *et al.*, 2006). HCN channels have been implicated in the control of pacemaker and oscillatory activity in the heart and brain respectively (see Chapter 1), setting of the resting membrane potential, as well as control of membrane resistance, dendritic integration and regulation of synaptic transmission (Robinson & Siegelbaum, 2003; Wahl-Schott & Biel, 2009). Central axons express HCN channels (Notomi & Shigemoto, 2004), and the current conducted by these channels has been proposed to be important in maintaining reliable conduction by counteracting membrane hyperpolarisation during high-frequency activity in axons. It has been proposed that activity-dependent hyperpolarisation as a result of the high activity of the electrogenic Na^+/K^+ pump during repetitive action potential firing, Na^+ being extruded out of the cell to oppose the large net-influx of Na^+ that results from high-frequency neuronal activity, is counteracted by I_h (Grafe *et al.*, 1997; Soleng *et al.*, 2003; Robinson & Siegelbaum, 2003). This is suggested to be related to I_h conducting a Na^+ inward current into the axoplasm, resulting in depolarisation. This in turn would drive the membrane potential back to its resting level, assisting the cell to reach threshold for triggering the next action potential. The finding that inhibition of HCN channels leads to membrane hyperpolarisation indicates that I_h is active at the resting membrane potential of the rat optic nerve, NO apparently setting the resting membrane potential, and, possibly, influencing excitability and reliable conduction via cGMP-mediated HCN channel modulation. The I_h conducted by HCN channels has also been demonstrated in retinal ganglion cells (Tabata & Ishida, 1996), where I_h is proposed to be activated during and following hyperpolarising light responses, transiently enhancing excitability after termination of light stimuli. A mechanism engaging NO-cGMP-mediated modulation of HCN channels may help explain why block of NOS activity inhibits light-evoked compound action potentials in the optic nerve (Maynard *et al.*, 1995), while modulation of dendritic or somatic HCN channels by the NO-cGMP signalling pathway may affect neuronal firing threshold or pattern (Pape & Mager, 1992; Abudara *et al.*, 2002).

The reason for using the isolated rat optic nerve preparation is its well established utility as a white matter model, allowing reproducible, quantitative

measurements of white matter function *in vitro* (Waxman *et al.*, 1991; Bolton & Butt, 2005). The cellular population of the optic nerve comprises axons of the retinal ganglion cells, glial cells and capillaries (Forrester & Peters, 1967; Butt & Ransom, 1993). Myelination begins around the sixth postnatal day and proceeds rapidly so that at the end-point of development the entire axonal population is fully myelinated. Also, there is an increase in size as maturation of the optic nerve ensues. Neonatal optic nerve axons have a diameter of about 0.14 µm, in contrast to a diameter of about 0.8 µm in the case of adult optic nerve axons (Forrester & Peters, 1967; Foster *et al.*, 1982). This study uses 10- to 11-day-old rat optic nerves which have been shown to have an average axonal diameter of approximately 0.4 µm, containing mixed populations of axons with respect to the degree of myelination and diameter (Foster *et al.*, 1982). The electrophysiological method used here is a standard extracellular gap technique, advantages of which include stable recordings over long periods of time, allowing repeatable drug wash-in and wash-out, as well as the monitoring of the average membrane potential of all axons of the optic nerve. In common with all extracellular recording methods, however, the grease-gap technique does not give the real value of membrane potential. Hypothetically, one could carry out intracellular patch-clamp recordings from axons. However, such an approach to record directly from optic nerve axons is not practical due to the small axonal diameter compared to the diameters of patch or sharp electrodes and would be highly unlikely to yield stable, long duration recordings. Since the electrophysiological technique used is not a direct readout of the actual changes in membrane potential, it was necessary to quantify these findings further. Calibration experiments estimated an actual shift in membrane potential of 2 mV in response to the NO donor PAPA/NO, and 6 mV for the overall scope of NO altering the membrane potential in optic nerve axons. Studies that looked at HCN channel modulation by NO-cGMP signalling in neurons (Pape & Mager, 1992; Ingram & Williams, 1996; Abudara *et al.*, 2002; Pose *et al.*, 2003; Kim *et al.*, 2005) observed effects on the membrane potential that are comparable with that observed on optic nerves. In addition, a small depolarisation of the presynaptic membrane potential has been shown to lead to enhanced probability of neurotransmitter release in rat brainstem (Awatramani *et al.*, 2005). Also, an

analogous modulation of membrane properties by tonic endogenous NO-cGMP signalling has been observed on rat striatal neurons *in vivo* (West & Grace, 2004).

Although a Ca^{2+}-dependent enzyme, eNOS is subjected to additional regulation through multiple phosphorylation sites, the tonic activity achieved also at resting levels of cytosolic Ca^{2+} being mainly attributable to PI3 kinase-Akt-mediated phosphorylation (Dudzinski *et al.*, 2006). The present study investigated whether it is this mechanism prevailing in the rat optic nerve, thereby governing ongoing NO release. The observation about NO tonically depolarising optic nerve axons is revealed as a membrane hyperpolarisation upon NOS inhibition. If NO maintains a constant depolarisation via PI3 kinase-mediated eNOS phosphorylation, exposure of the optic nerve to a PI3 kinase inhibitor should also evoke a hyperpolarisation, which in itself should be prevented in the presence of a broad spectrum NOS inhibitor. Moreover, the hyperpolarisation in response to the general NOS inhibitor should also be reduced in the presence of a PI3 kinase inhibitor. Moreover, the action of the PI3 kinase inhibitor would be sensitive to inhibition of the relevant mechanism, namely NO acting via its guanylyl cyclase-coupled receptors in axons (Garthwaite *et al.*, 2006). The results presented here are in line with these predictions, indicating a participation of the PI3 kinase pathway in sustaining tonic NO release from eNOS under resting conditions. However, while the hyperpolarisations in response to either of the used PI3 kinase inhibitors (wortmannin and LY 294002) were occluded in the presence of the general NOS inhibitor L-MeArg, only partial inhibition was observed *vice versa* (57% inhibition of L-MeArg-evoked hyperpolarisation by LY 294002 *vs.* 49% by wortmannin). This indicates only partial involvement of the PI3 kinase pathway, which is consistent with the PI3 kinase inhibitors evoking smaller hyperpolarisations than the broad-spectrum NOS inhibitor. One may ask why a broad-spectrum NOS inhibitor occludes the response observed upon application of the PI3 kinase inhibitors but not *vice versa*. This could possibly be answered by considering the point of the signalling pathway at which these inhibitors act. Applying the broad-spectrum inhibitor blocks the activity of NOS overall as it prevents the binding of L-arginine, the substrate required for NO formation (see Chapter 1). In contrast,

applying PI3 kinase inhibitors will only block that aspect of NOS activity regulation, meaning that any other factor, such as for example small fluctuations in the intracellular Ca^{2+} concentration, could still contribute to keeping eNOS to some degree active. Furthermore, from these types of experiments it is not possible to know whether the total eNOS population is in a phosphorylated state. It is likely that only a partial eNOS population is under the control of PI3 kinase-mediated phosphorylation, while the remaining population maintains tonic activity via a different regulatory mechanism.

There are proteins, for example, that may interact with eNOS and regulate its activity positively (Fulton *et al.*, 2001; Fleming & Busse, 2003). These include hsp90, which generally exists in association with eNOS within endothelial cells (Garcia-Cardena *et al.*, 1998). Furthermore, multiple phosphorylation sites on eNOS have been recognised, and it is suggested that there may still be more, as yet unidentified, sites (Boo & Jo, 2003; Mount *et al.*, 2007). Additionally, phosphorylation of eNOS at different sites can be regulated not only by PI3 kinase or its downstream kinase Akt, but also by various other protein kinases, such as PKA (Butt *et al.*, 2000; Boo *et al.*, 2002a; Boo *et al.*, 2002b; Michell *et al.*, 2002), PKG (Butt *et al.*, 2000), AMPK (Chen *et al.*, 1999; Thors *et al.*, 2004) and CaMKII (Fleming *et al.*, 2001). A further complication is the regulation of eNOS phosphorylation by different phosphatases, including PP2A, PP1 and calcineurin (Boo & Jo, 2003; Fleming & Busse, 2003; Mount *et al.*, 2007). In summary, the above demonstrates the complexity that underlies eNOS regulation. The main site of eNOS phosphorylation is considered to be the Ser-1179 (Dudzinski *et al.*, 2006). In the light of this, it has been shown, for example, that this residue on eNOS may be phosphorylated by at least five different protein kinases, including Akt (e.g. Butt *et al.*, 2000; Fleming *et al.*, 2001; Thors *et al.*, 2004). Moreover, different protein kinases may phosphorylate a number of different sites on eNOS (e.g. Chen *et al.*, 1999; Butt *et al.*, 2000; Michell *et al.*, 2002). Taken as a whole, which site on eNOS is phosphorylated or dephosphorylated by which protein kinase or phosphatase may depend on factors such as vascular type or origin, and on the general cellular context as well as on the given stimuli (Michel & Feron, 1997; Shaul, 2002). Overall, participation of any of the above mentioned

factors could account for the only partial contribution of PI3 kinase in the optic nerve with regard to tonic NO synthesis from eNOS.

Investigating the effects of PI3 kinase inhibitors on basal eNOS phosphorylation by means of Western blotting resulted in a discrepancy with the foregoing electrophysiological data. There was no detectable decline in the degree of basal eNOS phosphorylation in rat optic nerves that had been treated with LY 294002 or wortmannin as compared to control nerves. One possibility is that the effects of the inhibitors observed in the electrophysiological experiments are due to these inhibitors acting on some other unknown factor which ultimately contributes to tonic NO-mediated cGMP synthesis in the rat optic nerve. Alternatively, it can be argued that Western blotting is too insensitive to detect a change in basal eNOS phosphorylation upon PI3 kinase inhibition at the whole tissue level that may nevertheless be enough to bring about a change in eNOS output seen as hyperpolarisations in the electrophysiological experiments. Although this methodology is popularly used to establish the presence of a given protein, it is not suitable for detecting changing levels for all proteins – especially not relatively small changes. Large, obvious changes may be easily detectable as against a background of small variations caused by possible artefacts. However, the present work is investigating basal, unstimulated eNOS phosphorylation and several aspects of this method may make the detection of smaller changes problematic. Given that the bands appearing for S1179-phosphorylated eNOS are already fairly weak and undefined this may indicate that one is already at the verge of the detection limit. It should be taken into consideration that aspects such as differences in the background intensity are not taken into account, as the measurements obtained from the densitometry analysis do not correspond to absolute peak values from which the respective background densities had been subtracted. Additionally, the slightest variation in band density brought about perhaps artefactually, such as for example uneven film exposure or the slightest smearing of the bands at the edges of the blot, could make substantial differences to the values obtained later in the analysis, especially when dealing with relatively weak bands and/or rather small changes. Consequently, a significant change may be masked. This

possibility arose especially after comparing the raw numbers from one experiment to the other, as demonstrated below (see also Fig. 3.8):

Experiment #	P-eNOS/total eNOS Controls	P-eNOS/total eNOS LY 294002	P-eNOS/total eNOS Wortmannin	% of control LY 294002 *	% of control Wortmannin *
1	0.131	0.224	0.189	171	144
2	0.268	0.242	0.217	90	81
3	0.312	0.240	0.285	77	91

* Control = 100%

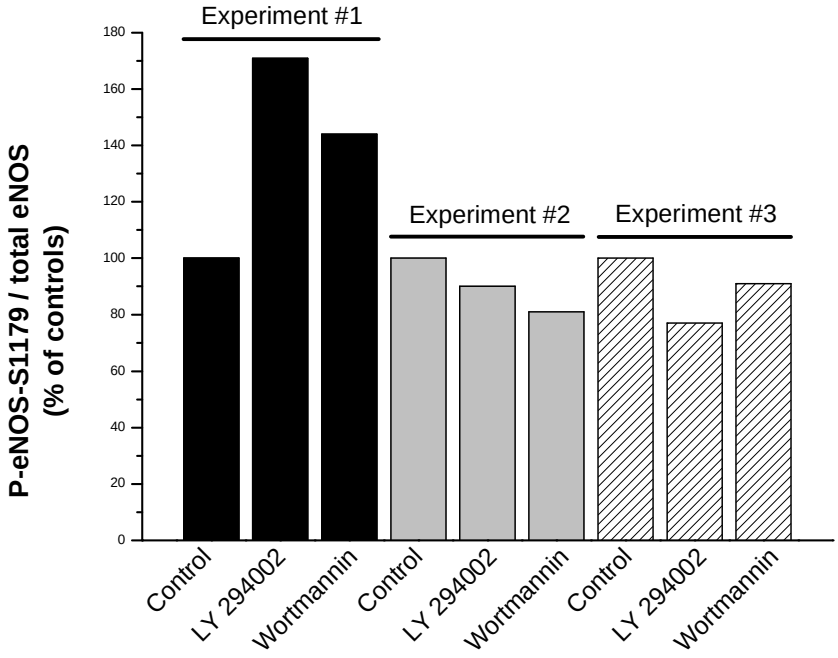

Looking at the results from the individual experiments depicted above it appears that in two experiments PI3 kinase inhibition caused some reduction in the level of phosphorylation ranging between 10 to 20%. However in another experiment the values suggest that there was in fact an increase in phosphorylation. This result is difficult to interpret. Nevertheless, if the lanes corresponding to experiment #1 were in fact ambiguous, it could be suggested that, although fairly small, there appears to be a trend in the other two experiments revealing some degree of reduction in the

basal level of eNOS-S1179 phosphorylation. Moreover, although statistically not significant, this extent of decline in the degree of eNOS phosphorylation may be sufficient to bring about a change in eNOS output that is revealed as small membrane hyperpolarisation in the electrophysiological recordings corresponding to some loss of ongoing endogenous NO synthesis in the whole nerve. Overall, perhaps increasing the *n* number of independent experiments may lead to the emergence of a clearer result. It is true that previous studies have successfully employed the same pharmacological and methodological approach in order to evaluate the impact of blocking the PI3 kinase on eNOS phosphorylation and activity. However, earlier studies establishing the importance of this phosphorylation pathway in regulating eNOS activity have compared the degree of inhibition to situations of selective stimulation and enhancement of eNOS phosphorylation, using agonists or applying shear stress. The scope of detection is most likely to be much greater in these cases as the signal is first increased before comparing it to the reduction brought about by preventing the action of the PI3 kinase. Furthermore, much of the published work has been carried out using cultured aortic smooth muscle cells, for example, or isolated endothelial cells, rather than a whole tissue. Previous work studying the role of the PI3 kinase pathway at the whole tissue level had to use large amounts of protein (0.4 mg or more) combined with subsequent protein purification to eliminate everything that does not bind NADPH (as eNOS does) in order to detect a clear, single band for phosphorylated eNOS (Hurt *et al.*, 2002). Looking at the result obtained in the present study, one can notice that the bands for phosphorylated eNOS are very weak compared to those corresponding to total eNOS, and non-specific bands were visible when probing against phosphorylated eNOS. The antibody directed against eNOS would detect all eNOS protein rather than only the S1179-phosphorylated population and the result may imply that only a small population of eNOS is in the S1179-phosphorylated state, enough to contribute to tonic eNOS activity. This idea would tie in with some of the suggestions brought forward above on the basis of the electrophysiological data. On the other hand, however, the weakness of the band corresponding to S1179-phosphorylated eNOS may solely be based on the anti-phospho-eNOS antibody binding more weakly to its antigen, and perhaps protein

purification would enhance the signal that is detected for phosphorylated eNOS at basal level also in this case. However, also here the question may yet arise whether normalisation of the relatively weak population of S1179-phosphorylated eNOS to total eNOS protein could possibly introduce some error to the final result.

In summary, the lack of a detectable effect of nNOS/iNOS inhibitors and the characteristics of bradykinin-evoked depolarisation further strengthens the implication of vascular eNOS as the principal source of the endogenous tonic NO level in the optic nerve that actively influences the axonal membrane potential. The role of eNOS is further underpinned by the finding that one of the key regulatory mechanisms for basal eNOS activity, namely the PI3 kinase phosphorylation pathway, appears to be at least partially contributing to ongoing NO synthesis. This notion is supported by the electrophysiological data. However, a discrepancy was revealed when investigating the role of PI3 kinase-mediated eNOS phosphorylation by means of Western blotting, seeing no measurable, significant reduction in eNOS-S1179-phosphorylation. It is most likely that this is due to this methodology being not sensitive enough to detect small changes in the signal under investigation.

A partial contribution of the PI3 kinase pathway to tonic eNOS-derived NO is consistent with findings in rat hippocampal slices (Hopper & Garthwaite, 2006), wherein it has been demonstrated that a basal eNOS-derived NO level is partially dependent on a PI3 kinase-mediated mechanism and is required for LTP (Hopper & Garthwaite, 2006). Deletion of eNOS has been reported to impair synaptic plasticity in the hippocampus (Wilson *et al.*, 1999), the cerebral cortex (Haul *et al.*, 1999), and striatum (Doreulee *et al.*, 2003). One of the main physiological stimulators for PI3 kinase-mediated eNOS phosphorylation is shear stress, the force imposed on blood vessel walls by blood flowing across them. This force would ultimately increase as blood flow increases (as would occur for instance during exercising), therefore boosting NO production in the vasculature. The finding of increases and decreases in eNOS activity changing cGMP levels and the membrane potential in opposite directions may provide a possible mechanism through which changes in blood flow and eNOS activity are coupled to changes in neuronal function, providing a possible

hypothesis for how factors that change eNOS activity *in vivo*, such as physical exercise (Green *et al.*, 2004), alter brain activity. In relation to this, physical exercise is also indicated to boost brain function and improve synaptic plasticity, to increase learning, and to enhance cognitive function (van Praag, 2009).

*

CHAPTER 4

Mechanism for tonic NO synthesis in the hippocampus

4.1 INTRODUCTION

The study presented in this chapter stemmed from work showing that there is a tonic level of NO continuously synthesised by eNOS in the rat optic nerve (Garthwaite *et al.*, 2006). Chapter 3 addressed the underlying mechanism for this tonic NO release, finding a partial involvement of PI3 kinase, phosphorylation of eNOS via the PI3 kinase-Akt pathway being among the key regulators of basal eNOS activity (Dimmeler *et al*., 1999; Fulton *et al.*, 1999; Michell *et al.*, 1999; Dudzinski *et al.*, 2006). Founded on the data obtained from electrophysiological recordings (see Chapter 3) it was intended to determine the level of basal eNOS phosphorylation in rat optic nerves by means of a more direct approach. One option was to employ Western blotting, which would give a more direct read out in terms of the level of basal eNOS phosphorylation relative to the amount of total protein. Additionally, this would test whether the PI3 kinase inhibitors, LY 294002 and wortmannin, are acting through the alleged mechanism in a more direct way. Previous work from this laboratory has shown that there is also a tonic level of NO in the adult rat hippocampus under basal conditions, the source being eNOS in blood vessels, finding this tonic NO level to be partly sensitive to PI3 kinase inhibition (Hopper & Garthwaite, 2006). Moreover, while in the optic nerve the eNOS-derived tonic NO appeared to modify the axonal membrane potential (Garthwaite *et al.*, 2006), in the adult rat hippocampus this basal level of NO was found to be a requisite for hippocampal LTP (Bon & Garthwaite, 2003; Hopper & Garthwaite, 2006). Based on these findings, the aim was to use the hippocampal slice preparation as the control tissue in the Western blot experiments in the rat optic nerve. As the forgoing work (Bon & Garthwaite, 2003; Hopper & Garthwaite, 2006) used adult rat hippocampus, to allow a more direct comparison with what had been found in immature rat optic nerves (Chapter 3), the primary aim was to determine the significance of the PI3 kinase pathway in maintaining tonic NO release in the immature rat hippocampus, replicating some of the experiments performed in Hopper and Garthwaite (2006).

The most sensitive and reliable method available at the time to monitor existing endogenous NO levels was the measurement of cGMP levels that are sensitive to NOS inhibition (Griffiths *et al.*, 2002). However, this method has a limit

of detection when looking at very low cGMP levels and/or changes of the cGMP signal upon pharmacological manipulation. One important hallmark of the hippocampus is very high activity of the cyclic nucleotide degrading enzyme phosphodiesterase (PDE), which contributes to the difficulty to measure detectable GMP levels. Therefore, in order to study endogenous NO production in unstimulated hippocampal slices, using cGMP as an index, it is necessary to firstly prevent cGMP breakdown and, secondly, to amplify the activity of the NO_{GC} receptors. Fortunately, there are good pharmacological tools available to date to do just this.

Several isoforms of PDE have been demonstrated to be localised in the rat hippocampus by means of *in situ* hybridisation and immunohistochemical approaches. These include PDE1, 2, 3 and 4 (Ludvig *et al.*, 1991; Repaske *et al.*, 1993; Furuyama *et al.*, 1994; Reinhardt & Bondy, 1996), as well as PDE9 and, to a weaker extent, PDE5 (van Staveren *et al.*, 2004). However, the principal PDE iso-enzyme responsible for cGMP hydrolysis in the hippocampus appears to be PDE2 (Repaske *et al.*, 1993; van Staveren *et al.*, 2001; Suvarna & O'Donnell, 2002), being expressed throughout postnatal development up until adulthood alongside PDE5 and 9 (van Staveren *et al.*, 2003; van Staveren *et al.*, 2004). The major role of PDE2 in cGMP hydrolysis in the hippocampus is emphasised by studies finding no detectable effect of PDE1 and PDE3 inhibition on cGMP accumulation in the hippocampus (van Staveren *et al.*, 2001; Suvarna & O'Donnell, 2002) and the fact that PDE4 is a cAMP-specific PDE (Bender & Beavo, 2006) the inhibition of which would be of no benefit to the current study. Intuitively, the first approach would be to use a general PDE inhibitor such as IBMX in order to prevent any given PDE activity that could be governing the profile of the cGMP signal. However, this could impose a number of possible complications. First of all, the one PDE isoform not affected by IBMX is PDE9, so that a combination of PDE inhibitors would be required if one wanted to ensure the inhibition of this PDE isoform (e.g. IBMX and BAY 73-6691; Wunder *et al.*, 2005; Bender & Beavo, 2006). Also, IBMX is not a 'very clean' compound, antagonising adenosine receptors (Choi *et al.*, 1988), which may modulate synaptic transmission and neuronal excitability (Dunwiddie & Fredholm, 1989; Greene & Haas, 1991). Activation of presynaptic A1 receptors leads normally to a reduction of

neuronal firing, which is suggested to be the result of suppressed glutamate release (Mitchell *et al.*, 1993; Wu & Saggau, 1994; Fowler *et al.*, 1999). Conversely, inhibition of adenosine receptors can lead to an increase in neuronal firing. An additional problem that may arise is related to the fact that IBMX would also prevent the breakdown of cAMP, so that crosstalk between cAMP and cGMP signalling pathways may ensue (Vigne *et al.*, 1994; Pelligrino & Wang, 1998; Bender & Beavo, 2006) making the interpretation of the data difficult. As mentioned above, the prevalent PDE isoform in the hippocampus appears to be the PDE2, which is not only strongly expressed in hippocampal neurons (Repaske *et al.*, 1993) but also in endothelial cells (Sadhu *et al.*, 1999). Despite it being able to degrade both cAMP and cGMP with similar K_m and V_{max} *in vitro* (Martins *et al.*, 1982; Bender & Beavo, 2006), evidence coming from studies on cortical neurons and hippocampal slices indicates that cGMP primarily is elevated upon PDE2 inhibition (Suvarna & O'Donnell, 2002; Boess *et al.*, 2004). This could be explained by the presence of PDE isoforms specifically degrading cAMP, binding this cyclic nucleotide with greater affinity than PDE2 (Bender & Beavo, 2006). A compound previously used as a PDE2 inhibitor is EHNA. However, not only does this compound exhibit a poor potency towards PDE2, it also potently inhibits adenosine deaminase (Sattin & Rall, 1970; Vargeese *et al.*, 1994; Caiolfa *et al.*, 1998), therefore potentially increasing extracellular adenosine levels (Cunha *et al.*, 1998).

The cGMP signal of main interest in this study corresponds to a low tonic NO level prevailing in unstimulated hippocampal slices. Therefore, to achieve an improvement in the signal-to-noise ratio, the compounds BAY 60-7550 and BAY 41-2272 were used. The former is a recently developed, highly selective and potent PDE2 inhibitor devoid of the other actions seen in the case of EHNA (Boess *et al.*, 2004). BAY 41-2272, is used to further amplify the cGMP signal, being an allosteric enhancer of NO_{GC} receptor activity sensitising NO_{GC} receptors towards very low (picomolar) concentrations of NO (Stasch *et al.*, 2001; Garthwaite, 2005; Roy *et al.*, 2008).

4.2 AIM

The initial aim of this study was to test the hypothesis that tonic NO release under basal conditions in immature rat hippocampal slices is mediated via PI3 kinase-dependent phosphorylation of eNOS, further evaluating that it is this NOS isoform that is the principal source of endogenous tonic NO levels.

4.3 METHODS

4.3.1 Hippocampal slice preparation and *in vitro* maintenance

Ten-day-old Sprague Dawley rats from Charles River UK Ltd were used. The animals were sacrificed by cervical dislocation followed by decapitation as approved by the UK Home Office Schedule 1 regulations. The cranium was cut along the midline and gently peeled away, followed by removal and placement of the brain into ice-cold, pre-oxygenated aCSF. Brains were first severed through the hemisphere-midline before the hippocampus of each hemisphere was isolated and carefully cleaned of adhering brain tissue. Transverse slices (400 µm; *Fig. 4.1*) were cut from the central portion of the hippocampus using a McIlwain tissue chopper (The Mickle Laboratory Engineering Co. Ltd). The slices from each hippocampus were kept in separate 50 ml Erlenmeyer flasks containing 20 ml pre-oxygenated, cold aCSF. Flasks were transferred to a shaking water bath for a recovery period of 1-2 hours at 37°C with a constant stream of 95% O_2 / 5% CO_2 flowing through the inlet stopper.

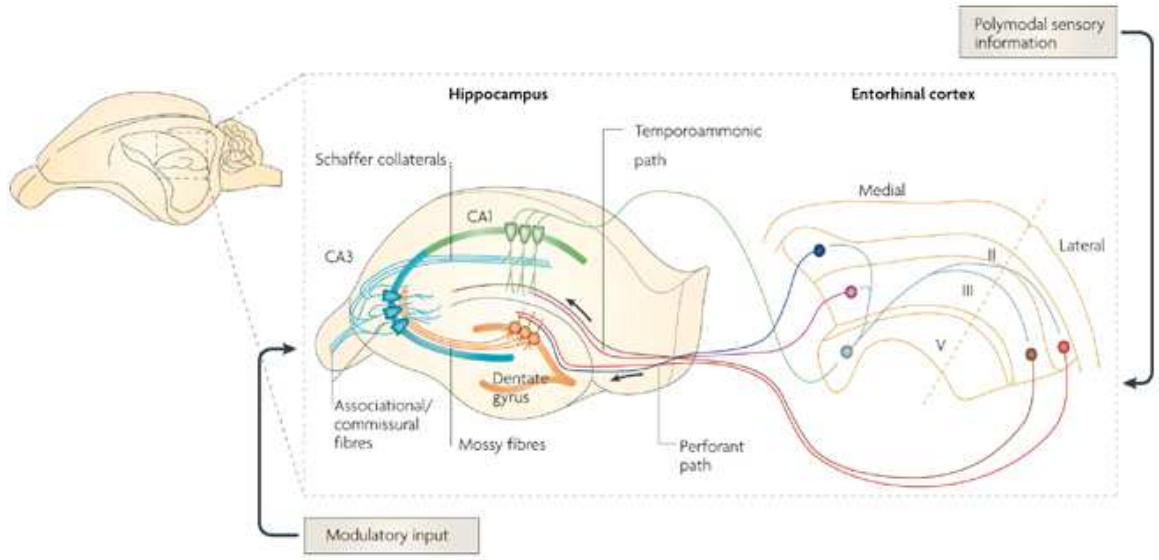

Fig. 4.1 Transverse hippocampal section, including a schematic outline of the basic anatomy of the hippocampus (Source: Neves et al., 2008)

4.3.2 Aortic ring preparation

Aortic rings were prepared from 10-day-old Sprague Dawley rats (Charles River, Margate, UK). The animals were sacrificed humanely according to Home office regulations by cervical dislocation. Upon exposure of the aorta, adhering perivascular connective tissue was gently cleaned away, and the thoracic portions rapidly removed and immediately immersed in cold aCSF that had been pre-equilibrated with 95% O_2 / 5% CO_2. Subsequent to gently flushing out the remaining blood from the aortas, 2-3 mm aortic ring segments were cut using a razor blade. On average 6 to 8 rings were obtained per aorta. Aortic rings were transferred into 50 ml Erlenmeyer flasks containing 20 ml pre-oxygenated, cold aCSF, and left to recover in a shaking water bath for 1-2 hours at 37ºC with a constant stream of 95% O_2 / 5% CO_2 flowing through the inlet stopper.

4.3.3 Experimental treatment of slices and cGMP measurements by means of radioimmunoassay (RIA)

Subsequent to the recovery period at 37ºC in the shaking water bath, rat hippocampal slices (or aortic rings) were randomised, transferring them to fresh aCSF before starting the pharmacological treatments. Equilibration with 95% O_2 / 5% CO_2 at 37°C occurred throughout the experiment. Except for the slices providing the measurements for 'basal' cGMP levels, hippocampal slices were pre-incubated with the PDE2 inhibitor BAY 60-7550 for 15 min before adding any agonists and left to be present throughout the experiment. Aortic rings were incubated for the same interval with the general PDE inhibitor IBMX. All antagonists to be tested were applied for a certain interval prior to BAY 60-7550 and then continued to be present for the remainder of the experiment. Except for LY 294002 and wortmannin, which were applied 20 min prior to BAY 60-7550, all other inhibitors tested were incubated for 10 min prior to BAY 60-7550 exposure. Exposure of hippocampal slices to PAPA/NO, NMDA and BAY 41-2272 were for 5 min, 2 min and 5 min respectively, and ACh was applied for 1 min in the case of aortic rings. To inactivate the biological reaction within the tissue, each of the slices or aortic rings were transferred into a separate Eppendorf tube containing 250 µl of boiling inactivation buffer at the appropriate time, and left to boil for at least 15 min. Tissue samples were then left to cool to room temperature and homogenised by sonication, and the protein content measured using the BCA Protein Assay Kit. Afterwards, samples were centrifuged at 800 rpm for 10 min, discarding the debris. The supernatant was used to determine the cGMP amount by means of RIA as described in detail in Chapter 2. The level of cAMP was quantified using the ^{3}H-cAMP kit (GE Healthcare, Amersham Bioscience, Bucks, UK).

4.3.4 Analysis

The procedure for determining cGMP content normalised to protein amount has been dealt with in detail in Chapter 2. All data are presented as means ± SEM obtained

from at least two different slices per animal, testing at least three rats. Statistical evaluation was carried out using ANOVA with Dunnett's test in GraphPad InStat version 3 (GraphPad Software, Inc., San Diego, CA, USA), statistical significance being accepted at $P < 0.05$.

4.4 RESULTS

4.4.1 Identification of suitable concentrations of BAY 41-2272 and the PDE2 inhibitor BAY 60-7550

The aim of this part of this study was to evaluate the basal NO synthesis under resting conditions in the immature rat hippocampus alongside examining hippocampal slice viability. To assess hippocampal slice viability first, the amount of cGMP formation in response to NMDA was determined. The rise in cGMP in response to NMDA depends on nNOS, therefore providing an index for neuronal NO formation within the slices. NMDA (1-300 µM) in the presence of BAY 60-7550 (1 µM) gave rise to concentration-dependent cGMP accumulation *(Fig. 4.2a)*, as did the NO donor PAPA/NO *(Fig. 4.2b)*.

Despite the presence of the PDE2 inhibitor BAY 60-7550 (1 µM), basal cGMP levels in hippocampal slices were near to being undetectable *(Fig. 4.2d,e)*. However, it is this basal level of cGMP that is related to the tonic endogenous NO level, the main subject of the study presented in this chapter. A pharmacological approach provides a solution to this problem. The compound BAY 41-2272 acts allosterically to sensitise NO_{GC} receptors to NO, pulling the equilibrium over to the active species of the NO_{GC} receptor (Roy *et al.*, 2008). The net result in general is enhanced activity of NO_{GC} receptors in the presence of low NO levels, where it has been suggested that in the presence of BAY 41-2272 the NO_{GC} receptors would exhibit low picomolar sensitivity for NO (Garthwaite, 2005; Roy *et al.*, 2008). Exposures of slices to BAY 41-2272 (0.3-30 µM) in the presence of BAY 60-7550 (1 µM) resulted in a concentration-dependent increase in cGMP levels *(Fig. 4.2c)*, which was inhibited by the broad-spectrum NOS inhibitor L-NNA (100 µM; *Fig. 4.2d*) and the NO_{GC} receptor inhibitor ODQ (10 µM;

Fig. 4.2e). This confirmed that the response to BAY 41-2272 is NO-dependent and corresponds to a boost in NO_{GC} receptor activity.

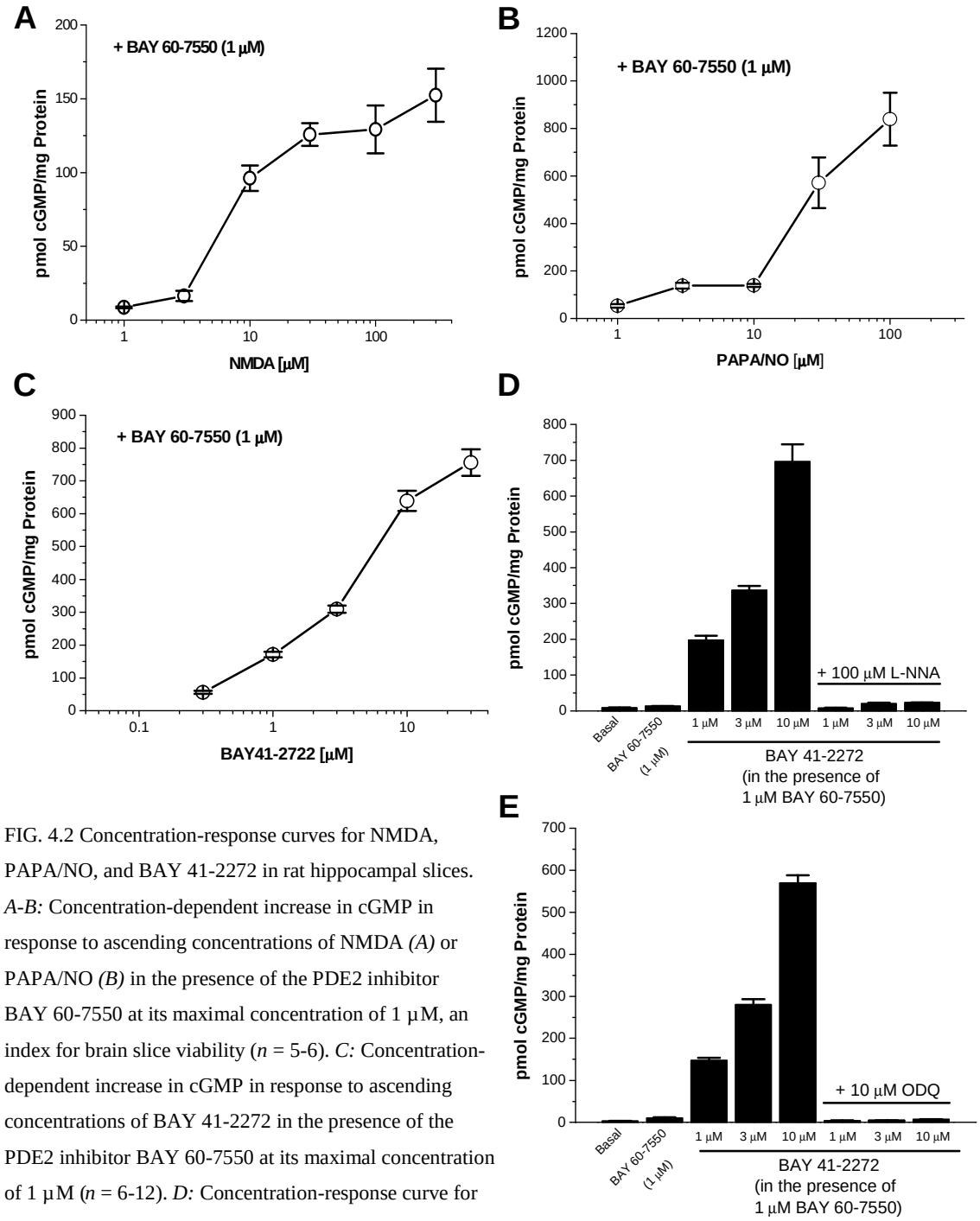

FIG. 4.2 Concentration-response curves for NMDA, PAPA/NO, and BAY 41-2272 in rat hippocampal slices. *A-B:* Concentration-dependent increase in cGMP in response to ascending concentrations of NMDA *(A)* or PAPA/NO *(B)* in the presence of the PDE2 inhibitor BAY 60-7550 at its maximal concentration of 1 µM, an index for brain slice viability (n = 5-6). *C:* Concentration-dependent increase in cGMP in response to ascending concentrations of BAY 41-2272 in the presence of the PDE2 inhibitor BAY 60-7550 at its maximal concentration of 1 µM (n = 6-12). *D:* Concentration-response curve for BAY 41-2272 in hippocampal slices incubated with the PDE2 inhibitor BAY 60-7550 in the absence and presence of L-NNA, verifying the dependence of the BAY 41-2272 effect on endogenous NO. The cGMP signal in response to all tested BAY 41-2272 concentrations was prevented by L-NNA (n = 4-6). *E:* Concentration-response curve for BAY 41-2272 in hippocampal slices incubated with the PDE2 inhibitor BAY 60-7550 in the absence and presence of ODQ, further verifying the NO-

dependence of the cGMP response evoked by BAY 41-2272. The cGMP signal in response to all tested BAY 41-2272 concentrations was prevented by ODQ (n = 5-6).

The present study uses the recently developed PDE2 inhibitor BAY 60-7550. In adult rat hippocampal slices this compound raised cAMP levels as well as cGMP, significant cAMP levels being detected when the concentration of BAY 60-7550 exceeded 1 µM (Boess *et al.*, 2004). Although, according to the observations made in adult hippocampal slices, 1 µM of BAY 60-7550 should be a reasonable concentration to use, it is yet possible that the potency of BAY 60-7550 to increase cAMP formation in young hippocampal slices differs, as appears to be the case for NMDA- and BAY 41-2272-evoked responses (compare Boess *et al.*, 2004 and Hopper & Garthwaite, 2006 with the present data). It has been reported that NO release from eNOS and its phosphorylation via the PI3 kinase-Akt pathway may also be stimulated directly by cAMP (Zhang & Hintze, 2006). Also PKA has been found to stimulate eNOS, but in this case in a PI3 kinase-independent manner (Boo *et al.*, 2002a; Boo *et al.*, 2002b). It has been implied that PKA does not necessarily act in association with cAMP in this respect. For example, among the cAMP-independent mechanisms proposed is direct activation of PKA by vasoactive peptides including endothelin-1 and angiotensin II (Dulin *et al.*, 2001). Nonetheless, a factor which directly increases cAMP in endothelial cells would also stimulate PKA. Additionally, it has been reported that the kinase Akt may be activated in a PI3 kinase-independent manner by cAMP (Sable *et al.*, 1997). For this to occur in the preparation investigated in the present study, cAMP would need to be raised within the blood vessels. The finding of PDE2 expression in a variety of microvessels, including within the brain (Sadhu *et al.*, 1999), makes the odds of cAMP interfering with the response under investigation more likely. Furthermore, BAY 60-7550 has been found to have inhibitory actions on purified PDE1 and PDE5 (Boess *et al.*, 2004). PDE5 inhibition (van Staveren *et al.*, 2003; van Staveren *et al.*, 2004; Rutten *et al.*, 2005), but not PDE1 inhibition (van Staveren *et al.*, 2001), has been shown to raise cGMP levels in the hippocampus marginally. To address the concentration of BAY 60-7550 required to avoid possible interference of the above with the response under investigation,

slices were tested for cAMP accumulation in the presence of different BAY 60-7550 concentrations. The previously reported effects of BAY 60-7550 on PDE1 and PDE5 were examined on purified enzyme (Boess *et al.*, 2004). Based on aspects such as diffusion properties of a compound in a whole tissue, it is likely that higher concentrations of BAY 60-7550 would be required in order to exhibit actions observed on purified PDEs. Nonetheless, the concentrations of BAY 60-7550 tested in the cAMP assays in the current work were kept below the ones which had been shown to inhibit PDE isoforms other than PDE2. One more aspect to consider is the potential crosstalk between cyclic nucleotides such as the ability of cGMP to inhibit cAMP-specific PDEs, which would in turn lead to enhanced cAMP levels (Bender & Beavo, 2006). Overall, the aim in this section was to identify a concentration of BAY 60-7550 that would not only be devoid of interfering actions, but would also nonetheless result in a good window of cGMP formation when applied in conjunction with BAY 41-2272. A good window of cGMP level was considered to be submaximal but large enough so that the signal-to-noise ratio would not impose a problem when looking at inhibition of the response.

Exposure of hippocampal slices to different concentrations of BAY 60-7550 (0.001-1 µM) in the presence of a set concentration of BAY 41-2272 (1 µM; *Fig. 4.3a*, or 3 µM; *Fig. 4.3b*) led to concentration-dependent increase in cGMP, which was prevented by L-NNA (100 µM) and ODQ (10 µM), the basal level of cGMP (with or without added BAY 60-7550) again being near to undetectable when BAY 41-2272 had not been applied *(Fig. 4.3a,b).*

To test whether cAMP was capable of evoking an increase in basal cGMP levels in the presence of the PDE2 inhibitor, the two highest concentrations of BAY 60-7550 tested (0.1 and 1 µM) were probed in the presence of the adenylyl cyclase activator forskolin (10 µM). Incubation of slices with these two test concentrations of BAY 60-7750, followed by exposure to forskolin, failed to evoke a significant rise in cGMP as compared to the basal level with or without added BAY 60-7550 (*Fig. 4.3b).* The lowest concentration of BAY 60-7550 that still resulted in an adequate window of cGMP accumulation, and should be devoid of interfering actions as outlined above, was found to be in the 10 nM range, combined with 3 µM BAY 41-2272. Two concentrations in that range (10 and 30 nM) were compared with the

general PDE inhibitor IBMX in the presence of either forskolin (1 and 10 µM) or BAY 41-2272 (3 µM), the latter determining whether cGMP accumulation under these conditions can raise cAMP levels. IBMX caused a greater increase in cAMP compared to the basal level with or without added BAY 60-7550 (*Fig. 4.4*; given in pmol cGMP/mg protein: 'IBMX only' *vs.* 'basal', '10 nM BAY 60-7550 only' and '30 nM BAY 60-7550 only' was 13.38 ± 0.73 *vs.* 3.47 ± 0.75, $p < 0.001$, 4.69 ± 0.67, $p < 0.001$, and 3.94 ± 0.39, $p < 0.001$ respectively), as would be expected when many different PDE isoforms are inhibited. Inhibition of PDE2 with 10 or 30 nM BAY 60-7550 also evoked an increase in cAMP when the adenylyl cyclase was activated by forskolin, albeit to lesser extent than IBMX (*Fig. 4.4*; given in pmol cGMP/mg protein: 'IBMX + 1 µM forskolin' *vs.* '10 nM BAY 60-7550/forskolin' and '30 nM BAY 60-7550/forskolin' was 75.79 ± 1.9 *vs.* 8.19 ± 1.77 and 13.04 ± 1.09 respectively, $p < 0.001$; 'IBMX + 10 µM forskolin' *vs.* '10 nM BAY 60-7550/forskolin' and '30 nM BAY 60-7550/forskolin' was 165.4 ± 6.4 *vs.* 55.5 ± 0.3 and 62.1 ± 10.4 respectively, $p < 0.001$). This is consistent with PDE2 being a dual substrate enzyme that hydrolyses both cAMP and cGMP (Bender & Beavo, 2006). However, stimulating cGMP synthesis by applying BAY 41-2272 failed to induce a significant rise in cAMP levels when the PDE2 inhibitor BAY 60-7550 was present, being not significantly different from cAMP levels measured under basal conditions in the absence or presence of BAY 60-7550 *(Fig. 4.4)*, suggesting that there is no crosstalk occurring between the two cyclic nucleotides under these conditions. Direct stimulation of cAMP accumulation by forskolin (1µM) in the presence of 10 nM BAY 60-7550 failed to raise cAMP levels significantly compared to the basal level with or without added BAY 60-7550, while in the presence of 30 nM BAY 60-7550 and forskolin (1 µM) this resulted in a significant difference in cAMP levels as compared to the basal level with or without added BAY 60-7550 (*Fig. 4.4*; given in pmol cGMP/mg protein: 30 nM BAY 60-7550 + forskolin *vs.* 'basal', '10 nM BAY 60-7550 only', and '30 nM BAY 60-7550 only' was 13.04 ± 1.09 *vs.* 3.47 ± 0.75, $p < 0.001$, 4.69 ± 0.67, $p < 0.001$, and 3.94 ± 0.39, $p < 0.001$ respectively). The levels of cAMP measured under conditions where only BAY 60-7550 was present at 10 or 30 nM were not significantly different from basal levels *(Fig. 4.4)*.

In summary, 10 nM of the PDE2 inhibitor BAY 60-7550 was chosen for all subsequent experiments. This concentration resulted in a good window of cGMP accumulation when slices were exposed to BAY 41-2272 (3 µM), and does not enhance cAMP formation or inhibit PDE isoforms other than PDE2, as described above. Moreover, at 10 nM BAY 60-7550, no crosstalk between the two cyclic nucleotides was apparent as forskolin failed to raise cGMP significantly and BAY 41-2272 did not evoke a significant increase in cAMP. As to the BAY 41-2272 concentration, 3 µM was chosen to be used in conjunction with the PDE2 inhibitor, a concentration at which BAY 41-2272 lacks PDE inhibitory activity (Stasch *et al.*, 2001; Mullershausen *et al.*, 2004a).

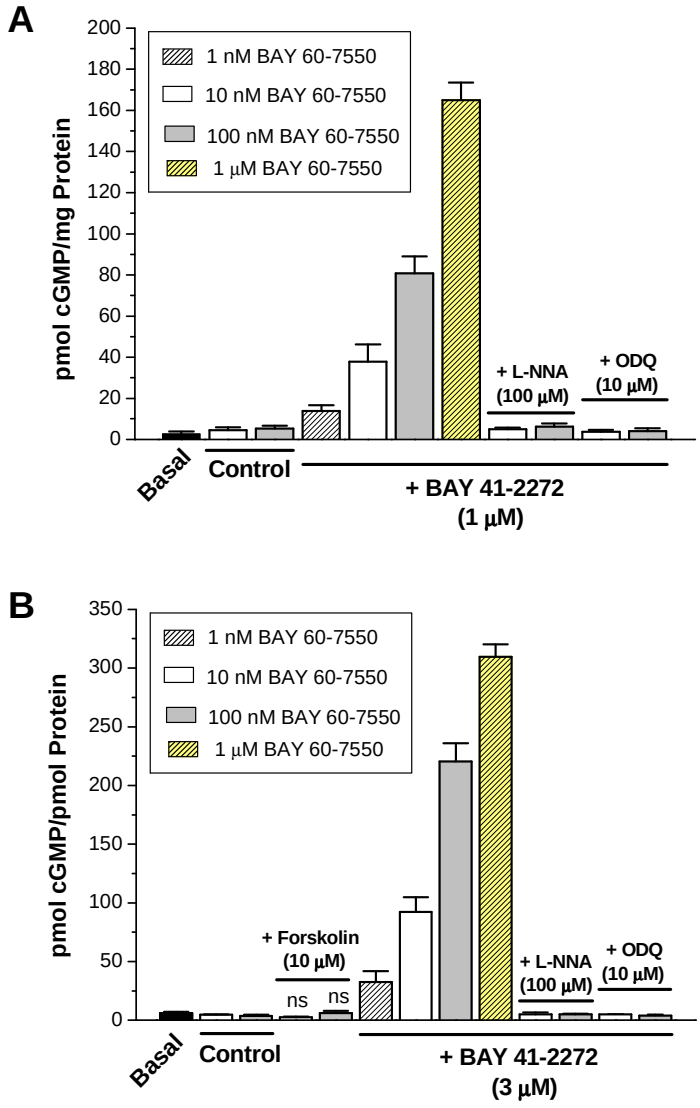

FIG. 4.3 Concentration profile of the PDE2 inhibitor BAY 60-7550 on cGMP accumulation. *A:* cGMP accumulation in response to 1 µM BAY 41-2272 in the presence of ascending concentrations of BAY 60-7550. The cGMP signal was prevented by both L-NNA and ODQ, confirming NO- and cGMP-dependence respectively (n = 3). *B:* cGMP accumulation in response to 3 µM BAY 41-2272 in the presence of ascending concentrations of BAY 60-7550. The cGMP signal was prevented by both L-NNA and ODQ, confirming NO- and cGMP-dependence respectively. Also, the adenylyl cyclase activator forskolin failed to evoke an increase in cGMP synthesis (n = 3). Note the low cGMP signal detectable under basal conditions in the absence or presence of BAY 60-7550.

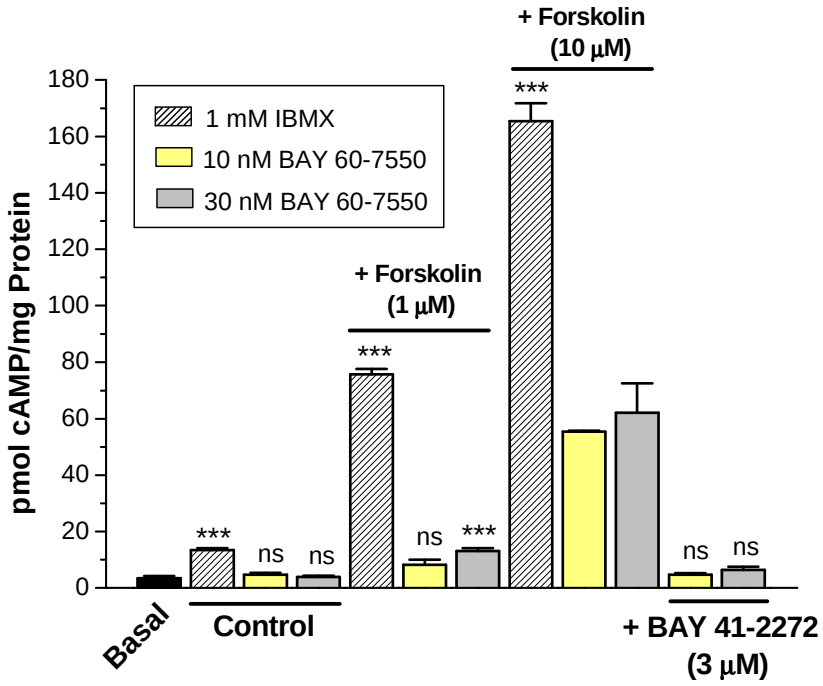

FIG. 4.4 Concentration profile of the PDE2 inhibitor BAY 60-7550 on cAMP accumulation. The adenylyl cyclase activator forskolin evoked a concentration-dependent increase in cAMP accumulation in the presence of the non-specific PDE inhibitor IBMX and the PDE2 inhibitor BAY 60-7550. The guanylyl cyclase sensitizer BAY 41-2272 failed to evoke a significant increase in cAMP synthesis (n = 3). *Note:* Except in the case of IBMX, the cAMP level detected under conditions of BAY 60-7550 application alone was not significantly different from that measured under basal conditions.

4.4.2 Underlying cause of tonic NO synthesis – the role of PI3 kinase

As described earlier, one of the key mechanisms thought to be responsible for tonic eNOS activity is the PI3 kinase-Akt pathway, which was found to be partially contributing to basal eNOS-derived NO synthesis in the immature rat optic nerve (Chapter 3) and in the adult rat hippocampus (Hopper & Garthwaite, 2006).

In immature rat hippocampal slices, the PI3 kinase inhibitors LY 294002 (100 µM) and wortmannin (1 µM) were tested against the cGMP accumulation in response to 3 µM BAY 41-2272 and 10 nM of the PDE2 inhibitor BAY 60-7550, a condition that gave a good window to work with in terms of the cGMP signal (see above). Neither of the two PI3 kinase inhibitors significantly reduced the cGMP response

(Fig. 4.5), questioning the involvement of the PI3 kinase pathway in the maintenance of basal eNOS activity in the developing rat hippocampus as opposed to the rat optic nerve (Chapter 3) and the adult rat hippocampus (Hopper & Garthwaite, 2006). In contrast, exposing the slices to the broad-spectrum NOS inhibitor L-NNA, inhibiting the enzyme more directly by preventing the substrate for NO synthesis (i.e. L-arginine) to bind to the enzyme, prevented the cGMP signal down to basal levels *(Fig. 4.5)*.

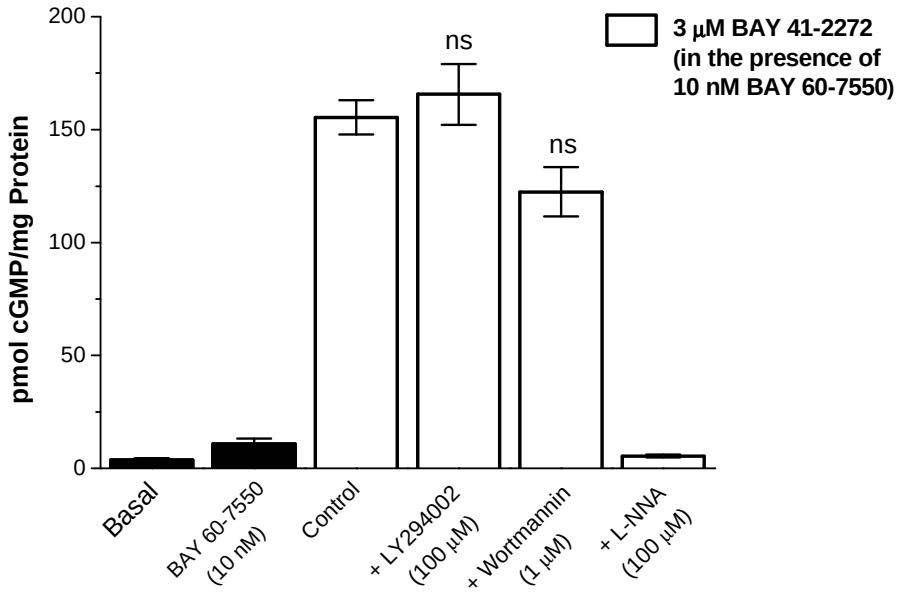

FIG. 4.5 Role of the PI3 kinase in the maintenance of basal NO release. Two different PI3 kinase inhibitors, LY 294002 and wortmannin, both failed to significantly affect the cGMP levels that were measured in the presence of BAY 41-2272 and PDE2 inhibitor (n = 6-9; $^{ns}p > 0.05$). In contrast, consistent with previous results, the NOS inhibitor L-NNA prevented the cGMP signal, in line with the response being dependent on endogenous NO. Also, as previously observed, only a very low cGMP signal could be detected both under basal conditions or when BAY 60-7550 was applied exclusively.

Apart from the likelihood of other factors (see Chapter 3) partially contributing to or being responsible for the level of tonic NO in the immature rat hippocampus, one alternative explanation for the lack of inhibitory effect of the PI3 kinase inhibitors could be related to the application time of the allosteric NO_{GC}

receptor enhancer BAY 41-2272. It is suggested that in the presence of BAY 41-2272, NO_{GC} receptors would exhibit low picomolar NO sensitivity (Garthwaite, 2005; Roy *et al.*, 2008). Such NO levels may persist in the hippocampal slices even following PI3 kinase inhibition. If this were the case, long enough application of BAY 41-2272 would more slowly, but yet eventually, drive the cGMP signal to a level that approaches that seen in the absence of a PI3 kinase inhibitor. Related to this argument, the scope of inhibition may depend on whether at 5 min application of BAY 41-2272 the cGMP response has reached steady-state or is still in its rising phase. A greater antagonistic effect would be expected during the rising phase of the agonist-evoked response. This has been shown, for example, in the case of the inhibitory action of ODQ on NO-induced cGMP increases (Mo *et al.*, 2004). To test this idea in the light of the present investigation, experiments were performed to look at the responses to BAY 41-2272 at different time points in the absence and presence of a PI3 kinase inhibitor. If the above arguments hold, one would predict a greater degree of inhibition by the PI3 kinase inhibitor at the early time points.

The level of cGMP was determined in response to BAY 41-2272 (1 µM) and the PDE2 inhibitor BAY 60-7550 (10 nM) at the time points 30 s, 1 min, 2 min and 5 min in the absence and presence of wortmannin (1 µM). No difference in the degree of inhibition was found among the different time points *(Fig. 4.6)*, further disputing the participation of the PI3 kinase pathway in preserving basal NO synthesis in the immature hippocampus.

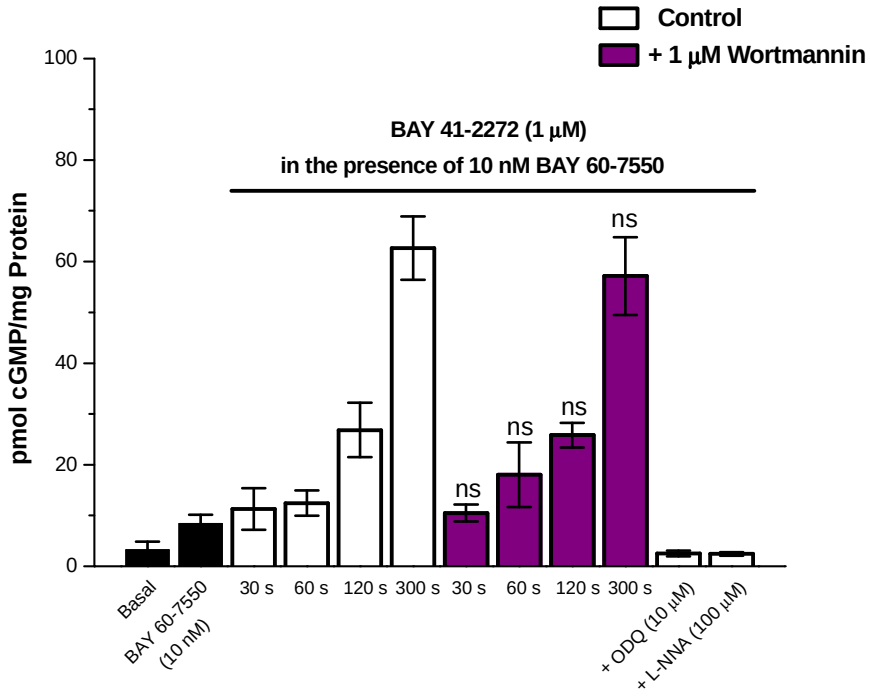

FIG. 4.6 Role of the PI3 kinase in the maintenance of tonic NO release – dependence on the application time of BAY 41-2272. In comparison with the respective controls, the PI3 kinase inhibitor wortmannin failed to reduce the cGMP accumulation significantly in response to BAY 41-2272, irrespective of the time BAY 41-2272 had been applied for (n = 3; $^{ns}p > 0.05$).

4.4.3 Identification of NOS isoforms responsible for tonic NO synthesis

Since the PI3 kinase pathway is apparently not involved in the maintenance of tonic NO release in the immature rat hippocampus, the mechanism(s) and the source(s) of basal tonic NO synthesis remained to be determined. Firstly, the aim was to try to dissect out which isoform(s) of NOS the tonic NO is coming from – eNOS and/or nNOS. To test the involvement of nNOS, two different nNOS inhibitors (L-VNIO and NPA) and an inhibitor that exerts greater inhibitory potency for iNOS than nNOS (1400W; Garvey *et al.*, 1997; Boer *et al.*, 2000; Young *et al.*, 2000) were employed.

The cGMP signal was measured in hippocampal slices that had been treated with BAY 41-2272 (3 µM) and BAY 60-7550 (10 nM) following pre-incubation with

one of the nNOS inhibitors, L-VNIO (100 nM) or NPA (1 µM), or the nNOS/iNOS inhibitor 1400W (1 µM; *Fig. 4.7*). All of the inhibitors used were applied at a concentration effective in the adult hippocampus (Hopper & Garthwaite, 2006). The cGMP response to BAY 41-2272, which corresponds to endogenous basal NO production, was unaffected by these inhibitors *(Fig. 4.7)*. This would immediately point to eNOS as being the major source for tonic NO synthesis. However, puzzlingly, control responses to NMDA (100 µM), which depend on nNOS, were also not affected significantly by the nNOS/iNOS inhibitors in the same experiments (*Fig. 4.7)*, making the interpretation of these data difficult. Overall, this result makes it impossible at this stage to conclude anything about the involvement of NOS isoforms other than eNOS as contributors to the ongoing basal NO synthesis. In contrast, L-NNA, which inhibits all NOS isoforms, prevented both the NMDA-induced and the BAY 41-2272-evoked cGMP accumulation accordingly *(Fig. 4.7).*

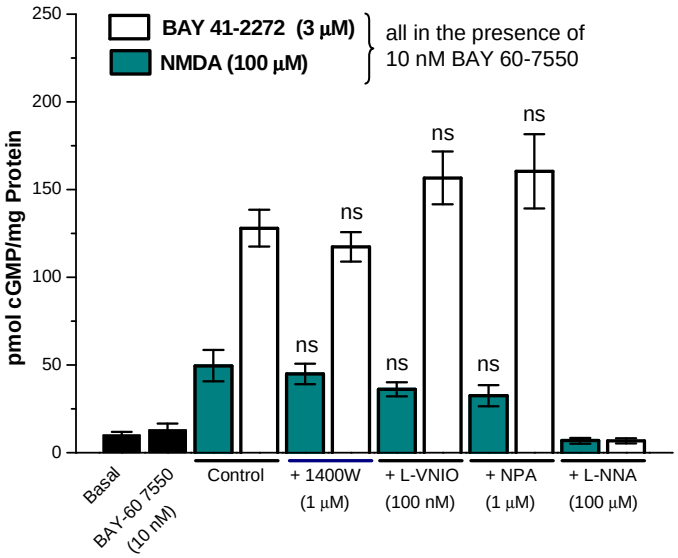

FIG. 4.7 Source of basal endogenous NO – nNOS/iNOS. The nNOS inhibitors NPA and L-VNIO, as well as the nNOS/iNOS inhibitor 1400W, at their usual working concentrations, all failed to reduce cGMP levels in the presence of BAY 41-2272 and the PDE2 inhibitor BAY 60-7550 as compared with their respective control (n = 6; $^{ns}p > 0.05$) . This would be indicative of NOS isoforms other than eNOS not being significant contributors to ongoing NO synthesis under basal conditions. However, unexpectedly, the same inhibitors also fell short in preventing the cGMP signal significantly in response to NMDA, making the interpretation of this data problematic (n = 6; $^{ns}p > 0.05$).

One reason for the above result shown in Fig. 4.7 may be that the applied concentrations of the nNOS/iNOS inhibitors are not maximal for inhibition in the immature hippocampus, despite showing clear inhibitory activity against the cGMP signal in response to NMDA in the adult hippocampus (Hopper & Garthwaite, 2006). This possibility can be extended based on comparison of the data presented here to those obtained from adult hippocampal slices (Hopper & Garthwaite, 2006). In the forgoing study by Hopper & Garthwaite (2006), the nNOS/iNOS inhibitors, used at the same concentrations as here, prevented the control responses to NMDA. However, 30 µM BAY 41-2272 was required to increase cGMP to levels that were only about a fifth of what is observed here in immature hippocampal slices exposed to only 3 µM of this compound. Also, 100 µM NMDA, the same concentration used here, produced cGMP levels in adult hippocampal slices that were only about a third of what is yielded here from immature hippocampal slices. These differences may indicate why higher concentrations of the nNOS/iNOS inhibitors may be required to accomplish significant inhibition of the cGMP signal in response to NMDA. To test this idea, the aim of the following set of experiments was to look at concentration-dependent inhibition of the NMDA-evoked cGMP signal by these inhibitors. As nNOS is of the main interest here, iNOS being usually only induced under certain pathological conditions over a course of several hours (Iadecola *et al.*, 1995; Iadecola *et al*., 1996; Moro *et al.*, 1998; Yamada *et al.*, 2003 and is absent in hippocampal slices subjected to standard treatment and incubation (Hopper & Garthwaite, 2006), only the inhibitory actions of L-VNIO and NPA were examined in the following set of experiments.

First, the concentrations of these inhibitors required to prevent the response to NMDA were established by producing concentration-inhibition curves *(Fig. 4.8)*. Surprisingly, approximately 10-fold higher concentrations of both inhibitors were necessary in order to achieve efficient inhibition (80-90%) of the response to NMDA *(Fig. 4.8)* and that was similar to the degree of inhibition observed in adult hippocampal slices (Hopper & Garthwaite. 2006).

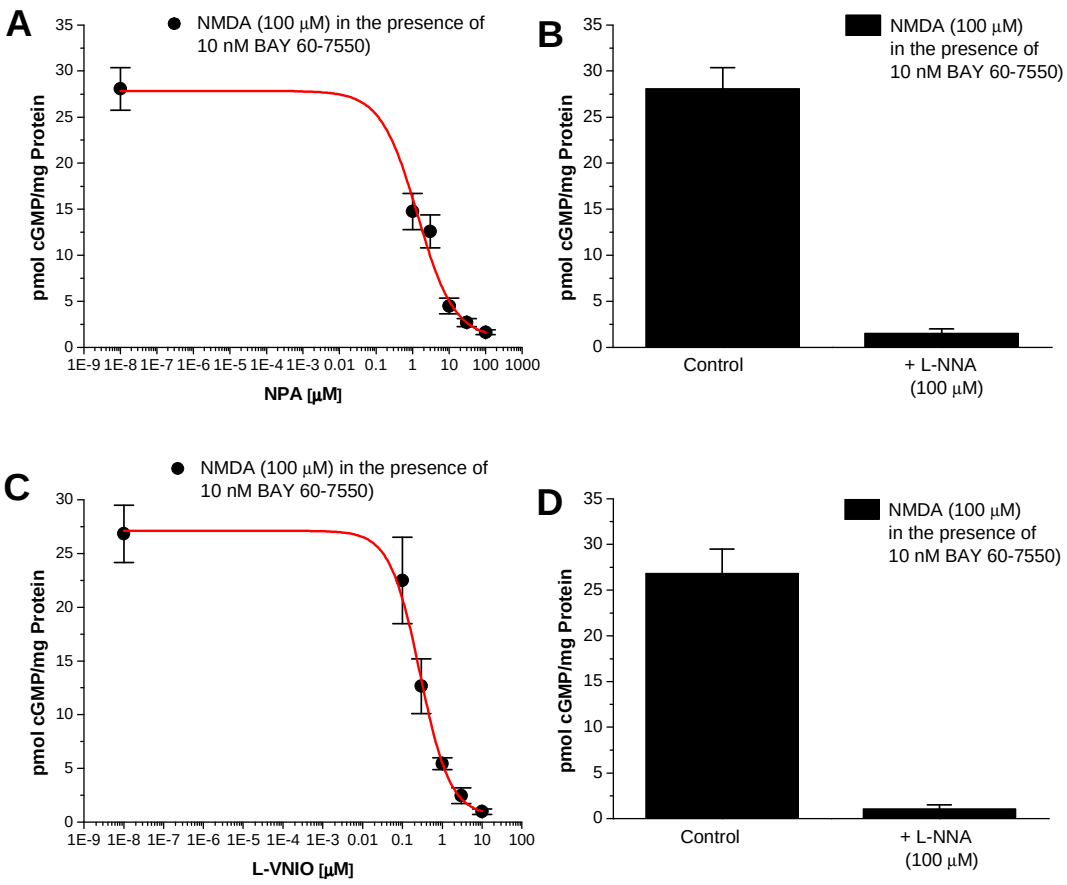

FIG. 4.8 Effect of nNOS inhibitors on NMDA-stimulated cGMP accumulation. *A-B:* Concentration-effect curve for NPA (n = 6; IC_{50} = 1.4 ± 0.43 µM). *C-D:* Concentration-effect curve for L-VNIO (n = 6; IC_{50} = 0.28 ± 0.08 µM). Note, for both inhibitors a concentration-dependent decrease in cGMP levels was observed in the presence of increasing concentrations of nNOS inhibitor. Furthermore, cGMP accumulation was prevented in the presence of L-NNA, providing confirmation of the NMDA-induced response entailing NO.

Having identified the profile of inhibition of the nNOS inhibitors in the immature hippocampus, the question now was whether the concentration at which the response to NMDA was prevented would also inhibit the cGMP signal upon BAY 41-2272 exposure. The prediction is that if eNOS is the solitary contributor to basal NO levels the response to BAY 41-2272 should not be prevented by inhibition of nNOS.

Exposure of hippocampal slices to BAY 41-2272 (3 µM) and BAY 60-7550 (10 nM) in the presence of L-VNIO (1 µM; *Fig. 4.9a*) or NPA (10 µM; *Fig. 4.9b*), both at a concentration that also prevented the NMDA-induced response *(Fig. 4.8a,c)*,

led to significant inhibition of the cGMP signals *(Fig. 4.9a,b)*. Lower concentrations of nNOS inhibitor failed to reduce the cGMP level in response to BAY 41-2272 markedly *(Fig. 4.9a)*, as was the case for NMDA-evoked responses *(Fig. 4.9a)*, the latter implying only partial inhibition of nNOS. As the cGMP response was only reduced by approximately 50%, these data indicate that both eNOS and nNOS may partially be involved in keeping up the NO production at basal level. As there are no inhibitors available for eNOS, it was not possible to test whether the remainder of the response could be prevented when both nNOS and eNOS were selectively inhibited. Also, there is still the likelihood that the degree of inhibition observed at higher concentrations of nNOS inhibitors is because they affect eNOS also. Therefore, a way was sought to find out whether the degree of inhibition observed was due to nNOS inhibition only (see *Fig. 4.10*). If this were the case, it would provide reason to hypothesise that both nNOS and eNOS may partially be responsible for tonic NO synthesis.

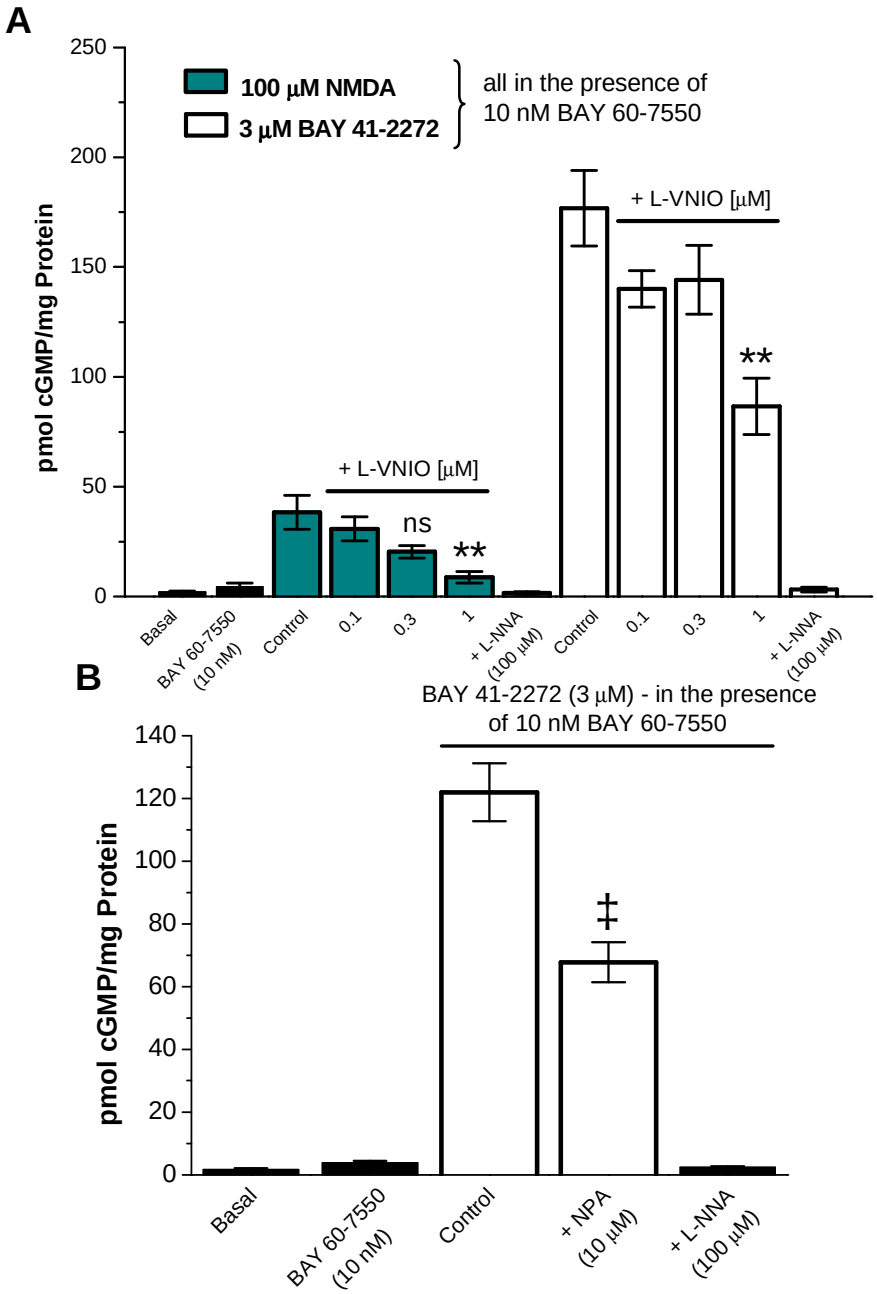

FIG. 4.9 Effect of nNOS inhibitors on NMDA-stimulated and BAY 41-2272-evoked cGMP accumulation *A:* The NMDA-induced cGMP response was concentration-dependently reduced in the presence of increasing concentrations of L-VNIO. In contrast, in the case of BAY 41-2272, only the maximal concentration of nNOS inhibitor tested (i.e. concentration of nNOS inhibitor required to prevent the cGMP level in response to NMDA) resulted in a significant decrease in the cGMP level (n = 3; **p < 0.01). *B:* The cGMP increase in response to BAY 41-2272 was only significantly reduced at the concentration of NPA that was required to prevent the cGMP level in response to NMDA (n = 3; ‡p < 0.002).

It is well known that stimulation of NO synthesis in blood vessels by ACh occurs via eNOS activation (Furchgott & Zawadzki, 1980) and aortas from mice lacking eNOS have been shown to lack a dilating response to ACh (Huang *et al.*, 1995). This standard way of generating NO from eNOS was exploited to test the selectivity of the nNOS inhibitors. The question was whether the concentrations of L-VNIO and NPA that significantly reduced the cGMP level in response to BAY 41-2272 (see *Fig. 4.9a,b*) were only due to nNOS inhibition or were also affecting the activity of eNOS.

Aortic rings cut from 10-day-old rat aortas were stimulated with ACh (10 µM) in the absence or presence of ascending concentrations of the two nNOS inhibitors *(Fig. 4.10)*. Concentrations that led to partial inhibition of the response to BAY 41-2272 *(Fig. 4.9a,b)* and prevention of the NMDA-evoked signal as well (*Fig. 4.8a,c and Fig. 4.9a)*, also resulted in partial reduction of the cGMP level evoked by ACh in the rat aorta *(Fig. 4.10)*.

From this it can be concluded that, at least in the immature rat hippocampus, the allegedly selective nNOS inhibitors L-VNIO and NPA, do not seem to be suitable tools for identifying the isoform of NOS involved in the biological response under investigation. From these data, showing a clear overlap of selectivity of these nNOS inhibitors between eNOS and nNOS, in conjunction with a lack of good eNOS inhibitors, it is impossible to determine whether only one or both of the two NOS isoforms are responsible for the persistent NO release under basal conditions in the immature rat hippocampus.

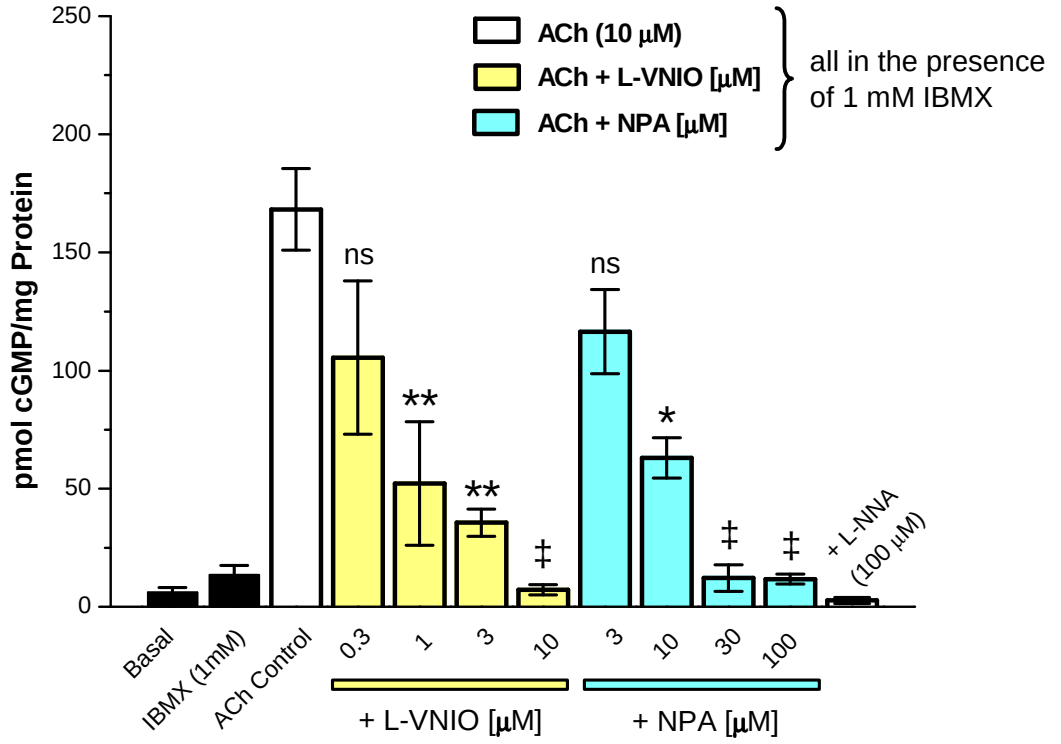

FIG. 4.10 Rat aorta control – effect of nNOS inhibitors on ACh-stimulated eNOS-dependent cGMP accumulation. Note, concentrations of both L-VNIO and NPA, which were previously found to significantly affect the cGMP increase in response to BAY 41-2272 in hippocampal slices, also reduced the ACh-evoked cGMP response in rat aortas (n = 4; *$p < 0.05$, **$p < 0.01$, $^{‡}p < 0.001$).

4.4.4 What maintains tonic NO?

Possible involvement of glutamate receptors, Na^+ channels and GABA

The cGMP response seen upon NMDA receptor activation is related to glutamate-evoked, Ca^{2+}-dependent activation of nNOS in neurons (Garthwaite *et al.*, 1988; Garthwaite, 1991). There is a possibility that basal neuronal activity sustains neurons in a depolarised state, which may result from basal glutamate release and some glutamate receptor activation. This could ultimately aid in establishing tonic nNOS activity. A further test for the involvement of nNOS in the basal NO

production was to determine whether the cGMP response associated with endogenous NO could be prevented when NMDA receptors were inhibited. Additionally, AMPA receptors and voltage-dependent Na^+ channels can also participate in the activation of nNOS (Southam *et al.*, 1991). Moreover, during certain stages of postnatal development the neurotransmitter GABA is excitatory before adopting its inhibitory nature (Ben-Ari, 2002; Ben-Ari *et al.*, 2007). This is the result of an initially high intracellular chloride concentration based on the delayed expression of the K^+ - Cl^- co-transporter. An interesting feature of the excitatory nature of GABA during development is the occurrence of so-called giant depolarising potentials (GDPs). This is a network-driven pattern of electrical activity in developing circuits which leads to the generation of large intracellular Ca^{2+} oscillations (Ben-Ari, 2001). In addition, the switch from an excitatory to an inhibitory nature of GABA during development is suggested to take place during the second postnatal week in the hippocampus (Khazipov *et al.*, 2004; Ben-Ari *et al.*, 2007). Noting that the present work is carried out on 10-day-old hippocampal slices, there is the possibility of GABA evoking Ca^{2+} oscillations that could ultimately lead to NO synthesis. Using pharmacological agents, the aim of the following set of experiments was to examine if any of the above neurotransmitters are linked to the tonic NO formation in the immature hippocampal slices.

The responses to BAY 41-2272 (3 µM), in the presence of PDE2 inhibitor, remained unaffected by the NMDA-R antagonist D-AP5 (100 µM), the AMPA-R/kainate-R antagonist CNQX (30 µM), and the Na^+ channel blocker TTX (1 µM; *Fig. 4.11a*), the inhibition of the responses to NMDA and veratrine by the respective antagonists serving as positive controls *(Fig. 4.11a)*. Also the $GABA_A$ receptor antagonist bicuculline (50 µM) and the $GABA_B$ receptor antagonist CGP 55845 (3 µM) failed to exhibit an effect on the cGMP signal *(Fig. 4.11b)*. The non-selective NOS inhibitor L-NNA prevented cGMP accumulation as expected *(Fig. 4.11a,b)*. These data suggest that, although cGMP levels in unstimulated hippocampal slices are NO-dependent, it is unlikely that any of the above systems are linked to tonic NO production.

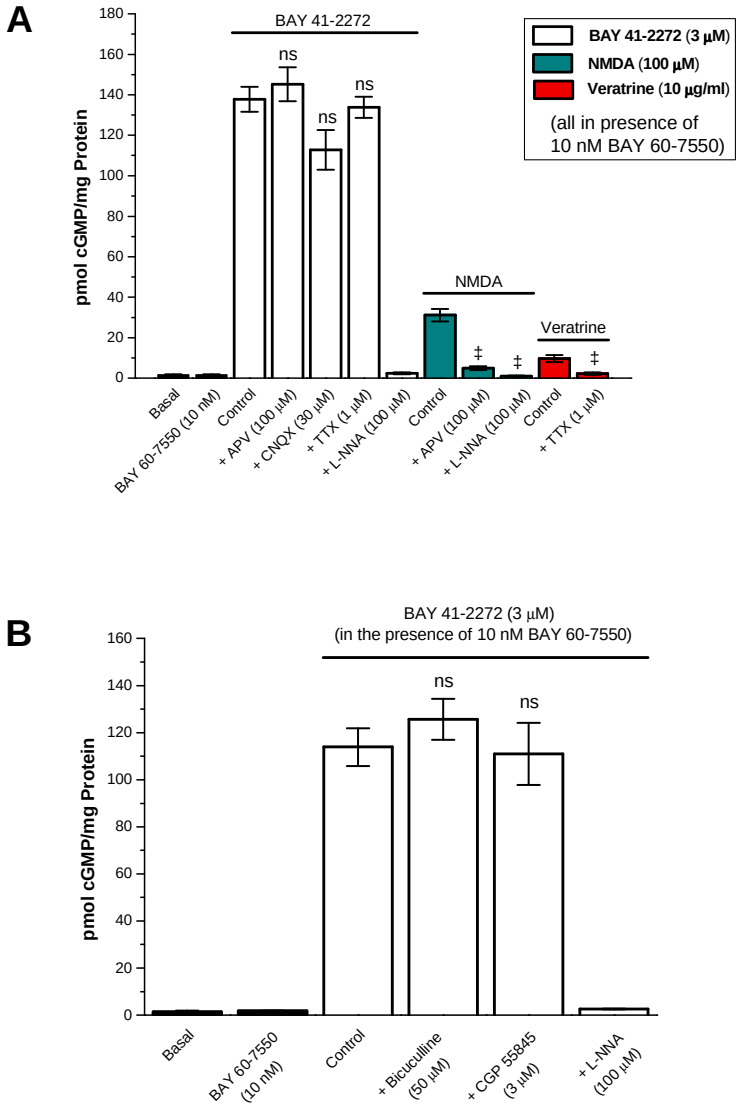

FIG. 4.11 Effect of pharmacological agents inhibiting GABA receptors, Na^+ channels, or glutamate receptors on cGMP levels. *A:* Effect of pharmacological agents, blocking Na^+ or GluRs, on cGMP levels. Incubation of hippocampal slices in aCSF containing the PDE2 inhibitor BAY 60-7550 and BAY 41-2272 in the absence or presence of APV to block NMDA receptors, CNQX to block AMPA receptors and TTX to block Na^+ channels. While causing clear inhibition when tested against the agonist, none of the agents produced significant inhibition of the cGMP level in response to BAY 41-2272, while L-NNA did, the latter being in line with the BAY 41-2272-evoked response being endogenous NO-dependent (n = 6-9; $^{‡}p < 0.001$). *B:* Effect of GABA receptor inhibition. Incubation of hippocampal slices in aCSF containing the PDE2 inhibitor BAY 60-7550 and BAY 41-2272 in the absence or presence of bicuculline or CGP 55845 to block $GABA_A$ or $GABA_B$ receptors respectively. No significant inhibition of the cGMP response to BAY 41-2272 occurred, while L-NNA abolished the cGMP signal as expected (n = 3-6; $^{ns}p > 0.05$).

Calcium dependence

As described in the main introduction (Chapter 1), both constitutive isoforms of NOS (eNOS and nNOS) are Ca^{2+}-dependent enzymes. One route for Ca^{2+} entry and consequent nNOS-dependent NO formation would be following NMDA receptor activation. However, as this study is looking at unstimulated hippocampal slices, this would mean that there is circuit activity occurring with neurons being in a depolarised state. Since inhibition of glutamate receptors, Na^{+} channels, and GABA receptors failed to affect the cGMP levels in response to BAY 41-2272 *(Fig. 4.11a)*, the scenario outlined above is highly unlikely. Other potential routes for Ca^{2+} entry into cells are via voltage-gated Ca^{2+} channels.

To investigate the Ca^{2+}-dependence of endogenous basal NO release in the immature hippocampus, slices were exposed to the general Ca^{2+} channel blocker cadmium (Cd^{2+}, 200 µM). This led to significant reduction of the BAY 41-2272-evoked cGMP signal *(Fig. 4.12a)*. To evaluate the total contribution of Ca^{2+}, slices were incubated in Ca^{2+}-free aCSF containing the Ca^{2+} chelator EGTA (1 mM). While Cd^{2+} caused approximately 60% inhibition, omission of any Ca^{2+} at all resulted in further reduction of the cGMP signal, producing a total of approximately 90% inhibition as compared to the control response *(Fig. 4.12a)*. Consistent with forgoing results, also ODQ and L-NNA prevented cGMP accumulation in response to BAY 41-2272 *(Fig. 4.12a)*.

To ensure that the conditions used so far for establishing the Ca^{2+} dependence were not causing inhibition of the response due to some direct action on the NO_{GC} receptors, control experiments were performed in which the responses to the NO donor PAPA/NO were assessed in the absence and presence of the same conditions tested above. The response to PAPA/NO remained unaffected by the presence of Cd^{2+}, while Ca^{2+}-free conditions led to a small, but yet statistically significant, increase in the cGMP level *(Fig. 4.12b)*. The latter may be due to relief of a small degree of inhibition, which the NO_{GC} receptors are experiencing in the presence of Ca^{2+} (Kazerounian *et al.*, 2002). As expected, ODQ fully prevented the response to exogenous NO *(Fig. 4.12b)*.

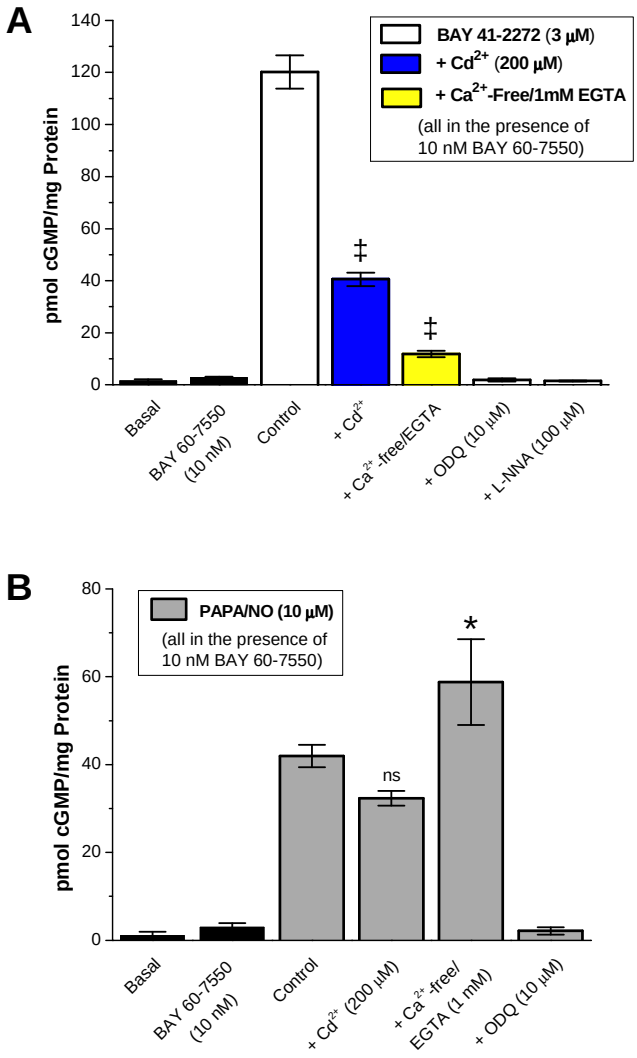

FIG. 4.12 Ca^{2+}-dependence of BAY 41-2272-evoked cGMP accumulation. *A:* Exposure of slices to the general Ca^{2+} channel inhibitor cadmium or incubation of slices in zero Ca^{2+}/ EGTA both significantly reduced the cGMP accumulation that is caused by BAY 41-2272 (n = 9; $^{‡}p < 0.001$). *B:* The same conditions now tested against cGMP accumulation that is caused by the NO donor PAPA/NO. No inhibitory effect was observed, excluding the possibility of these conditions directly interfering with cGMP production by affecting the NO_{GC} receptor. Under Ca^{2+}-free condition there appeared to be a slight increase in the cGMP response (n = 6; *p < 0.05).

The next question was whether it would be possible to isolate the subtype(s) of Ca^{2+} channels involved. Previous experiments discussed and illustrated above revealed that there is no spontaneous circuit activity occurring in the immature hippocampal slices and that the basal NO level is independent of glutamate receptors. Based on this, it is unlikely that the high-voltage activated Ca^{2+} channels (including L-, N-, P-, Q- and R-type Ca^{2+} channels, (Catterall *et al.*, 2005) are involved as their activation would require neurons to be in a depolarised state. Therefore, Ca^{2+} channel types were tested which could facilitate Ca^{2+} entry also under resting conditions. Low-voltage activated Ca^{2+} channels, which include the T-type Ca^{2+} channels, can activate at relatively negative membrane potentials (-50 mV to -70 mV; Catterall, 2000). An interesting feature of T-type channels is their exhibiting a so-called window current, which means that a fraction of these channels can maintain a current tonically under resting steady-state conditions as their inactivation and activation profiles overlap (Hughes *et al.*, 1999; Jones, 2003; Iftinca & Zamponi, 2009). This could provide a level of basal Ca^{2+} entry, which could in turn stimulate NOS activity. Importantly, these channels have also been shown to be expressed in hippocampal pyramidal neurons somato-dendritically (Talley *et al.*, 1999; McKay *et al.*, 2006), as well as in microvascular endothelial cells of the bovine adrenal medulla (Bossu *et al.*, 1989; Vinet & Vargas, 1999) and rat brain (Delpiano & Altura, 1996).

Hippocampal slices incubated in the presence of nickel (Ni^{2+}; 50 µM), at this concentration reported to be a selective R-/T-type Ca^{2+} channel inhibitor (Soong *et al.*, 1993; Zamponi *et al.*, 1996; Tottene *et al.*, 1996), revealed a marked reduction in BAY 41-2272-evoked cGMP accumulation *(Fig. 4.13a).*

Another potential candidate was the large family of channels referred to as transient receptor potential (TRP) channels, of which numerous different subtypes exist, some of which are thermosensitive (Pedersen *et al.*, 2005). Entry of Ca^{2+} via this putative route has been suggested to occur in the case of both neurons (Moran *et al.*, 2004; Talavera *et al.*, 2008) and endothelial cells (Wissenbach *et al.*, 2000; Güler *et al.*, 2002; Nilius *et al.*, 2003; Yao & Garland, 2005; Kwan *et al.*, 2007). In endothelial cells, for example, they are proposed to be constitutively open at body temperature, thereby providing a way for Ca^{2+} to enter cells under resting steady-state conditions.

Three different inhibitors, lanthanum (La^{3+}; 100 µM), gadolinium (Gd^{3+}; 30 µM) and SKF96365 (10 µM), suggested to generally block TRP channels (Leung & Kwan, 1999; Halaszovich *et al.*, 2000; Pinilla *et al.*, 2005), were examined. All three inhibitors produced significant inhibition of the cGMP signal induced by BAY 41-2272 *(Fig. 4.13a)*. Combining TRP channel inhibitors with the T-type channel blocker Ni^{2+} caused an additive degree of inhibition, which was comparable to that produced by the general Ca^{2+} channel blocker Cd^{2+} *(Fig. 4.13a)*. Taken all together, these data indicate that at least one or more subtypes of TRP channels, and T-type Ca^{2+} channels, appear to be likely routes for Ca^{2+} entry under resting conditions which allows for tonic NO synthesis to be sustained under basal conditions.

To certify that the inhibition seen under the above tested conditions is not due to a direct effect on the NO_{GC} receptors, control experiments were carried out in which they were tested against the response evoked by the NO donor PAPA/NO. None of the inhibitors on their own or combinations of inhibitors used in the foregoing experiments affected the cGMP signal in response to the NO donor significantly, while this was prevented upon inhibition of the NO_{GC} receptor by ODQ *(Fig. 4.13b)*.

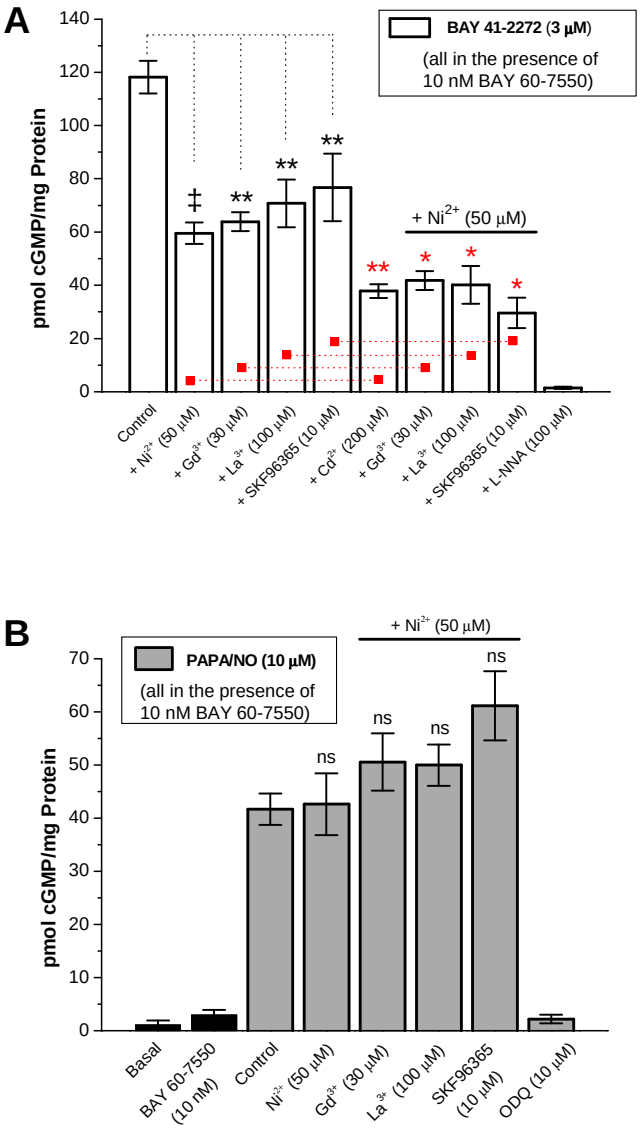

FIG. 4.13 Effect of subtype-selective Ca^{2+} - channel inhibitors on the BAY 41-2272-evoked cGMP response *A:* Exposure of slices to the R-/T-type Ca^{2+} channel blocker nickel or to three different TRP channel inhibitors (lanthanum, gadolinium and SKF96365) caused a significant reduction in the cGMP level. Additive inhibition occurred when a TRP channel inhibitor was applied in the presence of nickel, the overall extent of inhibition approximating the one seen in the presence of the general Ca^{2+} channel blocker cadmium (n = 5; $^{‡}p < 0.001$, $^{**}p < 0.01$, $^{*}p < 0.05$). Note: Statistical analysis shown in red employed ANOVA with Tukey's. *B:* The same Ca^{2+} channel blockers now tested against cGMP accumulation that is caused by the NO donor PAPA/NO. No inhibitory effect was observed, excluding the possibility of these conditions directly interfering with cGMP production by affecting the NO_{GC} receptor (n = 3; $^{ns}p > 0.05$).

4.5 DISCUSSION

Stemming from foregoing findings in the adult hippocampus (Hopper & Garthwaite, 2006), the initial objective of the present study was to investigate the involvement of the PI3 kinase pathway in the maintenance of basal NO production from eNOS in the immature hippocampus. This was intended to then serve as a comparison to what had been found in the immature rat optic nerve (Garthwaite *et al.*, 2006 and Chapter 3). Unexpectedly, this work took a new direction upon realisation that there appear to be marked differences in NO signalling – at least in the aspects investigated here – between the immature and adult rat hippocampus.

The measurement of a robust cGMP signal in immature hippocampal slices upon PDE2 inhibition with BAY 60-7550 in conjunction with BAY 41-2272 to amplify the NO_{GC} receptor output confirmed the presence of biologically active NO in the unstimulated tissue. Also, pharmacological tests using the general NOS inhibitor L-NNA and the NO_{GC} receptor inhibitor ODQ at concentrations that would ensure maximal inhibition (East & Garthwaite, 1991; Garthwaite *et al.*, 1995) confirmed that the cGMP signal resulting from PDE2 inhibition and NO_{GC} receptor sensitisation is indeed dependent on endogenous NO and corresponds to activity of NO_{GC} receptors. Suitable concentrations of both BAY 60-7550 and BAY 41-2272 in order to achieve a good working window in terms of the cGMP level and also a ‘clean’ cGMP response devoid of possible interferences (such as cAMP accumulation), as well as hippocampal slice viability were established. Subsequently, when moving on to investigating whether the tonic NO production in the unstimulated immature hippocampus was governed by the PI3 kinase pathway, the data disputed an involvement of this mechanism. Both PI3 kinase inhibitors tested (LY 294002 and wortmannin), shown previously to affect endogenous tonic NO-mediated cGMP production in the adult rat hippocampus (Hopper & Garthwaite, 2006), and indicated to at least partly sustain tonic NO levels in the immature rat optic nerve (Chapter 3), failed to affect the amount of cGMP accumulation in response to BAY 41-2272 in the immature hippocampus investigated here. The difference between the immature and adult hippocampi points to the possibility that, at least in this brain region, the profile

of basal NO synthesis may be differently controlled during development. In contrast, optic nerves were from rats of the same age as the immature hippocampal slices (i.e. 10- to 11-day old). This indicates that, in terms of sustenance of basal endogenous NO levels in an unstimulated tissue, the same mechanisms may not be common among different brain regions. A divergence could be related to the fact that, while the optic nerve is a white matter tract exclusively composed of axons, blood vessels and glial cells, the hippocampus consists of not only vascular elements and glial cells, but also a complex circuitry with synaptic connections and abundant expression of both eNOS and nNOS. There is the likelihood of not only different mechanisms being at play in maintaining a basal NO level, but also of this tonic NO production playing different roles at different developmental stages. This speculative possibility will be explored in more detail later.

Subsequently to the initial findings suggesting that the PI3 kinase pathway is not involved in controlling basal NO synthesis in the immature hippocampus, one of the first questions that arose concerned the isoforms of NOS at play. While evidence obtained from immature optic nerves and adult hippocampi pointed to eNOS as the primary source of basal NO with undetectable contribution of nNOS (Garthwaite *et al.*, 2006; Hopper & Garthwaite, 2006), this may not be the case in the immature hippocampus. To investigate a possible contribution of nNOS to basal NO levels in the immature hippocampus, the effect of nNOS inhibitors on the endogenous NO-dependent cGMP level was assessed. Concentrations of these inhibitors were employed that were previously shown to prevent the NMDA-evoked cGMP accumulation but not cGMP levels that depend on basal endogenous NO (East & Garthwaite, 1991; Hopper & Garthwaite, 2006). One of the inhibitors (1400W) also provided a way of testing the involvement of iNOS, exhibiting a greater inhibitory potency for iNOS than nNOS (Garvey *et al.*, 1997; Boer *et al.*, 2000; Young *et al.*, 2000). Inhibition of nNOS, or iNOS, failed to reduce the cGMP level in response to BAY 41-2272, the latter being consistent with iNOS being an unlikely candidate based on its principal involvement in pathological situations, its induction being initiated over the course of several hours (Iadecola *et al.*, 1995; Moro *et al.*, 1998; Yamada *et al.*, 2003). Additionally, iNOS was not detected in hippocampal slices

subjected to standard treatment and incubation (Hopper & Garthwaite, 2006). The lack of effect of nNOS inhibition would initially imply that there is no detectable constituent of neuronal NO release. Surprisingly, however, at the concentrations tested, the nNOS inhibitors also fell short in reducing the NMDA-evoked response significantly, indicating an inadequate degree of nNOS inhibition at these concentrations in immature hippocampal slices. One explanation for the failure of nNOS inhibitors to reduce the NMDA-induced cGMP signal may be insufficient concentrations used. Determining the potency of the nNOS inhibitors in the immature hippocampus led to the discovery that10-fold higher concentrations of the nNOS inhibitors were required to prevent NMDA-evoked cGMP accumulation compared to findings in adult hippocampi (Hopper & Garthwaite, 2006). Also worth mention is the observation that immature hippocampal slices were producing about three times as much cGMP in response to the same concentration of NMDA upon PDE2 inhibition as compared to findings in adult hippocampal slices. Moreover, also the cGMP response to BAY 41-2272 was noticeably greater in the immature hippocampal slices despite exposure to a 10-fold lower concentration of BAY 41-2272 than that applied to adult hippocampal slices (Hopper & Garthwaite, 2006), indicating that higher endogenous NO levels may prevail in the immature hippocampus.

An early study observed smaller cGMP responses to NMDA in adult hippocampal slices compared with immature tissue (East & Garthwaite, 1991), indicative of developmental differences. In the same study, it was found that supplementation of L-arginine, the substrate for NO synthesis, markedly enhanced the response to NMDA in the adult tissue. These findings indicate that there may be higher endogenous L-arginine levels in developing hippocampal slices. Moreover, the nNOS inhibitors that were used in the present study compete with L-arginine to exert their inhibitory action (Erdal *et al.,* 2005). Taken together, a difference in the amount of endogenous L-arginine may be an underlying reason for the necessity of higher concentrations of nNOS inhibitors to achieve the extent of inhibition of the response to NMDA as is observed in adult hippocampal slices. This is in concert with findings coming from studies investigating the potencies of inhibitors towards nNOS directly. The use of different concentrations of L-arginine has led to variations in the IC_{50} values reported (Wolff et al., 1998; Cowart *et al.,* 1998; Hagen *et al.,* 1998).

When probing the concentrations of the nNOS inhibitors that efficiently prevented NMDA-induced cGMP accumulation against BAY 41-2272-evoked cGMP levels, a partial reduction of the latter occurred. However, also this result failed to give any indications concerning the NOS isoforms involved in maintaining basal NO levels. Much higher concentrations of nNOS inhibitors were required to reduce the cGMP response to BAY 41-2272, and although with lower potency, the nNOS inhibitors have the potential to also compromise eNOS activity (Zhang *et al.*, 1997; Boer *et al.*, 2000). Selectivity towards nNOS at the higher concentrations of nNOS inhibitors required in the present study to efficiently inhibit nNOS was not preserved. Compromise of eNOS activity by the higher concentrations of nNOS inhibitors was evident by ACh-mediated eNOS-dependent cGMP production in rat aortas also being significantly reduced. Because of this overlap in potencies of the nNOS inhibitors, it is not possible to come to a clear conclusion regarding the source of basal NO in the immature hippocampus.

Arguably, the lack of reduction of the cGMP signal in response to BAY 41-2272 upon indirect inhibition of eNOS activity by means of preventing PI3 kinase activity could point to eNOS not being involved. However, the Ca^{2+}-dependence of eNOS activity should be taken into consideration. Preventing PI3 kinase-mediated phosphorylation of eNOS will reduce the sensitivity of the enzyme towards Ca^{2+} (Dudzinski *et al.*, 2006) but will not in itself entirely enable eNOS from being activated by other factors (see Chapter 3). Therefore, if there is sufficient Ca^{2+} present to preserve a basal state of eNOS activity, this could amount to enough basal NO output that would be detected upon sensitisation of the NO_{GC} receptors to very low NO levels by means of BAY 41-2272 (Garthwaite, 2005; Roy *et al.*, 2008). Equally, none of the data presented in the present study allows a firm conclusion to be made with regard to the contribution of nNOS. The possibility remains that both or only one of the isoforms may be at play to preserve ongoing NO formation under basal conditions. One issue these data reveal, however, concerns the questionable reliance on the selectivity of these nNOS inhibitors. Numerous studies use these compounds – as well-established nNOS antagonist – and interpret data for or against an involvement of nNOS based on the effects observed with these inhibitors. In addition, there may be false conclusion regarding the involvement of eNOS. The variations in

the observations made in studies that have investigated the potency and selectivity of nNOS inhibitors on isolated enzymes show clearly that results are sensitive to aspects such as different assay conditions (e.g. L-arginine concentration used) and species (Nakane *et al.*, 1995; Wolff *et al.*, 1998). This sensitivity will probably be aggravated when working on a whole tissue. Potencies of these inhibitors at the cellular level could be influenced by several factors. Permeability and/or intracellular metabolism of the compound may vary among different preparations, possibly depending on species, age and/or brain region investigated. Also, even if membrane permeability may not impose a problem for access *per se*, differences in the cellular context of the enzyme may impinge on the interaction between the inhibitor and its binding site. Considering the physical association of NMDA receptors and nNOS (Brenman *et al.*, 1996; Christopherson *et al.*, 1999; Valtschanoff & Weinberg, 2001), the presence of other proteins that may be targeted to the site of nNOS may shield the enzyme from an easy access of the inhibitor. For example, nNOS activity or its location may be influenced by interactions with various proteins such as synapsin and hsp90 (Billecke *et al.*, 2002; Jaffrey *et al.*, 2002; Dreyer *et al.*, 2004). As already mentioned above, another potential influence upon enzyme-inhibitor interaction may be differences in the concentration of endogenous L-arginine. As it appears to be a possibility in terms of the hippocampus, this may vary according to the age of the animal. While in the adult hippocampus the nNOS inhibitors were found to have higher potencies towards nNOS inhibiton compared with previous studies (Boer *et al.*, 2000; Cooper *et al.*, 2000; Hopper & Garthwaite, 2006), the results in the present study reveal that much higher concentrations need to be employed to achieve inhibition of the bulk nNOS activity. Moreover, different endogenous L-arginine levels may prevail in different brain areas. Overall, the data obtained in the present study, showing that at least in the hippocampus the inhibitory profile of the nNOS inhibitors differs between immature and adult tissue (Hopper & Garthwaite, 2006), underline the importance of the inclusion of appropriate controls when using these compounds. Failure to do so may lead to either nNOS being wrongly assumed to be a participant in the response under investigation or to eNOS being overlooked as a contributor.

To further test a possible contribution of a neuronal component to endogenous NO production, a number of neurotransmitter systems were investigated that could be involved in nNOS stimulation. It has been estimated that the presence of BAY 41-2272 shifts the potency of NO for its receptor to low picomolar concentrations (EC_{50} ~ 4 pM; Roy *et al.*, 2008). Spontaneous NO oscillations in the picomolar range have been measured in hippocampal neurons grown in culture (Sato *et al.*, 2006). Sato and colleagues observed periodic spontaneous NO release, which was NMDA receptor-dependent and relied on spontaneous neurotransmission, as revealed by its sensitivity to Na^+ channel block by TTX, as well as coincident with neuronal Ca^{2+} spikes. Spontaneous circuit activity in the hippocampal slices could lead to a basal level of glutamate being released, which could ultimately lead to activation of AMPA receptors and/or, given a sufficient degree of neuronal depolarisation, NMDA receptors. Both AMPA and NMDA receptors are permeable to Ca^{2+}, which in turn could stimulate NO formation from nNOS which is coupled to NMDA receptors (Brenman *et al.*, 1996; Christopherson *et al.*, 1999; Valtschanoff & Weinberg, 2001) and is expressed in pyramidal neurons at the protein level (Endoh *et al.*, 1994; Wendland *et al.*, 1994; Burette *et al.*, 2002; Blackshaw *et al.*, 2003). Block of neither glutamate receptors nor Na^+ channels revealed any significant change in the cGMP response evoked by BAY 41-2272. This implies that the tonic NO production in immature hippocampal slices is unlikely to be dependent on spontaneous neurotransmission. This is consistent with findings in adult hippocampal slices (Hopper & Garthwaite, 2006). Additionally, tonic NO generation from NOS that is independent of NMDA receptor activation and maintains a basal cGMP level – as revealed upon PDE inhibition – has been demonstrated previously in hippocampal and striatal slices (Chetkovich *et al.*, 1993; Griffiths *et al.*, 2002), On the other hand, the evidence taken together reveals a possible discrepancy between hippocampal neurons in their native environment and neurons that are grown and maintained in culture, perhaps arising from a different balance between excitation and inhibition. Overall, the finding that pharmacological manipulation of either of the above examined systems did not show a detectable impact on the cGMP signal that corresponds to the tonic NO level makes the involvement of nNOS even more doubtful. On the other hand these data are in favour of eNOS being the key player in

basal NO synthesis. However, based solely on the data obtained here, this is still speculative, bearing in mind that there are other potential routes by which nNOS could be stimulated in neurons such as, for example, Ca^{2+} entry via Ca^{2+} channels.

Both eNOS and nNOS are Ca^{2+}-dependent, another potential route of Ca^{2+} entry into cells being voltage-gated Ca^{2+} channels. Incubation of hippocampal slices with the general Ca^{2+} channel blocker cadmium markedly reduced the cGMP response to BAY 41-2272, while incubation of slices in Ca^{2+}-free aCSF prevented cGMP accumulation to a level approaching that measured in the absence of pharmacological treatment or upon NOS or NO_{GC} receptor inhibition. This result strongly indicates that in the immature hippocampus basal NO levels are chiefly Ca^{2+}-dependent. As to the Ca^{2+} channel types involved, the data obtained in the present study suggests T-type Ca^{2+} channels and TRP channels as possible contributors.

There are three isoforms of T-type Ca^{2+} channels (Perez-Reyes, 2003), all three having been found to be expressed in hippocampal pyramidal neurons (Talley *et al.*, 1999). Additionally, T-type channels have also been demonstrated on microvascular endothelial cells from rat brain (Delpiano & Altura; 1996). These channels exhibit a window current; that is they display an overlap between the curves describing their inactivation and activation, effectively allowing them to support a maintained current under steady-state conditions (Hughes *et al.*, 1999; Jones, 2003; Iftinca & Zamponi, 2009). The level of cGMP was significantly inhibited by nickel at concentrations reported to inhibit T-type (and R-type) Ca^{2+} channels (Soong *et al.*, 1993; Zamponi *et al.*, 1996; Tottene *et al.*, 1996), indicating a likely involvement of T-type channels in Ca^{2+}-dependent NOS activation. The involvement of the high-voltage activated R-type Ca^{2+} channels can probably be discounted, as their activation would require neurons to be depolarised. However, to ascertain that the effect of nickel is not due to R-type channel inhibition, further experiments should have been conducted, employing a selective R-type channel inhibitor such as SNX-482 (Newcomb *et al.*, 1998). T-type Ca^{2+} channels have been demonstrated to provide a route for sustained Ca^{2+} entry in the adrenal cortex (Cohen *et al.*, 1988) and in the heart (Nilius, 1985; Hagiwara *et al.*, 1988), regulating secretion from adrenal glomerulosa cells and pacemaker potentials in sino-atrial node cells respectively.

Also, mice lacking T-type channels were found to exhibit constitutively constricted coronary arterioles and focal myocardial fibrosis, displaying normal contractile responses but defective NO-mediated relaxation to ACh (Chen *et al.*, 2003). Chen and colleagues (2003) also demonstrated prevention of relaxation of coronary arteries by a low concentration of nickel.

The other possible contributor to Ca^{2+} entry under basal conditions that was assessed were TRP channels, which are permeable to Ca^{2+} and also can be open at the resting membrane potential (Clapham *et al.*, 2001) or be stimulated by extracellular signals such as the brain-derived neurotrophic factor (BDNF; Li *et al.*, 2005). The TRP channel family is one of the largest among the different groups of ion channels, comprising at least 28 genes that are subcategorised into six different protein families (Pedersen *et al.*, 2005). TRP channels are intimately involved in the processes of sensing and responding to environmental changes such as temperature, mechanical forces and taste (Damann *et al.*, 2008). With relevance to the present work, members of the TRP channel family have also been found to be expressed in endothelial cells (Wissenbach *et al.*, 2000; Güler *et al.*, 2002; Nilius *et al.*, 2003; Yao & Garland, 2005; Kwan *et al.*, 2007) and in neurons in various brain regions including the hippocampus (Moran *et al.*, 2004; Talavera *et al.*, 2008). Among the 28 different TRP channel isoforms, at least 19 are found in vascular endothelial cells. Some are open constitutively while others are activated by circulating vasoactive agents released from vascular cells (Yao & Garland, 2005; Kwan *et al.*, 2007). Either way, opening of these channels elicits a rise in Ca^{2+} in the endothelial cells, leading to the release of a number of vasodilating agents such as NO. For instance, the TRPV4 has been found to be highly expressed in endothelial cells (Wissenbach *et al.*, 2000) and to be constitutively open at body temperature, thereby potentially contributing to the maintenance of a steady-state Ca^{2+} level (Güler *et al.*, 2002; Nilius *et al.*, 2003). Additionally, mice lacking TRPV4 are devoid of NO-dependent vasorelaxation to ACh (Freichel *et al.*, 2001). TRP channels that have been found to be expressed in the hippocampus include TRPV1 and TRPV4, as well as subtypes 1, 3, 4, 5 and 6 of TRPC (Moran *et al.*, 2004; Talavera *et al.*, 2008). For example, TRPV4 channels have been demonstrated to allow basal Ca^{2+} influx at 37ºC in hippocampal neurons, potentially influencing neuronal excitability (Shibasaki *et al.*, 2007). Taking the data

obtained in the present study together with the other evidence outlined above, it is possible that T-type channels and TRP channels are at least partly responsible for the Ca^{2+}-dependent basal NO production in the immature hippocampal slices, the NO possibly originating from blood vessels (eNOS) and/or neurons (nNOS).

The overall picture of the present study reveals one major difference between the adult and the immature hippocampi. While in the adult hippocampus tonic NO release was found to be partly mediated by the PI3 kinase pathway (Hopper & Garthwaite, 2006), the basal NO production in the immature hippocampus appears to be mainly controlled in a Ca^{2+}-dependent manner, with no detectable contribution of the PI3 kinase pathway. Moreover, while pharmacological approaches in the adult hippocampus allowed differentiation between eNOS and nNOS, in the immature hippocampus overlap in potencies of available inhibitors prevented such a clear distinction between NOS isoforms. Several important issues arise from this work. What could be the significance of activity-independent, Ca^{2+}-mediated tonic NO synthesis in the immature hippocampus? What role may be served by possibly both eNOS and nNOS being locked into a state of basal activity? Is it possible that the readout obtained in these experiments corresponds to tonic NO release initiated artefactually in the unstimulated hippocampal slices?

Calcium is a ubiquitous intracellular signalling molecule that is involved in a vast array of different cellular processes. There is an impressive universality to calcium signalling, including its involvement in development. In the rat brain, angiogenesis, the formation of new vessels, is not complete until about postnatal day 20 (Plate, 1999). Endothelial cells play an important role in this process, and TRP channels, for instance, have been proposed to affect angiogenesis through several mechanisms such as activation by angiogenic growth factors including vascular-derived endothelial growth factor (VEGF) and platelet-derived growth factor (PDGF; Nilius *et al.*, 2003; Yao & Garland, 2005). Moreover, NO has also been implicated to play a role in angiogenesis (Ziche & Morbidelli, 2000; Donnini & Ziche, 2002), as has VEGF both in the developing and adult brain (Ment *et al.*, 1997; Plate, 1999; Greenberg & Jin, 2005). On the other hand, however, to date there is no evidence showing directly that dysfunctional endothelial TRP channels lead to impaired vessel

development or repair. Also in neurons, Ca^{2+} oscillations may have a purpose in development. For example, neuronal spontaneous Ca^{2+} signals that appear to be independent of synaptic activity have been observed in cultured immature spinal cord neurons by means of Ca^{2+} imaging (Fabbro *et al.*, 2007). The authors described mitochondrial Ca^{2+} uptake and release mechanisms to be a source for cytoplasmic repetitive Ca^{2+} transients in the neurons. Developmental processes such as neurite growth and neuronal differentiation are thought to be dependent on different patterns of Ca^{2+} transients (Gu & Spitzer, 1995; Gu & Spitzer, 1997; Gomez & Zheng, 2006). Interesting in this respect is the finding that, for example, types of the TRPC channel appear to be implicated in neurite outgrowth and axonal pathfinding (Greka *et al.*, 2003; Moran *et al.*, 2004; Talavera *et al.*, 2008). Spontaneous glial Ca^{2+} oscillations in acute brain slices have also been observed (Parri *et al.*, 2001; Nett *et al.*, 2002). Glial cells are known to release a number of substances including growth factors (Martin, 1992). Could there be a complex interplay among blood vessels, neurons and glia during development? For instance; could spontaneous Ca^{2+} activity in glia promote the release of substances which in turn could act on their receptors that my be expressed by neurons and/or endothelial cells, in turn causing spread of Ca^{2+} fluctuations (by, for example TRP channels) to these structures and ultimately stimulating tonic NO synthesis? Could it be possible that during postnatal development both neurons and blood vessels exhibit a basal level of continuous NO production, either being involved in their own maturation (e.g. angiogenesis, neurite growth) or influencing each other? Finally, to try to put this idea into context, NO has been shown to be involved in various processes during neuronal development in both vertebrates and invertebrates (Bicker, 2005; Bicker, 2007), NO being implicated in the granule cell migration in the rat cerebellum, for instance, and cGMP being proposed to play a role in growth cone behaviour. In snail neurons, growth cone morphology and neuronal pathfinding have been reported to be influenced in a NO-mediated, cGMP-dependent manner (van Wagenen & Rehder, 2001; Tornieri & Rehder, 2007). Here, the authors provided evidence that NO released from a given neuron can affect growth cone dynamics on neighbouring cells. Also in cultured hippocampal slices, for example, cGMP has been proposed to be a participant in mediating the correct targeting of mossy fibres of the dentate gyrus to the CA3 region

of the hippocampal formation (Mizuhashi *et al.*, 2001). However, the latter study on hippocampus claimed to have not observed evidence for NO involvement, unfortunately not showing the data and not describing the types of experiments executed to investigate the role of NO. Alternatively, it is likely that the effects the authors observed were related to cGMP production by the particulate natriuretic peptide-stimulated guanylyl cyclase, which is insensitive to NO. Although uncertain, this line of evidence could point to cGMP playing a role in aspects of hippocampal development, some of which may or may not be NO-mediated. Another purpose of basal NO-mediated cGMP production during development may be to engage the regulation of gene expression and protein synthesis, which could be mediated by phosphorylation of some transcription factors such as CREB by cGMP-dependent protein kinase (PKG; Pilz & Broderick, 2005).

To summarise, it is very tempting to reason and speculate that there may be a dual contribution of eNOS and nNOS to tonic NO levels in the immature hippocampus. However, from the present work the source(s) of NO remain unknown. The lack of good pharmacological tools makes it impossible to identify the origin of the endogenous basal NO in the immature hippocampus. Better pharmacology is crucial to build a new hypothesis concerning the role of tonic NO release in the immature hippocampus. Also, regarding the underlying mechanism for tonic NO release, this work only provides circumstantial evidence and more detailed investigation is required to clarify the components involved. It is also possible that the persistent NO production and corresponding cGMP levels were induced artefactually. Preventing normal degradation of cGMP greatly amplifies and prolongs the cGMP signal, which is an experimental way to detect the NO-mediated cGMP accumulation but is highly un-physiological. Hippocampal slices were pre-exposed to the PDE2 inhibitor BAY 60-7550 for at least 15 minutes before any further pharmacological manipulation. Since cGMP can modulate many downstream effectors, this prolonged cGMP accumulation may have led to continuous NO synthesis. For instance, both nNOS and eNOS may be phosphorylated by PKG, increasing enzyme activity (Butt *et al.*, 2000; Garthwaite, 2008), and the finding that the cGMP response corresponding to basal NO levels was prevented under Ca^{2+}-free conditions could simply reflect the

Ca^{2+}-dependence of constitutive NOS isoforms. Overall, many aspects of the present work remain inconclusive.

*

CHAPTER 5

Targets for NO in the hippocampus

5.1 INTRODUCTION

As described in more detail in Chapter 1, NO exerts its actions via a mechanism which commences with its synthesis by the NO synthase (NOS), the constitutive isoforms of this enzyme being neuronal (n)NOS, which is found in neurons (Bredt *et al.*, 1991b; Vincent & Kimura, 1992), and endothelial (e)NOS, which is expressed in blood vessels (Chiang *et al.*, 1994; Seidel *et al.*, 1997; Stanarius *et al.*, 1997; Topel *et al.*, 1998; Demas *et al.*, 1999; Blackshaw *et al.*, 2003; Chan *et al.*, 2004). This is followed by NO binding to its receptor, the guanylyl cyclase, generating the second messenger cGMP, which can then interact with a number of downstream targets, including ion channels, protein kinase G (PKG) and phosphodiesterases (PDEs; see Chapter 1). Nitric oxide can be produced in various brain constituents, including neurons and the vascular system, and is able to diffuse from its site of synthesis in a three-dimensional manner to target structures in its vicinity such as astrocytes, neurons, and blood vessels (Garthwaite & Boulton, 1995, Garthwaite, 2008). Since the discovery that NO is the missing transmitter that is generated in response to NMDA receptor activation (Garthwaite *et al.*, 1988; Garthwaite, 1991), the list on how NO may affect neuronal function has grown, including its implication in the long-term regulation of neuronal function (see Chapter 1) where neurons can undergo long-term changes in the efficacy of their synaptic connections. This event, referred to as long-term potentiation (LTP), has been observed in different brain regions, the most extensively studied being the hippocampus, and is considered to model the cellular events that underlie the acquisition and storage of information (Bliss & Collingridge, 1993; Neves *et al.*, 2008; Nader & Hardt, 2009). Nitric oxide via cGMP generation has been implicated in both pre- and postsynaptic changes such as modulation of neurotransmitter release (O'Dell *et al.*, 1991; Arancio *et al.*, 1995; Arancio *et al.*, 2001) or increase in AMPA receptor density respectively (Wang *et al.*, 2005; Serulle *et al.*, 2007), these changes being implicated in LTP (Garthwaite & Boulton, 1995; Prast & Philippu, 2001; Collingridge *et al.*, 2004; Kerchner & Nicoll, 2008). For example, Serulle et al. (2007) demonstrated cGMP-dependent PKG-mediated phosphorylation of GluR1 (the AMPA receptor subunit required for NMDA-dependent LTP), in this way apparently

facilitating the delivery of the GluRI subunit to extrasynaptic sites. Moreover, cGMP-mediated PKG-dependent phosphorylation of the transcription factor CREB has been reported to occur in the hippocampus, suggesting an involvement of the NO-signalling cascade in the component of LTP that relies on RNA and protein synthesis in the postsynaptic neuron (Lu *et al.*, 1999). Additionally, direct removal of NO from the postsynaptic neuron by means of injection of the NO scavenger CPTIO has been found to impair tetanus-evoked synaptic potentiation (Ko & Kelly, 1999).

Intuitively, based on the implications stemming from functional studies, one would expect to see cGMP accumulation in the appropriate structures upon NO_{GC} receptor activation, such as axons and neuronal somata. Unexpectedly, however, previous studies found no detectable cGMP formation in the principal neurons of the hippocampus, the pyramidal cells, despite the expression of the NO_{GC} receptor both at its mRNA and protein level (Matsuoka *et al.*, 1992; Teunissen *et al.*, 2001; Burette *et al.*, 2002; Gibb & Garthwaite, 2001; Ding *et al.*, 2004; Szabadits *et al.*, 2007). Conditions employed in previous studies found no cGMP accumulation in neuronal cell bodies of the hippocampus but predominant cGMP immunoreactivity (cGMP-IR) in astrocytes, particularly around the CA1 region. This was accompanied by cGMP staining in some interneurons and varicose fibres in different sub-regions of the hippocampus (de Vente *et al.*, 1988; de Vente *et al.*, 1996; van Staveren *et al.*, 2001; Teunissen *et al.*, 2001; van Staveren *et al.*, 2004; van Staveren *et al.*, 2005). Thus, it appears that there is a clear mismatch between anatomical and functional studies concerning the involvement of the NO-cGMP signalling pathway in neuronal function that can be either at the pre- or postsynaptic level, as discussed above.

One very important component of the NO-cGMP signalling pathway is PDE (see Chapter 1), as it provides great spatiotemporal control over the cGMP signal, rapidly breaking cGMP down to the inactive derivative GMP (Bender & Beavo, 2006). Therefore, the amount and duration of cGMP formation will highly depend not only on its rate of synthesis but also the presence and activity of PDE (Garthwaite, 2005). Moreover, the shape of the cGMP signal may also determine the downstream target and ensuing biological effect. For example, the concentration of cGMP accumulating at its site of synthesis in a neuron will determine whether the

downstream target is an ion channel or PKG, the two having different affinities for cGMP binding (Garthwaite, 2005). In the hippocampus, the presence and high activity of PDE is an important hallmark (see Chapter 4 – Introduction). Currently there are 11 PDE families known, the main ones found in the hippocampal formation being PDE2, 5 and 9 throughout various embryonic and postnatal developmental stages up until adulthood (van Staveren *et al.*, 2003). Previous evidence implicates PDE2 as the major PDE that shapes cGMP accumulation in the hippocampus (see Chapter 4 – Introduction).

In order to characterise signalling cascades and their impact on functional aspects, the availability of selective pharmacological tools is invaluable. Although there have been inhibitors available, the low potency and non-selectivity of available inhibitors could have confounded studies into the role of these enzymes. For PDE2, a commonly used inhibitor in the past has been the compound EHNA, which, however, not only has poor potency but is also used as a potent adenosine deaminase inhibitor (see Chapter 4 – Introduction). More recently, a highly selective and more potent PDE2 inhibitor, known as BAY 60-7550, has been developed and shown to enhance LTP of synaptic transmission and to improve the performance of rats in a number of memory tasks (Boess *et al.*, 2004). Other tools for manipulating the NO signalling pathway include the so-called NO donors. The NO_{GC} receptor can be activated independently of NOS-generated endogenous NO by these compounds. The choice of NO donor and the conditions they are used under are vital in terms of the outcome of the cGMP signal as both of these aspects will determine how NO is released (Morley & Keefer, 1993; Keefer *et al.*, 1996; Schmidt *et al.*, 1997; Feelisch, 1998). Another aspect to consider is the signal-to-noise ratio of the cGMP signal. Depending on the methodology utilised, a cGMP signal could remain undetected. Thus, additionally to inhibiting PDE, it is possible to further amplify the signal by using compounds such as BAY 41-2272, which sensitises the NO_{GC} receptors to NO, with the effect of shifting the potency of NO for its receptor from low nanomolar to low picomolar concentrations (Stasch *et al.*, 2001; Garthwaite, 2005; Roy *et al.*, 2008).

5.2 AIM

Taking advantage of the now available pharmacological tools, the aim of this study was to re-investigate the targets for NO in the hippocampus.

5.3 METHODS

5.3.1 Hippocampal tissue preparation

Hippocampi were isolated and sliced at 400 µm as described in detail in Chapter 4, and left to recover in a shaking water bath for 1-2 hours at 37°C with a constant stream of 95% O_2 / 5% CO_2 flowing through the inlet stopper. Brain slices were transferred to fresh aCSF before exposure to pharmacological treatment. For each experiment, a number of slices were processed for quantitative cGMP evaluation by means of radioimmunoassay, while the remaining slices were further processed for immunohistochemistry.

5.3.2 Quantitative analysis of cGMP accumulation

A number of hippocampal slices were processed for cGMP immunohistochemistry (see below) while some were treated for cGMP quantification by means of radioimmunoassay (RIA). Following a recovery period of 1-2 hours at 37ºC in a shaking water bath, rat hippocampal slices were transferred into fresh aCSF before starting the pharmacological treatments. Except for the slices providing the measurements for 'basal' cGMP levels, hippocampal slices were pre-incubated with the PDE2 inhibitor BAY 60-7550 for 15 min before adding any agonists, the PDE2 inhibitor being present throughout the experiment. Inhibitors such as L-NNA and ODQ were applied for a 10 min interval prior to BAY 60-7550 and were present for the remainder of the experiment. Exposure of hippocampal slices to DEA/NO and BAY 41-2272 was for 2 min and 5 min respectively, applying BAY 41-2272 first to

sensitise the NO_{GC} receptors before adding the NO donor. To inactivate the biological reaction within the tissue at the appropriate time, each of the slices was transferred into a separate Eppendorf tube containing 250 µl of boiling inactivation buffer, leaving it to boil for a minimum of 15 min. In parallel, hippocampal slices for the immunohistochemical analysis were transferred into fixative (see below). After tissue inactivation, samples were left to cool to room temperature, homogenised by sonication, and the protein content measured using the BCA Protein Assay Kit. Following this, samples were centrifuged at 800 rpm for 10 min, discarding the debris. The supernatant was used to determine the cGMP amount by means of RIA as described in detail in Chapter 2.

5.3.3 Fluorescence immunohistochemistry

The antibody against cGMP was kindly given to us by Jan de Vente, Maastricht University. Following pharmacological treatment, the slices used for histological evaluation of cGMP accumulation were placed onto a piece of filter paper and then transferred into 4% fresh depolymerised PFA fixative. Slices were fixed for 2 hours at 4ºC under constant motion, subsequent to which they were washed 4-5 times with 0.1 M PB (15-20 min each) and then placed into 5% sucrose for 2 hours standing at 4ºC. Subsequently, slices were transferred to 20% sucrose and left overnight standing at 4ºC. This was followed by placing the slices first into a 1: 1 mixture of OCT and 50% sucrose for 1 hour at room temperature and then into neat OCT for approximately 30 min before embedding in OCT in the appropriate embedding mould over dry ice / iso-pentane. Slices were then cryosectioned at 10 µm sections, mounted onto gelatine-coated slides, which were left to dry at room temperature overnight before storing them at -20ºC. Frozen tissue/OCT blocks that were not cryosectioned immediately were stored at -80ºC.

Staining procedure

Slides were allowed to thaw and were then re-hydrated with TBST at 2x 5 min. Non-specific binding was blocked by adding 10% serum (made in TBST) from the host of

the secondary antibody (in this case donkey) for 1 hour at room temperature, followed by applying primary antibody made up in TBST containing 1% serum, leaving it to incubate overnight for approximately 20 hours at 4ºC (negative controls were incubated with TBST-1% serum). Primary antibodies were used at the following dilutions: 1: 40 000 sheep-anti-cGMP, 1: 2000 mouse-anti-CNPase, 1: 1000 rabbit-anti-GFAP, 1: 1200 mouse-anti-NeuN, and 1: 500 mouse-anti-NF 200. Primary antibody incubation was followed by washing with TBST at 4-5x 10-15 min before applying the secondary antibody (made up in TBST) for 1 hour at room temperature in the dark. Secondary antibodies were used at the following dilutions: 1: 1000 donkey-anti-sheep-Alexa 488, 1: 1500 donkey-anti-rabbit-Alexa 594, and 1: 600 donkey-anti-mouse-Alexa 594. Slides were washed with TBST at 4-5x 10-15 min and then mounted and coverslipped in mounting medium (containing DAPI to stain the nuclei). Slides were stored at 4ºC in the dark.

5.3.4 Immunohistochemistry for $GC\beta_1$

For the $GC\beta_1$ immunohistochemistry, animals were deeply anaesthetised with 200 µl i/p of Pentoject (Pentobarbitone sodium – 200 mg/ml) per animal, followed by intracardial *in situ* fixation (this procedure was kindly carried out by Mr. Nick Davies). The *in situ* fixation consisted of one flush with cold PBS (0.1 M; sterile), to avoid blood contamination, followed by perfusion with cold, fresh depolymerised 1% PFA fixative. Whole hippocampi were transferred into 1% cold PFA and left for 3 hours at room temperature under continuous motion. Following fixation, hippocampi were washed 5 times with 0.1 M PB (20-30 min each), placed into 5% sucrose for 2-3 hours standing at 4ºC, transferred to 10% sucrose for 2 hours standing at 4ºC, and finally added to 25% sucrose in which they were left overnight standing at 4ºC. Subsequently, whole hippocampi were incubated for 1-2 hours in 1: 1 OCT and 50% sucrose, followed by approximately 30 min neat OCT. The hippocampi were then embedded in OCT in the appropriate mould over card ice / iso-pentane, dipping the bottom of the embedding mould into a plastic dish resting on the card ice and containing iso-pentane to ensure rapid freezing of the tissue. Slices were then cryosectioned at 10 µm sections, mounted onto gelatine-coated slides, which were left

to dry at room temperature overnight before storing them at -20ºC. Frozen tissue/OCT blocks that were not cryosectioned immediately were stored at -80ºC.

Staining procedure

Slides were allowed to thaw and were then re-hydrated with TBS (no triton) at 2x 5 min. Tissue was permeabilised with neat acetone for 5 min, continuously dropping some onto the slide, followed by 3x 5 min washes with TBS. Peroxidase suppressor was then applied for 15 min at room temperature, followed by 3x 5 min washes with TBS. Non-specific binding was blocked by adding 10% serum (made in TBS) from the host of the secondary antibody (in this case donkey) for 1 hour at room temperature. Primary antibody (rabbit-anti-GCβ_1; 1: 500) made up in TBS containing 1% serum was then applied and incubated overnight for approximately 20 hours at 4ºC (negative controls were incubated with TBS-1% serum), followed by 4x 10-15 min washes with TBS. Sections were then incubated with secondary antibody (donkey-anti-rabbit-biotin; made up in TBS at 1: 200) for 1-2 hours at room temperature, followed by 4x 10-15 min washes with TBS. Subsequently, ABC reagent was applied for 45 min at room temperature, followed by 4x 10-15 min washes with TBS, and DAB was then applied in excess for 4-5 min at room temperature. Slides were then rinsed with plenty dH_2O, counter-stained with haemalum (applying it for 20-25 seconds at room temperature and immediately rinsing it off with tap water), washed once with dH_2O, and finally allowed to air-dry overnight at room temperature. Slides were then mounted and coverslipped in DPX and allowed to dry overnight before taking pictures, storing them at room temperature.

5.3.5 Analysis

cGMP quantification by means of RIA

The procedure for determining cGMP content normalised to protein amount has been dealt with in detail in Chapter 2. All data are presented as means ± SEM obtained from at least two different slices per animal, testing at least three rats.

Immunohistochemistry

Images were taken, using a communal Leica TCS SP confocal microscope, running Leica LCS SP2 software (Leica Microsystems, Heidelberg, Germany). The Leica TCS SP confocal microscope is equipped with four lasers giving 5 selectable lines; Argon ion giving 458nm (blue) and 488nm (cyan), Krypton 568nm (green/yellow), HeNe 633nm (red) and a water-cooled Argon ion producing UV with lines at 351 and 364 nm. The Leica DM-R upright fluorescence microscope is fitted with standard FITC/TRITC filters. In the saved settings box of the Leica software, the appropriate filter was selected – e.g. DAPI (UV laser; blue emission, e.g. Hoechst and other UV dyes excited by 351 and 364 nm such as DAPI used in the present study), FITC (Argon laser; green emission, e.g. FITC, fluorescein, GFP and other green dyes excited by 488, 512 and 476 nm such as Alexa-488 used in the present study) or TRITC (HeNe laser; red emission, e.g. TRITC, rhodamine red, Texas red, Cy5 and other red dyes excited by 568-633 nm such as Alexa-594 used in the present study). For 10 µm tissue sections, 6 optical sections were taken and each was averaged 4-6 times. When comparing cGMP staining in different parts of the same tissue section, the same parameters were applied. Negative controls were also imaged in parallel with the same parameters. The images were then processed and merged in Leica LCS Lite. To determine cGMP-positive structures, the appropriate markers were stained and co-localisation was evaluated. Images presented here are qualitative representatives of at least three observations from different rats.

5.4 RESULTS

5.4.1 Localisation and characterisation of cGMP-positive structures

Stimulation of NO_{GC} receptors – in the absence of NO donor

cGMP signal corresponding to endogenous NO:

Incubation of hippocampal slices in the presence of PDE inhibitor only, resulted in barely detectable cGMP accumulation, as did incubation of slices under basal conditions without pharmacological treatment *(Fig. 5.4)*. In the presence of submaximal concentrations of both BAY 60-7550 (10 nM) and BAY 41-2272 (3 µM), cGMP levels were measured by RIA to be 151 ± 14 pmol/mg protein *(Fig. 5.4)*. Under these conditions, cGMP signals were observed mainly in astrocytes, especially around the CA1 region, a few interneurons, and blood vessels *(Fig. 5.1b and Fig. 5.2)*. A similar staining pattern was found when slices were incubated in the presence of the broad-spectrum PDE inhibitor IBMX (1 mM) and BAY 41-2272 (3 µM; *Fig. 5.1a and Fig. 5.2)*, a condition investigated previously in rat and mouse hippocampi, with a prominent cGMP signal in astrocytes (especially around the CA1 area) and varicose fibres (van Staveren *et al.*, 2004). Moreover, the similarity of the staining pattern that is obtained using either IBMX or BAY 60-7550 at a submaximal concentration echoes findings concerning the similarity observed when using IBMX and the PDE2 inhibitor EHNA in the absence or presence of an NO donor (van Staveren *et al.*, 2001).

In order to maximise the signal in response to endogenous NO the effects of maximal concentrations of these agents were investigated. When tested on purified PDE2, BAY 60-7550 showed maximal inhibition of enzyme activity at 0.1-1 µM (Boess *et al.*, 2004). Only the activity of PDE1 was noticeably affected by BAY 60-7550, while PDE5 activity was marginally enhanced. Bearing in mind, however, that these data correspond to observations made on purified enzymes, it is most likely that

a higher concentration would be required for these actions to occur when looking at the whole tissue level. A lower potency of inhibitors in slices is based on cell permeability or possible intracellular metabolism of the compound. For example, differences in potency were found for the PDE5 inhibitor DMPPO when comparing the inhibitory effect in an enzymatic assay to a cell model (Coste & Grondin, 1995). Furthermore, while inhibition of PDE5 has been shown to elevate cGMP to some extent, no increase in cGMP has been found to occur upon PDE1 inhibition in the hippocampus (de Vente *et al.*, 1996; van Staveren *et al.*, 2001). As it is well known, cyclic nucleotides can modulate each others' signal profile by, for example, one acting on a PDE affecting the breakdown of the other such as is the case with cGMP inhibition of PDE3 that may ultimately lead to enhanced cAMP levels (Vigne *et al.*, 1994; Pelligrino & Wang, 1997; Bender & Beavo, 2006). This could ultimately interfere with the signal of interest. The levels of cAMP in the presence of different BAY 60-7550 concentrations have been assessed previously in adult hippocampal slices, significant cAMP elevation being obtained when the concentration of BAY 60-7550 exceeded 1 µM (Boess *et al.*, 2004). Taken together, a maximal concentration of 1 µM was chosen for BAY 60-7550 in conjunction with a maximal concentration of 10 µM BAY 41-2272, the latter being devoid of non-selective effects such as PDE inhibition (Stasch *et al.*, 2001; Mullershausen *et al.*, 2004a). It should be noted, however, that even if cross talk occurred between the two cyclic nucleotides under these chosen conditions, or any other cGMP-hydrolysing PDE isoform were inhibited, this would not interfere with the primary aim of the present study, namely to evaluate structures in the hippocampus that are potential NO targets, being capable of synthesising cGMP. Moreover, direct elevation of cAMP via PDE4 inhibition has been reported to result in weak cGMP-IR in some astrocytes only (van Staveren *et al.*, 2001).

Under these chosen conditions in the present study (i.e. 1 µM BAY 60-7550 and 10 µM BAY 41-2272), the level of cGMP was found to be enhanced to 578 ± 53 pmol/mg protein *(Fig. 5.4)* and a quite distinct staining pattern revealed itself compared to previously tested conditions. In addition to broad astrocytic cGMP-IR throughout the hippocampal formation, a greater proportion of interneurons appeared to be immuno-positive for cGMP *(Fig. 5.1c)*. More strikingly, a brightly stained

cluster of unidentified cells, most likely pyramidal cells (as verified later by co-localisation with the neuronal marker NeuN), was apparent in the subiculum, as well as faintly stained pyramidal cells in the CA4 region *(Fig. 5.1c)*. In addition, cGMP-IR was noticeable throughout the neuropil of the slice *(Fig. 5.1c)*. The cGMP-IR resulting from incubation of slices with these maximal concentrations of BAY 60-7550 and BAY 41-2272 was absent in slices that had been exposed to the same treatment but in the presence of the broad-spectrum NOS inhibitor L-NNA or the NO_{GC} receptor inhibitor ODQ, confirming mediation by endogenous NO and specificity to NO_{GC} receptor activity respectively *(Fig. 5.1d-f)*.

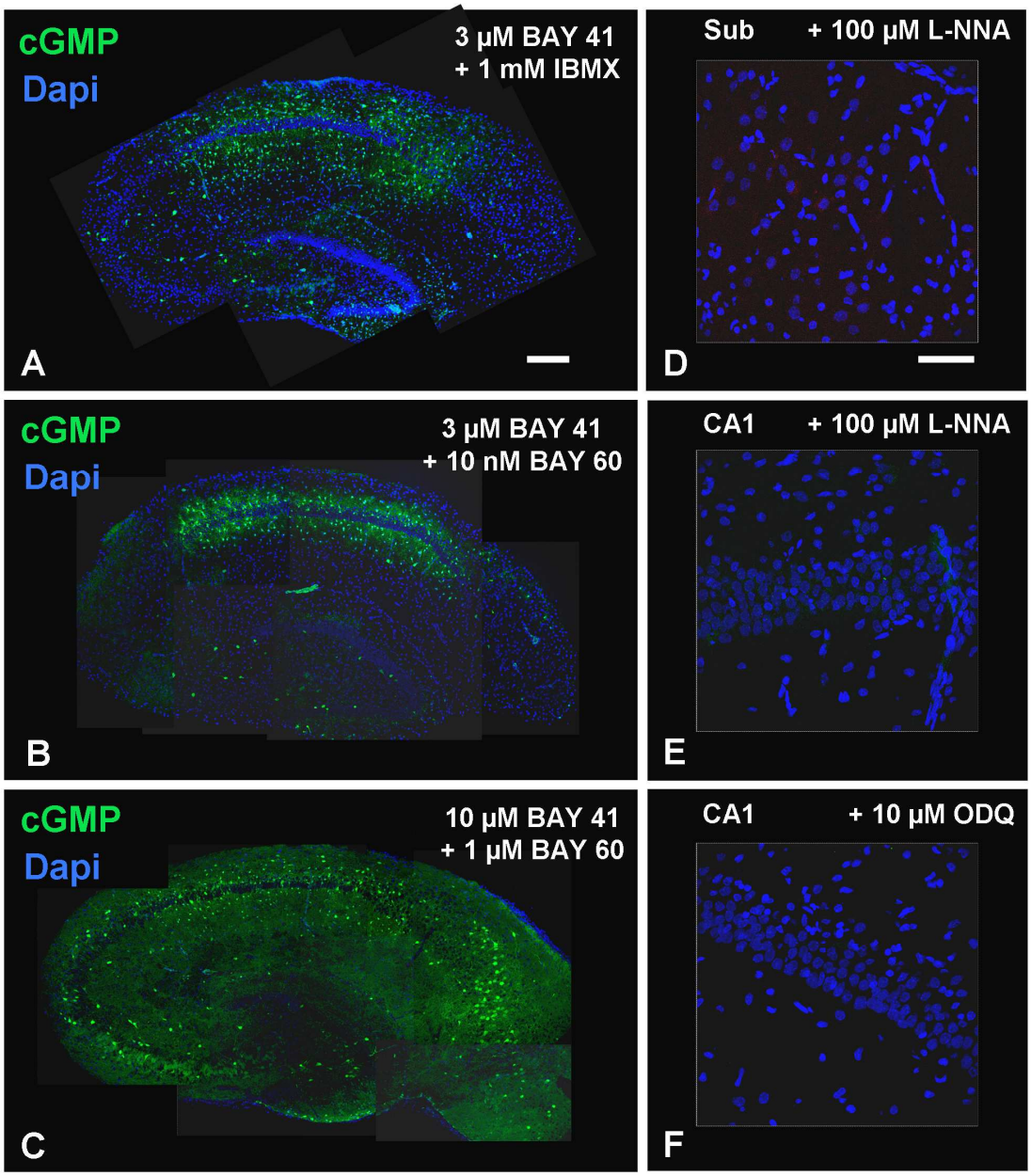

FIG. 5.1 cGMP-IR (green) in whole sections of rat hippocampal slices incubated *in vitro* under the conditions indicated in the upper right corner of each panel. (A, B) Predominant cGMP-IR in astrocytes surrounding the CA1, with a few interneurons throughout the hippocampal formation also stained for cGMP. **(C)** Onset of detectable cGMP-IR in the neuropil as well as in pyramidal cell bodies in CA4 and more strongly in the subiculum. **(D-F)** Representative controls for the treatment condition shown in (C). cGMP-IR was abolished in L-NNA and ODQ-incubated slices, confirming the NO-dependence of the signal and the specificity of the staining respectively. Nuclei are stained with DAPI (blue); Sub, subiculum; scale bar, 200 µm (A-C), 50 µm (D-F).

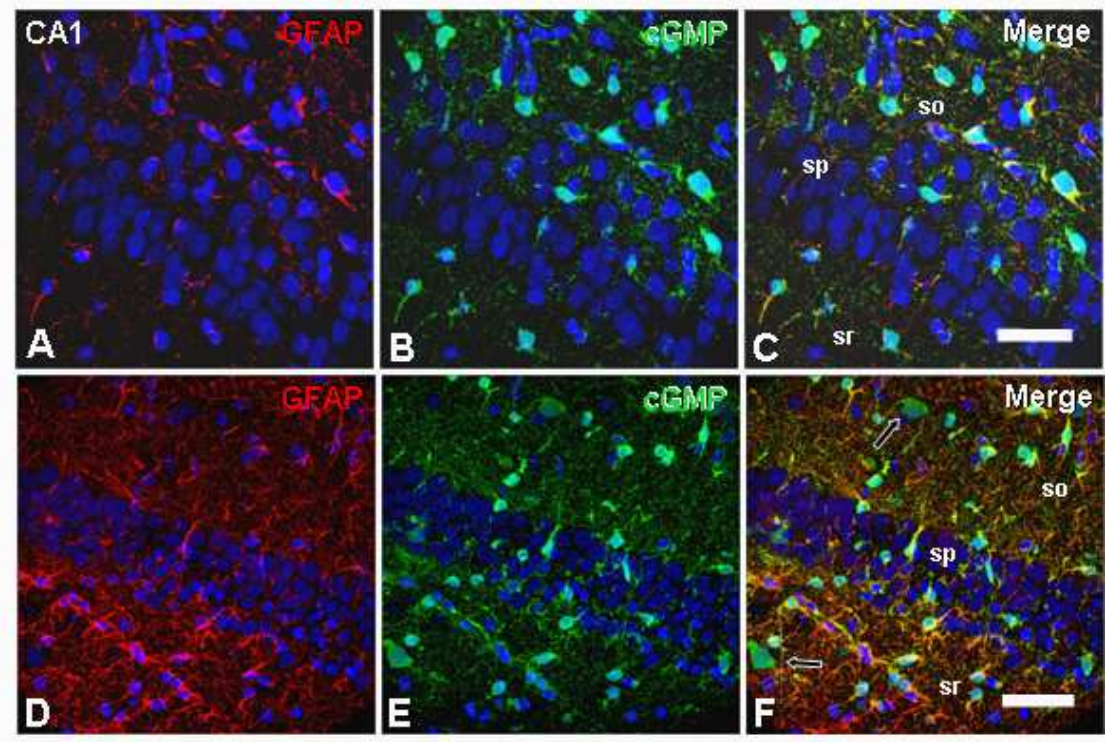

FIG. 5.2. Confocal images taken at a higher magnification, showing cGMP-IR (green) in astrocytes which are double immunostained for their marker GFAP (red). Photographs illustrating cGMP-IR in astrocytes around the CA1 region in sections of hippocampal slices incubated with submaximal concentrations of the PDE2 inhibitor BAY 60-7550 (10 nM) and Bay 41-2272 (3 µM) **(A-C)**, or the broad-spectrum PDE inhibitor IBMX (1 mM) and BAY 41-2272 (3 µM) **(D-F)** Note: indicated by the arrows are cGMP-positive cell bodies outside the pyramidal cell layer, most likely being interneurons. Nuclei are stained with DAPI (blue); so, stratum oriens; sp, stratum pyramidale; sr, stratum radiatum; scale bar in **C**, 30 µm; scale bar in **F**, 50 µm.

Stimulation of NO_{GC} receptors – in the presence of NO donor

Effect of BAY 60-7550 and BAY 41-2272 at maximal concentrations in the presence of an NO donor:

The cGMP signal presented in the foregoing data corresponded solely to endogenous NO. Therefore, the capacity for cGMP accumulation upon addition of an NO donor remained to be investigated. Thus, in addition to inhibiting PDE2 by means of BAY 60-7550 at the maximal concentration of 1 µM and sensitising the NO_{GC} receptor by means of BAY 41-2272 (10 µM), slices were exposed to the NO donor

DEA/NO (10 µM), this concentration of DEA/NO causing maximal cGMP elevation in rat hippocampal slices (Bon & Garthwaite, 2001). Under these conditions, the cGMP signal was pushed to a remarkable 1741 ± 45 pmol/mg protein as determined by RIA *(Fig. 5.4)*. This corresponded to a quite different staining pattern from that observed previously. Clear cGMP-IR was apparent throughout the neuropil, as well as in pyramidal cells of the subiculum, CA1, CA3 and CA4 *(Fig. 5.3a)*, recognisable by the distinct, compact arrangement of the cell bodies in the band of the stratum pyramidale. This staining for cGMP was entirely absent in sections from slices that were incubated in the presence of ODQ *(Fig. 5.3b)*. No staining appeared in the granule cell layer of the dentate gyrus *(Fig. 5.3a)*.

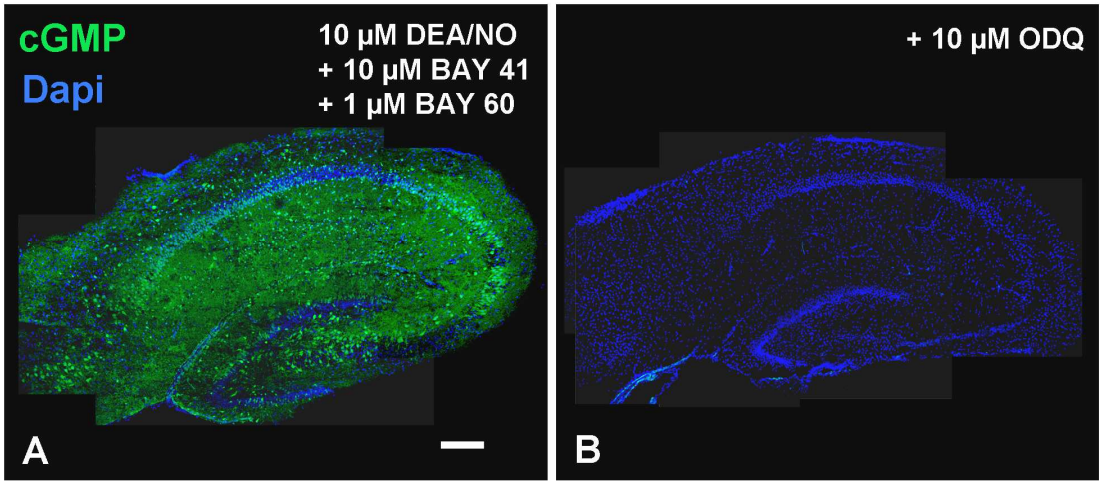

FIG. 5.3. cGMP-IR (green) in whole sections of rat hippocampal slices incubated *in vitro* under the conditions indicated in the upper right corner of each panel. (A) Marked cGMP-IR in the neuropil throughout the hippocampal formation with noticeable staining in pyramidal cell bodies in CA4, CA3, CA1 and subiculum. **(B)** No detectable cGMP-IR in sections from slices that were incubated in the presence of ODQ, confirming the specificity of the staining. Nuclei are stained with DAPI (blue); scale bar, 200 µm.

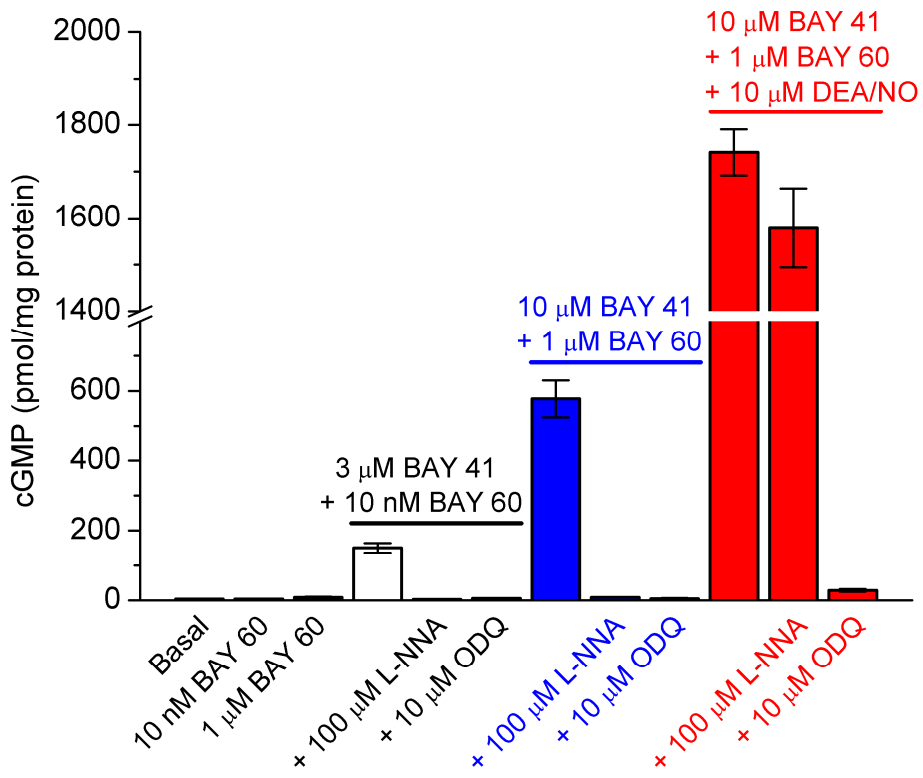

FIG. 5.4. Quantification of the cGMP signal by means of radioimmunoassay. For each animal tested, some of the hippocampal slices were processed for the quantitative evaluation of the cGMP-IR observed. Respective conditions are colour coded, showing the amount of cGMP accumulation that resulted when slices where incubated in aCSF containing the PDE2 inhibitor BAY 60-7550 and BAY 41-2272, with or without added NO donor, in the absence or presence of L-NNA or ODQ. Note, only in the 'red group' did L-NNA fail to prevent the cGMP response, which is consistent with exogenous NO being applied (n = 3-6).

Sections were counterstained for a number of cellular markers in order to localise cGMP accumulation. To look at the cGMP-IR in pyramidal cells, sections were co-stained with NeuN, a neuron-specific marker that stains the cytoplasm and nucleus of cell somata as well as dendrites in some cases (Mullen *et al.*, 1992; Weyer & Schillilng, 2003). Confocal images taken at higher magnification revealed a clear co-localisation of cGMP in the cell bodies of pyramidal cells in the region of the CA1, CA3, CA4 and subiculum *(Fig. 5.5)*. The most intense staining for cGMP appeared to be in the CA4 *(Fig. 5.5g-l)* and the subiculum *(Fig. 5.5j-l)*, followed by slightly weaker cGMP-IR in the CA3 and CA1 *(Fig. 5.5d-f)*. Among these regions, the CA1 showed the weakest intensity of cGMP-IR and fewer cells overall seemed to be

immuno-positive for cGMP as compared to the other regions investigated *(Fig. 5.5a-c)*. In the case of the CA3 region, an interesting feature was the stratum lucidum – the area in which the pyramidal cells receive their synaptic inputs from the mossy fibres originating from the granule cells in the dentate gyrus – appearing dark *(Fig. 5.5d-f)*. This implies that the presynaptic component of this synapse may be devoid of cGMP accumulation under these conditions. In contrast, there was evident cGMP-IR in the apical dendrites of CA3 pyramidal cells *(Fig. 5.5d-f)*. In all four hippocampal regions illustrated, there are some brightly stained cell bodies outside the stratum pyramidale on either side which are most likely interneurons as judged by co-staining with NeuN *(Fig. 5.5)*. Furthermore, in the subiculum, in which a distinct cluster of cells appears to be positive for cGMP, clearly co-localise with the neuronal marker NeuN. Yet, a number of cells stained for NeuN in this hippocampal sub-region evidently lack cGMP-IR *(Fig. 5.5j-l)*. Cell counts of neurons for Fig. 5.5 estimated 37% of neurons stained for cGMP in CA1 (43 cells out of 117), 76% in CA3 (35 out of 46), 48% in CA4 (33 out of 69), and 62% in subiculum (45 out of 73).

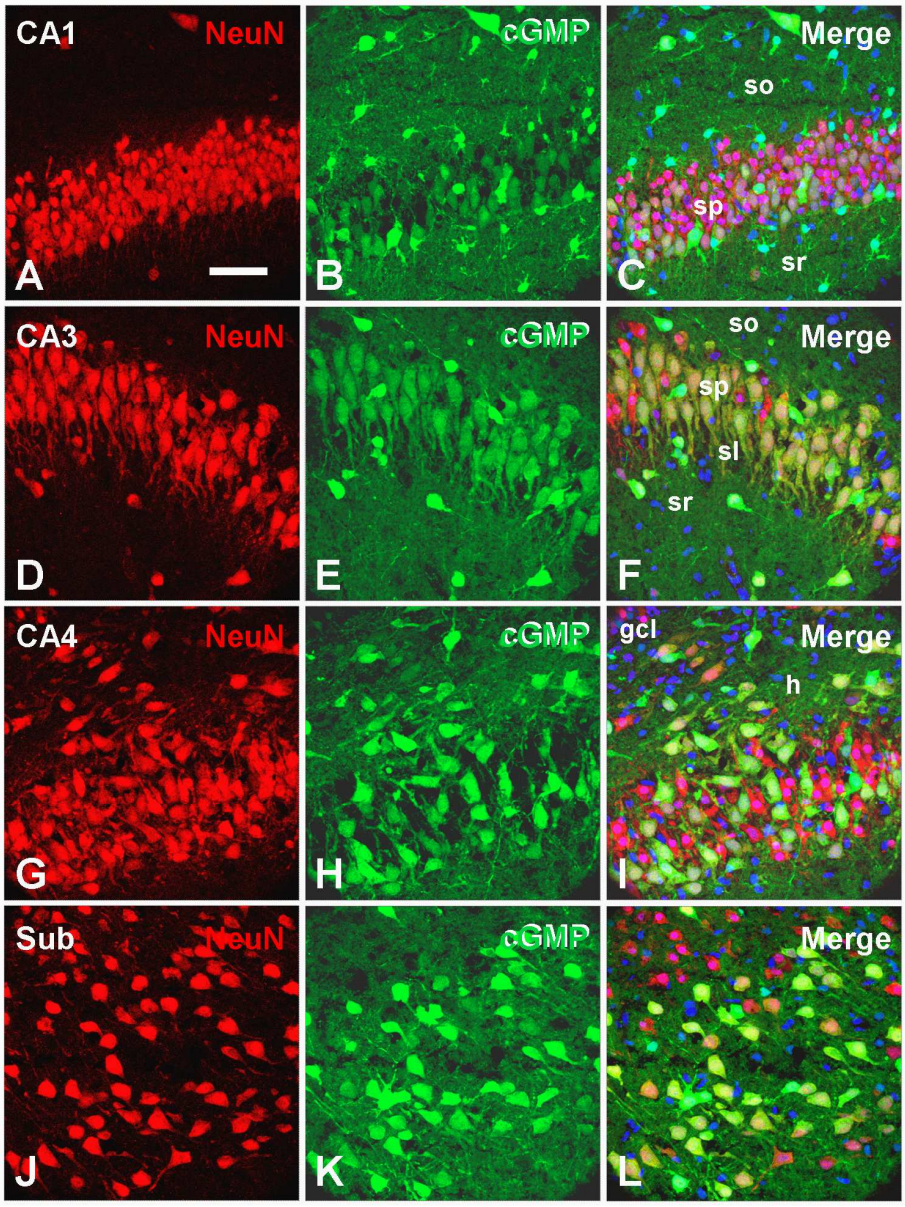

FIG. 5.5. Confocal images taken at a higher magnification, showing cGMP-IR (green) in pyramidal cell bodies which are double immunostained for NeuN (red) in hippocampal slices incubated with 1 µ BAY 60-7550, 10 µM Bay 41-2272, and 10 µM DEA/NO. Photographs show cGMP-IR in pyramidal cell bodies in CA1 **(A-C)**, CA3 **(D-F)**, CA4 **(G-I)** and subiculum **(J-L)**. Note the clear dendritic staining for cGMP in CA3. Nuclei are stained with DAPI (blue); Sub, subiculum; so, stratum oriens; sp, stratum pyramidale; sr, stratum radiatum; sl, stratum lucidum; gcl, granule cell layer; h, hilus; scale bar, 50 µm.

To investigate cGMP-accumulation in axons, sections were co-stained with the marker NF200, an intermediate filament protein expressed abundantly along axons. Axons positively immunolabelled for cGMP were found in all regions examined, namely CA1, CA3, CA4 and the subiculum *(Fig. 5.6).* Axons appeared to be more heavily stained for cGMP in the CA1 *(Fig. 5.6a-c),* CA3 *(Fig. 5.6d-f)* and the subiculum *(Fig. 5.6j-l),* while less intense cGMP-IR showed in the CA4 *(Fig. 5.6g-i).* Clear axonal staining was revealed both in the stratum oriens and stratum radiatum around the CA1 and CA3 regions *(Fig. 5.6a-f).* Around the CA4 region, most axons stained for cGMP were found to be in the polymorphic cell layer (or hilus) of the dentate gyrus *(Fig. 5.6g-i).* Also noticeable are some fibre-like structures that are clearly cGMP-positive but are not stained for NF200. These are most likely astrocyte processes or possibly dendrites *(Fig. 5.6).*

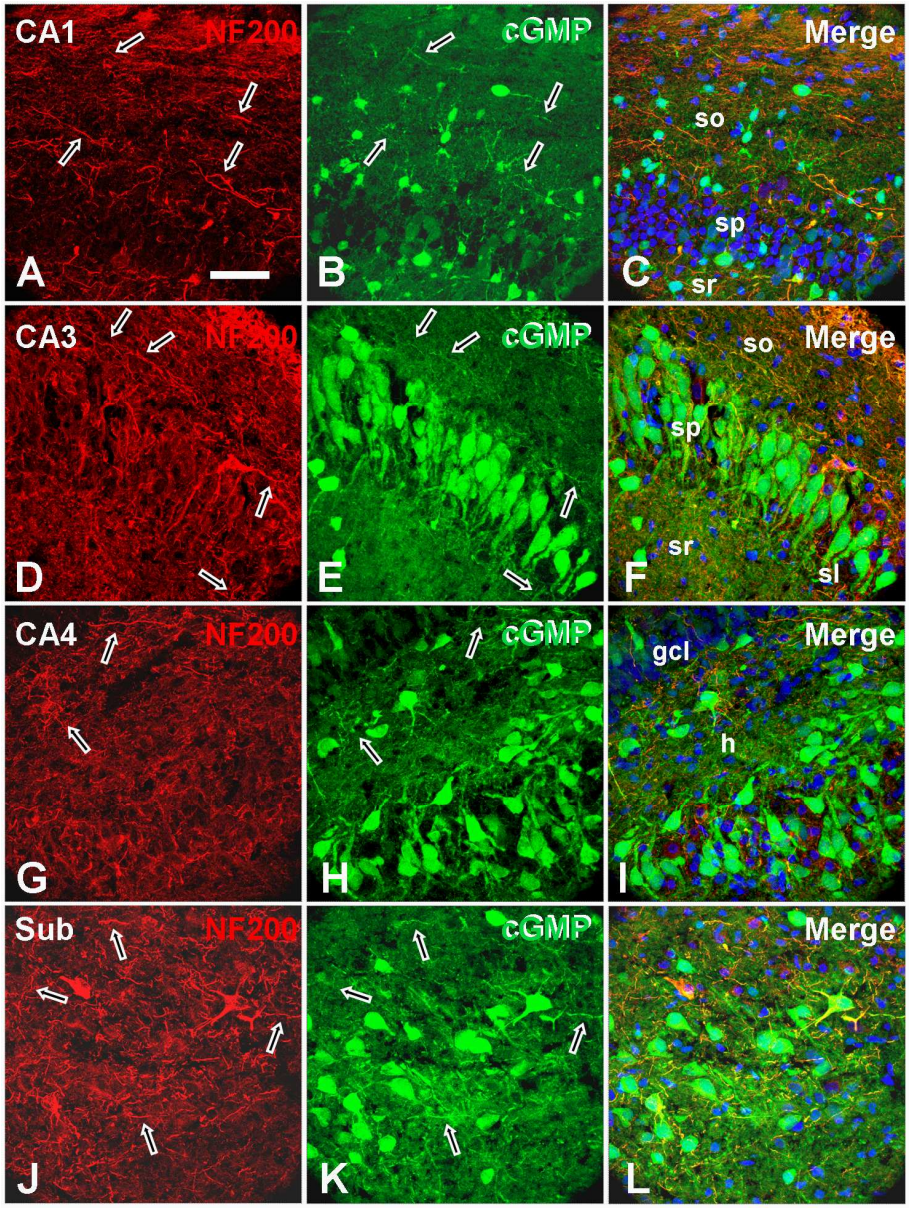

FIG. 5.6. Confocal images taken at a higher magnification, showing cGMP-IR (green) in axons which are double immunostained for NF200 (red) in hippocampal slices incubated with 1 µ BAY 60-7550, 10 µM Bay 41-2272, and 10 µM DEA/NO. Photographs show cGMP-IR in axons in CA1 **(A-C)**, CA3 **(D-F)**, CA4 **(G-I)** and subiculum **(J-L)**. Nuclei are stained with DAPI (blue); Sub, subiculum; so, stratum oriens; sp, stratum pyramidale; sr, stratum radiatum; sl, stratum lucidum; gcl, granule cell layer; h, hilus; scale bar, 50 µm.

Pronounced cGMP-IR was also found in astrocytes throughout the hippocampal formation *(Fig. 5.7a-c)*, co-localising with the astrocytic marker GFAP, which is a type of cytoskeletal intermediate filament protein abundant in this type of glial cell. No cGMP-IR was detected in oligodendrocytes *(Fig. 5.7d-f)*, perceptible as a lack of co-localisation of cGMP-IR with the staining for the enzyme CNPase which is prominent in oligodendrocytes. These data apply to all regions investigated, the illustrations of the CA3 being representative for observations made in the subiculum as well as the CA1 and CA4 regions of the hippocampus, and throughout the hippocampal section as a whole.

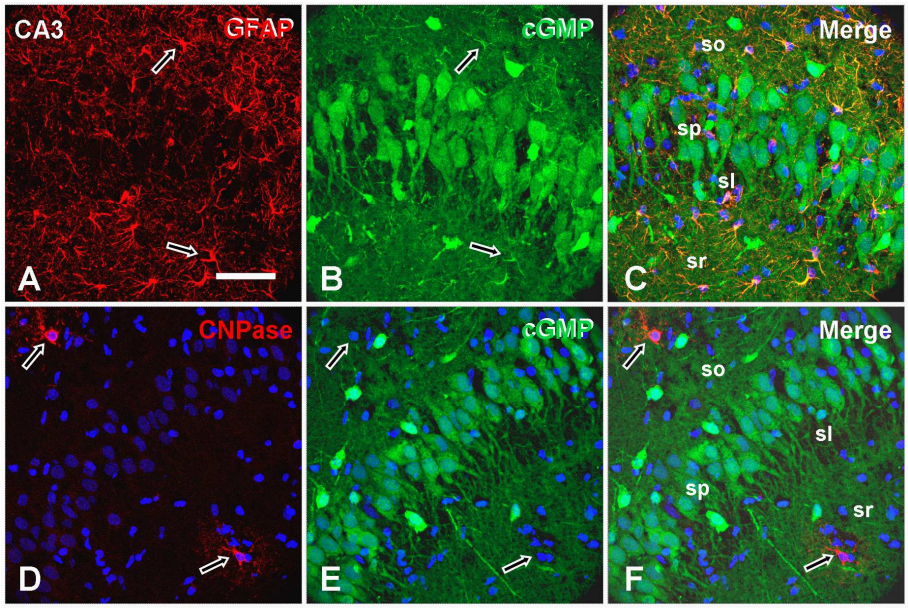

FIG. 5.7. Confocal images taken at a higher magnification, showing cGMP-IR (green) in glial cells which are double immunostained for their respective markers in hippocampal slices incubated with 1 µ BAY 60-7550, 10 µM Bay 41-2272, and 10 µM DEA/NO. (A-C) Photographs illustrating examples of cGMP-IR in astrocytes, here showing astrocytes in the CA3 double immunostained for GFAP (red). **(D-F)** Photographs illustrating examples of cGMP-IR in oligodendrocytes, here depicting these cells in the CA3 double-immunostained for CNPase (red). Nuclei are stained with DAPI (blue); so, stratum oriens; sp, stratum pyramidale; sr, stratum radiatum; sl, stratum lucidum; scale bar, 50 µm.

5.4.2 Localisation of the NO_{GC} receptor in the immature hippocampus

Previous results suggested that optimal protein staining for the NO_{GC} receptor was achieved only after a weak fixation paradigm (Burette *et al.*, 2002). The method optimised and applied by these authors was adopted in the present study, resulting in a staining pattern resembling the one demonstrated previously in the adult hippocampus (Burette *et al.*, 2002), as well as that of mRNA expression of the receptor in the immature hippocampus (Gibb & Garthwaite, 2001). Immunostaining for $GC\beta_1$ protein was evident in the pyramidal cell bodies of the CA1 area, the CA3 region, and also in neurons in the CA4 area and the subiculum *(Fig. 5.8a-d)*. Prominent staining was also recognised in the granule cell layer of the dentate gyrus *(Fig. 5.8e)*. Throughout the different sub-regions, intense immunostaining was also detected in cell bodies outside the defined neuronal cell layers, most likely being interneurons, which have been shown previously to express $GC\beta_1$ abundantly (Burette *et al.*, 2002; Szabadits *et al.*, 2007). Also striking was the prominent fibrous, punctate staining throughout the neuropil, which could be presynaptic, postsynaptic and/or astrocytic elements, consistent with their ability to synthesise cGMP.

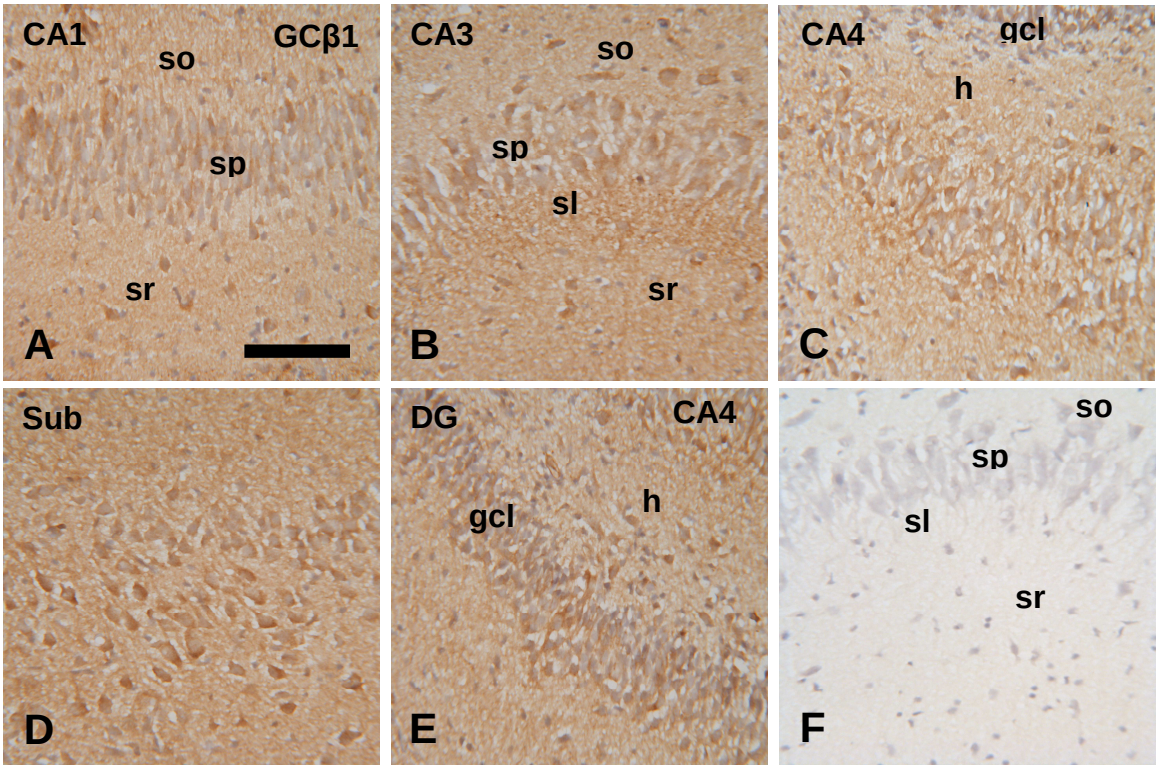

FIG. 5.8. Immunostaining for GCβ_1 in immature rat hippocampal slices. Photographs showing CA1 **(A)**, CA3 **(B)**, CA4 **(C)**, subiculum **(D)**, dentate gyrus **(E)** and a representative image of the negative control in which primary antibody was omitted, lacking GCβ_1 immunoreactivity **(F)**. So, stratum oriens; sp, stratum pyramidale; sr, stratum radiatum; sl, stratum lucidum; gcl, granule cell layer; h, hilus; scale bar, 100 µm.

5.5 DISCUSSION

In terms of NO sources in the hippocampus it is well known that these could be neurons and/or blood vessels. Less clear, however, has been the matter concerning the targets for NO in this brain region. The work presented here demonstrates that NO, via activation of its receptor, the guanylyl cyclase, initiates the formation of cGMP not only predominantly in astrocytes as observed in previous studies, but also in cell bodies of pyramidal neurons in the different sub-regions of the hippocampus, as well as in some dendrites and, possibly, axons. This concurred with the expression pattern of the NO_{GC} receptor found in the present study in immature hippocampal slices. The high specificity of the cGMP-directed antibody used in the present study

has been evaluated extensively in previous studies (de Vente *et al.*, 1987; Tanaka *et al.*, 1997), showing no cross-reactivity with cAMP, cyclic nucleotide monophosphate or triphosphates, or guanosine, indicating that the staining revealed in the present work exclusively reflects NO-responsive, cGMP-synthesising structures. This is also in harmony with the lack of staining for cGMP upon inhibition of NO_{GC} receptors, demonstrated in the present work.

Up until now, as visualised by means of immunohistochemistry, the general notion concerning cGMP-producing structures in the rat hippocampus either under basal conditions or exposed to exogenous NO in the absence or presence of PDE inhibitor, has been that the targets expressing functional NO_{GC} receptors are only astrocytes, a dense network of unidentified varicose fibres throughout this brain region, and blood vessel walls, with the occasional interneuron also displaying cGMP-IR (de Vente *et al.*, 1988; de Vente *et al.*, 1996; van Staveren et al., 2001; Teunissen et al., 2001; van Staveren *et al.*, 2004; van Staveren *et al.*, 2005). However, none has been detected in postsynaptic structures, including pyramidal or granule cell somata and dendrites. In contrast, functional studies have provided evidence that points to NO-mediated cGMP signal transduction taking place both pre- and postsynaptically in hippocampal neurons, a clear mismatch with anatomical studies (see Introduction). This mismatch is further highlighted by the clear expression of NO_{GC} receptors in pyramidal and granule neurons at the mRNA and protein level (Matsuoka *et al.*, 1992; Teunissen *et al.*, 2001; Burette *et al.*, 2002; Gibb & Garthwaite, 2001; Ding *et al.*, 2004; Szabadits *et al.*, 2007), not agreeing with the failure to detect cGMP accumulation in these structures upon NO challenge. The present study found clear expression of the $GC\beta_1$ subunit throughout the hippocampus, with prominent localisation in pyramidal cell bodies of the subiculum, CA1, CA3, and CA4, as well as neurons in the granule cell layer. Additionally, a dense, punctate staining was observed throughout the neuropil. This corroborates the previous demonstration of all three subunits being present in the immature hippocampus at their mRNA level (Gibb & Garthwaite, 2001).

The pattern revealed for the $GC\beta_1$ subunit largely complements the pattern of cGMP accumulation in the immature hippocampus, demonstrated in the present study.

Successful activation of the NO_{GC} receptor requires the α-subunit (α_1 or α_2) linked to the β_1-subunit, and the prosthetic haem (Harteneck *et al.*, 1990; Zabel *et al.*, 1998). A simple explanation for why no cGMP accumulation has been observed so far in all NO_{GC} receptor-bearing structures could be that not all structures in which the receptor has been detected contain receptors that are in this function-determining form. This is emphasised by the fact that only antibodies directed against one or the other subunit have been employed, the presence of one subunit not giving any information regarding the functional state of the receptor. Immature granule cells in the developing cerebellum, for instance, appear to express the α_2 subunit, as demonstrated by *in situ* hybridisation, but lack any other subunits (Gibb & Garthwaite, 2001). Alternatively, the receptors may be rendered inactive by some other factor(s). The idea of NO_{GC} receptors in cell somata being inhibited by some endogenous factor or by the absence of some vital cofactor has been put forward previously (Domek-Lopacinska *et al.*, 2005). In analogy, a mismatch between receptor-bearing and ligand-responding structures has also been observed in various regions of the rat brain upon exposure to atrial natriuretic peptide (ANP), the resulting response corresponding to cGMP output from the NO-insensitive form of the guanylyl cyclase (Saavedra, 1987; de Vente *et al.*, 1989; de Vente *et al.*, 1990a). For example, despite it revealing the highest density of ANP receptors (Saavedra, 1987), the supraoptic nucleus was found to not show ANP-responsive, cGMP-producing cells (de Vente *et al.*, 1990a). Moreover, cholinergic somata in the caudate putamen of adult rats were found to express NO_{GC} receptors, but, when exposed to NO, only fibres but not cell bodies appeared to accumulate cGMP (de Vente *et al.*, 2001a). Also in cerebella Purkinje cells no detectable cGMP accumulates (de Vente *et al.*, 1990b; de Vente *et al.*, 1998) despite the presence of NO_{GC} receptor subunits in these cells (Zwiller *et al.*, 1981; Nakane *et al.*, 1983; Ding *et al.*, 2004), mirroring the unexplained mismatch found in the hippocampus. Even in the presence of BAY 41-2272, to sensitise the NO_{GC} receptor to NO, and PDE inhibitor, no cGMP immunostaining has been observed in postsynaptic hippocampal structures (van Staveren *et al.*, 2004). The lack of cGMP accumulation in hippocampal pyramidal cell bodies, despite the presence of the NO_{GC} receptor, as indicated by $GC\beta_1$ expression, has also been demonstrated in the mouse brain (van Staveren *et al.*, 2004).

At this point two things should be considered. Firstly, immunohistochemistry allows to locate a given receptor and to investigate its functional activity by locating cells exhibiting immunostaining for the relevant signal. However, there is a limit to the sensitivity of immunohistochemistry, which could likely be the reason for why clear axonal cGMP-IR, for instance, was only observed under conditions of maximally evoked cGMP production (i.e. PDE2 inhibitor, BAY 41-2272 and NO donor). On the other hand, the presence of some brightly stained structures may mask very weakly stained structures. Overall, the absence of cGMP-IR is not an absolute indication for the non-existence of cGMP-producing structures in the region under investigation. Even complete failure to detect cyclic nucleotides by means of immunohistochemistry has been reported in the early days (Cumming *et al.*, 1977; Cumming *et al.*, 1980), in this case the paradigm of fixation appearing to be a crucial factor, with long fixation times found to destroy all cyclic nucleotide immunoreactivity (Rall & Lehne, 1982; de Vente *et al.*, 1987). Secondly, although not an aspect looked into experimentally in the present work, the age of the animal at which cGMP accumulation is investigated may be important in determining the scope of the detection limit of the cGMP-IR, as related to the amount of cGMP produced in the given tissue. Different patterns of cGMP-responding structures may reflect variations in the NO-cGMP signalling cascade at different developmental stages.

One of the key findings in the current study was the remarkable capacity of the immature tissue to produce cGMP. Purely corresponding to endogenous NO, incubation of the 10-day-old hippocampal slices with maximum concentrations of the PDE2 inhibitor and BAY 41-2272 to sensitise the NO_{GC} receptors produced approximately 600 pmol of cGMP per mg protein. Addition of the NO donor DEA/NO to this condition amounted in remarkable amounts of cGMP accumulation in the whole tissue, approaching 1800 pmol of cGMP per mg protein. These data reflect a cGMP-producing capacity never observed before in the hippocampus. While this work utilised immature hippocampal slices, the majority of previous work evaluated cGMP localisation in adult hippocampal tissue, finding the characteristic cGMP-IR mainly in varicose fibres, astrocytes, blood vessel walls, and the occasional interneuron, with a clear absence in postsynaptic elements as discussed above. In the rat cerebellum, for instance, there is an increase in cGMP content in astrocytes upon

maturation but a decreased responsiveness of the NO_{GC} receptor to NMDA (Garthwaite, 1982). A significant decrease in basal cGMP levels has been found in the olfactory bulb and the hippocampus of aged animals when compared to adult rats (de Vente *et al.*, 1990a), and *in vitro* slice studies have revealed changes in the functional activity of the NO_{GC} receptor during development (Markerink-van Ittersum *et al.*, 1997), noting that cGMP synthesis in cerebral neuronal somata in response to NO is more widespread during postnatal development than in adult and aged animals. Subsequent to the linkage of NO and cGMP production to NMDA receptor activation (Morris *et al.*, 1994), also in the spinal cord NOS-mediated cGMP synthesis has been proposed to be reduced upon maturation, NMDA-induced, NO-mediated cGMP-IR occurring in 2-week-old rats but none in adult (3-month-old) animals (Vles *et al.*, 2000). In the same study the authors described apparent ongoing NO synthesis in neonatal spinal cord slices which was, however, undetectable in the adult tissue slices. Furthermore, cholinergic neurons of the rat basal forebrain and the caudate putamen apparently lose the greater part of their capacity to synthesise cGMP in response to NO upon maturation, a marked reduction beginning during the second postnatal week (Domek-Lopacinska *et al.*, 2005). These age-dependent changes with regard to detectable cGMP accumulation may, however, be region-differentiated. Cholinergic fibres in the neocortex, for instance, retain their capacity to synthesise cGMP in response to NO throughout life (de Vente *et al.*, 2001a), whereas there is apparent loss of NO-responsiveness in the cholinergic fibres of the hippocampus during development (Domek-Lopacinska *et al.*, 2005). As to the reason for why there are higher levels of cGMP in the brain in general during postnatal development, this could be related to the proposed function of cGMP during maturation of neuronal networks both in vertebrates and invertebrates (Bicker, 2005; Bicker, 2007). For example, in the rat cortex, cGMP has been suggested to determine the direction of dendritic outgrowth during development (Polleux *et al.*, 2000), where inhibition of cGMP production or PKG was demonstrated to result in random orientation of dendrites. The indications concerning lower detectable levels of cGMP in the adult CNS parallels the finding of higher PDE activity in the aged brain of rats, resulting in more active cGMP degradation (Chalimoniuk & Strosznajder, 1998). Other studies have indicated changes not only in PDE activity, but also alterations in mRNA and

protein expression of some PDE isoforms such as PDE1 and PDE3 during brain development (Billingsley *et al.*, 1990; Reinhardt & Bondy, 1996). Additionally, more directly related to the present work, it appears that also the expression of PDE2, PDE5 and PDE9 increases during maturation of the hippocampus (van Staveren *et al.*, 2003).

In the present study, incubation of immature hippocampal slices with either the general PDE inhibitor IBMX or the PDE2 inhibitor BAY 60-7550 at its submaximal concentration in the presence of a submaximal concentration of BAY 41-2272 resulted in a similar distribution of cGMP-IR predominantly in astrocytes around the CA1 region, a few interneurons and blood vessels, which is in agreement with previous evidence cited above. However, upon exposure to maximal concentrations of BAY 60-7550 and BAY 41-2272, astrocytic cGMP-IR became more apparent throughout the different hippocampal regions and marked cGMP-immunofluorescence started to clearly appear in a cluster of neuronal cell bodies in the subiculum alongside diffuse neuropil staining and weak cGMP-IR in some cell bodies in the CA4. More pronounced staining throughout the neuropil as well as in pyramidal cell bodies of the subiculum, CA4, CA3 and, to a lesser extent, CA1 occurred only following the addition of the NO donor. Under conditions of added exogenous NO, granule cells still lacked cGMP-IR, which could be related to weaker expression of PDE2 in this region but greater abundance of PDE9 (van Staveren *et al.*, 2003; van Staveren *et al.*, 2004). On the other hand, clear cGMP accumulation was now evident in dendrites of pyramidal cells in the CA3 region, as well as axons surrounding or transecting the regions investigated. In terms of the axonal staining, however, the extent of investigation carried out in the present study does not allow further conclusions to be made concerning the identity of the cGMP-accumulating axons. The mere presence of NO-reactive axons in the different sub-regions of the hippocampus does not imply that these axons terminate in a particular region or make a particular functional contact within the hippocampus. Moreover, there is also the likelihood that some (if not the majority) of the cGMP-stained axons are interneuronal or are part of a pathway travelling through the hippocampus. Cholinergic neurons of the medial septum and diagonal band of Broca, for example, project to the

hippocampus, the varicose cholinergic fibres of these areas that innervate the hippocampus having been demonstrated to synthesise cGMP (Domek-Lopacinska *et al.*, 2005). Additionally, upon addition of DEA/NO, the cGMP-immunofluorescence seemed now to be brighter in the cell bodies of the subiculum and the CA4 area compared to when no NO donor was added.

The different conditions revealing a sequence of emergence of NO-responding targets, immunofluorescence intensity seemingly being brighter as cGMP levels are raised more, could reflect different profiles of PDE activity contained in cells in a given region. While PDE2, alongside PDE5 and PDE9, have been demonstrated at the mRNA level primarily in neuronal cell bodies (van Staveren *et al.*, 2003; van Staveren *et al.*, 2004), a different balance among these PDE isoforms in terms of their activity and/or abundance could be responsible for varying cGMP signals in the different hippocampal subregions. This possibility is strengthened by the lack of these PDE isoforms in astrocytes (van Staveren *et al.*, 2004) and the profile of cGMP accumulation in these cells, for example.

The identification of cGMP in astrocytes even in the presence of PDE inhibitor alone (van Staveren *et al.*, 2001) and cGMP appearing in blood vessel walls even in the absence of PDE inhibitor (de Vente *et al.*, 1996), is a good indication that PDE activity is a key determinant of detectable cGMP signals. Also, in the present study under all conditions tested, in the absence or presence of the NO donor, cGMP-immunofluorescence was obvious in astrocytes. It should be noted, however, that, while astrocytes in the CA1 region appeared cGMP-positive even under 'endogenous NO conditions', cGMP accumulation in astrocytes in the other areas investigated appeared clearly upon addition of exogenous NO by means of DEA/NO, or when maximal concentrations of BAY 60-7550 and BAY 41-2272 were applied. This could reflect different subpopulations of astroglia exhibiting different PDE activity. In analogy, a subregional heterogeneity of astroglia has been suggested previously, demonstrating that populations of these glial cells may contain either ANP-responding guanylyl cyclase or NO_{GC} receptors only, or both (de Vente *et al.*, 1989; de Vente *et al.*, 1990a; Teunissen *et al.*, 2001). In contrast, no cGMP-immunofluorescence was detectable in the oligodendrocytes with only a sparse number of these glial cells appearing immuno-positive for their marker CNPase. CNPase is an enzyme found in

oligodendrocytes and is thought to be involved in myelin formation. For example, in multiple sclerosis, where the main hallmark is the degeneration of myelin, plaque regions where myelin is lost also exhibit reduced levels of CNPase (Johnson *et al.*, 1986). Immunohistochemically, in the corpus callosum of the rat forebrain, oligodendrocytes have been demonstrated to have cGMP-producing capacity in response to NO (Tanaka *et al.*, 1997), using the same antibodies as the present study. Tanaka and colleagues found that the number of cGMP-producing oligodendrocytes decreases during maturation and appears to be absent in the adult brain, suggesting that the cGMP-dependent signalling pathway could be involved in the regulation of myelin formation. Tanaka et al. also showed that there is no cross-reactivity between the cGMP antibody, also used in the present study, and the 2'3'-analogues contained in oligodendrocytes. The limited number of CNPase-stained oligodendrocytes in the immature hippocampal slices could be explained by the expression profile of this oligodendrocyte marker in this brain region. Up to postnatal day 10 (the age of animals used in the current study), CNPase expression is very low, being nearly non-existent during the first 8 days of rat life, but sharply increases and approaches its peak around the fourth postnatal week (Virgili *et al.*, 1990). This trend of CNPase activity concurs with the beginning of myelination, myelinated fibres in the hippocampus being first seen between postnatal days 15 and 17 and progressively increasing until postnatal day 25 (Savaskan *et al.*, 1999; Meier *et al.*, 2004). Immature oligodendrocytes in the rat brain are suggested to express a number of different markers sequentially (Virgili *et al.*, 1990) and, although the few CNPase-positive oligodendrocytes did not reveal any cGMP accumulation in response to NO, it could be argued that there may be populations of oligodendrocytes at this developmental stage that may be targets for NO but could only be localised by means of a different marker. On the other hand there is no evidence of PDE2 in these glial cells, the only PDE subtype inhibited in the current work. Hence, it also becomes conceivable that, if there was any cGMP synthesis occurring in oligodendrocytes, one or more isoforms of PDE other than PDE2 could be degrading it, making it untraceable.

Another question remaining is as to why previous studies failed to observe cGMP-IR postsynaptically, particularly in neuronal cell somata. One previous

indication that cGMP may rise in dendrites derived from a previous study that also employed BAY 60-7550 (Boess *et al.*, 2004). Exposing hippocampal slices to similar conditions (i.e. maximal BAY 60-7550 concentration plus NO donor), the authors demonstrated diffuse, punctate neuropil staining for cGMP. This is similar to the observation made in the present study following incubation of the slices with maximal concentrations of BAY 60-7550 and BAY 41-2272 in the absence or presence of NO donor. However, Boess et al. found only minimal co-localisation of cGMP with the presynaptic marker synaptophysin, leading the authors to the conclusion that, although cGMP levels may be increased in a subset of presynaptic terminals, the main rise in cGMP may occur in postsynaptic parts of the neuron. However, also Boess and colleagues failed to detect cGMP-IR in pyramidal cell bodies, which could be related to the absence of BAY 41-2272 as compared to the present study. Moreover, the data presented here clearly show cGMP accumulation in dendrites emerging from CA3 pyramidal cell bodies, as evaluated by the co-localisation with the neuronal marker NeuN, which can also stain dendrites (Mullen *et al.*, 1992). While the study conducted by Boess et al. employed BAY 60-7550 just as the present work, a likely explanation for the absence of cGMP-IR in pyramidal cell bodies may be the pharmacological paradigm employed. Perhaps addition of a compound sensitising the NO_{GC} receptors so that the signal would be even further amplified would have revealed positive cGMP staining in the neuronal somata. Another aspect worthwhile considering, however, is the possibility of different splice variants of PDE occurring in a given tissue or cell. Different splice variants have been reported for PDE2, PDE2A1 being a cytosolic form, and PDE2A2 and PDE2A3 being membrane-bound variants (Bender & Beavo, 2006), where PDE2 in the hippocampus has been shown to appear ‘ring-like’ mainly around the plasma membrane of pyramidal neurons (van Staveren *et al.*, 2003). Studies that have investigated PDE2 in the hippocampus have focussed on mRNA expression, which does not necessarily give an accurate account concerning protein abundance. Also, the published work does not distinguish among different PDE2 splice variants. Therefore, previous tools employed to inhibit the PDE2, such as EHNA, may have not been effective against all possible PDE2 splice variants, expression of which in the hippocampus cannot be excluded to date.

Although not known, it may be that BAY 60-7550 has a more efficient inhibitory potency towards different variants of PDE2.

The absence of cGMP-IR in hippocampal pyramidal cell somata may also be brought about by the experimental and pharmacological paradigm used in previous studies in terms of NO application. The majority of previous work employed the NO donor SNP, which is a troublesome NO donor to work with. The interpretation of results generated from several NO donor compounds may be complicated by the production of NO-derivatives other than authentic NO. Decomposition of SNP can generate NO^+, NO^- and CN^- in addition to NO and its degradation is dependent on light and thiols (Feelisch, 1998; Miller & Megson, 2007). NO donors belonging to the family of NONOates on the other hand, including DEA/NO used in the present study, have been established to release authentic NO with known half-lives under physiological conditions (Maragos *et al.*, 1991; Morley & Keefer, 1993; Keefer *et al.*, 1996) and should therefore be used ideally. In this respect, differential stimulation of NO_{GC} receptors by SNP and DEA/NO has been reported to take place in cortical tissue for instance (Nedvetsky *et al.*, 2002), where application of compounds for the same amount of time revealed DEA/NO to stimulate NO_{GC} receptor activity with greater potency than SNP. Moreover, according to the findings by Nedvetsky *et al.* (2002), DEA/NO, used at a third of the concentration of SNP, evoked higher amounts of cGMP accumulation in various brain regions, including the medulla, hypothalamus, midbrain, and striatum. Also in the cerebellum there was a slightly greater effect of DEA/NO compared to SNP. Only a small number of previous studies that investigated NO-responding targets in the hippocampus have employed DEA/NO (van Staveren *et al.*, 2004; van Staveren *et al.*, 2005). However, in these studies DEA/NO was dissolved in aCSF and applied to the tissue slices for 10 minutes. The NONOates should be dissolved in alkaline solutions and be applied just before it is required to induce the biological response. DEA/NO is stable and kept in a non-releasing state in alkaline solutions but spontaneously decomposes with a half-life of 2 minutes at physiological pH and temperature (Morley & Keefer, 1993; Keefer *et al.*, 1996). Therefore, it is possibly that, given that the NO donor was dissolved in aCSF and applied for 10 minutes before inactivating the biological reaction, only minimal

cGMP production was evoked so that the real scope of cGMP accumulation remained undetected, associated with missing the optimal window of NO release.

To summarise, the present study revealed clear NO-responsiveness of postsynaptic structures in the hippocampus as demonstrated by cGMP-IR in pyramidal cell bodies in different sub-areas, explaining the previous mismatch between anatomical and functional investigations. The observation of dendritic and axonal cGMP accumulation requires more detailed investigation, the identity of the latter remaining unresolved in the present work. Overall, the present findings reveal a pharmacological paradigm that will be useful to determine NO targets in the brain and so possibly uncover new NO-responsive structures. Although the majority of pyramidal cell-cGMP-IR only appeared upon addition of an NO donor, it can be speculated that the same cGMP-producing cells can respond to endogenous NO, which, however, is beyond the detection limit of the immunohistochemical approach.

Demonstrating so far unidentified NO-responding structures in the CNS *in vitro* by means of cGMP-IR has certainly been a good aid to clarifying the neurobiological aspects of NO. However, immunohistochemistry only provides a ‘snapshot’ of the biological response, providing very poor or no spatiotemporal information. Aspects such as diffusion of cGMP from its initial site of synthesis prior to fixation cannot be determined by means of this methodology. The data shown here allows no firm conclusion concerning the ‘real’ cGMP-producing sites in the hippocampus. For example, it cannot be known with certainty whether cGMP is mainly synthesised in dendrites and/or closely around the soma membrane and then diffuses globally into neuronal cell bodies, or whether it is originally produced globally in pyramidal neurons. Given that PDE2 is inhibited in conjunction with evidence suggesting this PDE isoform to be located in a ‘ring-like’ appearance around the plasma membrane of pyramidal neurons (van Staveren *et al.*, 2003), diffusion of cGMP seems likely. Advances in the design of cGMP-sensitive indicators that can be expressed in a whole tissue may make it possible to investigate this matter in the future.

*

CHAPTER 6

Characterisation of a new method for real-time capture of cGMP signals in response to clamped NO concentrations

6 Characterisation of a new method for real-time capture of cGMP signals in response to clamped NO concentrations

6.1 INTRODUCTION

Based on the numerous functions of cGMP in cellular events and complex biological processes, there has been great interest in the development of sensitive tools that would allow monitoring of the spatial and temporal behaviour of cyclic nucleotide levels upon receptor stimulation. A commonly-used classical method to study NO-evoked cGMP accumulation has been radioimmunoassay (RIA), which allows the detection of changing levels of biological molecules at the whole tissue level. However, there are a number of downsides to this approach. In order to determine cGMP levels, using antibodies directed against the cyclic nucleotide, cells or tissues need to be homogenised. Moreover, although RIA has been a useful method to monitor endogenous NO levels by measuring cGMP levels that are sensitive to NOS inhibition (Griffiths *et al.*, 2002), it has a limit concerning its sensitivity and it does not allow examination of free cGMP levels as the antibody will also recognise pools of cGMP that are bound to downstream targets. Physiological effects of NO without detectable cGMP rises by RIA have been reported (Mergia *et al.*, 2006). Mergia et al. (2006) found that aortic rings from mice lacking about 94 % NO_{GC} receptors relax in response to NO with the corresponding cGMP accumulation being undetectable by means of RIA. A further important drawback of this biochemical assay is its low temporal and no spatial resolution. Previous studies have set out to study the temporal characteristics of NO-induced cGMP accumulation in tissues by terminating the biological reaction at different time points. However, acquisition of time courses in this way is very laborious and has a temporal limit, especially when considering the very fast kinetics of NO-evoked cGMP signals (Garthwaite, 2005). In rat cerebellar cells for instance, the kinetics for the reaction rate between NO and its receptor were found to be on a sub-second scale (Bellamy & Garthwaite, 2001a), significant increases in cGMP being observed at 40 ms. On the other hand, the importance of resolving cGMP signals spatially is underlined by the concept of cGMP compartmentalisation, which assumes different cGMP concentrations in various cellular compartments, ultimately determining the resultant physiological effect of a

NO-evoked cGMP signal. An intriguing aspect of cyclic nucleotide-mediated signal transduction has certainly been how specific cellular responses are achieved considering the vast number of effector systems coupled to cGMP signalling. As discussed in more detail in Chapter 1, the spatiotemporal profile of a given cGMP signal is not only determined by its rate of synthesis but also by its degradation by phosphodiesterase (PDE). In a different respect, it is not only desirable to understand the purpose of different cyclic nucleotide-generating systems being present in a given cell, but also the rationale for different PDEs with varying substrate specificity, affinity, and subcellular location occurring not only broadly in a given cell but even in microenvironments within that cell. A particular pattern of components present in a given microdomain of a cell may greatly influence the outcome of the cyclic nucleotide signal in terms of its ability to diffuse away from its site of production as well as its duration and amplitude, therefore determining the ensuing biological response based on the targets accessible to a given cGMP signal (Garthwaite, 2005; Fischmeister *et al.*, 2006).

Devising tools that would enable one to continuously monitor the changes in cGMP concentrations in living cells in real-time at high spatiotemporal resolution would substantially enrich our understanding of NO-cGMP signalling. A great deal of effort has been put into this objective by scientists in the past. One approach involves the use of recombinant CNG channels combined with electrophysiological recordings or Ca^{2+}-sensitive dyes, measuring or imaging the cation current or change in intracellular Ca^{2+} respectively that result upon channel activation in response to cGMP elevation. For example, CNG2 channels have been employed as cGMP sensors in rat cardiomyocytes (Castro *et al.*, 2006). The authors provided evidence for compartmentalisation of cGMP signals derived from either the natriuretic peptide- or NO-activated types of guanylyl cyclase. Castro and colleagues (2006) found that, while cGMP generated by the natriuretic peptide-activated enzyme was accessible at the plasma membrane and controlled exclusively by PDE2 activity, the cGMP signal generated by NO_{GC} receptors had access to the membrane only when PDE5 was

inhibited. While Castro et al. (2006) derived their findings from recording the Ca^{2+} current conducted by CNG channels, another study carried out by Piggott *et al.* (2006) also investigated the differential patterning of cGMP responses to NO donors and natriuretic peptide, finding also spatial segregation of cGMP signals in cultured vascular smooth muscle cells infected with adenovirus encoding the CNGα2 subunit. Here the readout for changes in GMP-modulated CNG channel activity was the Ca^{2+} influx through the channels using the Ca^{2+}-sensitive fluorescent dye fura-2 (Piggott *et al.*, 2006). A potential problem that may arise using this method is the fact that activated CNG channels conduct Ca^{2+} ions which in turn may influence downstream components of the signalling cascade that are sensitive to Ca^{2+}.

Another method that has attracted a lot of attention in the context of real-time measurements of cGMP dynamics in living cells involves the use of fluorescence resonance energy transfer (FRET)-based cGMP indicators. The principle of these indicators constitutes the interaction of cGMP with one of its natural binding domains, such as GAF-domains of PDE2 or PDE5 (Nikolaev *et al.*, 2006; Russwurm *et al.*, 2007), or parts of PKG (Sato *et al.*, 2000; Honda *et al.*, 2001; Russwurm *et al.*, 2007), which are fused between two fluorescent proteins, and which generally vary in their dynamic range, cGMP sensitivity, and selectivity. Binding of the cyclic nucleotide to the biosensor induces a conformational change which leads to an increase or decrease in the distance between the fluorescent proteins which in turn is translated into a change in FRET. It is the change in FRET that is ultimately monitored, providing information concerning the dynamics of cGMP signals.

The use of FRET-based cGMP indicators has provided insights into the spatiotemporal characteristics of cGMP signalling. For example, Cawley *et al.* (2007) provided information concerning temporal cGMP dynamics in cultured aortic smooth muscle cells. The authors demonstrated the concerted influence of NO_{GC} receptor activation and PDE5 activity on the kinetic profile of cGMP peaks in the smooth muscle cells, observing a sharp increase in cGMP followed by a rapid degradation phase, the decline in the response being prevented upon PDE5 inhibition. Other

interesting methods that have been developed recently include a PKG-based FRET sensor coupled to α and β subunits of the NO_{GC} receptor (Sato *et al.*, 2005). This construct had a detection limit of 0.1 nM NO. Employing this guanylyl cyclase-coupled cGMP indicator, the authors demonstrated that 1 nM NO, which is plenty to induce vasorelaxation, is generated in cultured vascular endothelial cells even in the absence of shear stress. The same laboratory then produced a reporter cell line named Piccell (Sato *et al.*, 2006), which can be used to monitor NO levels when grown in co-culture with the cells of interest. Sato and colleagues (2006) demonstrated remarkable NO sensitivity of their new system with a detection limit of 20 pM, and, in the course of their study in primary hippocampal neurons, uncovered an oscillatory release of picomolar NO concentrations from neurons which was synchronised with periodical neuronal Ca^{2+} spikes.

Though the use of FRET-based indicators has certainly added to the knowledge about NO-cGMP signal transduction, this method suffers from several disadvantages. Using this approach to study the spatiotemporal dynamics of cGMP requires technically laborious dual emission detection systems. Other limitations include low changes in the overall emission ratio and low sensitivity so that small fluctuations in cGMP levels can not be detected. Moreover, low NO concentrations are capable of initiating cGMP synthesis (Garthwaite, 2005), the amount of elevation of which may be physiologically relevant but yet not detected by the cGMP indicator used. Additionally, low selectivity, and poor reversibility and speed are a problem in FRET. Lastly, other attributes of available cGMP indicators to be improved include the problem of pH sensitivity, no applicability *in vivo* in mammals, and interactions of the biosensor with endogenous proteins, the latter possibly being responsible for the low maximal intensity changes observed in living cells (Nausch *et al.*, 2008). Very recently, a new non-FRET based cGMP biosensor named δ-FlincG has been developed and tested in Wolfgang Dostmann's laboratory in the University of Vermont, and was demonstrated to have superior spectral characteristics, fast association and dissociation kinetics, allowing capture of the very rapid rise and fall in cGMP, and greatly improved environmental stability (Nausch *et al.*, 2008).

FlincG and 'clamped' NO

The development of δ-FlincG (fluorescence indicator for cGMP) was largely based on the concept of non-FRET Ca^{2+} indicators (Baird *et al.*, 1999; Nakai *et al.*, 2001), which since have successfully been employed to visualise Ca^{2+} patterns during the cardiac cycle in the heart *in vivo* (Tallini *et al.*, 2006). The FlincG indicator constitutes two tandem PKG-derived cGMP binding sites that are fused to the N-terminus of a circularly permutated enhanced green fluorescent protein (cpEGFP), which permits substrate-indicator interactions to be directly translated into conformational changes and an increase in fluorescence intensity of a single cpEGFP molecule (Nausch *et al.*, 2008). A diagram of the FlincG construct is depicted in *Fig. 6.1*. The authors removed interactions between endogenous PKG and δ-FlincG by deleting the N-terminal domain of the PKG-derived cGMP binding domain which is responsible for dimerisation between PKG proteins. This latter modification led to improved maximal changes in fluorescence intensity. Furthermore, δ-FlincG was found to benefit from high selectivity for cGMP over cAMP (>280-fold) and to respond to low nanomolar NO-concentrations derived from the short-lived NO donor DEA/NO ($EC_{50,\ DEA/NO}$ = 4 nM; Nausch *et al.*, 2008). Another advantage of δ-FlincG was its resistance to small changes in pH under physiological conditions ($pK_{a,\ \delta\text{-FlincG}}$ = 6.1; Nausch *et al.*, 2008). Importantly, Nausch and colleagues (2008) have produced a novel cGMP biosensor with outstanding high-speed kinetics. Rapid temporal and spatial cGMP changes can be captured more accurately as the fast rates for cGMP association and dissociation with or from δ-FlincG ensure that the indicator does not act as a sink for cGMP. Moreover, the cGMP binding constant of δ-FlincG was estimated to be 170 nM, which is approximating the cGMP affinity for its endogenous binding partners such as PKG and PDE5 in vascular smooth muscle cells (Nausch *et al.*, 2008).

6 Characterisation of a new method for real-time capture of cGMP signals in response to clamped NO concentrations

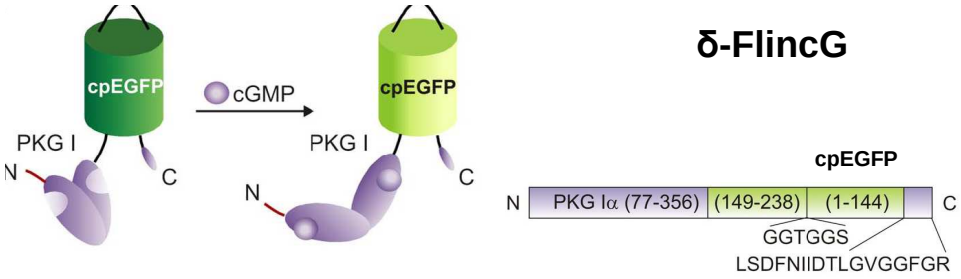

Fig. 6.1 Diagram of FlincG, published in Nausch et al., 2008.

A possible source of error in NO research is the way NO is applied. This has, for instance, led to inconsistent reports concerning the potency of NO for its receptor (Griffiths *et al.*, 2003; Garthwaite, 2005). Numerous studies have and are still deducing results from experiments in which NO is delivered in constantly changing concentrations. The basis of this problem is the continuous decomposition of the NO donor over time and the potential of NO to interact with oxygen, the latter known as autoxidation (Ford *et al.*, 1993). Previously an easy-to-use method has been developed to deliver NO concentrations under clamped conditions so that the biological response or profile of NO_{GC} receptor activation can be directly related to a known concentration of NO (Griffiths *et al.*, 2003). The principle of this method is a balanced state between NO release at a constant rate from an NO donor and an appropriate rate of NO consumption. This is achieved by combining a long-lived NO donor with the chemical NO scavenger CPTIO. The rationale of using an NO donor with a long half-life is to provide a slow rate of decomposition of the donor relative to the duration of the experiment so that a constant rate of NO release is achieved. On the other hand, CPTIO, which allegedly does not penetrate the cells (Griffiths *et al.*, 2003), scavenges NO extracellularly. The end result of combining a state of fast NO diffusion into the cells with continuous extracellular removal of NO is an existent dynamic equilibrium of NO across the cell barrier (Griffiths *et al.*, 2003).

6.2 AIM

The objective of the present study was to investigate NO-evoked cGMP dynamics in a heterologous expression system, combining real-time imaging and clamped delivery of NO at physiological concentrations.

6.3 METHODS

6.3.1 Cell culture of HEK cells

Four different HEK293 cell lines expressing the NO_{GC} receptor and/or PDE5 were chosen for study. One of the cell lines, generated by Jeffrey Vernon in the Garthwaite lab, permanently expresses the $\alpha_1\beta_1$ NO_{GC} receptor targeted to the cell plasma membrane. Three more HEK cell lines with different expression levels of the NO_{GC} receptor and/or the PDE5 were kindly provided by Doris Koesling, University of Bochum. Of these latter three, one had been transfected permanently with the normal $\alpha_1\beta_1$ NO_{GC} receptor only. The other two cell lines had been transfected permanently with the normal $\alpha_1\beta_1$ NO_{GC} receptor and PDE5, one expressing higher amounts of the PDE5 than the other (Mullershausen *et al.*, 2004b). The two respective PDE5-expressing cell lines will be referred to as HEK-GC/PDE5 and HEK-GC/$PDE5^{high}$. The PDE5 activity in HEK-GC/$PDE5^{high}$ cells is approximately 1.5-times higher than in HEK-GC/PDE5 cells (Mullershausen *et al.*, 2004b).

All of the four different HEK cell lines were cultured at 37ºC in a humidified 5% CO_2 atmosphere in DMEM supplemented with 5% heat-denatured fetal bovine serum, 1% penicillin / streptomycin and 1% non-essential amino acids, composing the basic culture medium for these cells. The basic culture medium for HEK cells expressing the membrane-targeted $\alpha_1\beta_1$ NO_{GC} receptor additionally contained the antibiotic zeocin at 300 µg/ml in order to select against the growth of wild type cells. For the

same purpose, basic culture media for the HEK cells expressing PDE5 additionally to the normal $\alpha_1\beta_1$ NO_{GC} receptor contained the antibiotics hygromycin, G418 and zeocin, each being at a final concentration of 200 µg/ml, while cells expressing only the normal $\alpha_1\beta_1$ NO_{GC} receptor were cultured in basic growth medium additionally containing hygromycin and G418 at 200 µg/ml each.

General procedure for cell maintenance

Cells were grown in filter-capped T175 flasks containing 20-30 ml of basic culture medium (see above), replenished with fresh medium approximately every 3-5 days as required. At approximately 80% confluence, cells were split as follows. Media were removed followed by one wash with 1x DPBS, taking care not to disturb or detach cells at this stage. Following removal of DPBS, 3 ml of trypsin solution was added and left for approximately 2 min or until cells had detached. In order to stop the trypsin reaction, 7 ml of basic culture medium was added, followed by triturating the cells. Depending on when confluence of cells was desired, the flask containing fresh basic culture medium was inoculated with an appropriate volume of the cell suspension, the remainder of which was discarded.

6.3.2 Infection of HEK cells with FlincG

FlincG was kindly donated by Wolfgang Dostmann, University of Vermont. To amplify the adenoviral stock, HEK293T cells were used and the procedure according to Invitrogen was followed. In brief, the day before the infection, 293T cells were trypsinised, counted, and plated at 3 x 10^6 cells per 10 cm plate, plating them in 10 ml of normal growth medium containing serum. Once the cells had reached 80-90% confluency, 100 µl of crude adenoviral stock was added to the cells. Cells were incubated at 37ºC in a humidified 5% CO_2 atmosphere, allowing the infection to proceed until 80-90% of cells had rounded up and were floating or only lightly attached to the tissue culture dish (typically 2-3 days post-infection). Adenovirus-

containing cells were harvested by squirting cells off the plate with a 10 ml pipette, transferring the cells and media to a sterile falcon tube. The tube was then placed at -80ºC for 30 min, followed by placing the tube in a 37ºC water bath for 15 min to thaw. This freeze / thaw cycle was repeated twice. Subsequently, cell lysates were centrifuged at 3000 rpm for 15 min at room temperature to pellet the debris. Finally, the supernatant containing viral particles were aliquoted under sterile conditions and stored at -80ºC.

All HEK cells lines containing the $\alpha_1\beta_1$ NO_{GC} receptor and/or PDE5 were plated in basic culture medium (at 2 ml per well) onto poly-D-lysine coated coverslips (No. 0 thickness, 0.08-0.12 mm; 13 mm diameter; VWR International, Dorset, UK) in 6-well plates (Falcon Discovery Labware, Marathon Laboratory Supplies, London, UK) at the desired density at least 24 hours prior to infection. Care was taken not to plate too densely as this would have made it difficult to select a field with the right balance of number of cells and cell-free background. Normally, a density of 30-40% confluence prior to infection was aimed for. On the day of infection, several hours before the addition of the virus, the medium was changed to basic culture medium devoid of the 'selection' antibiotics (i.e. no zeocin, hygromycin, or G418). For infection of HEK cells with the FlincG biosensor, adenovirus (10^7-10^9 per ml presumed titer) was first diluted at 1/ 100 in cold DPBS and then added to the wells containing 2 ml of medium and 30-40% confluent HEK cells at 1: 30 000, giving a final titer of 3.33×10^3-3.33×10^5 particles per ml. Cells were incubated in the presence of the viral construct for approximately 36 hours at 37ºC and 5% CO_2 atmosphere before imaging.

6.3.3 Imaging

On the day of imaging, approximately 1-2 hours before starting the experiments, the medium containing the FlincG-adenovirus was removed and replenished with complete culture medium devoid of the 'selection' antibiotics.

Before each experiment, flow rate and temperature were checked and, if necessary, were adjusted to 1.5-1.6 ml/min and 37ºC (± 0.1) respectively. To measure the delay between switching to a different solution and that solution reaching the chamber, the passage of a deliberately introduced air bubble was timed. All drug applications were corrected for this delay. Also, to determine the efficiency of wash-in and wash-out, fluorescein (1 nM) was perfused at the end of an experiment, and the equilibration parameters determined by fitting the rising and falling phases to the following logistic function:

$$y = \frac{A1 - A2}{1 + (\frac{x}{x_0})^p} + A2$$

Where:

A1 = start of wash-in or wash-off

A2 = equilibration of wash-in or wash-off

y = change in fluorescence in the chamber

x = time (sec)

x_0 = half-time of wash-in or wash-off

p = slope

A sample analysis is illustrated in *Fig. 6.2*. Overall, the mean half-time (x_0) for wash-in was 7.5 ± 0.72 sec with a mean slope (p) of 2.2 ± 0.77 (n = 24). For wash-out, the corresponding values were 8.6 ± 0.77 sec for x_0 and 2.4 ± 0.70 for p (n = 24).

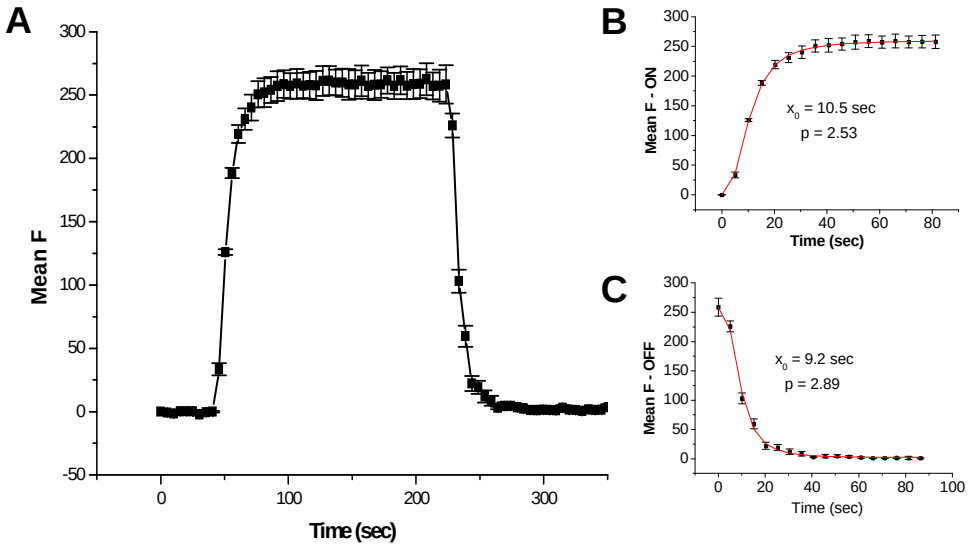

Fig. 6.2 Wash-in and wash-out of fluorescein for determining the mixing parameters. *A:* Whole graph showing 3 min application of fluorescein. *B:* Parameters determined for wash-in mixing time. *C:* Parameters determined for wash-out mixing time.

A coverslip was placed into the chamber (0.5 ml capacity) and a platinum ring (12 mm diameter) used to hold it down. The coverslip was perfused with clamp buffer and a field of cells brought into focus using the bright field. A field of cells was chosen on the basis of morphological criteria and reasonable expression levels of the FlincG. In general, the coverslips were screened for a field containing several cells positively expressing the FlincG, avoiding fields mainly containing very round or bright cells and/or lacking enough cell-free background space. The acquisition time (or frame rate) as well as exposure time were adjusted from one experiment to the other as required.

To achieve conditions of 'clamped' NO concentrations, the 'clamp buffer' contained the NO scavenger CPTIO (100 µM). Other constituents were urate (300 µM) to remove NO_2 that is formed by the reaction between NO and CPTIO, and SOD (100 U/ml) to scavenge any superoxide anions that would otherwise react with NO to form peroxynitrite (Griffiths *et al.*, 2003). To prevent any endogenous NO production, the

clamp buffer also contained the broad-spectrum NOS inhibitor L-NNA (30 µM). The potential problem of NO loss via autoxidation was negligible at the low concentrations of NO used (0.001-30 nM) based on the rate of the reaction between NO and oxygen being proportional to the square of the NO concentration (Ford *et al.*, 1993; Griffiths *et al.*, 2003). A mathematical model developed by Prof. John Garthwaite in Mathcad was used for determining the concentrations of NO donor and CPTIO to be added to the clamp buffer in order to achieve the desired clamped NO profile. As an example, *Fig. 6.3* shows an outline of the model, depicting the clamped profile of 1 nM NO:

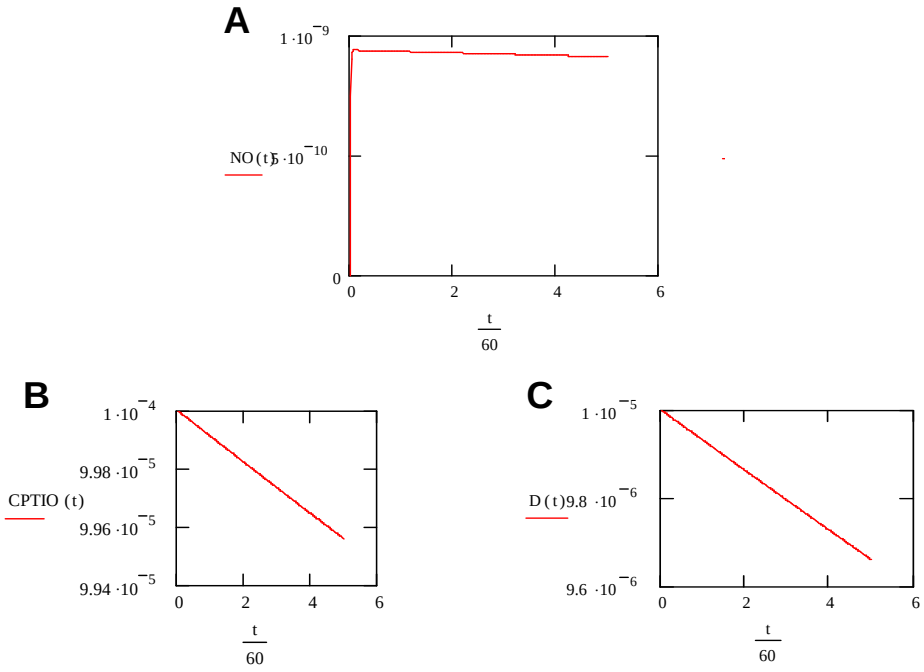

Fig. 6.3 Clamped NO concentrations as determined using a Mathcad document written by Prof. J. Garthwaite – A: Clamped profile of 1 nM NO. B: CPTIO consumption over time. C: Decomposition of NO donor over time.

The following parameters were employed to obtain the above profile:

$[Donor]_0$ = 10 µM, the initial concentration of NO donor added to the clamp buffer immediately before application in order to obtain 1 nM of 'clamped' NO;

eNO = 1.3, the mol of NO released per mol NO donor;

$[CPTIO]_0$ = 100 µM, the starting concentration of CPTIO that is added to the clamp buffer;

thalf = 100, the known half life of the NO donor NOC-12 in minutes at 37ºC and pH 7.4;

k1 = 1.155 x 10^{-4}, the rate constant for donor decomposition (s^{-1});

k2 = 1.6 x 10^4, the rate constant for reaction of NO with CPTIO;

Furthermore:

t = time in seconds

[NO](t) = concentration of NO at time t

[Donor](t) = concentration of NO donor at time t

[CPTIO](t) = concentration of CPTIO at time t

Finally, this is solved according to the following equation:

$$Donor \xrightarrow{k1} NO$$

$$NO + CPTIO \xrightarrow{k2} CPTI + NO_2$$

Assuming exponential decay of the donor, the decomposition reaction will follow first order kinetics with a rate of

$$\frac{d[Donor]}{dt}(t) = -k_1.[Donor](t)$$

Accordingly, the rate of NO formation is given by

$$\frac{d[NO]}{dt}(t) = k_1.[Donor](t).eNO$$

And will ultimately be determined by the amount of NO being removed by CPTIO, so that

$$\frac{d[NO]}{dt}(t) = k_1.[Donor](t).eNO - k_2.[CPTIO](t).[NO](t)$$

The decay of CPTIO will be given by its reaction rate with NO

$$\frac{d[CPTIO]}{dt}(t) = -k_2[CPTIO](t).[NO](t)$$

For all experiments, the concentration of CPTIO was kept constant (i.e. at 100 µM) and the concentration of NOC-12 to be added was adjusted as required to obtain the desired free NO concentration, which ranged from 1 pM to 30 nM.

Cells were continuously perfused with clamp buffer and imaged on an inverted microscope (Axiovert 135 TV Zeiss) using a x40 magnification oil immersion objective and a 12-bit monochrome camera (Q Imaging Rolera-XR; Microimaging Applications Group, Marlow, Buckinghamshire, UK) and a combined filterwheel and lamp (Prior Lumen200Pro; Prior Scientific Instruments Ltd). A standard filter set was used (Chroma filter set 49002 GFP containing an ET470±40 nm/40x excitation filter, a T495LP dichroic mirror and an ET525/50nm emitter; Chroma Technology Corp., Dorchester, Dorset, UK). The images were acquired using Image-Pro Plus 6.3 (MediaCybernetics, Inc., Bethesda, MD, USA). The FlincG has an absorption maximum at 491 nm, excitation at 480 nm yielding an emission maximum at 511 nm, which is shifted when cGMP binds (K_D ~ 170 nM; Nausch *et al.*, 2008). Cells were imaged at varying acquisition rates depending on their response profile. In general, HEK cells only expressing the NO_{GC} receptor were imaged at a frame rate of 0.2 Hz acquisition speed, while HEK cells expressing the NO_{GC} receptor and PDE5 at lower or higher levels were imaged at 0.5 Hz or 1 Hz respectively. Exposure times were

adjusted according to the level of FlincG expression and ranged from 90 to 110 msec. All inhibitors were pre-incubated for 5 min prior to NO application. The NO donor NOC-12 ($t_{1/2}$ = 100 min at pH 7.4 and 37ºC) was applied for 1 min, unless otherwise stated, at an appropriate concentration required to achieve the desired clamped concentration of NO. The cGMP analogue 8-Br-cGMP was perfused for 15 min. NO applications were at 10-15 min intervals unless otherwise indicated.

6.3.4 Analysis

FlincG-expressing cells that were very bright (near to saturated) or moved were excluded from the analysis. The data were analysed using Image-Pro Plus 6.3, Excel and OriginPro 8. Areas of interest (AOIs) were selected for each FlincG-expressing cell and the mean fluorescence intensity was measured over time. The background (F_0), which was selected in cell-free areas, was subtracted from all values of the mean fluorescence intensity (F) measured for the whole experiment, giving ΔF, and, to normalise the fluorescence intensity, ΔF was divided by F_0. Following normalisation of the data to $\Delta F/F_0$, all cells were averaged to show the mean FlincG readout of the experiment.

6.4 RESULTS

6.4.1 Evaluation of FlincG as a cGMP sensor

Influence of varying levels of FlincG on response profiles

To ensure that no errors are introduced due to a buffering effect on cGMP the cell line exhibiting the fastest response to NO (i.e. HEK-GC/PDE5^{high}; see later) was chosen for the comparison of the cGMP profiles among cells containing varying amounts of FlincG. No noticeable change in the response profiles was observed when

comparing different cells, with some expressing up to 5-fold higher FlincG content than others *(Fig. 6.4)*. No change in fluorescence occurred in control experiments testing cells which had not been infected with the FlincG-adenoviral construct *(Fig. 6.5)*.

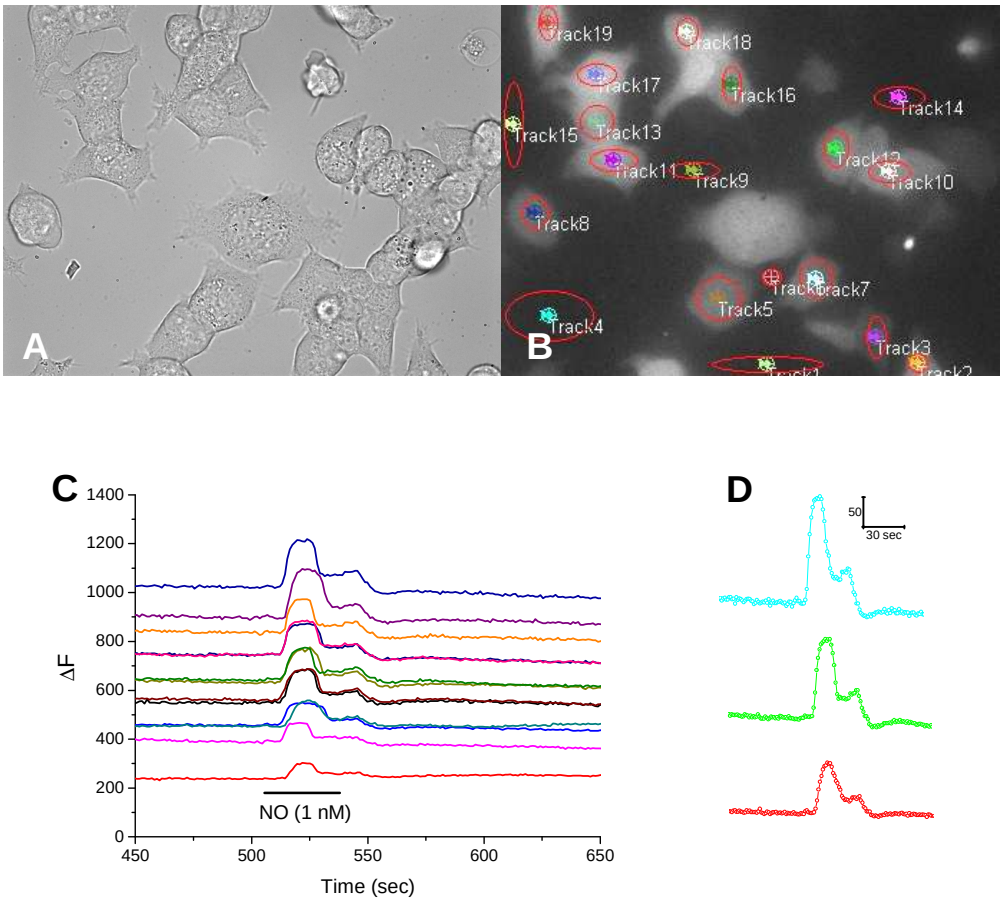

FIG. 6.4 Response profiles to 1 nM NO in HEK-GC/PDE5^{high} cells containing different amounts of FlincG. *A:* Bright-field image of HEK cells. *B:* Areas of interest. *C:* Read-out of areas of interest before normalisation to $\Delta F/F_0$. Up to a 5-fold difference in the level of FlincG expression had no noticeable impact on the shape of the response to 1 nM NO. *D:* Averaged traces of cells expressing lowest, intermediate, and highest levels of FlincG seen in panel *C*.

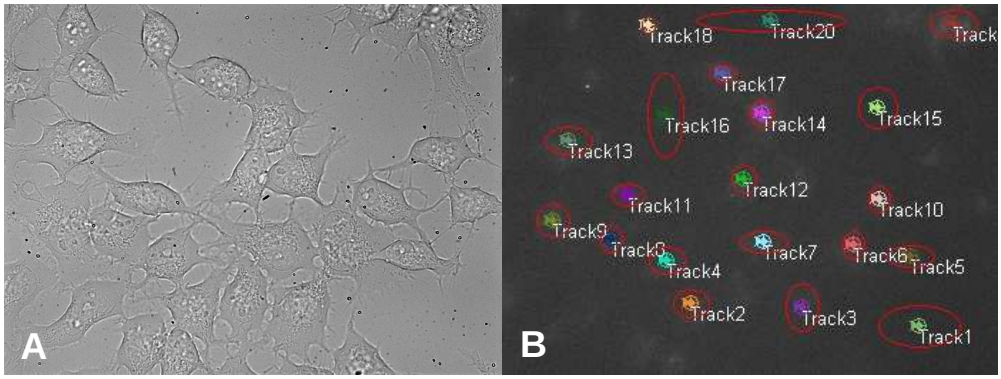

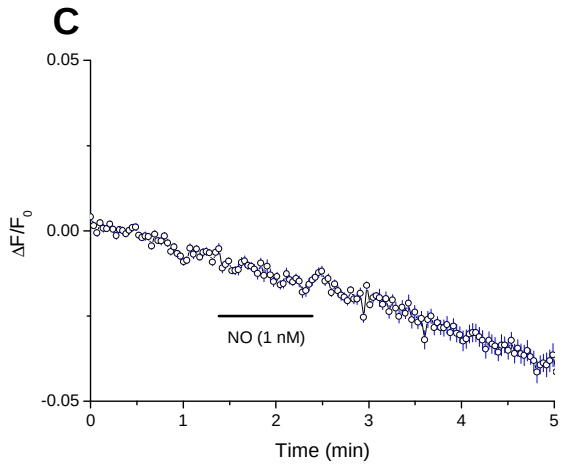

FIG. 6.5 Effect of NO in cells not infected with the FlincG. *A:* Bright-field image of cells. *B:* Areas of interest. *C:* Trace showing the mean readout of the response to 1 nM NO. No change in fluorescence intensity occurred. Shown are averaged traces of n = 16, representative of 3 observations. *Note:* Application time of NOC-12 is indicated by the horizontal bar. In blue are ± SEM.

Evaluation of FlincG as a sensor for changes in cGMP in response to clamped NO using HEK cells expressing the membrane-localised $\alpha_1\beta_1$ NO_{GC} receptor

The first aim was to test whether the fluorescence change in response to NO application was the result of activation of NO_{GC} receptors and ultimately corresponding to a change in cGMP. Cells were sequentially exposed to 1 nM NO, resulting in successive changes in fluorescence intensity, the response returning back to baseline upon removal of NO *(Fig. 6.6a,b)*. The response to NO was abolished in the presence of the NO_{GC} receptor inhibitor ODQ, signifying dependence on cGMP generation *(Fig. 6.6a,b)*. No change in the baseline occurred during pre-incubation of

ODQ. Additionally, the cGMP analogue 8-Br-cGMP also evoked a change in fluorescence intensity *(Fig. 6.6c,d)*.

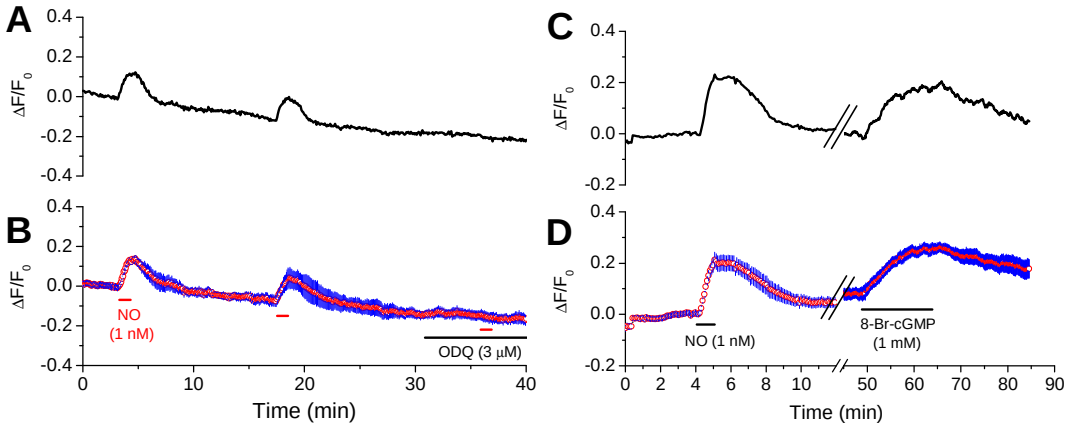

FIG. 6.6 NO_{GC} receptor-dependence of FlincG emitted fluorescence changes in response to NO exposure. *A-B:* Representative trace*(A)* and averaged traces of $n = 4$, representative of 3 observations *(B)* showing cGMP responses to 1 min applications of 1 nM clamped NO in the absence or presence of ODQ. *C-D:* Representative trace*(C)* and averaged traces of $n = 5$, representative of 4 observations *(D)* showing cGMP responses to 1 min application of 1 nM clamped NO and 8-Br-cGMP. Note, panels *C* and *D* depict data obtained in experiments shown in Fig. 6.9. *Note:* Application times of NO and ODQ are indicated by the horizontal bars. Red, mean; blue, ± SEM.

The profile of cGMP signals is determined by its rate of synthesis by NO_{GC} receptors and its degradation by phosphodiesterase (PDE; see Chapter 1). Having confirmed that the increase in fluorescence intensity is dependent on NO_{GC} receptor activation by NO *(Fig. 6.6)*, the aim was to assess whether the falling phase of the response upon NO removal was the result of cGMP breakdown by PDE. This test would further contribute to validating whether the changes in fluorescence intensity are based on changes in cGMP levels. Application of 1 nM NO resulted in the characteristic change in fluorescence intensity, gradually returning back to baseline upon wash-out of NO. In the presence of the broad-spectrum PDE inhibitor IBMX, the increase in fluorescence intensity persisted following NO removal and only returned to baseline upon wash-out of IBMX *(Fig. 6.7)*. Wash-out of IBMX and

restoration of PDE activity was confirmed by re-application and removal of NO resulting in the previously mentioned rise and fall in the fluorescence intensity.

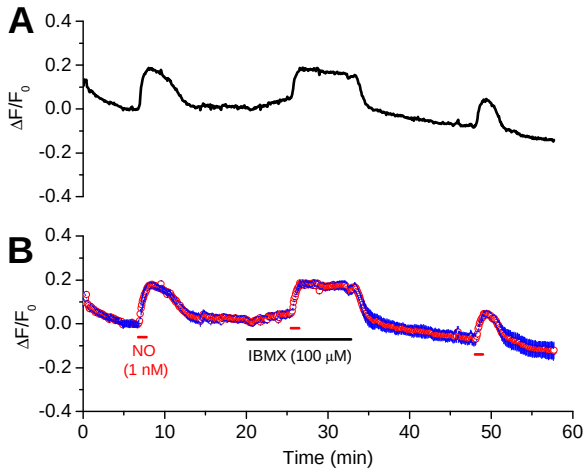

FIG. 6.7 Effect of PDE inhibition on NO-evoked cGMP-mediated FlincG responses *A:* Representative trace showing cGMP responses to 1 nM clamped NO in the absence or presence of the broad-spectrum inhibitor IBMX. *B:* Averaged traces of n = 5, representative of 5 observations. *Note:* Application times of NO and IBMX are indicated by the horizontal bars. Red, mean; blue, ± SEM.

The next set of experiments investigated the dynamics of the cGMP signal to different clamped NO concentrations. Exposure of HEK cells expressing the membrane-targeted $\alpha_1\beta_1$ isoform of the NO_{GC} receptor to 1 min of different clamped concentrations of NO generated a concentration-dependent increase in the mean fluorescence intensity *(Fig. 6.8a,b)*. A clear response was detected at 300 pM NO, the FlincG reaching its maximum fluorescence at 10 nM, resulting in a plateau phase of the response. The initial rate of the response rise accelerated with higher NO concentrations *(Fig. 6.8c,d)*, as did the decay rate *(Fig. 6.8e,f)*, the latter corresponding to the response falling back to baseline faster. Exposure to a high (30 nM) NO concentration was followed by a second application of 1 nM NO, the response to which appeared reduced and to have a slower rise time but faster decay time as compared to the response evoked by the first application of 1 nM NO *(Fig. 6.8g)*. Overall, the response to the second exposure of 1 nM NO (i.e. 'post-30 nM NO') appeared shallower with an accelerated rate of the fluorescence change returning to baseline. A submaximal concentration of 1 nM NO was chosen to serve as the control signal in all subsequent experiments as this allowed monitoring the

progression of the whole response without loss of the peak due to the FlincG saturating.

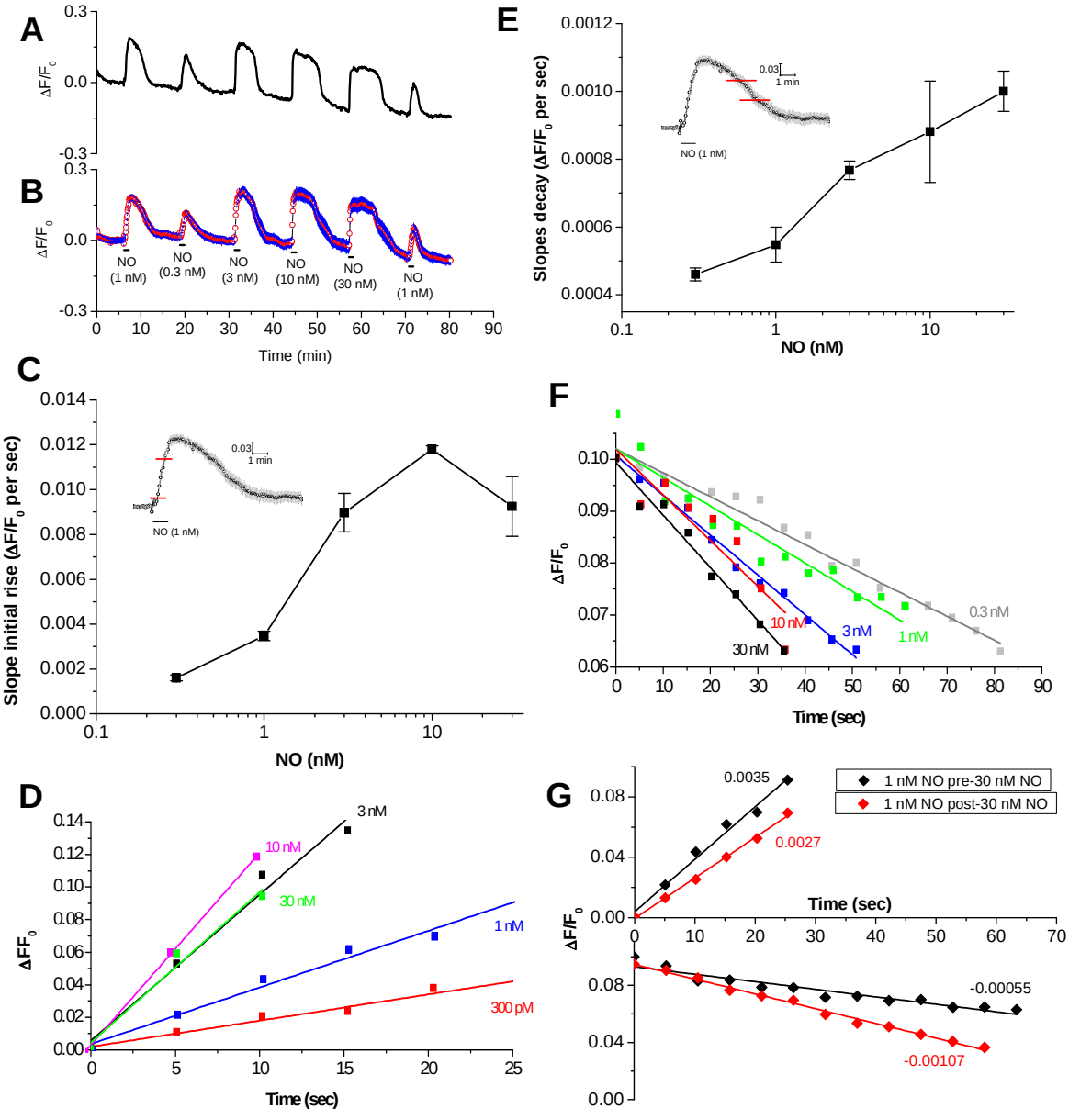

FIG. 6.8 Concentration-response of FlincG to clamped concentrations of NO. *A-B:* Representative trace *(A)* and averaged traces of n = 7 *(B)* showing cGMP responses to ascending clamped concentrations of NO, applied for 1 min. *C-F* Graphs showing mean initial rates of rise times *(C-D)* and the decay times *(E-F)* of responses to increasing NO concentrations. Indicated in panels *C* and *E* is an example of measurements taken of the initial rising phase and response decline. Panel *D* shows individual traces of mean initial rise times (normalised to zero),

the slopes of which are plotted in *C*. Panel *F* shows individual traces of mean decay times (normalised to a fixed point), the slopes of which are plotted in *E*. *G:* Comparison of the mean initial rates of rise and decay times of responses to 1 nM NO before ('1 nM NO pre-30 nM NO') and after ('1 nM NO post-30 nM NO') exposure to higher NO concentrations. Indicated in the graph are the slopes. *Note:* Application times of NO are indicated by the horizontal bars. In panel *B*, red is mean; blue is ± SEM.

From the changes in fluorescence intensity, estimations of the corresponding cGMP concentrations can be made by rearranging the Michaelis-Menten equation to:

$$[cGMP] = \left(\frac{r}{R_{\max} - r} \right)^{\frac{1}{n}} \times EC_{50}$$

Where:

[cGMP] = concentration of cGMP

$r = \Delta F$

$R_{max} = \Delta F_{max}$

n = 1.47, and is the slope of the calibration curve to known [cGMP] (Nausch *et al.*, 2008)

EC_{50} = 150 nM; the [cGMP] causing a half-maximal change in fluorescence (Nausch *et al.*, 2008)

In *Fig. 6.8*, ΔF_{max} was 0.21 units in fluorescence change (corresponding to the mean change in fluorescence caused by 3 nM, 10 nM and 30 nM NO), corresponding to 1 µM cGMP (Nausch *et al.*, 2008). Using the equation above, the change in fluorescence in response to 300 pM NO (0.10 units) corresponds to approximately 141 nM of cGMP, while the responses to the first 1 nM NO application (0.18 units) and the last 1 nM NO application (0.11 units) that followed a high (30 nM) NO

concentration correspond to approximately 507 nM and 160 nM cGMP respectively. From these estimates, it can be suggested that exposure to a high NO concentration caused over 60% loss of the response to a subsequent low NO concentration.

As revealed by the data shown in *Fig. 6.8,* following exposures to successive, ascending NO concentrations, the profile of control response to 1 nM NO was altered compared to that in response to the first application of 1 nM *(Fig. 6.8)*; the initial rising phase was found to be reduced, whereas the decay rate was found to be increased. The next set of experiments evaluated whether these changes in the control response profile were the result of the relatively long duration of the experiment, giving several NO challenges, or directly related to applying a high (30 nM) NO concentration. Following a single exposure to a high (30 nM) NO concentration, the response profile to the subsequent application of 1 nM exhibited a reduced initial rising rate and an accelerated falling phase compared to the control response to the first application of 1 nM NO *(Fig. 6.9a-c).*

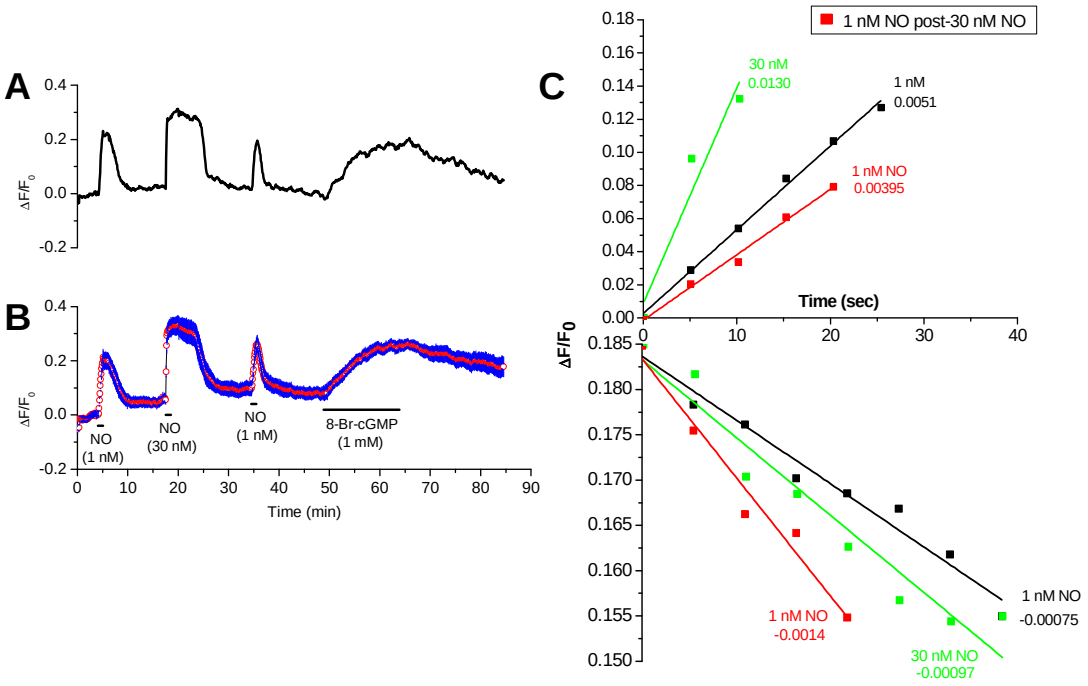

FIG. 6.9 Changes in the response profile to low NO following exposure to a high NO concentration. *A-B:* Representative trace *(A)* and averaged traces of $n = 5$, representative of 4 observations *(B)* showing cGMP responses to submaximal (1 nM) and saturating (30 nM) clamped NO concentrations, applied for 1 min. *C:* Plotted are mean initial rise and fall times of fluorescence changes normalised to zero or a fixed point respectively. Slopes are indicated in the graph. *Note:* Application times of NO and 8-Br-cGMP are indicated by the horizontal bars. In panel *B*, red is mean; blue is ± SEM.

6.4.2 NO sensitivity

FlincG response to clamped NO using HEK cells expressing the normal $\alpha_1\beta_1$ NO_{GC} receptor

The following set of experiments investigated the NO-evoked cGMP profile in HEK cells expressing the normal $\alpha_1\beta_1$ NO_{GC} receptor kindly provided by Doris Koesling. Cells were exposed to ascending concentrations of NO revealing concentration-dependent increases in fluorescence intensity. A change in fluorescence intensity resulted at NO concentrations as low as 3 pM, the FlincG saturating around

100 pM. Comparing these data to the concentration-response profile of HEK cells expressing the membrane-targeted $\alpha_1\beta_1$ NO_{GC} receptor *(Fig. 6.8)*, it is found that the HEK cells used in this set of experiments are nearly 100-fold more sensitive to NO (compare concentration-response profile illustrated in *Fig. 6.8a,b* with *Fig. 6.10a,b*). This observation is also consistent with the response to an approximately 30- to 100-fold lower concentration of NO exhibiting a similar initial rise time (compare *Fig. 6.8c,d* and *Fig. 6.10c*). Additionally, a much lower concentration of NO was able to cause saturation of the FlincG (i.e. 100 pM, *Fig. 6.10a,b vs.* 10 nM, *Fig. 6.8a,b*).

The remarkable sensitivity of this particular NO_{GC} receptor-HEK cell line was exploited to investigate whether a fluorescence change could be detected in response to environmental NO. An increase in fluorescence intensity was detected upon removal of the NO scavenger CPTIO, which reversed to baseline when the NO_{GC} receptor inhibitor ODQ was applied *(Fig. 6.10a,b)*. Application of 8-Br-cGMP evoked a response also in the presence of ODQ *(Fig. 10a,b)*, confirming that the loss of the fluorescence change upon NO exposure in the presence of ODQ is the result of NO_{GC} receptor inhibition and not due to a direct effect on the FlincG indicator. Additionally, this latter observation further provides evidence that the changes in fluorescence intensity are associated with changes in cGMP. Comparing the initial rise times of fluorescence changes, it was possible to estimate the level of environmental NO existing around the recording chamber. The level of environmental NO was estimated to be 10 pM *(Fig. 6.10c)*.

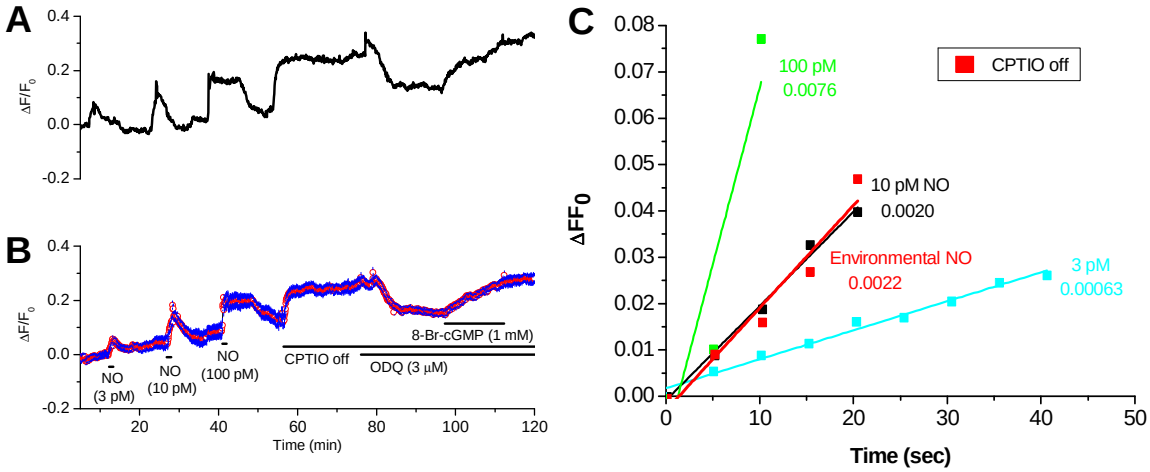

FIG. 6.10 NO sensitivity. *A-B:* Representative trace *(A)* and averaged traces of $n = 5$ *(B)* showing cGMP responses to ascending concentrations of clamped NO, revealing a FlincG signal to a NO concentration as low as 3 pM. Wash-off of the NO scavenger CPTIO resulted in an increase in fluorescence intensity, corresponding to a response to environmental NO, which was prevented upon exposure to ODQ. The response to 8-Br-cGMP was preserved in the presence of ODQ. *C:* Plotted are the mean initial rises in fluorescence intensity upon NO exposure, normalised to zero. Indicated in the graph are slopes, showing a much steeper rise in response to 100 pM NO as compared to 3 pM, corresponding to faster and slower rise times respectively. In red is the initial rise of the response to environmental NO. *Note:* Application times of compounds are indicated by the horizontal bars. In panel *B*, red is mean; blue is ± SEM.

6.4.3 Impact of PDE and NO_{GC} receptor activities on the profile of FlincG responses

The following series of experiments aimed to characterise the shape of the cGMP-mediated FlincG signal in HEK cell lines permanently expressing the normal $\alpha_1\beta_1$ NO_{GC} receptor and lower or higher levels of PDE5 (i.e. HEK-GC/PDE5 and HEK-GC/$PDE5^{high}$ respectively; Mullershausen *et al.*, 2004b), which were also kindly given to us by Doris Koesling.

Concentration-response profile

Exposure of HEK-GC/PDE5 and HEK-GC/PDE5^{high} cells to NO evoked FlincG responses that were markedly distinct from the ones observed in the forgoing experiments using HEK cell lines permanently expressing only NO_{GC} receptors (and their native PDE). Application of different clamped NO concentrations resulted in concentration-dependent FlincG signals, exhibiting a biphasic shape (*Fig. 6.11* and *Fig. 6.12*). The shape of the responses is exemplified in *Fig. 6.11c-e* and *Fig. 6.12c-e* for HEK-GC/PDE5 and HEK-GC/PDE5^{high} cells respectively. Each concentration of NO evoked a response comprised of a rapid rise and subsequent fall within approximately 1 min, the rise times being faster at higher NO concentrations as indicated by the steeper slopes of the initial rising phases (*Fig. 11f* and *Fig. 12f*). With increasing NO concentrations the rate of the initial rise in the response became steeper with faster onset of the response decline (*Fig. 11* and *Fig. 12*). In all cases, the FlincG signal in response to NO began to return towards baseline while the cells were still being perfused with NO, indicating cGMP-mediated switch-on of PDE5 (Rybalkin *et al.*, 2003; Mullershausen *et al.*, 2003). In the HEK-GC/PDE5 cells, at a low (30 pM) NO concentration the response reached a plateau and started to reverse within approximately 40 sec of response onset, which was found to be 20-25 sec and approximately 5 sec in the case of 1 nM and 30 nM NO respectively. In the case of the HEK-GC/PDE5^{high} cells, at 1 nM NO the response reached plateau and started to reverse within approximately 20 sec of response onset while the NO was still present, which was found to be approximately 10 sec in the case of 10 nM NO application. One difference that transpired between the HEK-GC/PDE5 and HEK-GC/PDE5^{high} cells concerned their sensitivity to NO. The threshold for detecting a response in HEK-GC/PDE5 cells was at 10-fold lower NO concentrations than in the HEK-GC/PDE5^{high} cells (10 pM *vs.* 100 pM; *Fig. 11a,b* and *Fig. 12a,b*). This latter observation is consistent with the HEK-GC/PDE5 having greater NO_{GC} activity than the HEK-GC/PDE5^{high} cells (Mullershausen *et al.*, 2004b) and is paralleled by the

initial rise times of responses to the same NO concentrations being steeper in the HEK-GC/PDE5 cells than in the HEK-GC/PDE5^{high} cells (*Fig. 11f* and *Fig. 12f*).

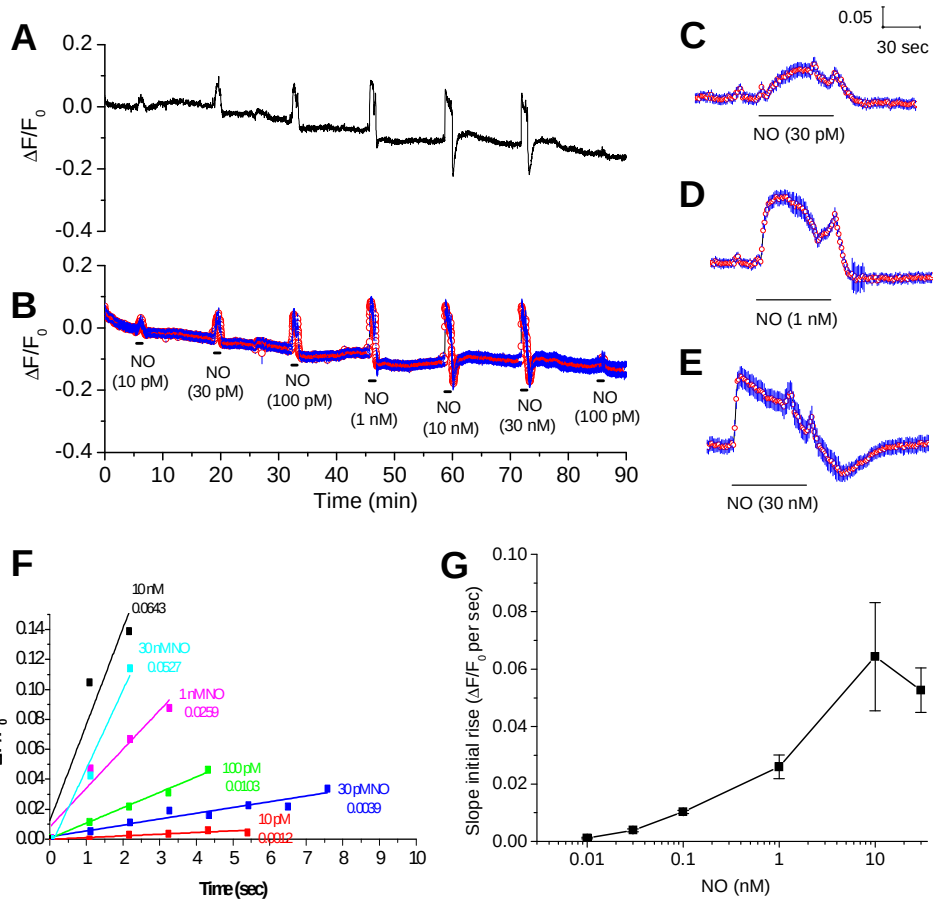

FIG. 6.11 Concentration-response profile of HEK-GC/PDE5 cells. *A-B:* Representative trace *(A)* and averaged traces of n = 10, representative of 3 observations *(B)*, showing cGMP responses to ascending concentrations of clamped NO, revealing FlincG responses to a NO concentration as low as 10 pM. Notice the almost complete loss of the response to a low (100 pM) NO concentration after exposure to a high (30 nM) NO concentration. Also note the 'undershoot' in the responses to higher NO concentrations. The distinct shapes of the responses to varying concentrations of NO are depicted in panels *C-E*, showing the enlarged traces of the response profiles to 30 pM *(C)*, 1 nM *(D)*, and 30 nM NO *(E)*. *F-G* Graphs showing mean initial rates of rise times of responses to increasing NO concentrations. Panel *F* shows individual traces of mean initial rise times (normalised to zero), the slopes of which are plotted in *G*. Indicated in the graph illustrated in panel *F* are slopes, being much steeper in the case of higher NO concentrations, corresponding to faster rise times. *Note:* Application times of compounds are indicated by the horizontal bars. In panels *B-E*, red is mean; blue is ± SEM.

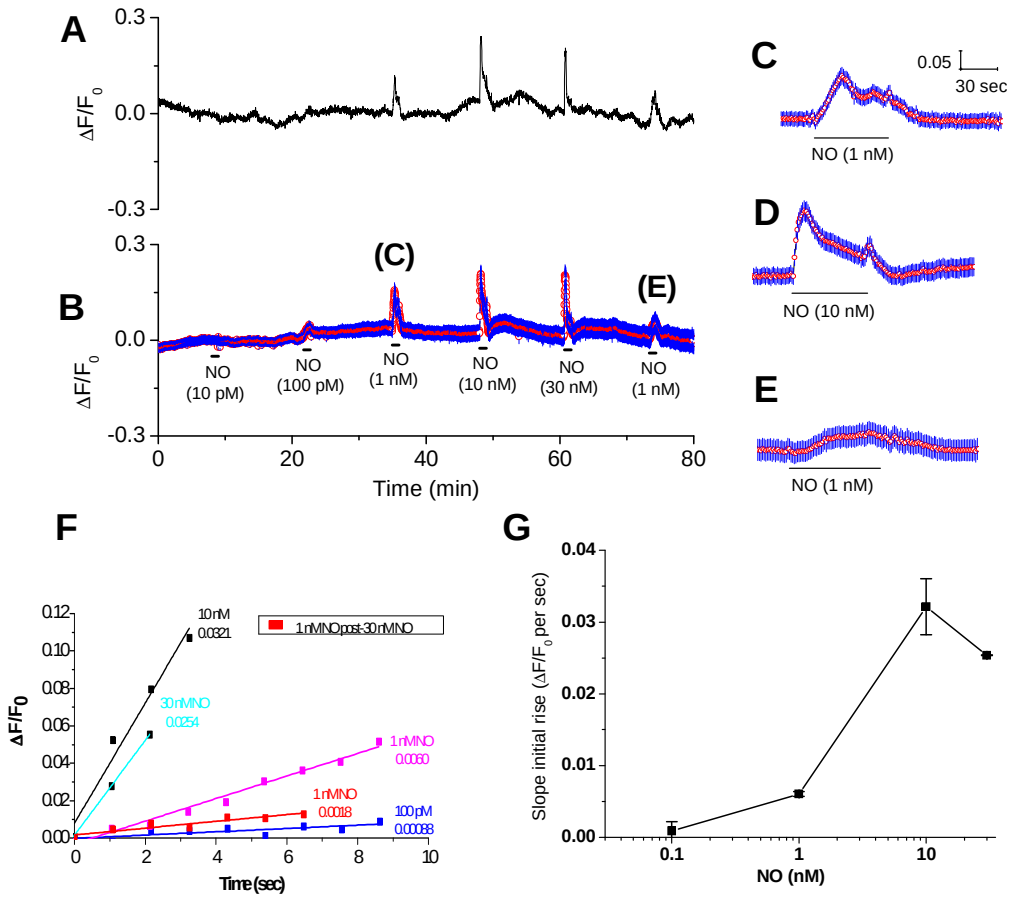

FIG. 6.12 Concentration-response profile of HEK-GC/PDE5^{high} cells. *A-B:* Representative trace *(A)* and averaged traces of *n* = 12, representative of 3 observations *(B)*, showing cGMP responses to ascending concentrations of clamped NO, revealing FlincG responses to a NO concentration as low as 100 pM. Notice the marked loss of the response to a low (1 nM) NO concentration after exposure to a high (30 nM) NO concentration. The distinct shapes of the responses to varying concentrations of NO are depicted in panels *C-E*, showing the enlarged traces of the response profiles to 1 nM *(C)*, 10 nM *(D)*, and the second application of 1 nM NO after a high NO concentration *(E)*. *F-G* Graphs showing mean initial rates of rise times of responses to increasing NO concentrations. Panel *F* shows individual traces of mean initial rise times (normalised to zero), the slopes of which are plotted in *G*. Indicated in the graph illustrated in panel *F* are slopes, being much steeper in the case of higher NO concentrations, corresponding to faster rise times; in red is the initial rise of the response to re-exposure to a low (1 nM) NO concentration after high (30 nM) NO, being slower compared to that measured upon the first application of 1 nM NO. *Note:* Application times of compounds are indicated by the horizontal bars. In panels *B-E*, red is mean; blue is ± SEM.

As was apparent in the forgoing experiments, the NO-evoked FlincG signal in both HEK-GC/PDE5 and HEK-GC/PDE5^{high} cells displayed a biphasic profile comprising a sharp rise followed by rapid reversal of the response back towards baseline while NO was still being perfused. The biphasic nature of the response was particularly pronounced in the HEK-GC/PDE5^{high} cells. The aim of the following set of experiments was to investigate the nature of this biphasic shape of the NO-evoked FlincG response further. Cells were repeatedly exposed to a submaximal (1 nM) NO concentration (i.e. a concentration at which the FlincG had not reached saturation) for 3 min (instead of 1 min). The first exposure revealed the first phase of the response comprising a fast rise, which was followed by a fast drop. The fast decline appeared to stabilise about half-way down, revealing the second phase of the response, which appeared to be in a steady-state until the NO was washed off *(Fig. 6.13a-d)*. The profile of the responses to subsequent NO challenges appeared altered in that they almost lacked the initial 'spike' phase *(Fig. 6.13c-d)*, with the second 'plateau' phase appearing to slowly decline while NO was still present *(Fig. 6.13a-b)*.

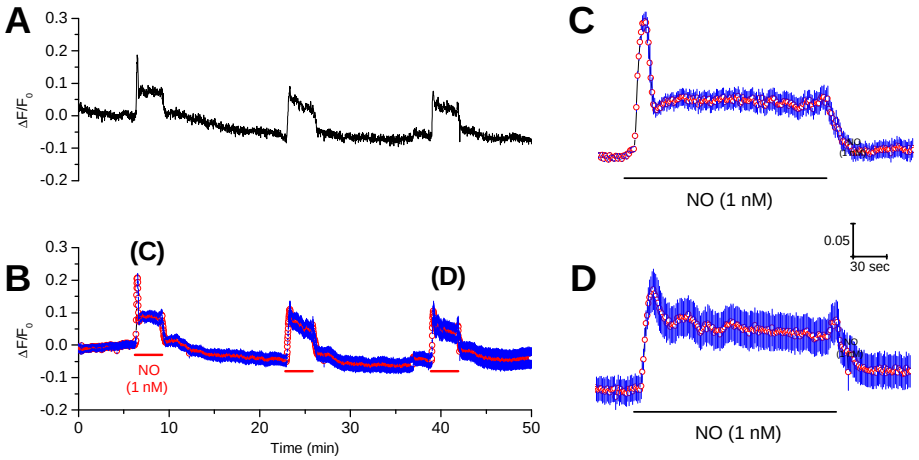

FIG. 6.13 Effect of prolonged repeated NO exposure on the response profile in HEK-GC/PDE5^{high} cells. *A-B:* Representative trace *(A)* and averaged traces of *n* = 7 *(B)* showing cGMP responses to repeated applications of 1 nM clamped NO, each NO challenge lasting for 3 min. Note the change in the response profile from one displaying a distinctive 'spike' phase followed by a 'plateau' phase seen in response to the first NO exposure, to one almost lacking the initial 'spike-like' phase of the response. *C-D:* Enlarged traces of responses to the first *(C)* and last *(D)* application of NO, indicated in panel *B*. *Note:* Application times of NO are indicated by the horizontal bars. In panels *B-D*, red is mean; blue is ± SEM.

Testing for basal NO_{GC} receptor activity

It was noticed in the forgoing experiment that the profile of the response consisted of an under-shoot passing the initial baseline following NO removal, which was particularly pronounced in the HEK-GC/PDE5 cells *(Fig. 6.11)*. This may be the result of a basal level of cGMP in the cells, the hydrolysis of which by the active PDE5 would be revealed as the fluorescence intensity decreasing beyond the baseline level. The next set of experiments assessed whether there was a basal level of cGMP in the cells. The prediction is that if there was basal NO_{GC} receptor activity in the cells, then inhibition of PDE5 to stop cGMP degradation would reveal a FlincG response. To avoid a possible interference of NO application, cells were first exposed to the PDE5 inhibitor sildenafil, revealing a clear increase in fluorescence intensity that returned to baseline upon wash out of sildenafil *(Fig. 14a,b)*. Subsequent exposure to NO resulted in the usual FlincG response. Surprisingly, a response to sildenafil was still observed in the presence of the NO_{GC} receptor inhibitor ODQ, while no FlincG response was evoked by NO, but the response to 8-Br-cGMP remained intact *(Fig. 14a,b)*. Closer examination revealed an over 50% shallower slope of the response to sildenafil in the presence of ODQ as compared to the response evoked by the first sildenafil exposure *(Fig. 14c)*, indicating that part of the initial (faster) response to sildenafil may be ODQ-sensitive and, thus, NO_{GC} receptor-dependent. Additionally, although not very marked, during pre-incubation of ODQ a small ‘dip’ could be seen in the baseline when looking at the averaged traces of individual cells *(Fig. 6.14b)*, which would be supportive of there being a basal cGMP level in unstimulated cells.

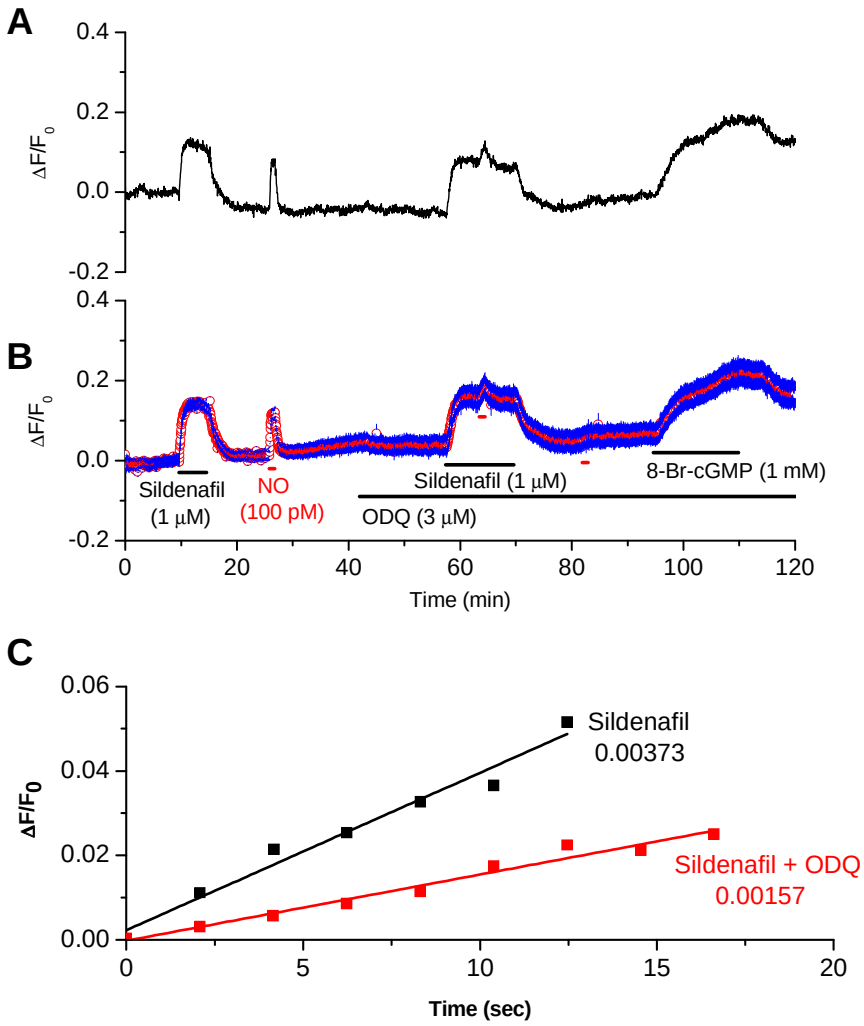

FIG. 6.14 Effect of PDE5 inhibition under basal conditions – HEK-GC/PDE5 cells. *A-B:* Representative trace *(A)* and averaged traces of n = 15, representative of 3 observations *(B)*. A marked FlincG response resulted upon sildenafil exposure prior to any NO application, where sildenafil evoked a response in the absence and presence of the NO_{GC} receptor inhibitor ODQ. The response to NO was prevented by ODQ, while 8-Br-cGMP still evoked a FlincG signal. *C:* Plotted are the mean initial rise phases, normalised to zero. Indicated in the graph are the slopes. Note the much shallower rise of the response to sildenafil in the presence of ODQ as compared to the first application of sildenafil. *Note:* Application times of compounds are indicated by the horizontal bars. In panel *B*, red is mean; blue is ± SEM.

6.4.4 Reproducibility of NO-evoked FlincG responses in fast responding HEK cells expressing the NO_{GC} receptor and PDE5

The next series of experiments investigated the capacity of the system characterised in the present study to provide readout of brief, successive NO-mediated responses. Cells expressing different proportions of NO_{GC} receptors and PDE5 were stimulated with a submaximal clamped NO concentration (i.e. concentrations at which the FlincG had not reached saturation) repeatedly for 30 sec at 2 min intervals. Both HEK-GC/PDE5 *(Fig. 6.15)* and HEK-GC/$PDE5^{high}$ cells *(Fig. 6.16)* were found to produce a reproducible readout of FlincG responses.

In the case of HEK-GC/PDE5 cells the main change observed was a subtle reduction in the response magnitude *(Fig. 6.15a,b)*, with the initial rates of rise times following a fairly stable trend at repeated 100 pM NO exposures *(6.15e,f)*. Comparing the response shape arising to the first and last NO exposure, no marked change was apparent *(Fig. 6.15c,d)*.

Also HEK-GC/$PDE5^{high}$ cells allowed monitoring of reproducible fluorescence changes in response to successive NO challenges *(Fig. 6.16a, b)*. However, a more pronounced change in the shape of the response was observed when comparing the responses to the first and last NO exposures *(Fig. 6.16c,d)*. While the cGMP profile resulting in response to the first NO application comprised a distinct biphasic shape as observed in foregoing experiments *(Fig. 6.16c)*, the response to the last NO exposure appeared to lack the distinct first phase that consisted of a rapid rise and fall *(Fig. 6.16d)*. Overall, the change in the response shape of the HEK-GC/$PDE5^{high}$ cells is consistent with the observations made in forgoing experiments *(Fig. 6.13)*. In the case of the HEK-GC/$PDE5^{high}$ cells a noticeable drop in the initial rising rate of the response occurred upon the first NO challenge, the subsequent response rising rates following a relatively stable trend with repeated 1 nM NO exposures *(6.16e,f)*.

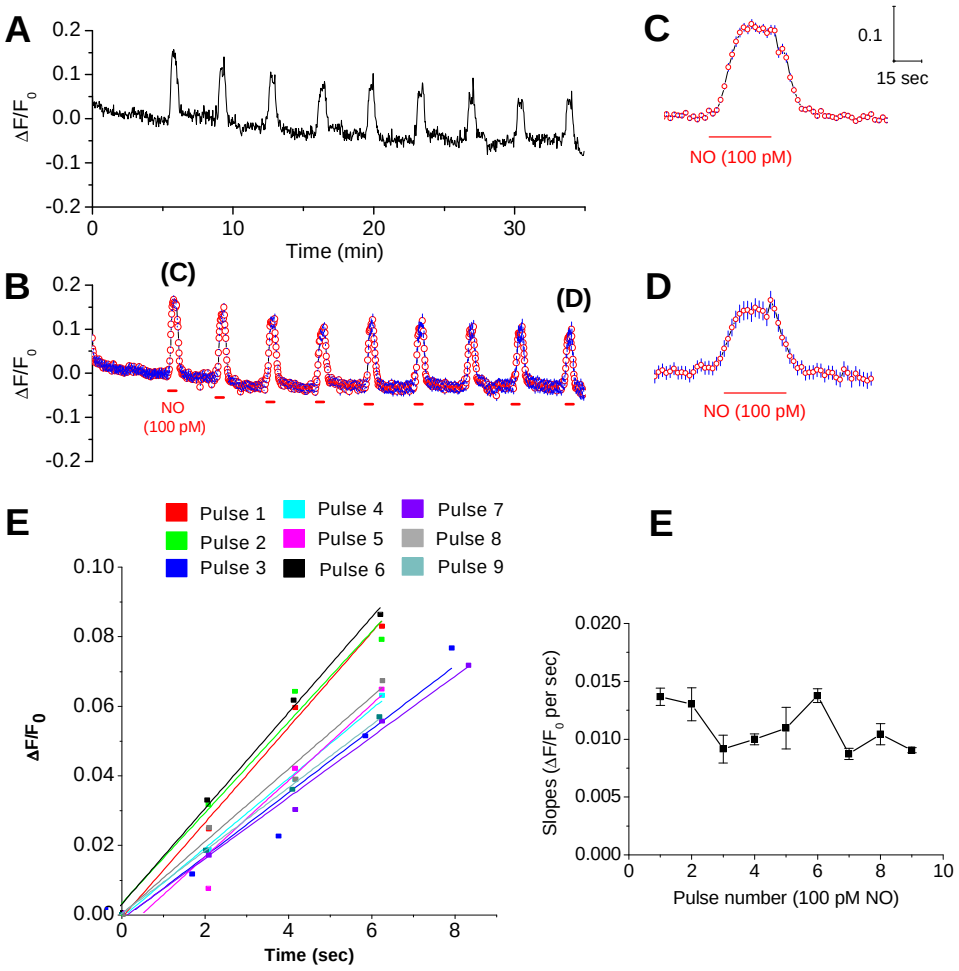

FIG. 6.15 Reproducibility of NO-evoked FlincG responses – HEK-GC/PDE5 cells. *A-B:* Representative trace *(A)* and averaged traces of *n* = 15 *(B)* showing cGMP responses to recurring NO exposures to a submaximal clamped NO concentration, each NO challenge lasting for 30 sec at 2 min intervals. *C-D:* Enlarged traces of responses indicated in panel *B*, showing the response profiles seen upon the first *(C)* and last *(D)* exposures to NO respectively. E-F: Illustrated are the individual mean initial rising phases of the fluorescence changes in response to NO, normalised to zero *(E)*, the slopes of which are plotted in panel *F*. *Note:* Application times of NO are indicated by the horizontal bars. In panels *B-D*, red is mean; blue is ± SEM.

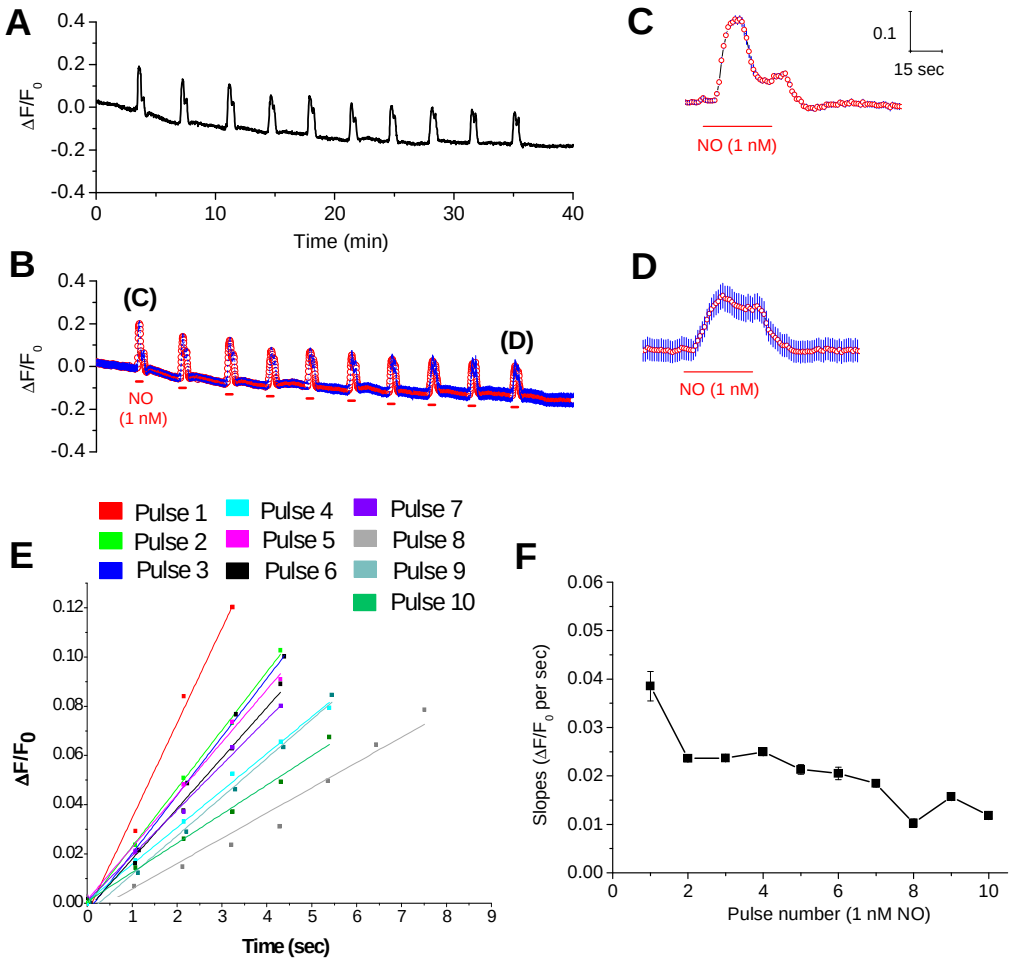

FIG. 6.16 Reproducibility of NO-evoked FlincG responses – HEK-GC/PDE5^{high} cells. *A-B:* Representative trace *(A)* and averaged traces of n = 13 *(B)* showing cGMP responses to recurring NO exposures to a submaximal clamped NO concentration, each NO challenge lasting for 30 sec at 2 min intervals. *C-D:* Enlarged traces of responses indicated in panel *B*, showing the response profiles seen upon the first *(C)* and last *(D)* exposures to NO respectively. *E-F:* Illustrated are the individual mean initial rising phases of the fluorescence changes in response to NO, normalised to zero *(E)*, the slopes of which are plotted in panel *F*. Note the value of the first point in panel *F* dropping, the subsequent points following a relatively stable trend. *Note:* Application times of NO are indicated by the horizontal bars. In panels *B-D*, red is mean; blue is ± SEM.

6.5 DISCUSSION

The present work combined the use of the new cGMP biosensor FlincG (Nausch *et al.*, 2008) and the delivery of known, steady-state (i.e. 'clamped') NO concentrations (Griffiths *et al.*, 2003) to begin to analyse NO transduction in real-time. Alongside a basic characterisation of this approach, the findings in the present work illustrate on a continuous timescale how the interplay between NO_{GC} receptor and PDE activities may serve to generate distinct cellular cGMP profiles.

The first part of the study assessed the methodology. All data obtained provided further evidence that the changes in fluorescence intensity correspond to NO-evoked changes in cGMP. Observations supporting this notion included ODQ-sensitive and concentration-dependent increases in fluorescence intensity upon NO exposure, and ODQ-insensitive FlincG responses upon application of a cGMP analogue. Additionally, prevention of the response decline back to baseline in the presence of a non-selective PDE inhibitor is consistent with the knowledge that the cGMP signal is governed by its rate of synthesis by NO_{GC} receptors and its rate of degradation by PDE (Garthwaite, 2005; Bender & Beavo, 2006; see Chapter 1), indicating the presence of cGMP-hydrolysing PDE(s) in HEK cells.

Buffering of cGMP by FlincG could alter free diffusion of cGMP. If the indicator is relatively immobile, free diffusion of cGMP may be hindered. On the other hand, if the indicator is mobile, diffusion may be enhanced as the indicator may act as a carrier that limits intrinsic binding to cGMP by cell constituents (e.g. PDE and PKG). Thus, high indicator levels may alter the kinetics of the response. This issue was assessed in cells that exhibited the fastest responses with a distinct biphasic shape, and no noticeable changes were found in the response profile among cells of varying brightness (see Fig. 6.4 and Fig. 6.5). The assumption is that the varying brightness of FlincG-transfected cells is related to the amount of FlincG. However, the path length (i.e. cell thickness) and basal cGMP levels could also affect the brightness, where a thick cell would fluoresce more than a thin cell. Also, the path

length may vary if the cell moves imperceptibly on the floor of the coverslip, which can cause apparent changes in cGMP. A solution to ensure a more accurate readout of changes in cGMP would be a ratiometric approach. Characterisation of FlincG (Nausch *et al.*, 2008) revealed that the indicator displays a second excitation peak at 410 nm in addition to the 491 excitation maximum. Therefore, as opposed to previous FRET-based cGMP biosensors, additionally to the advantage of a single wavelength excitation system being employable, the dual excitation spectrum of FlincG offers the possibility to combine the two excitation wavelengths and carry out ratiometric analysis which would cancel out issues of varying dye concentration and path length, and can be used to determine the intracellular cGMP concentration. On the other hand, a ratiometric approach would mean taking two pictures instead of just one for each frame, which may be problematic when investigating very fast signals. Further refinements are plausible. Due to the rate of bath exchange, it is likely that the initial rising rates and falling rates of the responses to NO are underestimates, particularly in the fast-responding HEK cells (i.e. HEK-GC/PDE5 and HEK-GC/PDE5^{high} cells). The assumption that can be made at this stage is that, although the actual concentration of NO in the cells is not at steady-state immediately, the rising and falling phases are likely to be proportional to the NO concentration applied. To avoid delays arising from a perfusion system (e.g. mixing time of compounds entering the chamber), there is the possibility of pressure-applying NO onto a given cell, allowing NO to be applied locally within much shorter intervals and acquiring responses at millisecond-timescales (Batchelor, unpublished). However, this approach may have a number of disadvantages which one would need to correct for, such as variations in the location of the pipette in relation to a given cell and uncertain concentration of NO a given cell is exposed to.

Four different HEK cell lines were chosen to investigate this novel approach of monitoring cGMP signals in real-time in response to known, steady-state NO concentrations. Some of the cell lines permanently expressed only the NO_{GC} receptor, while others permanently expressed the NO_{GC} receptor and PDE5. One proposed

mechanism by which the profile of NO-cGMP signalling may be regulated and is proposed to be the underlying cause of the loss of NO-responsiveness as a result of continued exposure of cells to NO is the gradual loss of mRNA levels of NO_{GC} receptor subunits and protein, which has been demonstrated upon long exposures of cultured rat smooth muscle cells to NO donors and to be cGMP-dependent (Filippov *et al.*, 1997; Scott & Nakayama, 1998). While this mechanism provides long-term regulation, short-term regulation of the sensitivity of the NO-cGMP pathway may be provided by NO_{GC} receptor desensitisation, cGMP-consumption by active PDE, or both, ultimately shaping acute cellular cGMP responses to NO and likely determining the selection of downstream pathways by cGMP (Garthwaite, 2005; Halvey *et al.*, 2009).

'Bell-shaped' responses were recorded in the two HEK cell lines permanently expressing NO_{GC} receptors only, which varied about two orders of magnitude in terms of their sensitivity to NO, indicating different amounts of NO_{GC} receptor. An increase in the initial rate of fluorescence change occurred with increasing NO concentrations, demonstrating faster switch-on of the NO_{GC} receptors at higher NO concentrations, the response decline being most likely governed by PDE-mediated hydrolysis of cGMP as suggested by non-selective PDE inhibition locking the response in a sustained plateau that only returned upon wash out of the PDE inhibitor. The plateau, which was reached within the 1 min NO application, reflects the point at which equilibrium exists between the rate of cGMP synthesis and breakdown. Following exposure to a high (30 nM) NO concentration, the responses to low NO concentrations exhibited a slower initial rising rate. This is likely to be the result of NO_{GC} receptor desensitisation, where it has been demonstrated in rat platelets that NO desensitises its receptor with an EC_{50} of 10-20 nM, the half-time for recovery being 16 min (Halvey *et al.*, 2009). Additionally, the response decline to a low NO concentration following a desensitising NO challenge was observed to be steeper compared to that of the response recorded upon the first application of low NO, indicating switch-on or acceleration of some factor that results in faster break-down of cGMP. One possibility is the switch-on of a cGMP-hydrolysing PDE following

exposure to a high NO concentration, ultimately causing faster decline of the subsequent response evoked by a lower NO concentration as the rate of hydrolysis would outcompete NO_{GC} receptor activity. The contribution of NO_{GC} receptor desensitisation to the shallower initial rise of the response is consistent with estimated cGMP accumulation being reduced by approximately 60% as compared to that in response to low NO before a desensitising NO concentration. Additionally, judging by the shape of the concentration-response curves of initial rising rates, it appears that NO at 10 nM evoked a degree of desensitisation, the initial rising rate to subsequent 30 nM NO being shallower.

In the HEK cell line that exhibited greater NO sensitivity, an increase in fluorescence was detected at NO concentrations as low as 3 pM, a breakthrough in the detection limit of NO-evoked cGMP signals and a validation of FlincG as a superlatively sensitive biosensor. As estimated from the initial rising rates of the responses to different NO concentrations, the environmental NO around the recording chamber was approximately 10 pM. Studies in cerebellar astrocytes suggested that an NO concentration of only 10 pM could theoretically generate enough cGMP (200 nM) to engage targets such as cGMP-dependent protein kinases (PKG; Roy & Garthwaite, 2006). The potential of small amounts of atmospheric NO generated by traffic and industrial combustion to cause cGMP accumulation has been demonstrated previously by studies on NO_{GC} receptors purified from bovine lung, which found 4-10 fold activation of NO_{GC} receptors by NO present in the atmosphere in close proximity to the Berlin inner city circular highway, which was prevented in the presence of an NO scavenger (Friebe *et al.*, 1996a). The sensitivity of NO_{GC} receptors and ensuing cGMP production to NO in polluted air highlights the importance of evaluating carefully the dependence of a given observation on endogenous NO produced within a tissue. The potential effect of environmental NO *in vivo* is implicated by reports that inhaled NO at amounts measured in atmospheric NO (Friebe *et al.*, 1996a) has beneficial consequences in patients suffering from pulmonary hypertension (Rossaint *et al.*, 1993).

In the case of the cells expressing NO_{GC} receptors and PDE5, biphasic responses were recorded, which is consistent with previous work that used a biochemical approach (Mullershausen *et al.*, 2004b). The initial fast rise of the FlincG response, giving rise to the first phase of the response, was followed by a rapid decline of the response while NO was still present. Both the initial rising rates of the responses as well as the onset of response decline were accelerated with ascending NO concentrations. These observations are consistent with activation of PDE5 by cGMP and allosteric enhancement of PDE5 activity by cGMP binding to the enzyme's GAF domain (Rybalkin *et al.*, 2003; Mullershausen *et al.*, 2003) so that PDE5 activity eventually exceeds NO_{GC} receptor activity, causing cGMP levels to fall. Additionally, at a non-desensitising NO concentration (Mo *et al.*, 2004; Halvey *et al.*, 2009) the initial 'spike-like' phase of the response was blunted following repeated NO exposures. This latter observation was indicative of a longer-term negative feedback on NO-evoked cGMP accumulation unlikely to involve receptor desensitisation at the low NO concentrations tested. Consistent with this idea are findings that sustained enhanced PDE5 activity can be initiated by NO via cGMP-PKG-mediated phosphorylation (Mullershausen *et al.*, 2003; Mullershuasen *et al.*, 2004b). It has been demonstrated in the same cell line that cGMP not only directly activates PDE5, therefore enhancing its catalytic activity, but also leads to phosphorylation of PDE5 which renders the enzyme able to bind cGMP with greater affinity and slows the rate at which PDE5 deactivates (Mullershausen *et al.*, 2004b). Additionally, endogenous cyclic nucleotide-activated kinase has been reported to be present in native HEK cells, and an increase in PDE5 phosphorylation under basal conditions and after NO application has been demonstrated in HEK cells over-expressing PKG (Mullershausen *et al.*, 2004b). On the other hand, the present work shows that the response to a low NO concentration following a high desensitising NO concentration was almost lost in cells expressing NO_{GC} receptors and PDE5, which is likely attributable to NO_{GC} receptor desensitisation and PDE5 activity out-competing the rate of cGMP synthesis (Garthwaite, 2005; Halvey *et al.*, 2009). A desensitising component at 10 nM was also evident by the concentration-response profile of the

initial rising rates of the responses of both HEK cell lines expressing both NO_{GC} receptor and PDE5, the initial rising rate of the response evoked by 30 nM being shallower compared to that of 10 nM NO. This range of NO concentration causing NO_{GC} receptor desensitisation is consistent with findings in rat platelets, which found an EC_{50} of 10-20 nM for NO to cause desensitisation (Halvey *et al.*, 2009).

The promising nature of the method characterised in the present study was highlighted by experiments showing reproducible changes in fluorescence intensity in cells permanently expressing both NO_{GC} receptors and PDE5 for up to ten successive, brief (30 sec) exposures to low (non-desensitising) NO concentrations at 2 min intervals. The reproducibility of responses to low NO concentrations was indicated by the initial rising phases of the response to successive NO applications following a relatively stable trend, indicating that no marked desensitisation occurred. However, in the case of the cells expressing higher levels of PDE5 (i.e. HEK-GC/$PDE5^{high}$), blunting of the first ('spike-like') phase of the biphasic response occurred when comparing the first response to the last one, consistent with the idea that there may be a long-term change such as PDE5 phosphorylation occurring as discussed above. This latter observation could also explain the drop in the initial rising rate upon the first NO challenge, which appeared to then continue a relatively stable trend in response to subsequent NO exposures. It may be that cGMP accumulation in response to the first NO application renders PDE5 more active, which stabilises in the course of the following NO challenges.

One surprising finding in the present studies on HEK-GC/PDE5 cell lines was a partly ODQ-insensitive FlincG response recorded upon PDE5 inhibition in the absence of added NO, but in the presence of the NO scavenger CPTIO as well as the broad-spectrum NOS inhibitor L-NNA, which would prevent any endogenous NO production. Part of the response seen upon PDE5 inhibition is likely to depend on basal NO_{GC} receptor activity as indicated by a much shallower gradient of the initial rising phase of the response upon NO_{GC} receptor inhibition as compared to that revealed in the absence of ODQ. On the contrary, no increase in fluorescence was

observed upon PDE inhibition in cells expressing only NO_{GC} receptors. The observation of basal cGMP production that appears to vary among the cell lines investigated suggests a possible flaw of procedure. A possible explanation for results indicating basal cGMP production in one cell line but not another is the rate of acquisition. While cells expressing only NO_{GC} receptor were imaged at 0.2 Hz, cells expressing both NO_{GC} receptors and PDE5 were imaged at 0.5 or 1.0 Hz. A greater speed of acquisition would mean that cells are exposed to more light. A phenomenon of light-induced smooth muscle relaxation, referred to as 'photorelaxation', has been reported (Ehrreich & Furchgott, 1968). The authors deduced that the light-evoked relaxation may be related to NO release, the suspected source being nitrite as indicated by relaxation of non-photosensitive tissue upon nitrite and light exposure. The phenomenon of light-induced relaxation has since been investigated further, aiming to identify and quantify the source that is apparently sensitive to light exposure and leads to NO liberation. More recent reports from studies in rat aorta are in support of S-nitrosothiols and nitrite being a light-sensitive source of NO that is independent of NOS activity (Rodriguez *et al.*, 2003; Batenburg *et al.*, 2009). Reynell and Batchelor in the Garthwaite lab (unpublished) conducted experiments in which cells were exposed to altering intervals of light exposure, finding that increasing the interval reduces the effect on basal cGMP and *vice versa*. Additionally, the NO scavenger CPTIO used in the present study is not very fast acting (Garthwaite, 2008), and the reaction of CPTIO and urate, which is also contained in the extracellular solution, produces nitrite. Hence, based on these latter considerations it is plausible to suggest that build up of nitrite may in fact be the source of NOS-independent, light-evoked basal cGMP production. This possible artefact may have influenced other results obtained in the present work. For example, the existence of basal cGMP levels may lead to a continuous state of PDE5 activation. On the other hand, basal cGMP production may explain the 'undershoot' of the response beyond the initial baseline upon NO removal, observed in cells expressing NO_{GC} receptors and PDE5. A possible explanation may be that the enhanced PDE5 activity brought about by NO-evoked increases in cGMP levels would hydrolyse basal cGMP levels, leading to the

fluorescence intensity reducing below the initial baseline intensity. Eventually, upon subsidence of PDE5 activity, the rate of basal cGMP synthesis may catch up and would reach equilibrium with its rate of hydrolysis, reverting back to the initial baseline. As artefactual, basal cGMP levels may be reduced by altering the extent of light exposure, there is scope for addressing this problem, either technologically or by preventing the build-up of NOS-independent NO sources directly.

As mentioned previously, there was also a marked ODQ-insensitive component of the sildenafil-evoked response. This may be explained by a tonic cGMP level produced by the NO-insensitive, natriuretic peptide-activated guanylyl cyclase. Due to the lack of appropriate pharmacological tools this possibility could not be investigated. Alternatively, mutations of the haem-coordinating his-105 residue of the β_1 subunit of the NO_{GC} receptor were shown to give rise to a guanylyl cyclase species that is NO-insensitive, haem-depleted, and constitutively active under basal conditions (Wedel *et al.*, 1994). The failure to prevent the sildenafil-evoked FlincG response by ODQ indicates that this effect may in fact be due to the presence of a haem-free population of the guanylyl cyclase since inhibition of NO_{GC} receptors by ODQ requires haem oxidation (Schrammel *et al.*, 1996). Therefore, it is plausible to suggest that the presence of a constitutively active, haem-free receptor species may account for the observed sildenafil-evoked effect in the absence of added NO that is insensitive to NO_{GC} receptor inhibition by ODQ.

The physiological relevance of the various NO-evoked FlincG response profiles observed in the expression systems assessed in the present study is indicated by the finding of similar NO-evoked cGMP signals occurring in human platelets and aortic smooth muscle, as deduced from biochemical measurements (Mullershausen *et al.*, 2001). In human platelets, NO has been demonstrated to evoke transient 'spike-like' cGMP responses with the rapid increase in cGMP peaking within approximately 5 sec and declining to almost basal levels in less then 1 min. This resembles very closely the NO-evoked response profiles captured in the HEK-GC/PDE5^{high} cells. On the contrary, responses monitored in HEK-GC/PDE5 cells were more similar to the

situation observed in aortic smooth muscle cells, where NO-evoked cGMP levels were found to approach maximum at *circa* 20-30 sec with a slower and less pronounced decline of cGMP. While PDE5 is the principal PDE isoform in platelets and smooth muscle, PDE2 plays an important role in cGMP hydrolysis in a number of brain regions including the hippocampus, cortex and striatum (van Staveren *et al.*, 2001; Suvarna & O'Donnell, 2002; Wykes *et al.*, 2002; van Staveren *et al.*, 2003). Similar to PDE5, PDE2 also contains regulatory GAF domains (Martins *et al.*, 1982; Martinez *et al.*, 2002; Bender & Beavo, 2006), so it may function similarly to PDE5. The FlincG response profiles recorded in cells expressing only the NO_{GC} receptor on the other hand may be more closely related to the situation in real-time in astrocytes. For example, in cerebellar astrocytes, which possess high levels of NO_{GC} receptors, the combination of rapid NO_{GC} receptor desensitisation and very low PDE activity results in a large increase in cGMP accumulation and a sustained plateau in response to NO, with the shape of the cGMP response being governed overwhelmingly by NO_{GC} receptor desensitisation (Bellamy *et al.*, 2000). These properties may allow astrocytes to respond to very low NO concentrations, possibly derived from the vasculature and/or neurons (Garthwaite, 2008), since to date there is no good evidence for astrocytes themselves synthesising NO.

Although the present study validated the method only on a temporal level, there is great potential to also study spatial dynamics of cGMP signalling by means of this novel approach. Nausch and colleagues (2008) illustrated spatially confined cGMP elevations in cultured aortic smooth muscle cells, recording global cGMP transients in response to NO, but membrane-confined cGMP elevations in response to activation of natriuretic peptide-sensitive guanylyl cyclase. The latter was shown to be transformed into a global signal upon inhibition of PDE5. This new method waits to be characterised at the single neuronal level. A recent study used a FRET-based cGMP biosensor expressed in cultured brain slices by viral-mediated gene transfer (Hepp *et al.*, 2007). The authors revealed a role of PDE2 in the regulation of basal cGMP levels in thalamic neurons, finding tonic NOS activity in these cells. However,

in experiments monitoring stimulated NO_{GC} receptor activity, concentrations of NO were not delivered at known steady-state concentrations, and a very small change in FRET started to occur at 50 nM of DEA/NO, with maximal FRET changes occurring at 50 µM and above, indicating poor sensitivity. Additionally, the readouts were relatively slow so that fast signalling events could not be monitored accurately. Following the characterisation of FlincG in HEK cell lines, a further aim of the present study was to investigate the spatiotemporal profile of cGMP accumulation in response to NO in cultured hippocampal neurons. As discussed in Chapter 5, the results obtained by means of immunohistochemistry provided only a 'snap shot' of the cGMP response. Global cGMP immunolabelling occurred in pyramidal cell somata throughout the different regions of the rat hippocampal formation, as well as in some dendrites and possibly axons (see Chapter 5). However, this result was only obtained by greatly amplifying cGMP accumulation in neurons by means of sensitising NO_{GC} receptors to NO (BAY 41-2272), inhibiting PDE2 (BAY 60-7550) and adding an NO donor. Attempts were made to express the FlincG in cultured hippocampal neurons by means of a Ca^{2+}-phosphate transfection approach (Jiang & Chen, 2006), using FlincG cDNA provided by Wolfgang Dostman and neurons kindly grown and provided by Lily Yu. However, no FlincG expression at all could be obtained in the neurons due to unknown reasons. A promising strategy in the future to express FlincG in neurons may be via Sindbis virus-mediated transfer of FlincG (currently investigated in the Garthwaite lab). Using Sindbis virus-mediated transfer of FlincG, it might be plausible to investigate the site of cGMP accumulation in pyramidal neurons, and to characterise the impact of PDE inhibition, Sindbis virus-mediated gene transfer having been shown to be highly efficient and selective to neurons compared to glial cells (Gwag *et al.*, 1998). Solely based on the histological evidence illustrated in Chapter 5 the neuronal domains of cGMP accumulation remain elusive. Is it localised only in dendrites and/or generally to membranes, or can it accumulate globally within the neuronal soma? If the former were the case, how does inhibition of different PDE isoforms impact on the spread of the cGMP signal from a spatial and temporal point of view? Or to pose the question in another way – at which

NO concentrations (or shapes of NO episodes) are different PDE isoforms recruited to the profiling of the cGMP signal? Unfortunately, due to lack of time, these questions could not be addressed as part of the present thesis.

In conclusion, the present study supports the combined use of δ-FlincG and the 'clamped' delivery method of NO to study fast, repetitive cGMP transients in response to very low NO concentrations. Moreover, the ability to capture distinct changes in cGMP profiles that are based on varying proportions of NO_{GC} receptor and/or PDE activities demonstrates the sensitivity of the method and its applicability in monitoring different cGMP signals in different types of cells, provided that the indicator can be delivered to the cell interior (e.g. astrocytes, neurons). Using this method, it may be possible to study the temporal profiles of events such as NO_{GC} receptor desensitisation, or even the temporal profile of pharmacological tools influencing cGMP signals. For example, it may be a useful tool in the future to assess properties of pharmacological agents acting on the NO_{GC} receptor, such as permeability properties, reversibility, and temporal profile of pharmacological action of the compound. Additionally, this method has the potential of becoming a valuable tool in investigating quantitatively how PDEs hydrolyse cGMP in intact cells, as well as in discerning how different PDE isoforms in a given cell may be contributing to shaping NO-mediated cGMP signals.

*

Reference list

Abudara V, Alvarez AF, Chase MH, Morales FR. Nitric oxide as an anterograde neurotransmitter in the trigeminal motor pool. J Neurophysiol. 2002; 88(1):497-506.

Accili EA, Proenza C, Baruscotti M, DiFrancesco D. From funny current to HCN channels: 20 years of excitation. News Physiol Sci. 2002; 17:32-7.

Ahmad I, Leinders-Zufall T, Kocsis JD, Shepherd GM, Zufall F, Barnstable CJ. Retinal ganglion cells express a cGMP-gated cation conductance activatable by nitric oxide donors. Neuron. 1994; 12(1):155-65.

Alderton WK, Cooper CE, Knowles RG. Nitric oxide synthases: structure, function and inhibition. Biochem J. 2001; 357(Pt 3):593-615.

Andreeva SG, Dikkes P, Epstein PM, Rosenberg PA. Expression of cGMP-specific phosphodiesterase 9A mRNA in the rat brain. J Neurosci. 2001; 21(22):9068-76.

Ang KL, Antoni FA. Reciprocal regulation of calcium dependent and calcium independent cyclic AMP hydrolysis by protein phosphorylation. J Neurochem. 2002; 81(3):422-33.

Antonova I, Arancio O, Trillat AC, Wang HG, Zablow L, Udo H, Kandel ER, Hawkins RD. Rapid increase in clusters of presynaptic proteins at onset of long-lasting potentiation. Science. 2001; 294(5546):1547-50.

Arancio O, Kandel ER, Hawkins RD. Activity-dependent long-term enhancement of transmitter release by presynaptic 3',5'-cyclic GMP in cultured hippocampal neurons. Nature. 1995; 376(6535):74-80.

Arancio O, Kiebler M, Lee CJ, Lev-Ram V, Tsien RY, Kandel ER, Hawkins RD. Nitric oxide acts directly in the presynaptic neuron to produce long-term potentiation in cultured hippocampal neurons. Cell. 1996; 87(6):1025-35.

Arancio O, Antonova I, Gambaryan S, Lohmann SM, Wood JS, Lawrence DS, Hawkins RD. Presynaptic role of cGMP-dependent protein kinase during long-lasting potentiation. J Neurosci. 2001; 21(1):143-9.

Ariano MA, Lewicki JA, Brandwein HJ, Murad F. Immunohistochemical localization of guanylate cyclase within neurons of rat brain. Proc Natl Acad Sci U S A. 1982; 79(4):1316-20.

Arnhold S, Fassbender A, Klinz FJ, Kruttwig K, Löhnig B, Andressen C, Addicks K. NOS-II is involved in early differentiation of murine cortical, retinal and ES cell-derived neurons-an immunocytochemical and functional approach. Int J Dev Neurosci. 2002; 20(2):83-92.

Arnold WP, Mittal CK, Katsuki S, Murad F. Nitric oxide activates guanylate cyclase and increases guanosine 3':5'-cyclic monophosphate levels in various tissue preparations. Proc Natl Acad Sci U S A. 1977; 74(8):3203-7.

Awatramani GB, Price GD, Trussell LO. Modulation of transmitter release by presynaptic resting potential and background calcium levels. Neuron. 2005; 48(1):109-21.

Ayajiki K, Kindermann M, Hecker M, Fleming I, Busse R. Intracellular pH and tyrosine phosphorylation but not calcium determine shear stress-induced nitric oxide production in native endothelial cells. Circ Res. 1996; 78(5):750-8.

Babu BR, Griffith OW. N5-(1-Imino-3-butenyl)-L-ornithine. A neuronal isoform selective mechanism-based inactivator of nitric oxide synthase. J Biol Chem. 1998; 273(15):8882-9.

Baird GS, Zacharias DA, Tsien RY. Circular permutation and receptor insertion within green fluorescent proteins. Proc Natl Acad Sci U S A. 1999; 96(20):11241-6.

Barbuti A, DiFrancesco D. Control of cardiac rate by "funny" channels in health and disease. Ann N Y Acad Sci. 2008; 1123:213-23.

Batenburg WW, Kappers MH, Eikmann MJ, Ramzan SN, de Vries R, Danser AH. Light-induced vs. bradykinin-induced relaxation of coronary arteries: do S-nitrosothiols act as endothelium-derived hyperpolarizing factors? J Hypertens. 2009; 27(8):1631-40.

Becker EM, Alonso-Alija C, Apeler H, Gerzer R, Minuth T, Pleiss U, Schmidt P, Schramm M, Schröder H, Schroeder W, Steinke W, Straub A, Stasch JP. NO-independent regulatory site of direct sGC stimulators like YC-1 and BAY 41-2272. BMC Pharmacol. 2001; 1:13.

Bellamy TC, Wood J, Goodwin DA, Garthwaite J. Rapid desensitization of the nitric oxide receptor, soluble guanylyl cyclase, underlies diversity of cellular cGMP responses. Proc Natl Acad Sci U S A. 2000; 97(6):2928-33.

Bellamy TC, Garthwaite J. Sub-second kinetics of the nitric oxide receptor, soluble guanylyl cyclase, in intact cerebellar cells. J Biol Chem. 2001a; 276(6):4287-92.

Bellamy TC, Garthwaite J. "cAMP-specific" phosphodiesterase contributes to cGMP degradation in cerebellar cells exposed to nitric oxide. Mol Pharmacol. 2001b; 59(1):54-61.

Bellamy TC, Garthwaite J. The receptor-like properties of nitric oxide-activated soluble guanylyl cyclase in intact cells. Mol Cell Biochem. 2002; 230(1-2):165-76.

Bellamy TC, Wood J, Garthwaite J. On the activation of soluble guanylyl cyclase by nitric oxide. Proc Natl Acad Sci U S A. 2002a; 99(1):507-10.

Bellamy TC, Griffiths C, Garthwaite J. Differential sensitivity of guanylyl cyclase and mitochondrial respiration to nitric oxide measured using clamped concentrations. J Biol Chem. 2002b; 277(35):31801-7.

Ben-Ari Y. Developing networks play a similar melody. Trends Neurosci. 2001; 24(6):353-60.

Ben-Ari Y. Excitatory actions of gaba during development: the nature of the nurture. Nat Rev Neurosci. 2002; 3(9):728-39.

Ben-Ari Y, Gaiarsa JL, Tyzio R, Khazipov R. GABA: a pioneer transmitter that excites immature neurons and generates primitive oscillations. Physiol Rev. 2007; 87(4):1215-84.

Bender AT, Beavo JA. Specific localized expression of cGMP PDEs in Purkinje neurons and macrophages. Neurochem Int. 2004; 45(6):853-7.

Bender AT, Beavo JA. Cyclic nucleotide phosphodiesterases: molecular regulation to clinical use. Pharmacol Rev. 2006; 58(3):488-520.

Bicker G. STOP and GO with NO: nitric oxide as a regulator of cell motility in simple brains. Bioessays. 2005; 27(5):495-505.

Bicker G. Pharmacological approaches to nitric oxide signalling during neural development of locusts and other model insects. Arch Insect Biochem Physiol. 2007; 64(1):43-58.

Biel M, Sautter A, Ludwig A, Hofmann F, Zong X. Cyclic nucleotide-gated channels--mediators of NO:cGMP-regulated processes. Naunyn Schmiedebergs Arch Pharmacol. 1998; 358(1):140-4.

Billecke SS, Bender AT, Kanelakis KC, Murphy PJ, Lowe ER, Kamada Y, Pratt WB, Osawa Y. hsp90 is required for heme binding and activation of apo-neuronal nitric-oxide synthase: geldanamycin-

mediated oxidant generation is unrelated to any action of hsp90. J Biol Chem. 2002; 277(23):20504-9.

Billingsley ML, Polli JW, Balaban CD, Kincaid RL. Developmental expression of calmodulin-dependent cyclic nucleotide phosphodiesterase in rat brain. Brain Res Dev Brain Res. 1990; 53(2):253-63.

Blackshaw S, Eliasson MJ, Sawa A, Watkins CC, Krug D, Gupta A, Arai T, Ferrante RJ, Snyder SH. Species, strain and developmental variations in hippocampal neuronal and endothelial nitric oxide synthase clarify discrepancies in nitric oxide-dependent synaptic plasticity. Neuroscience. 2003; 119(4):979-90.

Bliss TV, Lomo T. Long-lasting potentiation of synaptic transmission in the dentate area of the anaesthetized rabbit following stimulation of the perforant path. J Physiol. 1973; 232(2):331-56.

Bliss TV, Collingridge GL. A synaptic model of memory: long-term potentiation in the hippocampus. Nature. 1993; 361(6407):31-9.

Boer R, Ulrich WR, Klein T, Mirau B, Haas S, Baur I. The inhibitory potency and selectivity of arginine substrate site nitric-oxide synthase inhibitors is solely determined by their affinity toward the different isoenzymes. Mol Pharmacol. 2000; 58(5):1026-34.

Boess FG, Hendrix M, van der Staay FJ, Erb C, Schreiber R, van Staveren W, de Vente J, Prickaerts J, Blokland A, Koenig G. Inhibition of phosphodiesterase 2 increases neuronal cGMP, synaptic plasticity and memory performance. Neuropharmacology. 2004; 47(7):1081-92.

Bolton S, Butt AM. The optic nerve: a model for axon-glial interactions. J Pharmacol Toxicol Methods. 2005; 51(3):221-33.

Bon CL, Garthwaite J. Exogenous nitric oxide causes potentiation of hippocampal synaptic transmission during low-frequency stimulation via the endogenous nitric oxide-cGMP pathway. Eur J Neurosci. 2001; 14(4):585-94.

Bon CL, Garthwaite J. On the role of nitric oxide in hippocampal long-term potentiation. J Neurosci. 2003; 23(5):1941-8.

Bönigk W, Altenhofen W, Müller F, Dose A, Illing M, Molday RS, Kaupp UB. Rod and cone photoreceptor cells express distinct genes for cGMP-gated channels. Neuron. 1993; 10(5):865-77.

Boo YC, Sorescu G, Boyd N, Shiojima I, Walsh K, Du J, Jo H. Shear stress stimulates phosphorylation of endothelial nitric-oxide synthase at Ser1179 by Akt-independent mechanisms: role of protein kinase A. J Biol Chem. 2002a; 277(5):3388-96.

Boo YC, Hwang J, Sykes M, Michell BJ, Kemp BE, Lum H, Jo H. Shear stress stimulates phosphorylation of eNOS at Ser(635) by a protein kinase A-dependent mechanism. Am J Physiol Heart Circ Physiol. 2002b; 283(5):H1819-28.

Boo YC, Jo H. Flow-dependent regulation of endothelial nitric oxide synthase: role of protein kinases. Am J Physiol Cell Physiol. 2003; 285(3):C499-508.

Bossu JL, Feltz A, Rodeau JL, Tanzi F. Voltage-dependent transient calcium currents in freshly dissociated capillary endothelial cells. FEBS Lett. 1989; 255(2):377-80.

Boxall AR, Garthwaite J. Long-term depression in rat cerebellum requires both NO synthase and NO-sensitive guanylyl cyclase. Eur J Neurosci. 1996; 8(10):2209-12.

Bradley J, Zhang Y, Bakin R, Lester HA, Ronnett GV, Zinn K. Functional expression of the heteromeric "olfactory" cyclic nucleotide-gated channel in the hippocampus: a potential effector of synaptic plasticity in brain neurons. J Neurosci. 1997; 17(6):1993-2005.

Bredt DS, Snyder SH. Isolation of nitric oxide synthetase, a calmodulin-requiring enzyme. Proc Natl Acad Sci U S A. 1990; 87(2):682-5.

Bredt DS, Hwang PM, Snyder SH. Localization of nitric oxide synthase indicating a neural role for nitric oxide. Nature. 1990; 347(6295):768-70.

Bredt DS, Hwang PM, Glatt CE, Lowenstein C, Reed RR, Snyder SH. Cloned and expressed nitric oxide synthase structurally resembles cytochrome P-450 reductase. Nature. 1991a; 351(6329):714-8.

Bredt DS, Glatt CE, Hwang PM, Fotuhi M, Dawson TM, Snyder SH. Nitric oxide synthase protein and mRNA are discretely localized in neuronal populations of the mammalian CNS together with NADPH diaphorase. Neuron. 1991b; 7(4):615-24.

Brenman JE, Chao DS, Gee SH, McGee AW, Craven SE, Santillano DR, Wu Z, Huang F, Xia H, Peters MF, Froehner SC, Bredt DS. Interaction of nitric oxide synthase with the postsynaptic density protein PSD-95 and alpha1-syntrophin mediated by PDZ domains. Cell. 1996; 84(5):757-67.

Bretscher LE, Li H, Poulos TL, Griffith OW. Structural characterization and kinetics of nitric-oxide synthase inhibition by novel N5-(iminoalkyl)- and N5-(iminoalkenyl)-ornithines. J Biol Chem. 2003; 278(47):46789-97.

Brown GC. Nitric oxide regulates mitochondrial respiration and cell functions by inhibiting cytochrome oxidase. FEBS Lett. 1995; 369(2-3):136-9.

Bucci M, Gratton JP, Rudic RD, Acevedo L, Roviezzo F, Cirino G, Sessa WC. In vivo delivery of the caveolin-1 scaffolding domain inhibits nitric oxide synthesis and reduces inflammation. Nat Med. 2000; 6(12):1362-7.

Burette A, Zabel U, Weinberg RJ, Schmidt HH, Valtschanoff JG. Synaptic localization of nitric oxide synthase and soluble guanylyl cyclase in the hippocampus. J Neurosci. 2002; 22(20):8961-70.

Butt AM, Ransom BR. Morphology of astrocytes and oligodendrocytes during development in the intact rat optic nerve. J Comp Neurol. 1993; 338(1):141-58.

Butt E, Abel K, Krieger M, Palm D, Hoppe V, Hoppe J, Walter U. cAMP- and cGMP-dependent protein kinase phosphorylation sites of the focal adhesion vasodilator-stimulated phosphoprotein (VASP) in vitro and in intact human platelets. J Biol Chem. 1994; 269(20):14509-17.

Butt E, Bernhardt M, Smolenski A, Kotsonis P, Fröhlich LG, Sickmann A, Meyer HE, Lohmann SM, Schmidt HH. Endothelial nitric-oxide synthase (type III) is activated and becomes calcium independent upon phosphorylation by cyclic nucleotide-dependent protein kinases. J Biol Chem. 2000; 275(7):5179-87.

Caiolfa VR, Gill D, Parola AH. Probing the active site of adenosine deaminase by a pH responsive fluorescent competitive inhibitor. Biophys Chem. 1998; 70(1):41-56.

Campbell DS, Regan AG, Lopez JS, Tannahill D, Harris WA, Holt CE. Semaphorin 3A elicits stage-dependent collapse, turning, and branching in Xenopus retinal growth cones. J Neurosci. 2001; 21(21):8538-47.

Campello-Costa P, Fosse AM Jr, Ribeiro JC, Paes-De-Carvalho R, Serfaty CA. Acute blockade of nitric oxide synthesis induces disorganization and amplifies lesion-induced plasticity in the rat retinotectal projection. J Neurobiol. 2000; 44(4):371-81.

Carmeliet P, Tessier-Lavigne M. Common mechanisms of nerve and blood vessel wiring. Nature. 2005; 436(7048):193-200.

Casado M, Isope P, Ascher P. Involvement of presynaptic N-methyl-D-aspartate receptors in cerebellar long-term depression. Neuron. 2002; 33(1):123-30.

Castro LR, Verde I, Cooper DM, Fischmeister R. Cyclic guanosine monophosphate compartmentation in rat cardiac myocytes. Circulation. 2006; 113(18):2221-8.

Catterall WA. Structure and regulation of voltage-gated Ca2+ channels. Annu Rev Cell Dev Biol. 2000; 16:521-55.

Catterall WA, Perez-Reyes E, Snutch TP, Striessnig J. International Union of Pharmacology. XLVIII. Nomenclature and structure-function relationships of voltage-gated calcium channels. Pharmacol Rev. 2005; 57(4):411-25.

Cawley SM, Sawyer CL, Brunelle KF, van der Vliet A, Dostmann WR. Nitric oxide-evoked transient kinetics of cyclic GMP in vascular smooth muscle cells. Cell Signal. 2007; 19(5):1023-33.

Chalimoniuk M, Strosznajder JB. Aging modulates nitric oxide synthesis and cGMP levels in hippocampus and cerebellum. Effects of amyloid beta peptide. Mol Chem Neuropathol. 1998; 35(1-3):77-95.

Chan Y, Fish JE, D'Abreo C, Lin S, Robb GB, Teichert AM, Karantzoulis-Fegaras F, Keightley A, Steer BM, Marsden PA. The cell-specific expression of endothelial nitric-oxide synthase: a role for DNA methylation. J Biol Chem. 2004; 279(33):35087-100.

Chen CC, Lamping KG, Nuno DW, Barresi R, Prouty SJ, Lavoie JL, Cribbs LL, England SK, Sigmund CD, Weiss RM, Williamson RA, Hill JA, Campbell KP. Abnormal coronary function in mice deficient in alpha1H T-type Ca2+ channels. Science. 2003; 302(5649):1416-8.

Chen ZP, Mitchelhill KI, Michell BJ, Stapleton D, Rodriguez-Crespo I, Witters LA, Power DA, Ortiz de Montellano PR, Kemp BE. AMP-activated protein kinase phosphorylation of endothelial NO synthase. FEBS Lett. 1999; 443(3):285-9.

Cheng A, Wang S, Cai J, Rao MS, Mattson MP. Nitric oxide acts in a positive feedback loop with BDNF to regulate neural progenitor cell proliferation and differentiation in the mammalian brain. Dev Biol. 2003; 258(2):319-33.

Chetkovich DM, Klann E, Sweatt JD. Nitric oxide synthase-independent long-term potentiation in area CA1 of hippocampus. Neuroreport. 1993; 4(7):919-22.

Chevaleyre V, Castillo PE. Assessing the role of Ih channels in synaptic transmission and mossy fiber LTP. Proc Natl Acad Sci U S A. 2002; 99(14):9538-43.

Chiang LW, Schweizer FE, Tsien RW, Schulman H. Nitric oxide synthase expression in single hippocampal neurons. Brain Res Mol Brain Res. 1994; 27(1):183-8.

Chien WL, Liang KC, Teng CM, Kuo SC, Lee FY, Fu WM. Enhancement of long-term potentiation by a potent nitric oxide-guanylyl cyclase activator, 3-(5-hydroxymethyl-2-furyl)-1-benzyl-indazole. Mol Pharmacol. 2003; 63(6):1322-8.

Choi OH, Shamim MT, Padgett WL, Daly JW. Caffeine and theophylline analogues: correlation of behavioral effects with activity as adenosine receptor antagonists and as phosphodiesterase inhibitors. Life Sci. 1988; 43(5):387-98.

Christopherson KS, Hillier BJ, Lim WA, Bredt DS. PSD-95 assembles a ternary complex with the N-methyl-D-aspartic acid receptor and a bivalent neuronal NO synthase PDZ domain. J Biol Chem. 1999; 274(39):27467-73.

Chung HJ, Steinberg JP, Huganir RL, Linden DJ. Requirement of AMPA receptor GluR2 phosphorylation for cerebellar long-term depression. Science. 2003; 300(5626):1751-5.

Clapham JC, Wilderspin AF. Cloning of dog heart PDE1A - a first detailed characterization at the molecular level in this species. Gene. 2001; 268(1-2):165-71.

Clapham DE, Runnels LW, Strübing C. The TRP ion channel family. Nat Rev Neurosci. 2001; 2(6):387-96.

Clutton-Brock J. Two cases of poisoning by contamination of nitrous oxide with higher oxides of nitrogen during anaesthesia. Br J Anaesth. 1967; 39(5):388-92.

Cohen CJ, McCarthy RT, Barrett PQ, Rasmussen H. Ca2+ channels in adrenal glomerulosa cells: K+ and angiotensin II increase T-type Ca2+ channel current. Proc Natl Acad Sci U S A. 1988; 85(7):2412-6.

Collingridge GL, Isaac JT, Wang YT. Receptor trafficking and synaptic plasticity. Nat Rev Neurosci. 2004; 5(12):952-62.

Contestabile A. Roles of NMDA receptor activity and nitric oxide production in brain development. Brain Res Brain Res Rev. 2000; 32(2-3):476-509.

Cooper GR, Mialkowski K, Wolff DJ. Cellular and enzymatic studies of N(omega)-propyl-l-arginine and S-ethyl-N-[4-(trifluoromethyl)phenyl]isothiourea as reversible, slowly dissociating inhibitors selective for the neuronal nitric oxide synthase isoform. Arch Biochem Biophys. 2000; 375(1):183-94.

Corbin JD, Turko IV, Beasley A, Francis SH. Phosphorylation of phosphodiesterase-5 by cyclic nucleotide-dependent protein kinase alters its catalytic and allosteric cGMP-binding activities. Eur J Biochem. 2000; 267(9):2760-7.

Corson MA, James NL, Latta SE, Nerem RM, Berk BC, Harrison DG. Phosphorylation of endothelial nitric oxide synthase in response to fluid shear stress. Circ Res. 1996; 79(5):984-91.

Coste H, Grondin P. Characterization of a novel potent and specific inhibitor of type V phosphodiesterase. Biochem Pharmacol. 1995; 50(10):1577-85.

Cowart M, Kowaluk EA, Daanen JF, Kohlhaas KL, Alexander KM, Wagenaar FL, Kerwin JF Jr. Nitroaromatic amino acids as inhibitors of neuronal nitric oxide synthase. J Med Chem. 1998; 41(14):2636-42.

Cramer KS, Angelucci A, Hahm JO, Bogdanov MB, Sur M. A role for nitric oxide in the development of the ferret retinogeniculate projection. J Neurosci. 1996; 16(24):7995-8004.

Craven KB, Zagotta WN. CNG and HCN channels: two peas, one pod. Annu Rev Physiol. 2006; 68:375-401.

Cudeiro J, Rivadulla C, Rodríguez R, Grieve KL, Martínez-Conde S, Acuña C. Actions of compounds manipulating the nitric oxide system in the cat primary visual cortex. J Physiol. 1997; 504 (Pt 2):467-78.

Cumming R, Eccleston D, Steiner A. Immunohistochemical localization of cyclic GMP in rat cerebellum. J Cyclic Nucleotide Res. 1977; 3(4):275-82.

Cumming R, Dickison S, Arbuthnott G. Cyclic nucleotide losses during tissue processing for immunohistochemistry. J Histochem Cytochem. 1980; 28(1):54-5.

Cunha RA, Sebastião AM, Ribeiro JA. Inhibition by ATP of hippocampal synaptic transmission requires localized extracellular catabolism by ecto-nucleotidases into adenosine and channeling to adenosine A1 receptors. J Neurosci. 1998; 18(6):1987-95.

Damann N, Voets T, Nilius B. TRPs in our senses. Curr Biol. 2008; 18(18):R880-9.

Davies SP, Reddy H, Caivano M, Cohen P. Specificity and mechanism of action of some commonly used protein kinase inhibitors. Biochem J. 2000; 351(Pt 1):95-105.

Dedio J, König P, Wohlfart P, Schroeder C, Kummer W, Müller-Esterl W. NOSIP, a novel modulator of endothelial nitric oxide synthase activity. FASEB J. 2001; 15(1):79-89.

Degerman E, Belfrage P, Manganiello VC. Structure, localization, and regulation of cGMP-inhibited phosphodiesterase (PDE3). J Biol Chem. 1997; 272(11):6823-6.

Deguchi T, Yoshioka M. L-Arginine identified as an endogenous activator for soluble guanylate cyclase from neuroblastoma cells. J Biol Chem. 1982; 257(17):10147-51.

Delpiano MA, Altura BM. Modulatory effect of extracellular Mg2+ ions on K+ and Ca2+ currents of capillary endothelial cells from rat brain. FEBS Lett. 1996; 394(3):335-9.

Demas GE, Kriegsfeld LJ, Blackshaw S, Huang P, Gammie SC, Nelson RJ, Snyder SH. Elimination of aggressive behavior in male mice lacking endothelial nitric oxide synthase. J Neurosci. 1999; 19(19):RC30.

Detre JA, Nairn AC, Aswad DW, Greengard P. Localization in mammalian brain of G-substrate, a specific substrate for guanosine 3',5'-cyclic monophosphate-dependent protein kinase. J Neurosci. 1984; 4(11):2843-9.

De Vente J, Steinbusch HW, Schipper J. A new approach to immunocytochemistry of 3',5'-cyclic guanosine monophosphate: preparation, specificity, and initial application of a new antiserum against formaldehyde-fixed 3',5'-cyclic guanosine monophosphate. Neuroscience. 1987; 22(1):361-73.

De Vente J, Bol JG, Hudson L, Schipper J, Steinbusch HW. Atrial natriuretic factor-responding and cyclic guanosine monophosphate (cGMP)-producing cells in the rat hippocampus: a combined micropharmacological and immunocytochemical approach. Brain Res. 1988; 446(2):387-95.

De Vente J, Bol JG, Steinbusch HW. cGMP-Producing, Atrial Natriuretic Factor-Responding Cells in the Rat Brain. Eur J Neurosci. 1989; 1(5):436-460.

De Vente J, Manshanden CG, Sikking RA, Ramaekers FC, Steinbusch HW. A functional parameter to study heterogeneity of glial cells in rat brain slices: cyclic guanosine monophosphate production in atrial natriuretic factor (ANF)-responsive cells. Glia. 1990a; 3(1):43-54.

De Vente J, Bol JG, Berkelmans HS, Schipper J, Steinbusch HM. Immunocytochemistry of cGMP in the Cerebellum of the Immature, Adult, and Aged Rat: the Involvement of Nitric Oxide. A Micropharmacological Study. Eur J Neurosci. 1990b; 2(10):845-862.

De Vente J, Hopkins DA, Markerink-van Ittersum M, Steinbusch HW. Effects of the 3',5'-phosphodiesterase inhibitors isobutylmethylxanthine and zaprinast on NO-mediated cGMP accumulation in the hippocampus slice preparation: an immunocytochemical study. J Chem Neuroanat. 1996; 10(3-4):241-8.

De Vente J, Hopkins DA, Markerink-Van Ittersum M, Emson PC, Schmidt HH, Steinbusch HW. Distribution of nitric oxide synthase and nitric oxide-receptive, cyclic GMP-producing structures in the rat brain. Neuroscience. 1998; 87(1):207-41.

De Vente J, Markerink-van Ittersum M, Axer H, Steinbusch HW. Nitric-oxide-induced cGMP synthesis in cholinergic neurons in the rat brain. Exp Brain Res. 2001a; 136(4):480-91.

De Vente J, Asan E, Gambaryan S, Markerink-van Ittersum M, Axer H, Gallatz K, Lohmann SM, Palkovits M. Localization of cGMP-dependent protein kinase type II in rat brain. Neuroscience. 2001b; 108(1):27-49.

De Vente J, Markerink-van Ittersum M, Vles JS. The role of phosphodiesterase isoforms 2, 5, and 9 in the regulation of NO-dependent and NO-independent cGMP production in the rat cervical spinal cord. J Chem Neuroanat. 2006; 31(4):275-303.

Dhallan RS, Yau KW, Schrader KA, Reed RR. Primary structure and functional expression of a cyclic nucleotide-activated channel from olfactory neurons. Nature. 1990; 347(6289):184-7.

Dierks EA, Burstyn JN. Nitric oxide (NO), the only nitrogen monoxide redox form capable of activating soluble guanylyl cyclase. Biochem Pharmacol. 1996; 51(12):1593-600.

DiFrancesco D, Tortora P. Direct activation of cardiac pacemaker channels by intracellular cyclic AMP. Nature. 1991; 351(6322):145-7.

Dimmeler S, Fleming I, Fisslthaler B, Hermann C, Busse R, Zeiher AM. Activation of nitric oxide synthase in endothelial cells by Akt-dependent phosphorylation. Nature. 1999; 399(6736):601-5.

Dinerman JL, Dawson TM, Schell MJ, Snowman A, Snyder SH. Endothelial nitric oxide synthase localized to hippocampal pyramidal cells: implications for synaptic plasticity. Proc Natl Acad Sci U S A. 1994; 91(10):4214-8.

Ding JD, Burette A, Nedvetsky PI, Schmidt HH, Weinberg RJ. Distribution of soluble guanylyl cyclase in the rat brain. J Comp Neurol. 2004; 472(4):437-48.

Djordjevic S, Driscoll PC. Structural insight into substrate specificity and regulatory mechanisms of phosphoinositide 3-kinases. Trends Biochem Sci. 2002; 27(8):426-32.

Domek-Łopacińska K, van de Waarenburg M, Markerink-van Ittersum M, Steinbusch HW, de Vente J. Nitric oxide-induced cGMP synthesis in the cholinergic system during the development and aging of the rat brain. Brain Res Dev Brain Res. 2005; 158(1-2):72-81.

Donnini S, Ziche M. Constitutive and inducible nitric oxide synthase: role in angiogenesis. Antioxid Redox Signal. 2002; 4(5):817-23.

Doreulee N, Brown RE, Yanovsky Y, Gödecke A, Schrader J, Haas HL. Defective hippocampal mossy fiber long-term potentiation in endothelial nitric oxide synthase knockout mice. Synapse. 2001; 41(3):191-4.

Doreulee N, Sergeeva OA, Yanovsky Y, Chepkova AN, Selbach O, Gödecke A, Schrader J, Haas HL. Cortico-striatal synaptic plasticity in endothelial nitric oxide synthase deficient mice. Brain Res. 2003; 964(1):159-63.

Drab M, Verkade P, Elger M, Kasper M, Lohn M, Lauterbach B, Menne J, Lindschau C, Mende F, Luft FC, Schedl A, Haller H, Kurzchalia TV. Loss of caveolae, vascular dysfunction, and pulmonary defects in caveolin-1 gene-disrupted mice. Science. 2001; 293(5539):2449-52.

Dreyer J, Schleicher M, Tappe A, Schilling K, Kuner T, Kusumawidijaja G, Müller-Esterl W, Oess S, Kuner R. Nitric oxide synthase (NOS)-interacting protein interacts with neuronal NOS and regulates its distribution and activity. J Neurosci. 2004; 24(46):10454-65.

Dudzinski DM, Igarashi J, Greif D, Michel T. The regulation and pharmacology of endothelial nitric oxide synthase. Annu Rev Pharmacol Toxicol. 2006; 46:235-76.

Dulin NO, Niu J, Browning DD, Ye RD, Voyno-Yasenetskaya T. Cyclic AMP-independent activation of protein kinase A by vasoactive peptides. J Biol Chem. 2001; 276(24):20827-30.

Dunwiddie TV, Fredholm BB. Adenosine A1 receptors inhibit adenylate cyclase activity and neurotransmitter release and hyperpolarize pyramidal neurons in rat hippocampus. J Pharmacol Exp Ther. 1989; 249(1):31-7.

East SJ, Garthwaite J. NMDA receptor activation in rat hippocampus induces cyclic GMP formation through the L-arginine-nitric oxide pathway. Neurosci Lett. 1991; 123(1):17-9.

Eissa NT, Strauss AJ, Haggerty CM, Choo EK, Chu SC, Moss J. Alternative splicing of human inducible nitric-oxide synthase mRNA. tissue-specific regulation and induction by cytokines. J Biol Chem. 1996; 271(43):27184-7.

El-Husseini AE, Williams J, Reiner PB, Pelech S, Vincent SR. Localization of the cGMP-dependent protein kinases in relation to nitric oxide synthase in the brain. J Chem Neuroanat. 1999; 17(1):45-55.

Eliasson MJ, Blackshaw S, Schell MJ, Snyder SH. Neuronal nitric oxide synthase alternatively spliced forms: prominent functional localizations in the brain. Proc Natl Acad Sci U S A. 1997; 94(7):3396-401.

Ellerbroek SM, Wennerberg K, Burridge K. Serine phosphorylation negatively regulates RhoA in vivo. J Biol Chem. 2003; 278(21):19023-31.

Endo S, Suzuki M, Sumi M, Nairn AC, Morita R, Yamakawa K, Greengard P, Ito M. Molecular identification of human G-substrate, a possible downstream component of the cGMP-dependent protein kinase cascade in cerebellar Purkinje cells. Proc Natl Acad Sci U S A. 1999; 96(5):2467-72.

Endoh M, Maiese K, Wagner JA. Expression of the neural form of nitric oxide synthase by CA1 hippocampal neurons and other central nervous system neurons. Neuroscience. 1994; 63(3):679-89.

Eng DL, Gordon TR, Kocsis JD, Waxman SG. Current-clamp analysis of a time-dependent rectification in rat optic nerve. J Physiol. 1990; 421:185-202.

Erdal EP, Litzinger EA, Seo J, Zhu Y, Ji H, Silverman RB. Selective neuronal nitric oxide synthase inhibitors. Curr Top Med Chem. 2005; 5(7):603-24.

Ernst AF, Gallo G, Letourneau PC, McLoon SC. Stabilization of growing retinal axons by the combined signaling of nitric oxide and brain-derived neurotrophic factor. J Neurosci. 2000; 20(4):1458-69.

Ehrreich SJ, Furchgott RF. Relaxation of mammalian smooth muscles by visible and ultraviolet radiation. Nature. 1968 May 18;218(5142):682-4.

Fabbro A, Pastore B, Nistri A, Ballerini L. Activity-independent intracellular Ca2+ oscillations are spontaneously generated by ventral spinal neurons during development in vitro. Cell Calcium. 2007; 41(4):317-29.

Faraci FM, Breese KR. Nitric oxide mediates vasodilatation in response to activation of N-methyl-D-aspartate receptors in brain. Circ Res. 1993; 72(2):476-80.

Faraci FM, Brian JE Jr. 7-Nitroindazole inhibits brain nitric oxide synthase and cerebral vasodilatation in response to N-methyl-D-aspartate. Stroke. 1995; 26(11):2172-6.

Feelisch M, Noack EA. Correlation between nitric oxide formation during degradation of organic nitrates and activation of guanylate cyclase. Eur J Pharmacol. 1987; 139(1):19-30.

Feelisch M. Biotransformation to nitric oxide of organic nitrates in comparison to other nitrovasodilators. Eur Heart J. 1993; 14 Suppl I:123-32.

Feelisch M. The use of nitric oxide donors in pharmacological studies. Naunyn Schmiedebergs Arch Pharmacol. 1998; 358(1):113-22.

Feelisch M, Kotsonis P, Siebe J, Clement B, Schmidt HH. The soluble guanylyl cyclase inhibitor 1H-[1,2,4]oxadiazolo[4,3,-a] quinoxalin-1-one is a nonselective heme protein inhibitor of nitric oxide synthase and other cytochrome P-450 enzymes involved in nitric oxide donor bioactivation. Mol Pharmacol. 1999; 56(2):243-53.

Feil R, Hartmann J, Luo C, Wolfsgruber W, Schilling K, Feil S, Barski JJ, Meyer M, Konnerth A, De Zeeuw CI, Hofmann F. Impairment of LTD and cerebellar learning by Purkinje cell-specific ablation of cGMP-dependent protein kinase I. J Cell Biol. 2003; 163(2):295-302.

Feil S, Zimmermann P, Knorn A, Brummer S, Schlossmann J, Hofmann F, Feil R. Distribution of cGMP-dependent protein kinase type I and its isoforms in the mouse brain and retina. Neuroscience. 2005; 135(3):863-8.

Fergus A, Lee KS. Regulation of cerebral microvessels by glutamatergic mechanisms. Brain Res. 1997; 754(1-2):35-45.

Feron O, Belhassen L, Kobzik L, Smith TW, Kelly RA, Michel T. Endothelial nitric oxide synthase targeting to caveolae. Specific interactions with caveolin isoforms in cardiac myocytes and endothelial cells. J Biol Chem. 1996; 271(37):22810-4.

Feron O, Saldana F, Michel JB, Michel T. The endothelial nitric-oxide synthase-caveolin regulatory cycle. J Biol Chem. 1998; 273(6):3125-8.

Ferrendelli JA, Chang MM, Kinscherf DA. Elevation of cyclic GMP levels in central nervous system by excitatory and inhibitory amino acids. J Neurochem. 1974; 22(4):535-40.

Ferrendelli JA, Rubin EH, Kinscherf DA. Influence of divalent cations on regulation of cyclic GMP and cyclic AMP levels in brain tissue. J Neurochem. 1976; 26(4):741-8.

Fesenko EE, Kolesnikov SS, Lyubarsky AL. Induction by cyclic GMP of cationic conductance in plasma membrane of retinal rod outer segment. Nature. 1985; 313(6000):310-3.

Filippov G, Bloch DB, Bloch KD. Nitric oxide decreases stability of mRNAs encoding soluble guanylate cyclase subunits in rat pulmonary artery smooth muscle cells. J Clin Invest. 1997; 100(4):942-8.

Fischmeister R, Castro LR, Abi-Gerges A, Rochais F, Jurevicius J, Leroy J, Vandecasteele G. Compartmentation of cyclic nucleotide signaling in the heart: the role of cyclic nucleotide phosphodiesterases. Circ Res. 2006; 99(8):816-28.

Fleming I, Bauersachs J, Fisslthaler B, Busse R. Ca2+-independent activation of the endothelial nitric oxide synthase in response to tyrosine phosphatase inhibitors and fluid shear stress. Circ Res. 1998; 82(6):686-95.

Fleming I, Fisslthaler B, Dimmeler S, Kemp BE, Busse R. Phosphorylation of Thr(495) regulates Ca(2+)/calmodulin-dependent endothelial nitric oxide synthase activity. Circ Res. 2001; 88(11):E68-75.

Fleming I, Busse R. Molecular mechanisms involved in the regulation of the endothelial nitric oxide synthase. Am J Physiol Regul Integr Comp Physiol. 2003; 284(1):R1-12.

Foerster J, Harteneck C, Malkewitz J, Schultz G, Koesling D. A functional heme-binding site of soluble guanylyl cyclase requires intact N-termini of alpha 1 and beta 1 subunits. Eur J Biochem. 1996; 240(2):380-6.

Ford PC, Wink DA, Stanbury DM. Autoxidation kinetics of aqueous nitric oxide. FEBS Lett. 1993; 326(1-3):1-3.

Forrester J, Peters A. Nerve fibres in optic nerve of rat. Nature. 1967; 214(5085):245-7.

Foster RE, Connors BW, Waxman SG. Rat optic nerve: electrophysiological, pharmacological and anatomical studies during development. Brain Res. 1982; 255(3):371-86.

Fowler JC, Gervitz L, Partridge LD. Hydroxylamine blocks pre- but not postsynaptic adenosine A(1) receptor-mediated actions in rat hippocampus. Brain Res. 1999; 837(1-2):309-13.

Francis SH, Bessay EP, Kotera J, Grimes KA, Liu L, Thompson WJ, Corbin JD. Phosphorylation of isolated human phosphodiesterase-5 regulatory domain induces an apparent conformational change and increases cGMP binding affinity. J Biol Chem. 2002; 277(49):47581-7.

Freichel M, Suh SH, Pfeifer A, Schweig U, Trost C, Weissgerber P, Biel M, Philipp S, Freise D, Droogmans G, Hofmann F, Flockerzi V, Nilius B. Lack of an endothelial store-operated Ca2+ current impairs agonist-dependent vasorelaxation in TRP4-/- mice. Nat Cell Biol. 2001; 3(2):121-7.

Friebe A, Malkewitz J, Schultz G, Koesling D. Positive effects of pollution. Nature. 1996a; 382(6587):120.

Friebe A, Schultz G, Koesling D. Sensitizing soluble guanylyl cyclase to become a highly CO-sensitive enzyme. EMBO J. 1996b; 15(24):6863-8.

Friebe A, Koesling D. Mechanism of YC-1-induced activation of soluble guanylyl cyclase. Mol Pharmacol. 1998; 53(1):123-7.

Friebe A, Müllershausen F, Smolenski A, Walter U, Schultz G, Koesling D. YC-1 potentiates nitric oxide- and carbon monoxide-induced cyclic GMP effects in human platelets. Mol Pharmacol. 1998; 54(6):962-7.

Friebe A, Koesling D. Regulation of nitric oxide-sensitive guanylyl cyclase. Circ Res. 2003; 93(2):96-105.

Fujishige K, Kotera J, Omori K. Striatum- and testis-specific phosphodiesterase PDE10A isolation and characterization of a rat PDE10A. Eur J Biochem. 1999; 266(3):1118-27.

Fulton D, Gratton JP, McCabe TJ, Fontana J, Fujio Y, Walsh K, Franke TF, Papapetropoulos A, Sessa WC. Regulation of endothelium-derived nitric oxide production by the protein kinase Akt. Nature. 1999; 399(6736):597-601.

Fulton D, Gratton JP, Sessa WC. Post-translational control of endothelial nitric oxide synthase: why isn't calcium/calmodulin enough? J Pharmacol Exp Ther. 2001; 299(3):818-24.

Furchgott RF, Zawadzki JV. The obligatory role of endothelial cells in the relaxation of arterial smooth muscle by acetylcholine. Nature. 1980; 288(5789):373-6.

Furchgott RF. Endothelium-derived relaxing factor: discovery, early studies, and identification as nitric oxide. Biosci Rep. 1999; 19(4):235-51.

Furuyama T, Iwahashi Y, Tano Y, Takagi H, Inagaki S. Localization of 63-kDa calmodulin-stimulated phosphodiesterase mRNA in the rat brain by in situ hybridization histochemistry. Brain Res Mol Brain Res.1994; 26(1-2):331-6.

Gallo G, Ernst AF, McLoon SC, Letourneau PC. Transient PKA activity is required for initiation but not maintenance of BDNF-mediated protection from nitric oxide-induced growth-cone collapse. J Neurosci. 2002; 22(12):5016-23.

Gamm DM, Francis SH, Angelotti TP, Corbin JD, Uhler MD. The type II isoform of cGMP-dependent protein kinase is dimeric and possesses regulatory and catalytic properties distinct from the type I isoforms. J Biol Chem. 1995; 270(45):27380-8.

García-Cardeña G, Fan R, Stern DF, Liu J, Sessa WC. Endothelial nitric oxide synthase is regulated by tyrosine phosphorylation and interacts with caveolin-1. J Biol Chem. 1996; 271(44):27237-40.

García-Cardeña G, Martasek P, Masters BS, Skidd PM, Couet J, Li S, Lisanti MP, Sessa WC. Dissecting the interaction between nitric oxide synthase (NOS) and caveolin. Functional significance of the nos caveolin binding domain in vivo. J Biol Chem. 1997; 272(41):25437-40.

García-Cardeña G, Fan R, Shah V, Sorrentino R, Cirino G, Papapetropoulos A, Sessa WC. Dynamic activation of endothelial nitric oxide synthase by Hsp90. Nature. 1998; 392(6678):821-4.

Garthwaite J. Excitatory amino acid receptors and guanosine 3',5'-cyclic monophosphate in incubated slices of immature and adult rat cerebellum. Neuroscience. 1982; 7(10):2491-7.

Garthwaite J. Cellular uptake disguises action of L-glutamate on N-methyl-D-aspartate receptors. With an appendix: diffusion of transported amino acids into brain slices. Br J Pharmacol. 1985; 85(1):297-307.

Garthwaite J, Garthwaite G. Cellular origins of cyclic GMP responses to excitatory amino acid receptor agonists in rat cerebellum in vitro. J Neurochem. 1987; 48(1):29-39.

Garthwaite J, Charles SL, Chess-Williams R. Endothelium-derived relaxing factor release on activation of NMDA receptors suggests role as intercellular messenger in the brain. Nature. 1988; 336(6197):385-8.

Garthwaite J, Garthwaite G, Palmer RM, Moncada S. NMDA receptor activation induces nitric oxide synthesis from arginine in rat brain slices. Eur J Pharmacol. 1989; 172(4-5):413-6.

Garthwaite J. Glutamate, nitric oxide and cell-cell signalling in the nervous system. Trends Neurosci. 1991; 14(2):60-7.

Garthwaite J, Boulton CL. Nitric oxide signaling in the central nervous system. Annu Rev Physiol. 1995; 57:683-706.

Garthwaite J, Southam E, Boulton CL, Nielsen EB, Schmidt K, Mayer B. Potent and selective inhibition of nitric oxide-sensitive guanylyl cyclase by 1H-[1,2,4]oxadiazolo[4,3-a]quinoxalin-1-one. Mol Pharmacol. 1995; 48(2):184-8.

Garthwaite J, Batchelor AM. A biplanar slice preparation for studying cerebellar synaptic transmission. J Neurosci Methods. 1996; 64(2):189-97.

Garthwaite G, Brown G, Batchelor AM, Goodwin DA, Garthwaite J. Mechanisms of ischaemic damage to central white matter axons: a quantitative histological analysis using rat optic nerve. Neuroscience. 1999a; 94(4):1219-30.

Garthwaite G, Goodwin DA, Garthwaite J. Nitric oxide stimulates cGMP formation in rat optic nerve axons, providing a specific marker of axon viability. Eur J Neurosci. 1999b; 11(12):4367-72.

Garthwaite G, Goodwin DA, Batchelor AM, Leeming K, Garthwaite J. Nitric oxide toxicity in CNS white matter: an in vitro study using rat optic nerve. Neuroscience. 2002a; 109(1):145-55.

Garthwaite G, Goodwin DA, Neale S, Riddall D, Garthwaite J. Soluble guanylyl cyclase activator YC-1 protects white matter axons from nitric oxide toxicity and metabolic stress, probably through Na(+) channel inhibition. Mol Pharmacol. 2002b; 61(1):97-104.

Garthwaite J. Dynamics of cellular NO-cGMP signaling. Front Biosci. 2005; 10:1868-80.

Garthwaite G, Bartus K, Malcolm D, Goodwin D, Kollb-Sielecka M, Dooldeniya C, Garthwaite J. Signaling from blood vessels to CNS axons through nitric oxide. J Neurosci. 2006; 26(29):7730-40.

Garthwaite J. Concepts of neural nitric oxide-mediated transmission. Eur J Neurosci. 2008; 27(11):2783-802.

Garvey EP, Oplinger JA, Furfine ES, Kiff RJ, Laszlo F, Whittle BJ, Knowles RG. 1400W is a slow, tight binding, and highly selective inhibitor of inducible nitric-oxide synthase in vitro and in vivo. J Biol Chem. 1997; 272(8):4959-63.

Geiselhöringer A, Gaisa M, Hofmann F, Schlossmann J. Distribution of IRAG and cGKI-isoforms in murine tissues. FEBS Lett. 2004; 575(1-3):19-22.

Ghamari-Langroudi M, Bourque CW. Ionic basis of the caesium-induced depolarisation in rat supraoptic nucleus neurons. J Physiol. 2001; 536(Pt 3):797-808.

Gibb BJ, Garthwaite J. Subunits of the nitric oxide receptor, soluble guanylyl cyclase, expressed in rat brain. Eur J Neurosci. 2001; 13(3):539-44.

Gibb BJ, Wykes V, Garthwaite J. Properties of NO-activated guanylyl cyclases expressed in cells. Br J Pharmacol. 2003; 139(5):1032-40.

Gillespie PG, Beavo JA. Characterization of a bovine cone photoreceptor phosphodiesterase purified by cyclic GMP-sepharose chromatography. J Biol Chem. 1988; 263(17):8133-41.

Giordano D, De Stefano ME, Citro G, Modica A, Giorgi M. Expression of cGMP-binding cGMP-specific phosphodiesterase (PDE5) in mouse tissues and cell lines using an antibody against the enzyme amino-terminal domain. Biochim Biophys Acta. 2001; 1539(1-2):16-27.

Gold ME, Wood KS, Byrns RE, Fukuto J, Ignarro LJ. NG-methyl-L-arginine causes endothelium-dependent contraction and inhibition of cyclic GMP formation in artery and vein. Proc Natl Acad Sci U S A. 1990; 87(12):4430-4.

Gomez TM, Zheng JQ. The molecular basis for calcium-dependent axon pathfinding. Nat Rev Neurosci. 2006; 7(2):115-25.

Grafe P, Quasthoff S, Grosskreutz J, Alzheimer C. Function of the hyperpolarization-activated inward rectification in nonmyelinated peripheral rat and human axons. J Neurophysiol. 1997; 77(1):421-6.

Gratton JP, Fontana J, O'Connor DS, Garcia-Cardena G, McCabe TJ, Sessa WC. Reconstitution of an endothelial nitric-oxide synthase (eNOS), hsp90, and caveolin-1 complex in vitro. Evidence that hsp90 facilitates calmodulin stimulated displacement of eNOS from caveolin-1. J Biol Chem. 2000; 275(29):22268-72.

Green LC, Tannenbaum SR, Goldman P. Nitrate synthesis in the germfree and conventional rat. Science. 1981; 212(4490):56-8.

Green DJ, Maiorana A, O'Driscoll G, Taylor R. Effect of exercise training on endothelium-derived nitric oxide function in humans. J Physiol. 2004; 561(Pt 1):1-25.

Greenberg DA, Jin K. From angiogenesis to neuropathology. Nature. 2005; 438(7070):954-9.

Greene RW, Haas HL. The electrophysiology of adenosine in the mammalian central nervous system. Prog Neurobiol. 1991; 36(4):329-41.

Greka A, Navarro B, Oancea E, Duggan A, Clapham DE. TRPC5 is a regulator of hippocampal neurite length and growth cone morphology. Nat Neurosci. 2003; 6(8):837-45.

Griffiths C, Garthwaite G, Goodwin DA, Garthwaite J. Dynamics of nitric oxide during simulated ischaemia-reperfusion in rat striatal slices measured using an intrinsic biosensor, soluble guanylyl cyclase. Eur J Neurosci. 2002; 15(6):962-8.

Griffiths C, Wykes V, Bellamy TC, Garthwaite J. A new and simple method for delivering clamped nitric oxide concentrations in the physiological range: application to activation of guanylyl cyclase-coupled nitric oxide receptors. Mol Pharmacol. 2003; 64(6):1349-56.

Gruetter CA, Barry BK, McNamara DB, Gruetter DY, Kadowitz PJ, Ignarro L. Relaxation of bovine coronary artery and activation of coronary arterial guanylate cyclase by nitric oxide, nitroprusside and a carcinogenic nitrosoamine. J Cyclic Nucleotide Res. 1979; 5(3):211-24.

Gruetter CA, Gruetter DY, Lyon JE, Kadowitz PJ, Ignarro LJ. Relationship between cyclic guanosine 3':5'-monophosphate formation and relaxation of coronary arterial smooth muscle by glyceryl trinitrate, nitroprusside, nitrite and nitric oxide: effects of methylene blue and methemoglobin. J Pharmacol Exp Ther. 1981; 219(1):181-6.

Gu X, Spitzer NC. Distinct aspects of neuronal differentiation encoded by frequency of spontaneous Ca2+ transients. Nature. 1995; 375(6534):784-7.

Gu X, Spitzer NC. Breaking the code: regulation of neuronal differentiation by spontaneous calcium transients. Dev Neurosci. 1997; 19(1):33-41.

Güler AD, Lee H, Iida T, Shimizu I, Tominaga M, Caterina M. Heat-evoked activation of the ion channel, TRPV4. J Neurosci. 2002; 22(15):6408-14.

Gupta G, Azam M, Yang L, Danziger RS. The beta2 subunit inhibits stimulation of the alpha1/beta1 form of soluble guanylyl cyclase by nitric oxide. Potential relevance to regulation of blood pressure. J Clin Invest. 1997; 100(6):1488-92.

Gwag BJ, Kim EY, Ryu BR, Won SJ, Ko HW, Oh YJ, Cho YG, Ha SJ, Sung YC. A neuron-specific gene transfer by a recombinant defective Sindbis virus. Brain Res Mol Brain Res. 1998 Dec

10;63(1):53-61.

Hagen TJ, Bergmanis AA, Kramer SW, Fok KF, Schmelzer AE, Pitzele BS, Swenton L, Jerome GM, Kornmeier CM, Moore WM, Branson LF, Connor JR, Manning PT, Currie MG, Hallinan EA. 2-Iminopyrrolidines as potent and selective inhibitors of human inducible nitric oxide synthase. J Med Chem. 1998; 41(19):3675-83.

Haghikia A, Mergia E, Friebe A, Eysel UT, Koesling D, Mittmann T. Long-term potentiation in the visual cortex requires both nitric oxide receptor guanylyl cyclases. J Neurosci. 2007; 27(4):818-23.

Hagiwara N, Irisawa H, Kameyama M. Contribution of two types of calcium currents to the pacemaker potentials of rabbit sino-atrial node cells. J Physiol. 1988; 395:233-53.

Halaszovich CR, Zitt C, Jungling E, Luckhoff A. Inhibition of TRP3 channels by lanthanides. Block from the cytosolic side of the plasma membrane. J Biol Chem. 2000; 275(48):37423-8.

Hall CN, Garthwaite J. Inactivation of nitric oxide by rat cerebellar slices. J Physiol. 2006; 577(Pt 2):549-67.

Hall CN, Keynes RG, Garthwaite J. Cytochrome P450 oxidoreductase participates in nitric oxide consumption by rat brain. Biochem J. 2009; 419(2):411-8.

Hall CN, Garthwaite J. What is the real physiological NO concentration in vivo? Nitric Oxide. 2009; 21(2):92-103.

Hall KU, Collins SP, Gamm DM, Massa E, DePaoli-Roach AA, Uhler MD. Phosphorylation-dependent inhibition of protein phosphatase-1 by G-substrate. A Purkinje cell substrate of the cyclic GMP-dependent protein kinase. J Biol Chem. 1999; 274(6):3485-95.

Halvey EJ, Vernon J, Roy B, Garthwaite J. Mechanisms of activity-dependent plasticity in cellular no-cGMP signaling. J Biol Chem. 2009 [Epub ahead of print]

Han NL, Ye JS, Yu AC, Sheu FS. Differential mechanisms underlying the modulation of delayed-rectifier K+ channel in mouse neocortical neurons by nitric oxide. J Neurophysiol. 2006; 95(4):2167-78.

Harris MB, Ju H, Venema VJ, Liang H, Zou R, Michell BJ, Chen ZP, Kemp BE, Venema RC. Reciprocal phosphorylation and regulation of endothelial nitric-oxide synthase in response to bradykinin stimulation. J Biol Chem. 2001 May; 276(19):16587-91.

Harris NC, Constanti A. Mechanism of block by ZD 7288 of the hyperpolarization-activated inward rectifying current in guinea pig substantia nigra neurons in vitro. J Neurophysiol. 1995; 74(6):2366-78.

Hartell NA. cGMP acts within cerebellar Purkinje cells to produce long term depression via mechanisms involving PKC and PKG. Neuroreport. 1994; 5(7):833-6.

Harteneck C, Koesling D, Söling A, Schultz G, Böhme E. Expression of soluble guanylyl cyclase. Catalytic activity requires two enzyme subunits. FEBS Lett. 1990; 272(1-2):221-3.

Hashimoto Y, Sharma RK, Soderling TR. Regulation of Ca2+/calmodulin-dependent cyclic nucleotide phosphodiesterase by the autophosphorylated form of Ca2+/calmodulin-dependent protein kinase II. J Biol Chem. 1989; 264(18):10884-7.

Haug LS, Jensen V, Hvalby O, Walaas SI, Ostvold AC. Phosphorylation of the inositol 1,4,5-trisphosphate receptor by cyclic nucleotide-dependent kinases in vitro and in rat cerebellar slices in situ. J Biol Chem. 1999; 274(11):7467-73.

Haul S, Gödecke A, Schrader J, Haas HL, Luhmann HJ. Impairment of neocortical long-term potentiation in mice deficient of endothelial nitric oxide synthase. J Neurophysiol. 1999; 81(2):494-7.

Hauser W, Knobeloch KP, Eigenthaler M, Gambaryan S, Krenn V, Geiger J, Glazova M, Rohde E, Horak I, Walter U, Zimmer M. Megakaryocyte hyperplasia and enhanced agonist-induced platelet activation in vasodilator-stimulated phosphoprotein knockout mice. Proc Natl Acad Sci U S A. 1999; 96(14):8120-5.

Hayashi Y, Nishio M, Naito Y, Yokokura H, Nimura Y, Hidaka H, Watanabe Y. Regulation of neuronal nitric-oxide synthase by calmodulin kinases. J Biol Chem. 1999; 274(29):20597-602.

He Y, Yu W, Baas PW. Microtubule reconfiguration during axonal retraction induced by nitric oxide. J Neurosci. 2002; 22(14):5982-91.

Hegesh E, Shiloah J. Blood nitrates and infantile methemoglobinemia. Clin Chim Acta. 1982; 125(2):107-15.

Heginbotham L, Abramson T, MacKinnon R. A functional connection between the pores of distantly related ion channels as revealed by mutant K+ channels. Science. 1992; 258(5085):1152-5.

Hepp R, Tricoire L, Hu E, Gervasi N, Paupardin-Tritsch D, Lambolez B, Vincent P. Phosphodiesterase type 2 and the homeostasis of cyclic GMP in living thalamic neurons. J Neurochem. 2007; 102(6):1875-86.

Hibbs JB Jr, Vavrin Z, Taintor RR. L-arginine is required for expression of the activated macrophage effector mechanism causing selective metabolic inhibition in target cells. J Immunol. 1987; 138(2):550-65.

Hibbs JB Jr, Taintor RR, Vavrin Z, Rachlin EM. Nitric oxide: a cytotoxic activated macrophage effector molecule. Biochem Biophys Res Commun. 1988; 157(1):87-94.

Hinds HL, Goussakov I, Nakazawa K, Tonegawa S, Bolshakov VY. Essential function of alpha-calcium/calmodulin-dependent protein kinase II in neurotransmitter release at a glutamatergic central synapse. Proc Natl Acad Sci U S A. 2003; 100(7):4275-80.

Hogg N. The biochemistry and physiology of S-nitrosothiols. Annu Rev Pharmacol Toxicol. 2002; 42:585-600.

Honda A, Adams SR, Sawyer CL, Lev-Ram V, Tsien RY, Dostmann WR. Spatiotemporal dynamics of guanosine 3',5'-cyclic monophosphate revealed by a genetically encoded, fluorescent indicator. Proc Natl Acad Sci U S A. 2001; 98(5):2437-42.

Hopper R, Lancaster B, Garthwaite J. On the regulation of NMDA receptors by nitric oxide. Eur J Neurosci. 2004; 19(7):1675-82.

Hopper RA, Garthwaite J. Tonic and phasic nitric oxide signals in hippocampal long-term potentiation. J Neurosci. 2006; 26(45):11513-21.

Huang CC, Chan SH, Hsu KS. cGMP/protein kinase G-dependent potentiation of glutamatergic transmission induced by nitric oxide in immature rat rostral ventrolateral medulla neurons in vitro. Mol Pharmacol 2003; 64:521-532.

Huang PL, Dawson TM, Bredt DS, Snyder SH, Fishman MC. Targeted disruption of the neuronal nitric oxide synthase gene. Cell. 1993; 75(7):1273-86.

Huang PL, Huang Z, Mashimo H, Bloch KD, Moskowitz MA, Bevan JA, Fishman MC. Hypertension in mice lacking the gene for endothelial nitric oxide synthase. Nature. 1995; 377(6546):239-42.

Hughes SW, Cope DW, Tóth TI, Williams SR, Crunelli V. All thalamocortical neurones possess a T-type Ca2+ 'window' current that enables the expression of bistability-mediated activities. J Physiol. 1999; 517 (Pt 3):805-15.

Hurt KJ, Musicki B, Palese MA, Crone JK, Becker RE, Moriarity JL, Snyder SH, Burnett AL. Akt-dependent phosphorylation of endothelial nitric-oxide synthase mediates penile erection. Proc Natl Acad Sci U S A. 2002; 99(6):4061-6.

Iadecola C, Zhang F, Xu S, Casey R, Ross ME. Inducible nitric oxide synthase gene expression in brain following cerebral ischemia. J Cereb Blood Flow Metab. 1995; 15(3):378-84.

Iadecola C, Zhang F, Casey R, Clark HB, Ross ME. Inducible nitric oxide synthase gene expression in vascular cells after transient focal cerebral ischemia. Stroke. 1996; 27(8):1373-80.

Iftinca MC, Zamponi GW. Regulation of neuronal T-type calcium channels. Trends Pharmacol Sci. 2009; 30(1):32-40.

Ignarro LJ, Lippton H, Edwards JC, Baricos WH, Hyman AL, Kadowitz PJ, Gruetter CA. Mechanism of vascular smooth muscle relaxation by organic nitrates, nitrites, nitroprusside and nitric oxide: evidence for the involvement of S-nitrosothiols as active intermediates. J Pharmacol Exp Ther. 1981; 218(3):739-49.

Ignarro LJ, Byrns RE, Buga GM, Wood KS. Endothelium-derived relaxing factor from pulmonary artery and vein possesses pharmacologic and chemical properties identical to those of nitric oxide radical. Circ Res. 1987a; 61(6):866-79.

Ignarro LJ, Buga GM, Wood KS, Byrns RE, Chaudhuri G. Endothelium-derived relaxing factor produced and released from artery and vein is nitric oxide. Proc Natl Acad Sci U S A. 1987b; 84(24):9265-9

Ingram SL, Williams JT. Modulation of the hyperpolarization-activated current (Ih) by cyclic nucleotides in guinea-pig primary afferent neurons. J Physiol. 1996; 492 (Pt 1):97-106.

Ito M. Cerebellar long-term depression: characterization, signal transduction, and functional roles. Physiol Rev. 2001; 81(3):1143-95.

Jaffrey SR, Benfenati F, Snowman AM, Czernik AJ, Snyder SH. Neuronal nitric-oxide synthase localization mediated by a ternary complex with synapsin and CAPON. Proc Natl Acad Sci U S A. 2002; 99(5):3199-204.

Jiang M, Chen G. High Ca2+-phosphate transfection efficiency in low-densitiy neuronal cultures. Nature Protocols. 2006; 1(2):695-700.

Johnson D, Sato S, Quarles RH, Inuzuka T, Brady RO, Tourtellotte WW. Quantitation of the myelin-associated glycoprotein in human nervous tissue from controls and multiple sclerosis patients. J Neurochem. 1986; 46(4):1086-93.

Jones SW. Calcium channels: unanswered questions. J Bioenerg Biomembr. 2003; 35(6):461-75.

Ju H, Zou R, Venema VJ, Venema RC. Direct interaction of endothelial nitric-oxide synthase and caveolin-1 inhibits synthase activity. J Biol Chem. 1997; 272(30):18522-5.

Ju H, Venema VJ, Marrero MB, Venema RC. Inhibitory interactions of the bradykinin B2 receptor with endothelial nitric-oxide synthase. J Biol Chem. 1998; 273(37):24025-9.

Kang Y, Dempo Y, Ohashi A, Saito M, Toyoda H, Sato H, Koshino H, Maeda Y, Hirai T. Nitric oxide activates leak K+ currents in the presumed cholinergic neuron of basal forebrain. 2007; 98(6):3397-410.

Kantor DB, Lanzrein M, Stary SJ, Sandoval GM, Smith WB, Sullivan BM, Davidson N, Schuman EM. A role for endothelial NO synthase in LTP revealed by adenovirus-mediated inhibition and rescue. Science. 1996; 274(5293):1744-8.

Kara P, Friedlander MJ. Arginine analogs modify signal detection by neurons in the visual cortex. J Neurosci. 1999; 19(13):5528-48.

Katsuki S, Arnold W, Mittal C, Murad F. Stimulation of guanylate cyclase by sodium nitroprusside, nitroglycerin and nitric oxide in various tissue preparations and comparison to the effects of sodium azide and hydroxylamine. J Cyclic Nucleotide Res. 1977; 3(1):23-35.

Kaupp UB, Niidome T, Tanabe T, Terada S, Bönigk W, Stühmer W, Cook NJ, Kangawa K, Matsuo H, Hirose T, Miyata T, Numa S. Primary structure and functional expression from complementary DNA of the rod photoreceptor cyclic GMP-gated channel. Nature. 1989; 342(6251):762-6.

Kaupp UB, Seifert R. Cyclic nucleotide-gated ion channels. Physiol Rev. 2002; 82(3):769-824.

Kazerounian S, Pitari GM, Ruiz-Stewart I, Schulz S, Waldman SA. Nitric oxide activation of soluble guanylyl cyclase reveals high and low affinity sites that mediate allosteric inhibition by calcium. Biochemistry. 2002; 41(10):3396-404.

Keefer LK, Nims RW, Davies KM, Wink DA. "NONOates" (1-Substituted Diazen-1-ium-1,2-diolates) as Nitric Oxide Donors: Convenient Nitric oxide Dosage Forms. Meth. Enzymol. 1996; 268:281-293.

Keilhoff G, Seidel B, Noack H, Tischmeyer W, Stanek D, Wolf G. Patterns of nitric oxide synthase at the messenger RNA and protein levels during early rat brain development. Neuroscience. 1996; 75(4):1193-201.

Kerchner GA, Nicoll RA. Silent synapses and the emergence of a postsynaptic mechanism for LTP. Nat Rev Neurosci. 2008; 9(11):813-25.

Keynes RG, Duport S, Garthwaite J. Hippocampal neurons in organotypic slice culture are highly resistant to damage by endogenous and exogenous nitric oxide. Eur J Neurosci. 2004; 19(5):1163-73.

Kharitonov VG, Russwurm M, Magde D, Sharma VS, Koesling D. Dissociation of nitric oxide from soluble guanylate cyclase. Biochem Biophys Res Commun. 1997; 239(1):284-6.

Khazipov R, Khalilov I, Tyzio R, Morozova E, Ben-Ari Y, Holmes GL. Developmental changes in GABAergic actions and seizure susceptibility in the rat hippocampus. Eur J Neurosci. 2004; 19(3):590-600.

Kim HY, Kim SJ, Kim J, Oh SB, Cho H, Jung SJ. Effect of nitric oxide on hyperpolarization-activated current in substantia gelatinosa neurons of rats. Biochem Biophys Res Commun. 2005; 338(3):1648-53.

Kimura H, Mittal CK, Murad F. Increases in cyclic GMP levels in brain and liver with sodium azide an activator of guanylate cyclase. Nature. 1975; 257(5528):700-2.

Kincaid RL, Stith-Coleman IE, Vaughan M. Proteolytic activation of calmodulin-dependent cyclic nucleotide phosphodiesterase. J Biol Chem. 1985 Jul 25;260(15):9009-15.

Kingston PA, Zufall F, Barnstable CJ. Rat hippocampal neurons express genes for both rod retinal and olfactory cyclic nucleotide-gated channels: novel targets for cAMP/cGMP function. Proc Natl Acad Sci U S A. 1996; 93(19):10440-5.

Kingston PA, Zufall F, Barnstable CJ. Widespread expression of olfactory cyclic nucleotide-gated channel genes in rat brain: implications for neuronal signalling. Synapse. 1999; 32(1):1-12.

Kleppisch T, Wolfsgruber W, Feil S, Allmann R, Wotjak CT, Goebbels S, Nave KA, Hofmann F, Feil R. Hippocampal cGMP-dependent protein kinase I supports an age- and protein synthesis-dependent component of long-term potentiation but is not essential for spatial reference and contextual memory. J Neurosci. 2003; 23(14):6005-12.

Klyachko VA, Ahern GP, Jackson MB. cGMP-mediated facilitation in nerve terminals by enhancement of the spike afterhyperpolarization. Neuron. 2001; 31(6):1015-25.

Ko GY, Kelly PT. Nitric oxide acts as a postsynaptic signaling molecule in calcium/calmodulin-induced synaptic potentiation in hippocampal CA1 pyramidal neurons. J Neurosci. 1999; 19(16):6784-94.

Koesling D. Studying the structure and regulation of soluble guanylyl cyclase. Methods. 1999; 19(4):485-93.

Koppenol WH. NO nomenclature? Nitric Oxide. 2002; 6(1):96-8.

Kornau HC, Schenker LT, Kennedy MB, Seeburg PH. Domain interaction between NMDA receptor subunits and the postsynaptic density protein PSD-95. Science. 1995; 269(5231):1737-40.

Kotera J, Yanaka N, Fujishige K, Imai Y, Akatsuka H, Ishizuka T, Kawashima K, Omori K. Expression of rat cGMP-binding cGMP-specific phosphodiesterase mRNA in Purkinje cell layers during postnatal neuronal development. Eur J Biochem. 1997; 249(2):434-42.

Kotera J, Fujishige K, Omori K. Immunohistochemical localization of cGMP-binding cGMP-specific phosphodiesterase (PDE5) in rat tissues. J Histochem Cytochem. 2000; 48(5):685-93.

Kuchan MJ, Frangos JA. Role of calcium and calmodulin in flow-induced nitric oxide production in endothelial cells. Am J Physiol. 1994; 266(3 Pt 1):C628-36.

Kuzmiski JB, MacVicar BA. Cyclic nucleotide-gated channels contribute to the cholinergic plateau potential in hippocampal CA1 pyramidal neurons. J Neurosci. 2001; 21(22):8707-14.

Kwan HY, Huang Y, Yao X. TRP channels in endothelial function and dysfunction. Biochim Biophys Acta. 2007; 1772(8):907-14.

Langnaese K, Richter K, Smalla KH, Krauss M, Thomas U, Wolf G, Laube G. Splice-isoform specific immunolocalization of neuronal nitric oxide synthase in mouse and rat brain reveals that the PDZ-complex-building nNOSalpha beta-finger is largely exposed to antibodies. Dev Neurobiol. 2007; 67(4):422-37.

Launey T, Endo S, Sakai R, Harano J, Ito M. Protein phosphatase 2A inhibition induces cerebellar long-term depression and declustering of synaptic AMPA receptor. Proc Natl Acad Sci U S A. 2004; 101(2):676-81.

Leamey CA, Ho-Pao CL, Sur M. Disruption of retinogeniculate pattern formation by inhibition of soluble guanylyl cyclase. J Neurosci. 2001; 21(11):3871-80.

Lein ES, Hawrylycz MJ, Ao N, Ayres M, Bensinger A, Bernard A, et al. Genome-wide atlas of gene expression in the adult mouse brain. Nature. 2007; 445(7124):168-76.

Leinders-Zufall T, Zufall F. Block of cyclic nucleotide-gated channels in salamander olfactory receptor neurons by the guanylyl cyclase inhibitor LY83583. J Neurophysiol. 1995; 74(6):2759-62.

Leinders-Zufall T, Rosenboom H, Barnstable CJ, Shepherd GM, Zufall F. A calcium-permeable cGMP-activated cation conductance in hippocampal neurons. Neuroreport. 1995; 6(13):1761-5.

Leppanen L, Stys PK. Ion transport and membrane potential in CNS myelinated axons I. Normoxic conditions. J Neurophysiol. 1997; 78(4):2086-94.

Leung YM, Kwan CY. Current perspectives in the pharmacological studies of store-operated Ca2+ entry blockers. Jpn J Pharmacol. 1999; 81(3):253-8.

Lev-Ram V, Jiang T, Wood J, Lawrence DS, Tsien RY. Synergies and coincidence requirements between NO, cGMP, and Ca2+ in the induction of cerebellar long-term depression. Neuron. 1997; 18(6):1025-38.

Li Y, Jia YC, Cui K, Li N, Zheng ZY, Wang YZ, Yuan XB. Essential role of TRPC channels in the guidance of nerve growth cones by brain-derived neurotrophic factor. Nature. 2005; 434(7035):894-8.

Li DP, Chen SR, Pan HL. Nitric oxide inhibits spinally projecting paraventricular neurons through potentiation of presynaptic GABA release. J Neurophysiol. 2002; 88(5):2664-74.

Li DP, Chen SR, Finnegan TF, Pan HL. Signalling pathway of nitric oxide in synaptic GABA release in the rat paraventricular nucleus. J Physiol. 2004; 554(Pt 1):100-10.

Lin LH, Taktakishvili O, Talman WT. Identification and localization of cell types that express endothelial and neuronal nitric oxide synthase in the rat nucleus tractus solitarii. Brain Res. 2007; 1171:42-51.

Lipton SA, Choi YB, Takahashi H, Zhang D, Li W, Godzik A, Bankston LA. Cysteine regulation of protein function--as exemplified by NMDA-receptor modulation. Trends Neurosci. 2002; 25(9):474-80.

Lohmann SM, Vaandrager AB, Smolenski A, Walter U, De Jonge HR. Distinct and specific functions of cGMP-dependent protein kinases. Trends Biochem Sci. 1997; 22(8):307-12.

Lu YF, Kandel ER, Hawkins RD. Nitric oxide signaling contributes to late-phase LTP and CREB phosphorylation in the hippocampus. J Neurosci. 1999; 19(23):10250-61.

Lu YF, Hawkins RD. Ryanodine receptors contribute to cGMP-induced late-phase LTP and CREB phosphorylation in the hippocampus. J Neurophysiol. 2002; 88(3):1270-8.

Ludvig N, Burmeister V, Jobe PC, Kincaid RL. Electron microscopic immunocytochemical evidence that the calmodulin-dependent cyclic nucleotide phosphodiesterase is localized predominantly at postsynaptic sites in the rat brain. Neuroscience. 1991; 44(2):491-500.

Ludwig A, Zong X, Jeglitsch M, Hofmann F, Biel M. A family of hyperpolarization-activated mammalian cation channels. Nature. 1998; 393(6685):587-91.

Lumme A, Soinila S, Sadeniemi M, Halonen T, Vanhatalo S. Nitric oxide synthase immunoreactivity in the rat hippocampus after status epilepticus induced by perforant pathway stimulation. Brain Res. 2000; 871(2):303-10.

Luo D, Das S, Vincent SR. Effects of methylene blue and LY83583 on neuronal nitric oxide synthase and NADPH-diaphorase. Eur J Pharmacol. 1995; 290(3):247-51.

MacMicking J, Xie QW, Nathan C. Nitric oxide and macrophage function. Annu Rev Immunol. 1997; 15:323-50.

Manganiello VC, Degerman E. Cyclic nucleotide phosphodiesterases (PDEs): diverse regulators of cyclic nucleotide signals and inviting molecular targets for novel therapeutic agents. Thromb Haemost. 1999; 82(2):407-11.

Maragos CM, Morley D, Wink DA, Dunams TM, Saavedra JE, Hoffman A, Bove AA, Isaac L, Hrabie JA, Keefer LK. Complexes of .NO with nucleophiles as agents for the controlled biological release of nitric oxide. Vasorelaxant effects. J Med Chem. 1991; 34(11):3242-7.

Markerink-Van Ittersum M, Steinbusch HW, De Vente J. Region-specific developmental patterns of atrial natriuretic factor- and nitric oxide-activated guanylyl cyclases in the postnatal frontal rat brain. Neuroscience. 1997; 78(2):571-87.

Marrero MB, Venema VJ, Ju H, He H, Liang H, Caldwell RB, Venema RC. Endothelial nitric oxide synthase interactions with G-protein-coupled receptors. Biochem J. 1999; 343 Pt 2:335-40.

Martin E, Berka V, Bogatenkova E, Murad F, Tsai AL. Ligand selectivity of soluble guanylyl cyclase: effect of the hydrogen-bonding tyrosine in the distal heme pocket on binding of oxygen, nitric oxide, and carbon monoxide. J Biol Chem. 2006; 281(38):27836-45.

Martin DL. Synthesis and release of neuroactive substances by glial cells. Glia. 1992; 5(2):81-94.

Martin W, Villani GM, Jothianandan D, Furchgott RF. Selective blockade of endothelium-dependent and glyceryl trinitrate-induced relaxation by hemoglobin and by methylene blue in the rabbit aorta. J Pharmacol Exp Ther. 1985a; 232(3):708-16.

Martin W, Villani GM, Jothianandan D, Furchgott RF. Blockade of endothelium-dependent and glyceryl trinitrate-induced relaxation of rabbit aorta by certain ferrous hemoproteins. J Pharmacol Exp Ther. 1985b; 233(3):679-85.

Martinez SE, Beavo JA, Hol WG. GAF domains: two-billion-year-old molecular switches that bind cyclic nucleotides. Mol Interv. 2002; 2(5):317-23.

Martins TJ, Mumby MC, Beavo JA. Purification and characterization of a cyclic GMP-stimulated cyclic nucleotide phosphodiesterase from bovine tissues. J Biol Chem. 1982; 257(4):1973-9.

Matarredona ER, Murillo-Carretero M, Moreno-López B, Estrada C. Nitric oxide synthesis inhibition increases proliferation of neural precursors isolated from the postnatal mouse subventricular zone. Brain Res. 2004; 995(2):274-84.

Matsuoka I, Giuili G, Poyard M, Stengel D, Parma J, Guellaen G, Hanoune J. Localization of adenylyl and guanylyl cyclase in rat brain by in situ hybridization: comparison with calmodulin mRNA distribution. J Neurosci. 1992; 12(9):3350-60.

Matulef K, Zagotta WN. Cyclic nucleotide-gated ion channels. Annu Rev Cell Dev Biol. 2003; 19:23-44.

Mayer B, Klatt P, Böhme E, Schmidt K. Regulation of neuronal nitric oxide and cyclic GMP formation by Ca2+. J Neurochem. 1992; 59(6):2024-9.

Mayer B, Brunner F, Schmidt K. Inhibition of nitric oxide synthesis by methylene blue. Biochem Pharmacol. 1993; 45(2):367-74.

Mayer B, Koesling D. cGMP signalling beyond nitric oxide. Trends Pharmacol Sci. 2001; 22(11):546-8.

Maynard KI, Yanez P, Ogilvy CS. Nitric oxide modulates light-evoked compound action potentials in the intact rabbit retina. Neuroreport. 1995;6(6):850-2.

McCormick DA, Bal T. Sleep and arousal: thalamocortical mechanisms. Annu Rev Neurosci. 1997; 20:185-215.

McKay BE, McRory JE, Molineux ML, Hamid J, Snutch TP, Zamponi GW, Turner RW. Ca(V)3 T-type calcium channel isoforms differentially distribute to somatic and dendritic compartments in rat central neurons. Eur J Neurosci. 2006; 24(9):2581-94.

Meier S, Bräuer AU, Heimrich B, Nitsch R, Savaskan NE. Myelination in the hippocampus during development and following lesion. Cell Mol Life Sci. 2004; 61(9):1082-94.

Menniti FS, Faraci WS, Schmidt CJ. Phosphodiesterases in the CNS: targets for drug development. Nat Rev Drug Discov. 2006; 5(8):660-70.

Ment LR, Stewart WB, Fronc R, Seashore C, Mahooti S, Scaramuzzino D, Madri JA. Vascular endothelial growth factor mediates reactive angiogenesis in the postnatal developing brain. Brain Res Dev Brain Res. 1997; 100(1):52-61.

Mergia E, Russwurm M, Zoidl G, Koesling D. Major occurrence of the new alpha2beta1 isoform of NO-sensitive guanylyl cyclase in brain. Cell Signal. 2003; 15(2):189-95.

Mergia E, Friebe A, Dangel O, Russwurm M, Koesling D. Spare guanylyl cyclase NO receptors ensure high NO sensitivity in the vascular system. J Clin Invest. 2006; 116(6):1731-7.

Michel JB, Feron O, Sase K, Prabhakar P, Michel T. Caveolin versus calmodulin. Counterbalancing allosteric modulators of endothelial nitric oxide synthase. J Biol Chem. 1997; 272(41):25907-12.

Michel T, Feron O. Nitric oxide synthases: which, where, how, and why? J Clin Invest. 1997; 100(9):2146-52.

Michell BJ, Griffiths JE, Mitchelhill KI, Rodriguez-Crespo I, Tiganis T, Bozinovski S, de Montellano PR, Kemp BE, Pearson RB. The Akt kinase signals directly to endothelial nitric oxide synthase. Curr Biol. 1999; 9(15):845-8.

Michell BJ, Harris MB, Chen ZP, Ju H, Venema VJ, Blackstone MA, Huang W, Venema RC, Kemp BE. Identification of regulatory sites of phosphorylation of the bovine endothelial nitric-oxide synthase at serine 617 and serine 635. J Biol Chem. 2002; 277(44):42344-51.

Micheva KD, Holz RW, Smith SJ. Regulation of presynaptic phosphatidylinositol 4,5-biphosphate by neuronal activity. J Cell Biol. 2001; 154(2):355-68.

Micheva KD, Buchanan J, Holz RW, Smith SJ. Retrograde regulation of synaptic vesicle endocytosis and recycling. Nat Neurosci. 2003; 6(9):925-32.

Miller MR, Megson IL. Recent developments in nitric oxide donor drugs. Br J Pharmacol. 2007; 151(3):305-21.

Milligan CJ, Edwards IJ, Deuchars J. HCN1 ion channel immunoreactivity in spinal cord and medulla oblongata. Brain Res. 2006; 1081(1):79-91.

Mironov SL, Langohr K. Modulation of synaptic and channel activities in the respiratory network of the mice by NO/cGMP signalling pathways. Brain Res. 2007; 1130(1):73-82.

Mitchell D, Tyml K. Nitric oxide release in rat skeletal muscle capillary. Am J Physiol. 1996; 270(5 Pt 2):H1696-703.

Mitchell JB, Lupica CR, Dunwiddie TV. Activity-dependent release of endogenous adenosine modulates synaptic responses in the rat hippocampus. J Neurosci. 1993; 13(8):3439-47.

Mizuhashi S, Nishiyama N, Matsuki N, Ikegaya Y. Cyclic nucleotide-mediated regulation of hippocampal mossy fiber development: a target-specific guidance. J Neurosci. 2001; 21(16):6181-94.

Mo E, Amin H, Bianco IH, Garthwaite J. Kinetics of a cellular nitric oxide/cGMP/phosphodiesterase-5 pathway. J Biol Chem. 2004; 279(25):26149-58.

Moore PK, al-Swayeh OA, Chong NW, Evans RA, Gibson A. L-NG-nitro arginine (L-NOARG), a novel, L-arginine-reversible inhibitor of endothelium-dependent vasodilatation in vitro. Br J Pharmacol. 1990; 99(2):408-12.

Moosmang S, Biel M, Hofmann F, Ludwig A. Differential distribution of four hyperpolarization-activated cation channels in mouse brain. Biol Chem. 1999; 380(7-8):975-80.

Moosmang S, Stieber J, Zong X, Biel M, Hofmann F, Ludwig A. Cellular expression and functional characterization of four hyperpolarization-activated pacemaker channels in cardiac and neuronal tissues. Eur J Biochem. 2001; 268(6):1646-52.

Moran MM, Xu H, Clapham DE. TRP ion channels in the nervous system. Curr Opin Neurobiol. 2004; 14(3):362-9.

Moreno-López B, Noval JA, González-Bonet LG, Estrada C. Morphological bases for a role of nitric oxide in adult neurogenesis. Brain Res. 2000; 869(1-2):244-50.

Moreno-López B, Romero-Grimaldi C, Noval JA, Murillo-Carretero M, Matarredona ER, Estrada C. Nitric oxide is a physiological inhibitor of neurogenesis in the adult mouse subventricular zone and olfactory bulb. J Neurosci. 2004; 24(1):85-95.

Morley D, Keefer LK. Nitric oxide/nucleophile complexes: a unique class of nitric oxide-based vasodilators. J Cardiovasc Pharmacol. 1993; 22 Suppl 7:S3-9.

Moro MA, De Alba J, Leza JC, Lorenzo P, Fernández AP, Bentura ML, Boscá L, Rodrigo J, Lizasoain I. Neuronal expression of inducible nitric oxide synthase after oxygen and glucose deprivation in rat forebrain slices. Eur J Neurosci. 1998; 10(2):445-56.

Morris R, Southam E, Gittins SR, de Vente J, Garthwaite J. The NO-cGMP pathway in neonatal rat dorsal horn. Eur J Neurosci. 1994; 6(5):876-9.

Mount PF, Kemp BE, Power DA. Regulation of endothelial and myocardial NO synthesis by multi-site eNOS phosphorylation. J Mol Cell Cardiol. 2007; 42(2):271-9.

Mullen RJ, Buck CR, Smith AM. NeuN, a neuronal specific nuclear protein in vertebrates. Development. 1992; 116(1):201-11.

Mullershausen F, Russwurm M, Thompson WJ, Liu L, Koesling D, Friebe A. Rapid nitric oxide-induced desensitization of the cGMP response is caused by increased activity of phosphodiesterase type 5 paralleled by phosphorylation of the enzyme. J Cell Biol. 2001; 155(2):271-8.

Mullershausen F, Friebe A, Feil R, Thompson WJ, Hofmann F, Koesling D. Direct activation of PDE5 by cGMP: long-term effects within NO/cGMP signaling. J Cell Biol. 2003; 160(5):719-27.

Mullershausen F, Russwurm M, Friebe A, Koesling D. Inhibition of phosphodiesterase type 5 by the activator of nitric oxide-sensitive guanylyl cyclase BAY 41-2272. Circulation. 2004a; 109(14):1711-3.

Mullershausen F, Russwurm M, Koesling D, Friebe A. In vivo reconstitution of the negative feedback in nitric oxide/cGMP signaling: role of phosphodiesterase type 5 phosphorylation. Mol Biol Cell. 2004b; 15(9):4023-30.

Muradov H, Boyd KK, Artemyev NO. Structural determinants of the PDE6 GAF A domain for binding the inhibitory gamma-subunit and noncatalytic cGMP. Vision Res. 2004; 44(21):2437-44.

Murthy KS. Modulation of soluble guanylate cyclase activity by phosphorylation. Neurochem Int. 2004; 45(6):845-51.

Nader K, Hardt O. A single standard for memory: the case for reconsolidation. Nat Rev Neurosci. 2009; 10(3):224-34.

Nakai J, Ohkura M, Imoto K. A high signal-to-noise Ca(2+) probe composed of a single green fluorescent protein. Nat Biotechnol. 2001; 19(2):137-41.

Nakane M, Ichikawa M, Deguchi T. Light and electron microscopic demonstration of guanylate cyclase in rat brain. Brain Res. 1983; 273(1):9-15.

Nakane M, Klinghofer V, Kuk JE, Donnelly JL, Budzik GP, Pollock JS, Basha F, Carter GW. Novel potent and selective inhibitors of inducible nitric oxide synthase. Mol Pharmacol. 1995; 47(4):831-4.

Nausch LW, Ledoux J, Bonev AD, Nelson MT, Dostmann WR. Differential patterning of cGMP in vascular smooth muscle cells revealed by single GFP-linked biosensors. Proc Natl Acad Sci U S A. 2008; 105(1):365-70.

Nedvetsky PI, Kleinschnitz C, Schmidt HH. Regional distribution of protein and activity of the nitric oxide receptor, soluble guanylyl cyclase, in rat brain suggests multiple mechanisms of regulation. Brain Res. 2002; 950(1-2):148-54.

Nett WJ, Oloff SH, McCarthy KD. Hippocampal astrocytes in situ exhibit calcium oscillations that occur independent of neuronal activity. J Neurophysiol. 2002; 87(1):528-37.

Neves G, Cooke SF, Bliss TV. Synaptic plasticity, memory and the hippocampus: a neural network approach to causality. Nat Rev Neurosci. 2008; 9(1):65-75.

Newcomb R, Szoke B, Palma A, Wang G, Chen X, Hopkins W, Cong R, Miller J, Urge L, Tarczy-Hornoch K, Loo JA, Dooley DJ, Nadasdi L, Tsien RW, Lemos J, Miljanich G. Selective peptide antagonist of the class E calcium channel from the venom of the tarantula Hysterocrates gigas. Biochemistry. 1998; 37(44):15353-62.

Nikolaev VO, Gambaryan S, Lohse MJ. Fluorescent sensors for rapid monitoring of intracellular cGMP. Nat Methods. 2006; 3(1):23-5.

Nikonenko I, Boda B, Steen S, Knott G, Welker E, Muller D. PSD-95 promotes synaptogenesis and multiinnervated spine formation through nitric oxide signaling. J Cell Biol. 2008; 183(6):1115-27.

Nilius B, Hess P, Lansman JB, Tsien RW. A novel type of cardiac calcium channel in ventricular cells. Nature. 1985; 316(6027):443-6.

Nilius B, Watanabe H, Vriens J. The TRPV4 channel: structure-function relationship and promiscuous gating behaviour. Pflugers Arch. 2003; 446(3):298-303.

Ninan I, Arancio O. Presynaptic CaMKII is necessary for synaptic plasticity in cultured hippocampal neurons. Neuron. 2004; 42(1):129-41.

Notomi T, Shigemoto R. Immunohistochemical localization of Ih channel subunits, HCN1-4, in the rat brain. J Comp Neurol. 2004; 471(3):241-76.

O'Connor V, Genin A, Davis S, Karishma KK, Doyère V, De Zeeuw CI, Sanger G, Hunt SP, Richter-Levin G, Mallet J, Laroche S, Bliss TV, French PJ. Differential amplification of intron-containing transcripts reveals long term potentiation-associated up-regulation of specific Pde10A phosphodiesterase splice variants. J Biol Chem. 2004; 279(16):15841-9.

O'Dell TJ, Hawkins RD, Kandel ER, Arancio O. Tests of the roles of two diffusible substances in long-term potentiation: evidence for nitric oxide as a possible early retrograde messenger. Proc Natl Acad Sci U S A. 1991; 88(24):11285-9.

Ogura T, Yokoyama T, Fujisawa H, Kurashima Y, Esumi H. Structural diversity of neuronal nitric oxide synthase mRNA in the nervous system. Biochem Biophys Res Commun. 1993; 193(3):1014-22.

Packer MA, Stasiv Y, Benraiss A, Chmielnicki E, Grinberg A, Westphal H, Goldman SA, Enikolopov G. Nitric oxide negatively regulates mammalian adult neurogenesis. Proc Natl Acad Sci U S A. 2003; 100(16):9566-71.

Palmer RM, Ferrige AG, Moncada S. Nitric oxide release accounts for the biological activity of endothelium-derived relaxing factor. Nature. 1987; 327(6122):524-6.

Panda K, Ghosh S, Stuehr DJ. Calmodulin activates intersubunit electron transfer in the neuronal nitric-oxide synthase dimmer. J Biol Chem. 2001; 276(26):23349-56.

Papapetropoulos A, García-Cardeña G, Madri JA, Sessa WC. Nitric oxide production contributes to the angiogenic properties of vascular endothelial growth factor in human endothelial cells. J Clin Invest. 1997; 100(12):3131-9.

Pape HC, Mager R. Nitric oxide controls oscillatory activity in thalamocortical neurons. Neuron. 1992; 9(3):441-8.

Pape HC. Queer current and pacemaker: the hyperpolarization-activated cation current in neurons. Annu Rev Physiol. 1996; 58:299-327.

Parent A, Schrader K, Munger SD, Reed RR, Linden DJ, Ronnett GV. Synaptic transmission and hippocampal long-term potentiation in olfactory cyclic nucleotide-gated channel type 1 null mouse. J Neurophysiol. 1998; 79(6):3295-301.

Park C, Sohn Y, Shin KS, Kim J, Ahn H, Huh Y. The chronic inhibition of nitric oxide synthase enhances cell proliferation in the adult rat hippocampus. Neurosci Lett. 2003; 339(1):9-12.

Parri HR, Gould TM, Crunelli V. Spontaneous astrocytic Ca2+ oscillations in situ drive NMDAR-mediated neuronal excitation. Nat Neurosci. 2001; 4(8):803-12.

Pawlik G, Rackl A, Bing RJ. Quantitative capillary topography and blood flow in the cerebral cortex of cats: an in vivo microscopic study. Brain Res. 1981; 208(1):35-58.

Pedersen SF, Owsianik G, Nilius B. TRP channels: an overview. Cell Calcium. 2005; 38(3-4):233-52.

Pelligrino DA, Wang Q. Cyclic nucleotide crosstalk and the regulation of cerebral vasodilation. Prog Neurobiol. 1998; 56(1):1-18.

Peng C, Rich ED, Varnum MD. Subunit configuration of heteromeric cone cyclic nucleotide-gated channels. Neuron. 2004; 42(3):401-10.

Perez-Reyes E. Molecular physiology of low-voltage-activated t-type calcium channels. Physiol Rev. 2003; 83(1):117-61.

Pian P, Bucchi A, Robinson RB, Siegelbaum SA. Regulation of gating and rundown of HCN hyperpolarization-activated channels by exogenous and endogenous PIP2. J Gen Physiol. 2006; 128(5):593-604.

Piggott LA, Hassell KA, Berkova Z, Morris AP, Silberbach M, Rich TC. Natriuretic peptides and nitric oxide stimulate cGMP synthesis in different cellular compartments. J Gen Physiol. 2006; 128(1):3-14.

Pilz RB, Broderick KE. Role of cyclic GMP in gene regulation. Front Biosci. 2005; 10:1239-68.

Pinilla PJ, Hernández AT, Camello MC, Pozo MJ, Toescu EC, Camello PJ. Non-stimulated Ca2+ leak pathway in cerebellar granule neurones. Biochem Pharmacol. 2005; 70(5):786-93.

Plate KH. Mechanisms of angiogenesis in the brain. J Neuropathol Exp Neurol. 1999; 58(4):313-20.

Podda MV, Marcocci ME, Oggiano L, D'Ascenzo M, Tolu E, Palamara AT, Azzena GB, Grassi C. Nitric oxide increases the spontaneous firing rate of rat medial vestibular nucleus neurons in vitro via a cyclic GMP-mediated PKG-independent mechanism. Eur J Neurosci. 2004; 20(8):2124-32.

Podda MV, D'Ascenzo M, Leone L, Piacentini R, Azzena GB, Grassi C. Functional role of cyclic nucleotide-gated channels in rat medial vestibular nucleus neurons. J Physiol. 2008; 586(3):803-15.

Polleux F, Morrow T, Ghosh A. Semaphorin 3A is a chemoattractant for cortical apical dendrites. Nature. 2000; 404(6778):567-73.

Pose I, Sampogna S, Chase MH, Morales FR. Mesencephalic trigeminal neurons are innervated by nitric oxide synthase-containing fibers and respond to nitric oxide. Brain Res. 2003; 960(1-2):81-9.

Prado GN, Taylor L, Zhou X, Ricupero D, Mierke DF, Polgar P. Mechanisms regulating the expression, self-maintenance, and signaling-function of the bradykinin B2 and B1 receptors. J Cell Physiol. 2002; 193(3):275-86.

Prast H, Philippu A. Nitric oxide as modulator of neuronal function. Prog Neurobiol. 2001; 64(1):51-68.

Proenza C, Tran N, Angoli D, Zahynacz K, Balcar P, Accili EA. Different roles for the cyclic nucleotide binding domain and amino terminus in assembly and expression of hyperpolarization-activated, cyclic nucleotide-gated channels. J Biol Chem. 2002; 277(33):29634-42.

Puzzo D, Vitolo O, Trinchese F, Jacob JP, Palmeri A, Arancio O. Amyloid-beta peptide inhibits activation of the nitric oxide/cGMP/cAMP-responsive element-binding protein pathway during hippocampal synaptic plasticity. J Neurosci. 2005; 25(29):6887-97.

Rall TW, Lehne RA. Evidence for cross-linking of cyclic AMP to constituents of brain tissue by aldehyde fixatives: potential utility in histochemical procedures. J Cyclic Nucleotide Res. 1982; 8(4):243-65.

Rameau GA, Chiu LY, Ziff EB. Bidirectional regulation of neuronal nitric-oxide synthase phosphorylation at serine 847 by the N-methyl-D-aspartate receptor. J Biol Chem. 2004; 279(14):14307-14.

Rameau GA, Tukey DS, Garcin-Hosfield ED, Titcombe RF, Misra C, Khatri L, Getzoff ED, Ziff EB Biphasic coupling of neuronal nitric oxide synthase phosphorylation to the NMDA receptor regulates AMPA receptor trafficking and neuronal cell death. J Neurosci. 2007; 27(13):3445-55.

Rapoport RM, Murad F. Agonist-induced endothelium-dependent relaxation in rat thoracic aorta may be mediated through cGMP. Circ Res. 1983; 52(3):352-7.

Rapoport RM, Draznin MB, Murad F. Endothelium-dependent relaxation in rat aorta may be mediated through cyclic GMP-dependent protein phosphorylation. Nature. 1983; 306(5939):174-6.

Reed TM, Repaske DR, Snyder GL, Greengard P, Vorhees CV. Phosphodiesterase 1B knock-out mice exhibit exaggerated locomotor hyperactivity and DARPP-32 phosphorylation in response to dopamine agonists and display impaired spatial learning. J Neurosci. 2002; 22(12):5188-97.

Reinhardt RR, Bondy CA. Differential cellular pattern of gene expression for two distinct cGMP-inhibited cyclic nucleotide phosphodiesterases in developing and mature rat brain. Neuroscience. 1996; 72(2):567-78.

Repaske DR, Corbin JG, Conti M, Goy MF. A cyclic GMP-stimulated cyclic nucleotide phosphodiesterase gene is highly expressed in the limbic system of the rat brain. Neuroscience. 1993; 56(3):673-86.

Robello M, Amico C, Bucossi G, Cupello A, Rapallino MV, Thellung S. Nitric oxide and GABAA receptor function in the rat cerebral cortex and cerebellar granule cells. Neuroscience. 1996; 74(1):99-105.

Robinson RB, Siegelbaum SA. Hyperpolarization-activated cation currents: from molecules to physiological function. Annu Rev Physiol. 2003; 65:453-80.

Rodrigo J, Springall DR, Uttenthal O, Bentura ML, Abadia-Molina F, Riveros-Moreno V, Martínez-Murillo R, Polak JM, Moncada S. Localization of nitric oxide synthase in the adult rat brain. Philos Trans R Soc Lond B Biol Sci. 1994; 345(1312):175-221.

Rodriguez J, Maloney RE, Rassaf T, Bryan NS, Feelisch M. Chemical nature of nitric oxide storage forms in rat vascular tissue. Proc Natl Acad Sci U S A. 2003; 100(1):336-41.

Rodríguez-Crespo I, Straub W, Gavilanes F, Ortiz de Montellano PR. Binding of dynein light chain (PIN) to neuronal nitric oxide synthase in the absence of inhibition. Arch Biochem Biophys. 1998; 359(2):297-304.

Rosenbaum T, Gordon SE. Quickening the pace: looking into the heart of HCN channels. Neuron. 2004; 42(2):193-6.

Rossaint R, Falke KJ, López F, Slama K, Pison U, Zapol WM. Inhaled nitric oxide for the adult respiratory distress syndrome. N Engl J Med. 1993; 328(6):399-405.

Roy B, Garthwaite J. Nitric oxide activation of guanylyl cyclase in cells revisited. Proc Natl Acad Sci U S A. 2006; 103(32):12185-90.

Roy B, Halvey EJ, Garthwaite J. An enzyme-linked receptor mechanism for nitric oxide-activated guanylyl cyclase. J Biol Chem. 2008; 283(27):18841-51.

Ruiz-Stewart I, Tiyyagura SR, Lin JE, Kazerounian S, Pitari GM, Schulz S, Martin E, Murad F, Waldman SA. Guanylyl cyclase is an ATP sensor coupling nitric oxide signaling to cell metabolism. Proc Natl Acad Sci U S A. 2004; 101(1):37-42.

Russell KS, Haynes MP, Caulin-Glaser T, Rosneck J, Sessa WC, Bender JR. Estrogen stimulates heat shock protein 90 binding to endothelial nitric oxide synthase in human vascular endothelial cells. Effects on calcium sensitivity and NO release. J Biol Chem. 2000; 275(7):5026-30.

Russwurm M, Wittau N, Koesling D. Guanylyl cyclase/PSD-95 interaction: targeting of the nitric oxide-sensitive alpha2beta1 guanylyl cyclase to synaptic membranes. J Biol Chem. 2001; 276(48):44647-52.

Russwurm M, Koesling D. Isoforms of NO-sensitive guanylyl cyclase. Mol Cell Biochem. 2002; 230(1-2):159-64.

Russwurm M, Mullershausen F, Friebe A, Jäger R, Russwurm C, Koesling D. Design of fluorescence resonance energy transfer (FRET)-based cGMP indicators: a systematic approach. Biochem J. 2007; 407(1):69-77.

Rutten K, Vente JD, Sik A, Ittersum MM, Prickaerts J, Blokland A. The selective PDE5 inhibitor, sildenafil, improves object memory in Swiss mice and increases cGMP levels in hippocampal slices. Behav Brain Res. 2005; 164(1):11-6.

Rutten K, Prickaerts J, Hendrix M, van der Staay FJ, Sik A, Blokland A. Time-dependent involvement of cAMP and cGMP in consolidation of object memory: studies using selective phosphodiesterase type 2, 4 and 5 inhibitors. Eur J Pharmacol. 2007; 558(1-3):107-12.

Rybalkin SD, Rybalkina IG, Shimizu-Albergine M, Tang XB, Beavo JA. PDE5 is converted to an activated state upon cGMP binding to the GAF A domain. EMBO J. 2003; 22(3):469-78.

Saavedra JM. Regulation of atrial natriuretic peptide receptors in the rat brain. Cell Mol Neurobiol. 1987; 7(2):151-73.

Sable CL, Filippa N, Hemmings B, Van Obberghen E. cAMP stimulates protein kinase B in a Wortmannin-insensitive manner. FEBS Lett. 1997; 409(2):253-7.

Sadhu K, Hensley K, Florio VA, Wolda SL. Differential expression of the cyclic GMP-stimulated phosphodiesterase PDE2A in human venous and capillary endothelial cells. J Histochem Cytochem. 1999; 47(7):895-906.

Salerno JC, Harris DE, Irizarry K, Patel B, Morales AJ, Smith SM, Martasek P, Roman LJ, Masters BS, Jones CL, Weissman BA, Lane P, Liu Q, Gross SS. An autoinhibitory control element defines calcium-regulated isoforms of nitric oxide synthase. J Biol Chem. 1997; 272(47):29769-77.

Santoro B, Chen S, Luthi A, Pavlidis P, Shumyatsky GP, Tibbs GR, Siegelbaum SA. Molecular and functional heterogeneity of hyperpolarization-activated pacemaker channels in the mouse CNS. J Neurosci. 2000; 20(14):5264-75.

Sato M, Hida N, Ozawa T, Umezawa Y. Fluorescent indicators for cyclic GMP based on cyclic GMP-dependent protein kinase Iα and green fluorescent proteins. Anal Chem. 2000; 72(24):5918-24.

Sato M, Hida N, Umezawa Y. Imaging the nanomolar range of nitric oxide with an amplifier-coupled fluorescent indicator in living cells. Proc Natl Acad Sci U S A. 2005; 102(41):14515-20.

Sato M, Nakajima T, Goto M, Umezawa Y. Cell-based indicator to visualize picomolar dynamics of nitric oxide release from living cells. Anal Chem. 2006; 78(24):8175-82.

Sattin A, Rall TW. The effect of adenosine and adenine nucleotides on the cyclic adenosine 3', 5'-phosphate content of guinea pig cerebral cortex slices. Mol Pharmacol. 1970; 6(1):13-23.

Sattler R, Xiong Z, Lu WY, Hafner M, MacDonald JF, Tymianski M. Specific coupling of NMDA receptor activation to nitric oxide neurotoxicity by PSD-95 protein. Science. 1999; 284(5421):1845-8.

Savaskan NE, Plaschke M, Ninnemann O, Spillmann AA, Schwab ME, Nitsch R, Skutella T. Myelin does not influence the choice behaviour of entorhinal axons but strongly inhibits their outgrowth length in vitro. Eur J Neurosci. 1999; 11(1):316-26.

Savchenko A, Barnes S, Kramer RH. Cyclic-nucleotide-gated channels mediate synaptic feedback by nitric oxide. Nature. 1997; 390(6661):694-8.

Schlossmann J, Feil R, Hofmann F. Insights into cGMP signalling derived from cGMP kinase knockout mice. Front Biosci. 2005; 10:1279-89.

Schmidt H, Werner M, Heppenstall PA, Henning M, Moré MI, Kühbandner S, Lewin GR, Hofmann F, Feil R, Rathjen FG. cGMP-mediated signaling via cGKIalpha is required for the guidance and connectivity of sensory axons. J Cell Biol. 2002; 159(3):489-98.

Schmidt K, Desch W, Klatt P, Kukovetz WR, Mayer B. Release of nitric oxide from donors with known half-life: a mathematical model for calculating nitric oxide concentrations in aerobic solutions. Naunyn Schmiedebergs Arch Pharmacol. 1997; 355(4):457-62.

Schrammel A, Behrends S, Schmidt K, Koesling D, Mayer B. Characterization of 1H-[1,2,4]oxadiazolo[4,3-a]quinoxalin-1-one as a heme-site inhibitor of nitric oxide-sensitive guanylyl cyclase. Mol Pharmacol. 1996; 50(1):1-5.

Scott WS, Nakayama DK. Sustained nitric oxide exposure decreases soluble guanylate cyclase mRNA and enzyme activity in pulmonary artery smooth muscle. J Surg Res. 1998; 79(1):66-70.

Seeger TF, Bartlett B, Coskran TM, Culp JS, James LC, Krull DL, Lanfear J, Ryan AM, Schmidt CJ, Strick CA, Varghese AH, Williams RD, Wylie PG, Menniti FS. Immunohistochemical localization of PDE10A in the rat brain. Brain Res. 2003; 985(2):113-26.

Seidel B, Stanarius A, Wolf G. Differential expression of neuronal and endothelial nitric oxide synthase in blood vessels of the rat brain. Neurosci Lett. 1997; 239(2-3):109-12.

Senter PD, Eckstein F, Mülsch A, Böhme E. The stereochemical course of the reaction catalyzed by soluble bovine lung guanylate cyclase. J Biol Chem. 1983; 258(11):6741-5.

Serulle Y, Zhang S, Ninan I, Puzzo D, McCarthy M, Khatri L, Arancio O, Ziff EB. A GluR1-cGKII interaction regulates AMPA receptor trafficking. Neuron. 2007; 56(4):670-88.

Sessa WC. eNOS at a glance. J Cell Sci. 2004 May 15;117(Pt 12):2427-9.

Shakur Y, Takeda K, Kenan Y, Yu ZX, Rena G, Brandt D, Houslay MD, Degerman E, Ferrans VJ, Manganiello VC. Membrane localization of cyclic nucleotide phosphodiesterase 3 (PDE3). Two N-terminal domains are required for the efficient targeting to, and association of, PDE3 with endoplasmic reticulum. J Biol Chem. 2000; 275(49):38749-61.

Sharma RK, Wang JH. Differential regulation of bovine brain calmodulin-dependent cyclic nucleotide phosphodiesterase isoenzymes by cyclic AMP-dependent protein kinase and calmodulin-dependent phosphatase. Proc Natl Acad Sci U S A. 1985; 82(9):2603-7.

Shaul PW. Regulation of endothelial nitric oxide synthase: location, location, location. Annu Rev Physiol. 2002; 64:749-74.

Shaw PJ, Charles SL, Salt TE. Actions of 8-bromo-cyclic-GMP on neurones in the rat thalamus in vivo and in vitro. Brain Res. 1999; 833(2):272-7.

Shi W, Wymore R, Yu H, Wu J, Wymore RT, Pan Z, Robinson RB, Dixon JE, McKinnon D, Cohen IS. Distribution and prevalence of hyperpolarization-activated cation channel (HCN) mRNA

expression in cardiac tissues. Circ Res. 1999; 85(1):e1-6.

Shibasaki K, Suzuki M, Mizuno A, Tominaga M. Effects of body temperature on neural activity in the hippocampus: regulation of resting membrane potentials by transient receptor potential vanilloid 4. J Neurosci. 2007; 27(7):1566-75.

Shimizu-Albergine M, Rybalkin SD, Rybalkina IG, Feil R, Wolfsgruber W, Hofmann F, Beavo JA. Individual cerebellar Purkinje cells express different cGMP phosphodiesterases (PDEs): in vivo phosphorylation of cGMP-specific PDE (PDE5) as an indicator of cGMP-dependent protein kinase (PKG) activation. J Neurosci. 2003; 23(16):6452-9.

Shin JH, Linden DJ. An NMDA receptor/nitric oxide cascade is involved in cerebellar LTD but is not localized to the parallel fiber terminal. J Neurophysiol. 2005; 94(6):4281-9.

Smith JA, Francis SH, Walsh KA, Kumar S, Corbin JD. Autophosphorylation of type Ibeta cGMP-dependent protein kinase increases basal catalytic activity and enhances allosteric activation by cGMP or cAMP. J Biol Chem. 1996; 271(34):20756-62.

Soderling SH, Bayuga SJ, Beavo JA. Isolation and characterization of a dual-substrate phosphodiesterase gene family: PDE10A. Proc Natl Acad Sci U S A. 1999; 96(12):7071-6.

Soleng AF, Chiu K, Raastad M. Unmyelinated axons in the rat hippocampus hyperpolarize and activate an H current when spike frequency exceeds 1 Hz. J Physiol. 2003; 552(Pt 2):459-70.

Son H, Hawkins RD, Martin K, Kiebler M, Huang PL, Fishman MC, Kandel ER. Long-term potentiation is reduced in mice that are doubly mutant in endothelial and neuronal nitric oxide synthase. Cell. 1996; 87(6):1015-23.

Song T, Hatano N, Horii M, Tokumitsu H, Yamaguchi F, Tokuda M, Watanabe Y. Calcium/calmodulin-dependent protein kinase I inhibits neuronal nitric-oxide synthase activity through serine 741 phosphorylation. FEBS Lett. 2004; 570(1-3):133-7.

Song T, Hatano N, Kume K, Sugimoto K, Yamaguchi F, Tokuda M, Watanabe Y. Inhibition of neuronal nitric-oxide synthase by phosphorylation at Threonine1296 in NG108-15 neuronal cells. FEBS Lett. 2005; 579(25):5658-62.

Song Y, Zweier JL, Xia Y. Heat-shock protein 90 augments neuronal nitric oxide synthase activity by enhancing Ca2+/calmodulin binding. Biochem J. 2001; 355(Pt 2):357-60.

Song H, Ming G, He Z, Lehmann M, McKerracher L, Tessier-Lavigne M, Poo M. Conversion of neuronal growth cone responses from repulsion to attraction by cyclic nucleotides. Science. 1998; 281(5382):1515-8.

Sonnenburg WK, Seger D, Kwak KS, Huang J, Charbonneau H, Beavo JA. Identification of inhibitory and calmodulin-binding domains of the PDE1A1 and PDE1A2 calmodulin-stimulated cyclic nucleotide phosphodiesterases. J Biol Chem. 1995; 270(52):30989-1000.

Soong TW, Stea A, Hodson CD, Dubel SJ, Vincent SR, Snutch TP. Structure and functional expression of a member of the low voltage-activated calcium channel family. Science. 1993; 260(5111):1133-6.

Southam E, East SJ, Garthwaite J. Excitatory amino acid receptors coupled to the nitric oxide/cyclic GMP pathway in rat cerebellum during development. J Neurochem. 1991; 56(6):2072-81.

Southam E, Garthwaite J. The nitric oxide-cyclic GMP signalling pathway in rat brain. Neuropharmacology. 1993; 32(11):1267-77.

Sprigge JS. Sir Humphry Davy; his researches in respiratory physiology and his debt to Antoine Lavoisier. Anaesthesia. 2002; 57(4):357-64.

Stamler JS, Lamas S, Fang FC. Nitrosylation. the prototypic redox-based signaling mechanism. Cell. 2001; 106(6):675-83.

Stanarius A, Töpel I, Schulz S, Noack H, Wolf G. Immunocytochemistry of endothelial nitric oxide synthase in the rat brain: a light and electron microscopical study using the tyramide signal amplification technique. Acta Histochem. 1997; 99(4):411-29.

Stasch JP, Becker EM, Alonso-Alija C, Apeler H, Dembowsky K, Feurer A, Gerzer R, Minuth T, Perzborn E, Pleiss U, Schröder H, Schroeder W, Stahl E, Steinke W, Straub A, Schramm M. NO-independent regulatory site on soluble guanylate cyclase. Nature. 2001; 410(6825):212-5.

Steinbach K, Volkmer H, Schlosshauer B. Semaphorin 3E/collapsin-5 inhibits growing retinal axons. Exp Cell Res. 2002; 279(1):52-61.

Stern JE, Li Y, Zhang W. Nitric oxide: a local signalling molecule controlling the activity of pre-autonomic neurones in the paraventricular nucleus of the hypothalamus. Acta Physiol Scand. 2003; 177(1):37-42.

Straub A, Stasch JP, Alonso-Alija C, Benet-Buchholz J, Ducke B, Feurer A, Fürstner C NO-independent stimulators of soluble guanylate cyclase. Bioorg Med Chem Lett. 2001; 11(6):781-4.

Strijbos PJ, Pratt GD, Khan S, Charles IG, Garthwaite J. Molecular characterization and in situ localization of a full-length cyclic nucleotide-gated channel in rat brain. Eur J Neurosci. 1999; 11(12):4463-7.

Stuehr DJ, Marletta MA. Mammalian nitrate biosynthesis: mouse macrophages produce nitrite and nitrate in response to Escherichia coli lipopolysaccharide. Proc Natl Acad Sci U S A. 1985; 82(22):7738-42.

Stys PK, Sontheimer H, Ransom BR, Waxman SG. Noninactivating, tetrodotoxin-sensitive Na+ conductance in rat optic nerve axons. Proc Natl Acad Sci U S A. 1993; 90(15):6976-80.

Stys PK, Lehning E, Saubermann AJ, LoPachin RM Jr. Intracellular concentrations of major ions in rat myelinated axons and glia: calculations based on electron probe X-ray microanalyses. J Neurochem. 1997; 68(5):1920-8.

Stys PK, Hubatsch DA, Leppanen LL. Effects of K+ channel blockers on the anoxic response of CNS myelinated axons. Neuroreport. 1998; 9(3):447-53.

Suvarna NU, O'Donnell JM. Hydrolysis of N-methyl-D-aspartate receptor-stimulated cAMP and cGMP by PDE4 and PDE2 phosphodiesterases in primary neuronal cultures of rat cerebral cortex and hippocampus. J Pharmacol Exp Ther. 2002; 302(1):249-56.

Szabadits E, Cserép C, Ludányi A, Katona I, Gracia-Llanes J, Freund TF, Nyíri G. Hippocampal GABAergic synapses possess the molecular machinery for retrograde nitric oxide signaling. J Neurosci. 2007; 27(30):8101-11.

Tabata T, Ishida AT. Transient and sustained depolarization of retinal ganglion cells by Ih. J Neurophysiol. 1996; 75(5):1932-43.

Talavera K, Nilius B, Voets T. Neuronal TRP channels: thermometers, pathfinders and life-savers. Trends Neurosci. 2008; 31(6):287-95.

Talley EM, Cribbs LL, Lee JH, Daud A, Perez-Reyes E, Bayliss DA. Differential distribution of three members of a gene family encoding low voltage-activated (T-type) calcium channels. J Neurosci. 1999; 19(6):1895-911.

Tallini YN, Ohkura M, Choi BR, Ji G, Imoto K, Doran R, Lee J, Plan P, Wilson J, Xin HB, Sanbe A, Gulick J, Mathai J, Robbins J, Salama G, Nakai J, Kotlikoff MI. Imaging cellular signals in the heart in vivo: Cardiac expression of the high-signal Ca2+ indicator GCaMP2. Proc Natl Acad Sci U S A. 2006; 103(12):4753-8.

Takahashi S, Mendelsohn ME. Calmodulin-dependent and -independent activation of endothelial nitric-oxide synthase by heat shock protein 90. J Biol Chem. 2003a; 278(11):9339-44.

Takahashi S, Mendelsohn ME. Synergistic activation of endothelial nitric-oxide synthase (eNOS) by HSP90 and Akt: calcium-independent eNOS activation involves formation of an HSP90-Akt-CaM-bound eNOS complex. J Biol Chem. 2003b; 278(33):30821-7

Takigawa T, Alzheimer C, Quasthoff S, Grafe P. A specific blocker reveals the presence and function of the hyperpolarization-activated cation current IH in peripheral mammalian nerve fibres. Neuroscience. 1998; 82(3):631-4.

Tanaka J, Markerink-van Ittersum M, Steinbusch HW, De Vente J. Nitric oxide-mediated cGMP synthesis in oligodendrocytes in the developing rat brain. Glia. 1997; 19(4):286-97.

Taqatqeh F, Mergia E, Neitz A, Eysel UT, Koesling D, Mittmann T. More than a retrograde messenger: nitric oxide needs two cGMP pathways to induce hippocampal long-term potentiation. J Neurosci. 2009; 29(29):9344-50.

Teng CM, Wu CC, Ko FN, Lee FY, Kuo SC. YC-1, a nitric oxide-independent activator of soluble guanylate cyclase, inhibits platelet-rich thrombosis in mice. Eur J Pharmacol. 1997; 320(2-3):161-6.

Teunissen C, Steinbusch H, Markerink-van Ittersum M, Koesling D, de Vente J. Presence of soluble and particulate guanylyl cyclase in the same hippocampal astrocytes. Brain Res. 2001; 891(1-2):206-12.

Thomas MK, Francis SH, Corbin JD. Substrate- and kinase-directed regulation of phosphorylation of a cGMP-binding phosphodiesterase by cGMP. J Biol Chem. 1990; 265(25):14971-8.

Thors B, Halldórsson H, Thorgeirsson G. Thrombin and histamine stimulate endothelial nitric-oxide synthase phosphorylation at Ser1177 via an AMPK mediated pathway independent of PI3K-Akt. FEBS Lett. 2004; 573(1-3):175-80.

Töpel I, Stanarius A, Wolf G. Distribution of the endothelial constitutive nitric oxide synthase in the developing rat brain: an immunohistochemical study. Brain Res. 1998; 788(1-2):43-8.

Tojima T, Itofusa R, Kamiguchi H. The nitric oxide-cGMP pathway controls the directional polarity of growth cone guidance via modulating cytosolic Ca2+ signals. J Neurosci. 2009; 29(24):7886-97.

Tornieri K, Rehder V. Nitric oxide release from a single cell affects filopodial motility on growth cones of neighboring neurons. Dev Neurobiol. 2007; 67(14):1932-43.

Tottene A, Moretti A, Pietrobon D. Functional diversity of P-type and R-type calcium channels in rat cerebellar neurons. J Neurosci. 1996; 16(20):6353-63.

Tsou K, Snyder GL, Greengard P. Nitric oxide/cGMP pathway stimulates phosphorylation of DARPP-32, a dopamine- and cAMP-regulated phosphoprotein, in the substantia nigra. Proc Natl Acad Sci U S A. 1993; 90(8):3462-5.

Tsoukias NM, Popel AS. A model of nitric oxide capillary exchange. Microcirculation. 2003;10(6):479-95.

Turko IV, Francis SH, Corbin JD. Binding of cGMP to both allosteric sites of cGMP-binding cGMP-specific phosphodiesterase (PDE5) is required for its phosphorylation. Biochem J. 1998; 329 (Pt 3):505-10.

Turko IV, Ballard SA, Francis SH, Corbin JD. Inhibition of cyclic GMP-binding cyclic GMP-specific phosphodiesterase (Type 5) by sildenafil and related compounds. Mol Pharmacol. 1999; 56(1):124-30.

Ulens C, Tytgat J. Functional heteromerization of HCN1 and HCN2 pacemaker channels. J Biol Chem. 2001; 276(9):6069-72.

Umans JG, Levi R. Nitric oxide in the regulation of blood flow and arterial pressure. Annu Rev Physiol. 1995; 57:771-90.

Vaandrager AB, Ehlert EM, Jarchau T, Lohmann SM, de Jonge HR. N-terminal myristoylation is required for membrane localization of cGMP-dependent protein kinase type II. J Biol Chem. 1996; 271(12):7025-9.

Valtschanoff JG, Weinberg RJ, Kharazia VN, Nakane M, Schmidt HH. Neurons in rat hippocampus that synthesize nitric oxide. J Comp Neurol. 1993; 331(1):111-21.

Valtschanoff JG, Weinberg RJ. Laminar organization of the NMDA receptor complex within the postsynaptic density. J Neurosci. 2001; 21(4):1211-7.

Van Praag H. Exercise and the brain: something to chew on. Trends Neurosci. 2009; 32(5):283-90.

Van Staveren WC, Markerink-van Ittersum M, Steinbusch HW, de Vente J. The effects of phosphodiesterase inhibition on cyclic GMP and cyclic AMP accumulation in the hippocampus of the rat. Brain Res. 2001; 888(2):275-286.

Van Staveren WC, Glick J, Markerink-van Ittersum M, Shimizu M, Beavo JA, Steinbusch HW, de Vente J. Cloning and localization of the cGMP-specific phosphodiesterase type 9 in the rat brain. J Neurocytol. 2002; 31(8-9):729-41.

Van Staveren WC, Steinbusch HW, Markerink-Van Ittersum M, Repaske DR, Goy MF, Kotera J, Omori K, Beavo JA, De Vente J. mRNA expression patterns of the cGMP-hydrolyzing phosphodiesterases types 2, 5, and 9 during development of the rat brain. J Comp Neurol. 2003; 467(4):566-80.

Van Staveren WC, Steinbusch HW, Markerink-van Ittersum M, Behrends S, de Vente J. Species differences in the localization of cGMP-producing and NO-responsive elements in the mouse and rat hippocampus using cGMP immunocytochemistry. Eur J Neurosci. 2004; 19(8):2155-68

Van Staveren WC, Markerink-van Ittersum M, Steinbusch HW, Behrends S, de Vente J. Localization and characterization of cGMP-immunoreactive structures in rat brain slices after NO-dependent and NO-independent stimulation of soluble guanylyl cyclase. Brain Res. 2005; 1036(1-2):77-89.

Van Wagenen S, Rehder V. Regulation of neuronal growth cone filopodia by nitric oxide depends on soluble guanylyl cyclase. J Neurobiol. 2001; 46(3):206-19.

Vargas G, Lucero MT. Modulation by PKA of the hyperpolarization-activated current (Ih) in cultured rat olfactory receptor neurons. J Membr Biol. 2002; 188(2):115-25.

Vargeese C, Sarma MS, Pragnacharyulu PV, Abushanab E, Li SY, Stoeckler JD. Adenosine deaminase inhibitors. Synthesis and biological evaluation of putative metabolites of (+)-erythro-9-(2S-hydroxy-3R-nonyl)adenine. J Med Chem. 1994; 37(22):3844-9.

Vigne P, Lund L, Frelin C. Cross talk among cyclic AMP, cyclic GMP, and Ca(2+)-dependent intracellular signalling mechanisms in brain capillary endothelial cells. J Neurochem. 1994; 62(6):2269-74.

Vincent SR, Kimura H. Histochemical mapping of nitric oxide synthase in the rat brain. Neuroscience. 1992; 46(4):755-84.

Vinet R, Vargas FF. L- and T-type voltage-gated Ca2+ currents in adrenal medulla endothelial cells. Am J Physiol. 1999; 276(4 Pt 2):H1313-22.

Virgili M, Barnabei O, Contestabile A. Regional maturation of neurotransmitter-related and glial markers during postnatal development in the rat. Int J Dev Neurosci. 1990; 8(2):159-66.

Viswanathan M, Rivera O, Short BL. Heat shock protein 90 is involved in pulsatile flow-induced dilation of rat middle cerebral artery. J Vasc Res. 1999; 36(6):524-7.

Vles JS, de Louw AJ, Steinbusch H, Markerink-van Ittersum M, Steinbusch HW, Blanco CE, Axer H, Troost J, de Vente J. Localization and age-related changes of nitric oxide- and ANP-mediated cyclic-GMP synthesis in rat cervical spinal cord: an immunocytochemical study. Brain Res. 2000; 857(1-2):219-34.

Wagner LE 2nd, Li WH, Yule DI. Phosphorylation of type-1 inositol 1,4,5-trisphosphate receptors by cyclic nucleotide-dependent protein kinases: a mutational analysis of the functionally important sites in the S2+ and S2- splice variants. J Biol Chem. 2003; 278(46):45811-7.

Wagner DA, Young VR, Tannenbaum SR. Mammalian nitrate biosynthesis: incorporation of 15NH3 into nitrate is enhanced by endotoxin treatment. Proc Natl Acad Sci U S A. 1983; 80(14):4518-21.

Wahl-Schott C, Biel M. HCN channels: structure, cellular regulation and physiological function. Cell Mol Life Sci. 2009; 66(3):470-94.

Wainger BJ, DeGennaro M, Santoro B, Siegelbaum SA, Tibbs GR. Molecular mechanism of cAMP modulation of HCN pacemaker channels. Nature. 2001; 411(6839):805-10.

Walker EH, Pacold ME, Perisic O, Stephens L, Hawkins PT, Wymann MP, Williams RL. Structural determinants of phosphoinositide 3-kinase inhibition by wortmannin, LY294002, quercetin, myricetin, and staurosporine. Mol Cell. 2000; 6(4):909-19.

Wall MJ. Endogenous nitric oxide modulates GABAergic transmission to granule cells in adult rat cerebellum. Eur J Neurosci. 2003; 18(4):869-78.

Wang HG, Lu FM, Jin I, Udo H, Kandel ER, de Vente J, Walter U, Lohmann SM, Hawkins RD, Antonova I. Presynaptic and postsynaptic roles of NO, cGK, and RhoA in long-lasting potentiation and aggregation of synaptic proteins. Neuron. 2005; 45(3):389-403.

Wang P, Wu P, Egan RW, Billah MM. Identification and characterization of a new human type 9 cGMP-specific phosphodiesterase splice variant (PDE9A5). Differential tissue distribution and subcellular localization of PDE9A variants. Gene. 2003; 314:15-27.

Wang J, Chen S, Siegelbaum SA. Regulation of hyperpolarization-activated HCN channel gating and cAMP modulation due to interactions of COOH terminus and core transmembrane regions. J Gen Physiol. 2001; 118(3):237-50.

Wang YT, Linden DJ. Expression of cerebellar long-term depression requires postsynaptic clathrin-mediated endocytosis. Neuron. 2000; 25(3):635-47.

Waxman SG, Ransom BR, Stys PK. Non-synaptic mechanisms of Ca(2+)-mediated injury in CNS white matter. Trends Neurosci. 1991; 14(10):461-8.

Wedel B, Humbert P, Harteneck C, Foerster J, Malkewitz J, Böhme E, Schultz G, Koesling D. Mutation of His-105 in the beta 1 subunit yields a nitric oxide-insensitive form of soluble guanylyl cyclase. Proc Natl Acad Sci U S A. 1994; 91(7):2592-6.

Weitz D, Ficek N, Kremmer E, Bauer PJ, Kaupp UB. Subunit stoichiometry of the CNG channel of rod photoreceptors. Neuron. 2002; 36(5):881-9.

Wendland B, Schweizer FE, Ryan TA, Nakane M, Murad F, Scheller RH, Tsien RW. Existence of nitric oxide synthase in rat hippocampal pyramidal cells. Proc Natl Acad Sci U S A. 1994; 91(6):2151-5.

West AR, Grace AA. The nitric oxide-guanylyl cyclase signaling pathway modulates membrane activity States and electrophysiological properties of striatal medium spiny neurons recorded in vivo. J Neurosci. 2004; 24(8):1924-35.

Weyer A, Schilling K. Developmental and cell type-specific expression of the neuronal marker NeuN in the murine cerebellum. J Neurosci Res. 2003; 73(3):400-9.

Wilson RI, Gödecke A, Brown RE, Schrader J, Haas HL. Mice deficient in endothelial nitric oxide synthase exhibit a selective deficit in hippocampal long-term potentiation. Neuroscience. 1999; 90(4):1157-65.

Wissenbach U, Bödding M, Freichel M, Flockerzi V. Trp12, a novel Trp related protein from kidney. FEBS Lett. 2000; 485(2-3):127-34.

Wolff DJ, Lubeskie A, Gauld DS, Neulander MJ. Inactivation of nitric oxide synthases and cellular nitric oxide formation by N6-iminoethyl-L-lysine and N5-iminoethyl-L-ornithine. Eur J Pharmacol. 1998; 350(2-3):325-34.

Wolin MS, Cherry PD, Rodenburg JM, Messina EJ, Kaley G. Methylene blue inhibits vasodilation of skeletal muscle arterioles to acetylcholine and nitric oxide via the extracellular generation of superoxide anion. J Pharmacol Exp Ther. 1990; 254(3):872-6.

Wu CC, Ko FN, Kuo SC, Lee FY, Teng CM. YC-1 inhibited human platelet aggregation through NO-independent activation of soluble guanylate cyclase. Br J Pharmacol. 1995; 116(3):1973-8.

Wu SN, Hwang T, Teng CM, Li HF, Jan CR. The mechanism of actions of 3-(5'-(hydroxymethyl-2'-furyl)-1-benzyl indazole (YC-1) on Ca(2+)-activated K(+) currents in GH(3) lactotrophs. Neuropharmacology. 2000a; 39(10):1788-99

Wu HH, Cork RJ, Huang PL, Shuman DL, Mize RR. Refinement of the ipsilateral retinocollicular projection is disrupted in double endothelial and neuronal nitric oxide synthase gene knockout mice. Brain Res Dev Brain Res. 2000b; 120(1):105-11.

Wu HH, Cork RJ, Mize RR. Normal development of the ipsilateral retinocollicular pathway and its disruption in double endothelial and neuronal nitric oxide synthase gene knockout mice. J Comp Neurol. 2000c; 426(4):651-65.

Wu HH, Selski DJ, El-Fakahany EE, McLoon SC. The role of nitric oxide in development of topographic precision in the retinotectal projection of chick. J Neurosci. 2001; 21(12):4318-25.

Wu LG, Saggau P. Adenosine inhibits evoked synaptic transmission primarily by reducing presynaptic calcium influx in area CA1 of hippocampus. Neuron. 1994; 12(5):1139-48.

Wunder F, Tersteegen A, Rebmann A, Erb C, Fahrig T, Hendrix M. Characterization of the first potent and selective PDE9 inhibitor using a cGMP reporter cell line. Mol Pharmacol. 2005; 68(6):1775-81.

Wykes V, Bellamy TC, Garthwaite J. Kinetics of nitric oxide-cyclic GMP signalling in CNS cells and its possible regulation by cyclic GMP. J Neurochem. 2002; 83(1):37-47.

Xiang Y, Li Y, Zhang Z, Cui K, Wang S, Yuan XB, Wu CP, Poo MM, Duan S. Nerve growth cone guidance mediated by G protein-coupled receptors. Nat Neurosci. 2002; 5(9):843-8.

Yamada T, Fujino T, Yuhki K, Hara A, Karibe H, Takahata O, Okada Y, Xiao CY, Takayama K, Kuriyama S, Taniguchi T, Shiokoshi T, Ohsaki Y, Kikuchi K, Narumiya S, Ushikubi F. Thromboxane A2 regulates vascular tone via its inhibitory effect on the expression of inducible nitric oxide synthase. Circulation. 2003; 108(19):2381-6.

Yamazaki M, Chiba K, Mohri T, Hatanaka H. Activation of the mitogen-activated protein kinase cascade through nitric oxide synthesis as a mechanism of neuritogenic effect of genipin in PC12h cells. J Neurochem. 2001; 79(1):45-54.

Yang Q, Chen SR, Li DP, Pan HL. Kv1.1/1.2 channels are downstream effectors of nitric oxide on synaptic GABA release to preautonomic neurons in the paraventricular nucleus. Neuroscience. 2007; 149(2):315-27.

Yao X, Garland CJ. Recent developments in vascular endothelial cell transient receptor potential channels. Circ Res. 2005; 97(9):853-63.

Young RJ, Beams RM, Carter K, Clark HA, Coe DM, Chambers CL, Davies PI, et al., Knowles RG. Inhibition of inducible nitric oxide synthase by acetamidine derivatives of hetero-substituted lysine and homolysine. Bioorg Med Chem Lett. 2000; 10(6):597-600.

Yu X, Duan KL, Shang CF, Yu HG, Zhou Z. Calcium influx through hyperpolarization-activated cation channels (I(h) channels) contributes to activity-evoked neuronal secretion. Proc Natl Acad Sci U S A. 2004; 101(4):1051-6.

Zabel U, Weeger M, La M, Schmidt HH. Human soluble guanylate cyclase: functional expression and revised isoenzyme family. Biochem J. 1998; 335 (Pt 1):51-7.

Zagotta WN, Olivier NB, Black KD, Young EC, Olson R, Gouaux E. Structural basis for modulation and agonist specificity of HCN pacemaker channels. Nature. 2003; 425(6954):200-5.

Zamponi GW, Bourinet E, Snutch TP. Nickel block of a family of neuronal calcium channels: subtype- and subunit-dependent action at multiple sites. J Membr Biol. 1996; 151(1):77-90.

Zeng G, Quon MJ. Insulin-stimulated production of nitric oxide is inhibited by wortmannin. Direct measurement in vascular endothelial cells. J Clin Invest. 1996; 98(4):894-8.

Zhang XP, Hintze TH. cAMP signal transduction induces eNOS activation by promoting PKB phosphorylation. Am J Physiol Heart Circ Physiol. 2006; 290(6):H2376-84.

Zhang HQ, Fast W, Marletta MA, Martasek P, Silverman RB. Potent and selective inhibition of neuronal nitric oxide synthase by N omega-propyl-L-arginine. J Med Chem. 1997; 40(24):3869-70.

Zhao Y, Brandish PE, Ballou DP, Marletta MA. A molecular basis for nitric oxide sensing by soluble guanylate cyclase. Proc Natl Acad Sci U S A. 1999; 96(26):14753-8.

Zheng J, Zagotta WN. Stoichiometry and assembly of olfactory cyclic nucleotide-gated channels. Neuron. 2004; 42(3):411-21.

Ziche M, Morbidelli L. Nitric oxide and angiogenesis. J Neurooncol. 2000; 50(1-2):139-48.

Zolles G, Klöcker N, Wenzel D, Weisser-Thomas J, Fleischmann BK, Roeper J, Fakler B. Pacemaking by HCN channels requires interaction with phosphoinositides. Neuron. 2006; 52(6):1027-36.

Zoraghi R, Bessay EP, Corbin JD, Francis SH. Structural and functional features in human PDE5A1 regulatory domain that provide for allosteric cGMP binding, dimerization, and regulation. J Biol Chem. 2005; 280(12):12051-63.

Zwiller J, Ghandour MS, Revel MO, Basset P. Immunohistochemical localization of guanylate cyclase in rat cerebellum. Neurosci Lett. 1981; 23(1):31-6.